Theory Manual

Regional Simulation Model (RSM)

South Florida Water Management District (SFWMD)
Office of Modeling (OoM)
3301 Gun Club Road
West Palm Beach, FL 33406

Updated on May 16, 2005

This page will intentionally be left blank in the final draft

Table 1: *Revision history for the RSM Theory Manual.*

Version	Name	Date	Comments
1.0	Lal	4/4/05	Generated document side-by-side with theory presentation
1.1	Fulton	4/9/05	Added Bibliography, title page, revision page, preface
1.2	Lal	4/13/05	Changes to document
1.3	Fulton	4/13/05	(3 hrs) Added graphics, Eric HPM section, Karen MSE section
1.4	Fulton	4/13/05	(1.5 hrs) Worked on references, rescaling graphics, equations
1.5	Fulton	4/14/05	(1 hr) Worked on appendices, references, front pages
1.6	Fulton	4/15/05	(3 hrs) Incorporated Ken and Zaki changes
1.7	Fulton	4/19/05	(30 mins) Replaced chapter 3 from Joseph
1.8	Fulton	4/20/05	(4 hrs) Incorporated Ken and Zaki changes for chapter 3
1.9	Lal	4/21/05	(4 hrs) Updated equations and figures in chapter 2
2.0	Fulton	4/22/05	(10 hrs) Updated chapter 2 through Overland Flow Watermover, cover page, bibliography, minor tweaks elsewhere
2.1	Fulton	4/25/05	(6 hrs) Updated remainder of chapter 2
2.2	Fulton	4/26/05	(6 hrs) Updated bibliography, chapter 1, front sections
2.3	Fulton	4/28/05	(3 hrs) Updated chapter 1, minor tweaks, biblio
2.4	Fulton	4/29/05	(5 hrs) Updated chapters 1, 2 and biblio
2.5	Fulton	5/2-4/05	(11 hrs) Updated chapters 1,2, Appendix A,C, figures and biblio
2.6	Black	5/13-14/05	Latex fixes, bibliography fixes

Contents

List of Figures

List of Tables

Acknowledgements

The South Florida Water Management District gratefully acknowledges the contributions of all professionals and support staff who have made this model a reality. The Regional Simulation Model has been developed over many years, and many people have contributed to this development. All contributors are South Florida Water Management District (SFWMD) staff except where noted.

Project Management: Jayantha Obeysekera, Director of the Office of Modeling, wrote the original statement of work for this model in 1993. He has nurtured the technical staff all these years to bring the model to fruition, and we gratefully acknowledge his technical and managerial oversight. In the last few years, Jack Maloy has infused a new level of energy into the RSM project, fast-tracking the completion of the model by providing support in obtaining both human and financial resources. Ken Tarboton is now serving as project manager of both model development and implementation activities.

Principal Contributors: Wasantha Lal, Lead Hydrologic Modeler, is the principal developer of the hydrologic/hydraulic tenets upon which the RSM is built. Randy VanZee, Chief Hydrologic Modeler, is the principal architect of the model, and developer of the majority of the object-oriented code. Wasantha Lal served as the principal author of this manual. Other contributors include David Welter, Lead Hydrologic Modeler, Joseph Park, Lead Hydrologic Modeler, Eric Flaig, Senior Engineer, Clay Brown, Senior Hydrologic Modeler, and Mark Belnap, Senior Engineer at NTI/Verio and former SFWMD Engineer.

For Further Information Please Contact:

For theory questions:

Wasantha Lal, Ph.D., P.E.

Office of Modeling

South Florida Water Management District

3301 Gun Club Road, West Palm Beach, FL 33406

561-682-6826

wlal@sfwmd.gov

For additional copies of the RSM Documentation, please contact the District's Reference Center at 561-682-

2850. The complete set of RSM documents is also available on the World Wide Web at http://www.sfwmd.gov

Acronyms

Acronym	Description
BC	Boundary Conditions
CERP	Comprehensive Everglades Restoration Plan
ET	Evapotranspiration
FIFO	First In First Out
FV	Finite Volume
GIS	Geographic Information Systems
GLPK	GNU Linear Programming Kit
HEC/DSS	Hydrologic Engineering Center Data Storage System
HPM	Hydrologic Process Module
HUB	Collection of HPM
HSE	Hydrologic Simulation Engine
LP	Linear Programming
MSE	Management Simulation Engine
NetCDF	Network Common Data Form
MISO	Multi Input Multi Output
OO	Object-Oriented
PDE	Partial Differential Equation
PETSC	Portable, Extensible Toolkit for Scientific Computation (the RSM 'solver')
RSM	Regional Simulation Model
SFWMM	South Florida Water Management Model (the 2 X 2)
SFWMD	South Florida Water Management District (aka District)
STL	Standard Template Library
SV	Stage to volume conversion
SVD	Single Value Decomposition
USACE	U.S. Army Corps of Engineers
VS	Volume to stage conversion
WCU	Water Control Unit
XML	Extensible Markup Language

Chapter 1

Introduction

The advent of software packages for computational and numerical simulation has produced a profound impact on the ability of scientists and engineers to model a wide variety of physical phenomena across a broad spectrum of disciplines. The discipline of hydrology has leveraged these developments to the point where there currently exists a nearly overwhelming proliferation of hydraulic and hydrologic numerical models aimed at addressing the major engineering issues facing the hydrologic community.

Along with these standard engineering issues, South Florida faces complex problems related to water supply deliveries, flood control and water quality management. While tools exist to address individual water resource management needs, the complexity of south Florida requires a comprehensive modeling tool with greater flexibility for simulating various planning and management options, and the ability to integrate multiple disciplines into one model (e.g., hydrology, hydraulics, ecology, and water quality).

Numerous simulation models have been developed to provide predictive application which have included both groundwater and surface water components. Some of these models were mainly developed as groundwater models, and then added surface water components to the original model (e.g., Modflow), while others were developed as surface water models, and then a groundwater component was added (e.g., MODNET). The limitation of such an approach is that more attention is given to one component over the other (i.e., groundwater vs. surface water), with more details included in one component while little or minimal mathematical representation is included in the other. This modeling constraint was due to the inability of existing technology (e.g., software matrix, computer language) to allow concurrent model development and integration of both surface water and groundwater.

In south Florida, both groundwater and surface water components need to be equally represented to address this unique region. In addition, a comprehensive hydraulic component must be provided to simulate and manage numerous and different types of man-made struc-

tures and canals in south Florida. The hydraulic component must be capable of responding to preset rules and operations as well as to extreme weather patterns (wet/dry) that affect competing urban, environmental and agricultural demands.

To address these needs, the South Florida Water Management District (SFWMD) is developing the Regional Simulation Model (RSM). While this regional hydrologic model is developed on a sound conceptual and mathematical framework, simulating a wide range of hydrologic conditions, RSM has been developed principally for application in South Florida, and accounts for interactions among surface water and groundwater hydrology, structure and canal hydraulics, and management of these hydraulic components.

The RSM simulates and integrates the coupled movement and distribution of groundwater, surface water, man-made structures and network canals in south Florida. The RSM has two principal components, the Hydrologic Simulation Engine (HSE) and the Management Simulation Engine (MSE) (Figure 1.1). The HSE simulates natural hydrology, water control features, water conveyance systems and water storage systems. The HSE component solves the governing equations of water flow through both the natural hydrologic system and the man-made structures (future versions of RSM will include water quality and system ecology)

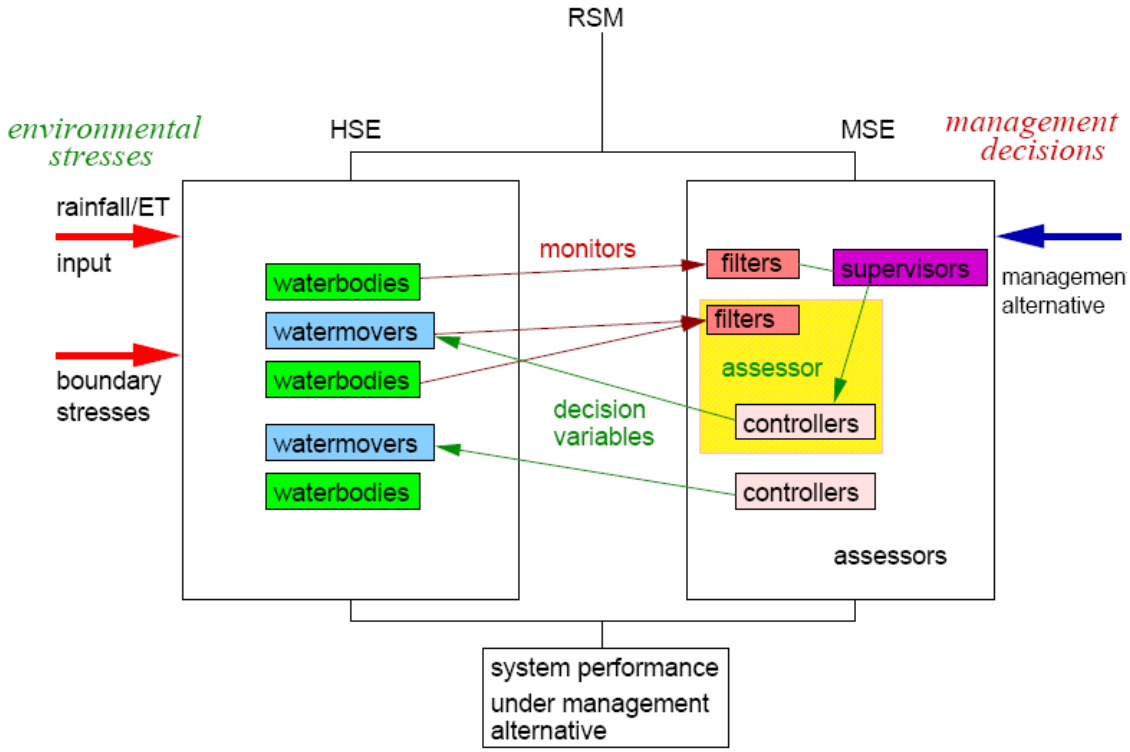

Figure 1.1: *Principal components of the RSM: a) HSE, b) MSE, c) HPM*

The MSE component provides a wide range of operational and management capabilities to the HSE (Figure 1.1). The MSE is capable of simulating a wide range of management operations for the water control features of the South Florida system. Considering that there is not a single unique way that operations can be executed, the MSE is designed to simulate a variety of management options including those used in the past or planned for the future under both normal and extreme conditions.

This manual presents the theory of the Regional Simulation Model in three main sections and several appendices. The remainder of this introductory chapter presents a brief history of the development of the RSM, followed by an overview of model concepts, capabilities, and features. A summary of refinement and testing efforts that have enhanced RSM development is also provided.

Chapter two of the RSM Theory Manual describes the concepts, theory, governing equations and algorithms used in the Hydrologic Simulation Engine to numerically simulate the hydrologic process. The concept and theory of the local hydrologic process modules (HPMs) are also described, which provide an upper boundary condition to the integrated numerical solution.

Chapter three presents the concepts and the theory of the Management Simulation Engine (MSE). In Chapter 3, different levels of management control are described to simulate both local and regional water management options. At the higher level of management control is the capability to assign an overall mission (e.g., unexpected or unplanned water supply needs in a specific area within the model domain). At the lower level of control are capabilities that will make that mission happen (e.g., release more water through a group of structures to meet the water supply needs at that specific area). In addition, Chapter 3 describes the concepts of the decision making process and the interaction between the HSE and MSE.

Additional background information are provided in Appendix A, regarding RSM model philosophy, limitations and usage guidelines. Appendix B presents the shallow water overland equations traditionally used in many existing models, while Appendix C contains a subset of RSM referenced materials.

The RSM Theory Manual is the first of three main Regional Simulation Model Documents. The other principal documents are the Hydrologic System Engine User Manual and the Management Simulation Engine User Manual. Many other published manuscripts, documents and reports regarding the RSM are also available, most via the Internet.

1.1 Brief History of Regional Modeling in South Florida

Regional simulation models have always been a key tool to manage the vast and unique systems of south Florida. Analog models were the first generation regional modeling tools used in south Florida. They were used for a brief period in the 1970's to simulate steady state groundwater flow problems. As digital computers became available, simple digital simulation models based on principles of mass balance became popular initially. One of the first computer models introduced to south Florida and used by the District was the Regional Water Routing Model, also known as the POT model (Fan, 1986). It was a lumped parameter model applied over part of the regional system simulating Lake Okeechobee and various storage areas (e.g., conservation areas). However, the model evolved over many generations with added capabilities to simulate processes such as evaporation and soil moisture as well as to simulate various management options. Over time, it became clear that processes such as canal seepage and sheet flow have to be simulated in two dimensions (x-y) to obtain realistic results (Lin, 2003). This need resulted in the development of the South Florida Water Management Model (SFWMM); also known as the 2X2 model (South Florida Water Management District, 1999).

The SFWMM is the first 2-D distributed parameter model to simulate the regional system of south Florida to determine the distribution of flow in this complex landscape. The model simulates 2-D overland flow, groundwater flow, canal flow, canal seepage, levee seepage, well pumping, and a substantial portion of water management activities. The SFWMM has been used to estimate flows and water levels resulting from historical, current and proposed management scenarios under a wide range of climatic and boundary conditions. The SFWMM uses a 2-mile square horizontal grid spatial resolution and a one-day time step for the computations (Figure 1.2). The model domain extends from Lake Okeechobee in the north to Florida Bay in the south, covering an area of 7600 square miles. The selected spatial and temporal resolutions were the optimum discretizations that were practical using 1980s' slow computers.

The SFWMM is used to evaluate current and proposed water management protocols and operational rules, to make planning decisions regarding significant changes to the system while maintaining water supply, the environment, and other water needs. Over the years, the type of structure management operations carried out within the model has become complex, and the hard-coded sites and operational conditions of the model have become difficult to maintain. However, the SFWMM is still a useful tool capable of performing a large number of regional simulation functions.

The Natural System Model (NSM) is the counterpart to the SFWMM, designed to simulate pre-drainage conditions (i.e., no canals or man-made structures) to assist in establishing and maintaining water management goals, while sustaining and restoring natural systems. The NSM covers the same area as the SFWMM and includes an additional 728 square mile portion of Hendry County that was considered tributary to the Everglades.

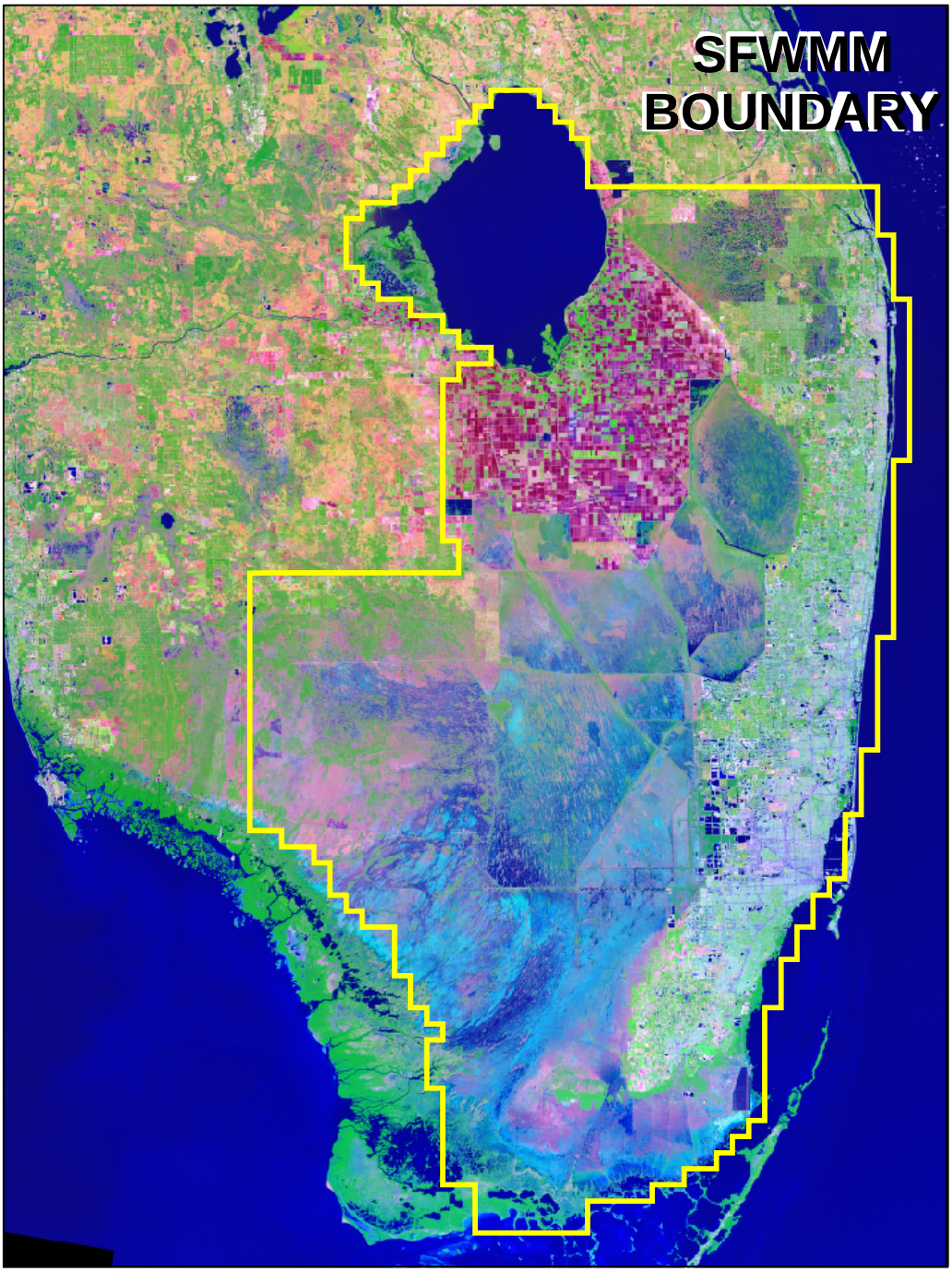

Figure 1.2: *Spatial extent of SFWMM model grid (2X2 model)*

Seeing a need to modernize these two models, SFWMD began engineering a replacement model which could accommodate the goals and objectives of both the SFWMM and NSM models. The RSM, currently under development, is the modeling tool used to implement both the South Florida Regional Simulation Model (SFRSM) and the Natural System Regional System Model (NSRSM). These two implementations extend the boundaries of the original models, and are being implemented using a triangular mesh (Figure 1.3).

1.2 RSM Design Requirements and Building Blocks

One of the primary goals in the development of the RSM is that its South Florida implementation, SFRSM, must be both flexible and adaptable to changing conditions within South Florida. With the expansive planned changes to South Florida drainage basins under the Comprehensive Everglades Restoration Plan (CERP) [1] and new water management strategies [2], it is necessary to develop a model that can be adapted to simulate changing and complex management strategies. It is imperative that this model be easier to use than the South Florida Water Management Model, with shorter learning curves, improved documentation and benchmark examples. There will be no hard-coding of site or operational conditions within the RSM or its implementations to allow maximum flexibility in model application.

RSM development relies mainly on three building blocks, object-oriented (OO) code design, new computational methods (i.e., grid resolution and numerical errors) and new and efficient numerical solvers for large matrices. Without these three building blocks, RSM could not meet the needs of south Florida.

The first area of technological contribution came from recent developments in information technology and the use of OO code design methods. The use of extensible markup language XML (Bosak and Bray, 1999), geographic information system (GIS) technology and database support has allowed us to achieve a level of code flexibility and data integration that did not exist before. Object-oriented methods have been used in the past for hydraulic model design by Solomantine (1996), Tisdale (1996), and many others. Although OO design may have been previously considered to be outside the expertise of many hydrologists, the increased complexity of the hydrologic processes modeled and the need to incorporate methods developed by professionals from many other disciplines such as biology, hydrogeology and ecology, have changed this view.

The strong dependencies between hydrology, nutrient transport and ecology have created a need to develop a comprehensive and integrated software package using a modular approach. Simple models that address issues within one discipline at a time have become

[1] http://www.evergladesplan.org
[2] http://www.sfwmd.gov/org/wsd/waterreservations/index.html

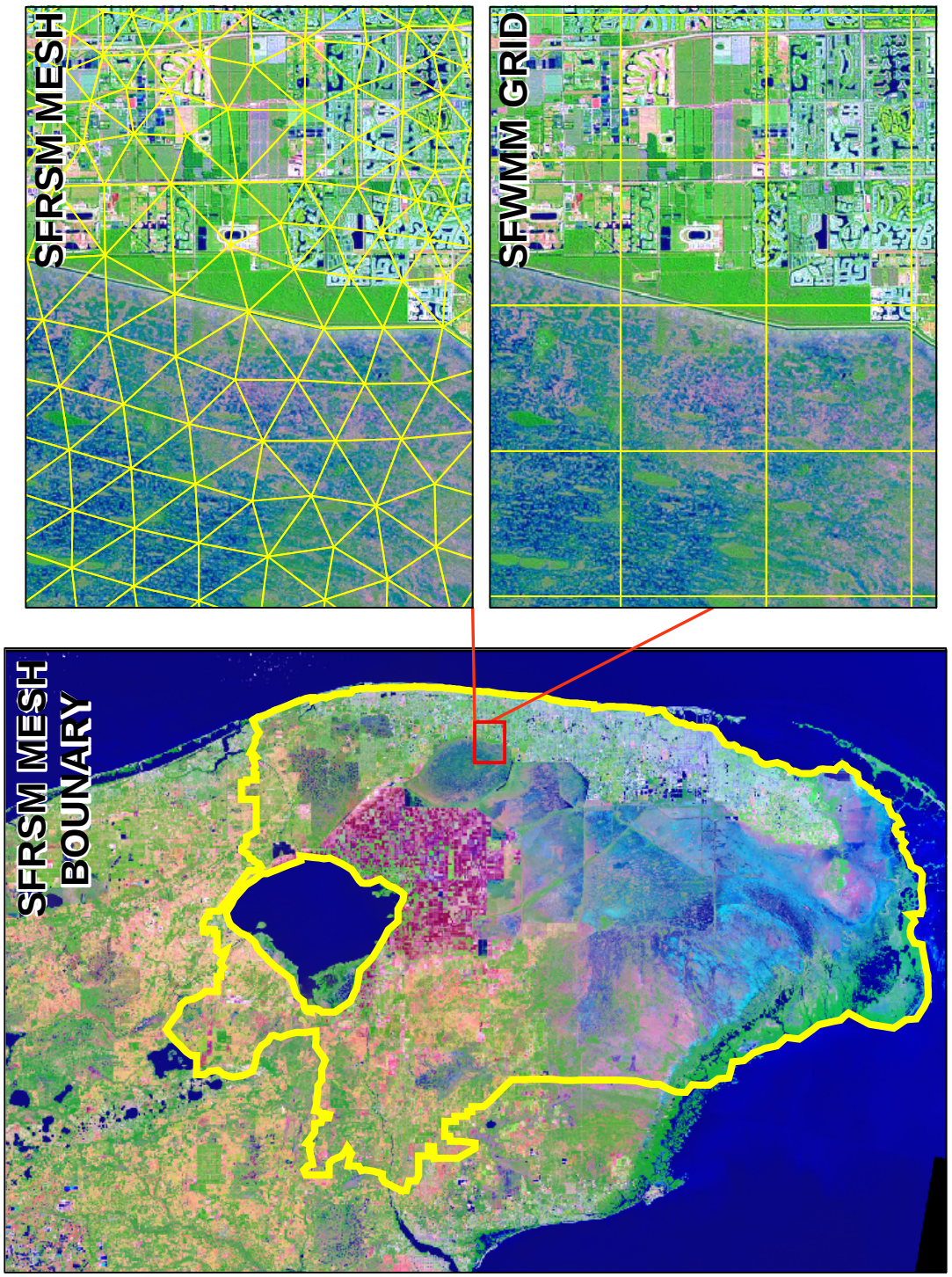

Figure 1.3: *Spatial extent of SFRSM and SFWMM model boundary and an example of grid resolution used by both models*

inadequate for studying complex systems. The improved use of GIS support tools, OO code design and XML language have made it possible to organize large amounts of complex data and to model complex systems.

The mathematical foundation for RSM has been around for many years (Chow et al., 1988; Hirsch, 1989). However, implementation of these equations was only made possible through the advancement of certain new technologies. The second technological contribution came from developments in computational methods. For example, the use of unstructured meshes of variable size to simulate 2-D integrated overland and groundwater flow in irregular shaped domains has become common (Zhao et al., 1994; Shen et al., 1997). Full and partial integration with canal networks and lakes is now possible. In the past two decades, a number of physically based, distributed-parameter models have emerged with such features. The early models include MODBRANCH (Swain and Wexler, 1996), MODNET (Walton et al., 1999), MikeSHE/Mike11 based on Abbott et al. (1986a) and Abbott et al. (1986b), WASH123 (Yeh et al., 1998), MODFLOW-HMS (HydroGeoLogic, 2000), and models by VanderKwaak (1999), Schmidt and Roig (1997), and Lal (1998b). The computational engines of these models are based on solving a form of the shallow water equation for overland flow and either the variably saturated Richards' Equation or the fully saturated groundwater flow equation. Inertia terms in the shallow water equations are neglected, and the solution to the governing equations is obtained using a single global matrix. A number of features, such as lookup tables, approximate linearization methods, and regression methods, are available in these models to simulate structures, urban areas and agricultural areas. The choice of features depends on the intended application of the model.

Advanced developments in numerical error analysis by Hirsch (1989) and Lal (2000) also helped in the selection of optimal grid discretizations for integrated modeling approach. Results of error analysis are useful in developing model meshes that produce more accurate solutions and avoid large errors and incipient instabilities. Large-scale integration using an implicit method is practically impossible without understanding numerical errors and instability. Because of unconditional stability, implicit models can be run with practically any time step regardless of whether the solution is accurate or not.

The third area of technical contribution came from a new generation of computer packages that can be used to solve large sparse systems of equations efficiently (Schenk and Gartner, 2004; Gupta et al., 1997). It is now possible to develop implicit finite volume algorithms and solve many complex equations simultaneously without iterating between various model components. Modern solvers support parallel processing and have a variety of built-in tools and options to achieve fast model runs. These solvers are easy to use because details, such as matrix storage methods, are automated and transparent to the user. RSM uses the software package PETSC (Balay et al., 2001) to solve its matrices, due to PETSC's advantages (e.g., it uses parallel processing, in the public domain, fast, and easy to use and implement).

The RSM uses advanced computational techniques and other technologies such as: object-oriented design methods, extensible markup language(XML), geographic information system (GIS), and a finite volume (FV) method to simulate 2-D overland and groundwater flow. RSM uses an unstructured triangular mesh to discretize the model domain. The discretized control volumes for surface water, groundwater, canals and lakes are treated as abstract "waterbodies" that are connected by abstract "watermovers." The numerical procedure is flexible enough to allow the use of several representations for the same equation without the constraint of a preset single approach (e.g., Manning's equation, flow resistance in wetlands, or lookup tables).

An object-oriented (OO) code design is used to provide robust and highly extensible software architecture. The object-oriented design of the RSM allows an implementation to consist of an assembly of different water management objects that can be interchanged as the model evolves. A weighted implicit numerical method is used to keep the model fully integrated and stable. We conducted a limited error analysis to ensure that the results of the implicit scheme used in the RSM falls within acceptable criteria using well posed analytical solutions.

The RSM has been tested at a subregional scale to analyze its applicability to south Florida conditions. For example, the HSE has been used to simulate flow in the Kissimmee River (Lal, 1998c), and in the Everglades National Park (Lal, 1998b, Brion et al., 2000, Brion et al., 2001, Senarath et al., 2001). The accuracy of the model was verified using the MODFLOW model (McDonald and Harbaugh, 1984) and an analytical solution for stream-aquifer interaction Lal, 2001.

1.3 Special Features and Capabilities of RSM

South Florida is a unique environment requiring specialized models to simulate regional operations. South Florida has a complex regional hydrologic system that includes:

- Approximately 2267 of miles of primary and secondary networked canals
- A total of 263 of man-made control structures (flow)
- Groundwater/seepage influence of Lake Okeechobee, a 730 square mile, relatively shallow lake with an average depth of 9 feet
- Extreme weather patterns of rain events and frequent droughts
- Water reservation needs
- Highly pervious aquifers that are connected to the surficial aquifer
- Considerable groundwater and overland flow interaction
- Extensive wetlands systems adjacent to rapidly expanding urban areas and agricultural sectors

- Open areas subjected to overland flow and sheet flow
- Unique sheet flow characteristics in the Everglades and the Water Conservation Areas (i.e., extremely slow flow due to low slope, shallow depth, and the ridge and slough vegetation affecting flow direction).

This complex system requires that the model perform quickly, offer tremendous flexibility, and clear interpretation of input data sets. The use of modeling to assist in water supply planning requires quick scenario changes, usually with an expected turnaround time of less than 48 hours per simulation. Also, due to south Florida's extreme rain events and droughts, it is imperative that models be capable of running long-term regional simulations of 35-40 years, covering wet, dry and average rainfall conditions. Over this length of time, water demands continue to change as the south Florida population steadily increases, land use constantly changes as agricultural land is converted to urban use, marshes or reservoirs, and regional operational policies change to distribute water resources fairly as competition increases for limited water supplies. This requires both flexibility and ease of use in building and modifying input data sets, as well as an ability to use generalized data sets to optimize performance.

Advanced computational methods and very fast computers alone have limited success in solving modern day problems such as these because the challenge is to model the complexity of the hydrologic system, while maintaining computational efficiency and an acceptable level of numerical errors. Consequently, more efficient computational methods, more flexible computer code, better code development environments, and better code maintenance procedures are needed to keep pace with these growing demands. The need for clean code design, participation by multiple developers from a variety of disciplines, and regular use of test cases to routinely check code integrity has become critical. RSM uses XML to format input data sets, and tools are being developed to aid error-checking of these data sets. The OO code modularity makes it easy to insert new functionality into the model. For example, water quality and ecological modules will be added with access to the same hydrologic data as other model components, and operational rules can be added or updated as water management policies are revised. Output from the model can be specified in a number of standard formats (e.g., HEC/DSS and NetCDF), allowing a quicker analysis of results using a wide variety of tools.

The following provides a list of RSM primary hydrologic processes and capabilities:

- Two-dimensional overland flow over arbitrary water bodies.
- Two-dimensional or three-dimensional groundwater flow coupled to surface water bodies.
- One-dimensional diffusion flow in canal networks.
- Independent layouts of 2-D meshes and 1-D flow networks overlapping fully or partially. The model can be used to simulate overland flow, canal flow, lake flow or any

combination of them. The model is fully integrated, and all the equations for regional flow are solved simultaneously.

- Constant or variable storage coefficients that can describe soil storage capacity varying with depth. The variation can be described using lookup tables.
- Various overland flow conveyance behaviors based on Manning's equations, wetland flow equations and look-up table type functions with values varying with depth.
- Various transmissivity functions for confined and unconfined aquifers including lookup table type functions with values changing with depth.
- Reservoirs, or large water bodies, in full interaction with aquifers.
- Ponds or small water bodies residing within meshes but in full interaction.
- Many common types of structures, weirs, pipes, bridges etc. with more than one flow regime. All the structure types used in National Weather Service (NWS) models and the CASCADE model are available for use. Some of the USACE models are available as well.
- Virtual water movers based on 1-D, 2-D, or water level difference based lookup table functions. These water movers can move water from any water body to any other water body controlled by state variables in a third water body. A lookup table is used as a mapping function. A number of pumping and flood control conditions can be simulated using these lookup tables.
- Full three-dimensional simulation of groundwater flow, with any number of layers. Different numbers of layers can cover different parts of the horizontal domain.
- Water budget features that can track the movement of water throughout the model.
- A feature known as Hydrologic Process Modules (HPMs) that can capture a wide variety of local hydrologic functions associated with urban and natural land use, agricultural management practices, irrigation practices, and routing.
- Features capable of simulating detention storage, and unsaturated moisture within HPMs.

1.4 Refinement and Testing of RSM

Development and application of new models can happen only because of the growth of many scientific ideas and disciplines. Since newly developed models are expected to have capabilities beyond any existing models, new developments in surface and sub-surface hydrology, theoretical solution methods, numerical methods, software techniques, and GIS methods are essential to make progress in model development and application. Some of the refinements and tests that have allowed the movement from subregional to regional use of RSM include:

Determining the computational efficiencies of various algorithms. Understanding of the computational efficiencies and run times of various solution methods is critical in the selection of

a solution method for surface and subsurface flow. Lal (1998b) describes a comparison of various iterative and non-iterative solution methods for the same discretization. The paper also explains the influence of mesh resolution on model error and run time.

Estimating numerical errors associated with the solution of model application. Numerical errors are common to all numerical models. These errors have to be evaluated and considered before accepting model results. In addition to mesh resolution, the numerical error of a solution depends on the type of the problem solved. The error associated with dynamic boundary conditions, for example, is different from the error associated with a pumping well located in a single cell inside the model domain. Lal (2000) has estimated numerical errors of the diffusion equation for problems including the steady state solution, source term (e.g., rainfall), point pumping, and dynamic boundary influences (e.g., tidal boundaries).

Testing implicit finite volume methods and their numerical errors. A comparison of two of the implicit finite volume approaches is also described by Lal (1998a). Numerical error in the fully implicit solution implemented in the RSM model, is also described in Lal (2005). The numerical error in RSM model is equal to the numerical error of the MODFLOW model when both are solving the linear diffusion equations using the same cell and mesh areas.

Testing and quantifying canal-aquifer interaction. Mathematical expression of canal-aquifer interaction involves the solution of a fully coupled 1-D canal equation and a 2-D groundwater flow equation. Lal (2001, 2005) showed that the solution depends on a number of dimensionless parameter groups. Depending on the values of the dimensionless groups, canal-aquifer interaction can be insignificant or dominant. These papers also describe analytical expressions against which numerical solutions can be checked.

Identifying model parameters and their uncertainty. Parameters of most models are underdetermined (Menke, 1989). This is mainly because it is practically impossible to collect all the observed data needed to determine all these parameters. Even if average parameter values are used during regional calibrations, field observations are needed if accurate results are expected under south Florida conditions, mainly because of the heterogeneous limestone base, which causes sporadic and huge variability in seepage, particularly in South Miami-Dade County (Cunningham et al., 2004). A number of dynamic field tests have been introduced by Lal (2005) to calibrate a number of parameters under such difficult conditions. Parameter calibration and uncertainty analysis methods are also useful in identifying parameter values and ranges prior to model application (see Appendix C for additional references with details regarding some of this research).

Chapter 2

Hydrologic Simulation Engine Theory and Concepts

2.1 HSE Concepts

The HSE simulates the physical processes in the hydrologic system, including the major processes of water storage and conveyance driven by rainfall, potential evapotranspiration, and boundary and initial conditions. The basic conceptualization of the HSE is coupling sets of control volumes (waterbodies) with different forms of flow between them (watermovers) based on the properties and state of the respective control volumes (Figure 2.1).

In the RSM, the HSE is integrally linked to the Management Simulation Engine (MSE), which allows managed water routing between control volumes, based on different levels of management control rules. The HSE provides hydrologic state information to the MSE, which imposes management control on selected control volumes. This conceptualization allows the RSM to be applied to a wide range of hydrologic systems, from natural systems with no management intervention, to a complex system of water storage areas plus a canal network with numerous structures operated using a sophisticated set of rules.

The RSM is implemented using the object-oriented C++ computer language, with high level abstractions used to represent different hydrologic states in control volumes and different forms of flow between control volumes. In the HSE two basic abstractions, "waterbodies" and "watermovers", are used to represent the state within the control volume and the flux between control volumes, respectively. Waterbodies and watermovers are central to the organizational hierarchy of the HSE. These objects allow simulation of two-dimensional overland flow, two or three dimensional groundwater flow, canal flow and lake representation (storage and flow) in an integrated system of waterbodies with watermover fluxes between the waterbodies.

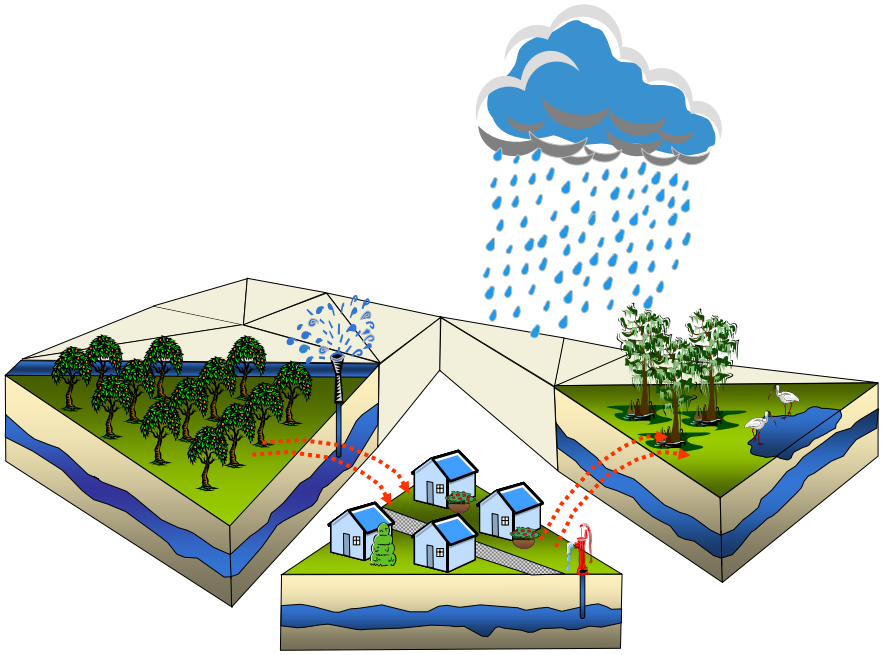

Figure 2.1: *HSE representation of the hydrologic system*

The development and the application of the regional simulation model are based on a theoretical foundation that requires the consideration of a number of technical aspects including:

1. governing equations that describe the physical processes of fluid flow
2. numerical methods useful in obtaining efficient solutions for the governing equations
3. flexible software design, such as object-oriented methods, that allow organization of data and computational methods to solve complex problems involving irregular geometries, heterogeneous materials and complicated operations.
4. established analytical tools that can be used to check if the numerical solution is accurate and within acceptable bounds
5. theoretical guidelines to assist in the selection of time steps and cell sizes for optimization of model performance and prediction of model accuracy
6. useful analytical tools that can be used in verifying the model
7. analytical tools to evaluate the results of a model application and determine the reliability of the results based on a variety of uncertainties.

The first four considerations are important for the development of models and the last three considerations are important for the implementation and application of models. During both

the development and the application, it is important to have a thorough understanding of the physical problem, governing equations, assumptions and their limitations.

2.2 Theoretical Overview

The governing equations of RSM include the equation for conservation of mass and the equation for the conservation of momentum. In addition to these primary laws, constitutive equations and equations of state are also used. Because a continuous medium is assumed for the model domain, the governing equations are expressed as partial differential equations (PDEs) and solved as initial-boundary value problems. The solution depends simultaneously on the initial and boundary conditions. For numerical simulation purposes the continuous medium is discretized into a finite number of points in space and solved at discrete points in time.

In the HSE, a finite volume method is used to simulate the hydrology and the hydraulics of the entire system. The governing equations used in the formulation are based on the Reynolds transport theorem. Because the model functions as a result of interplay between the control volume objects or waterbodies and the surface integral objects or watermovers, in the HSE groundwater and overland flow are described as objects performing designated functions under appropriate conditions. The integral form has many advantages, and is the key to seamless integration of various flow, discretization, and land use types in the implicit finite volume method. With this approach, various control volumes become metamorphic objects that change according to the type of flow, such as overland flow, groundwater flow and canal flow, without regard to the type of discretization. Parts of the surface integral become metamorphic objects that change for overland flow, canal flow, structure flow etc. Hydrologic process module objects and a variety of other objects are similarly metamorphic. The object-oriented design of the model makes it possible to write one computational algorithm for all generic flow objects eliminating the need to have separate overland flow, groundwater flow, canal flow models, and the need to integrate the separate models. A unique feature of the HSE is the integration of object-oriented design methodology with an implicit formulation.

This object-oriented approach is particularly useful in representing a complex system in an integrated fashion in the model, however it differs from a more traditional approach where overland and groundwater flow can be described using sequentially placed conditional statements. In this document a mixture of traditional and more object-oriented (OO) approaches is used to better describe the HSE to those who may not be familiar with OO methods. The HSE is described in more detail in a traditional sense in Lal (1998b) as well as Appendix B and in an OO approach in Lal et al. (2005), which is included in Appendix C.

2.3 HSE Governing Equations

The finite volume method is built around governing equations in integral form. The Reynolds transport theorem is at the core of the RSM model. Reynolds transport theorem is generally used to describe physical laws written for fluid systems applied to control volumes fixed in space. More recently, it has been used as a first step in the derivation of many conservative laws in partial differential equation form (Chow et al., 1988). The Reynolds transport theorem is expressed for an arbitrary control volume (Figure 2.2) as:

$$\frac{D\mathbf{N}}{Dt} = \frac{\partial}{\partial t}\int_{cv} \eta\rho \, d\mathcal{V} + \int_{cs} \eta\rho(\mathbf{E}\cdot\mathbf{n}) \, dA \tag{2.1}$$

in which $\mathbf{N}$ = an arbitrary extensive property such as the total mass; η = arbitrary intensive property, or property per unit mass such as concentration; $\mathbf{E}$ = flux vector; $\mathbf{n}$ = unit normal vector; $d\mathcal{V}$ = volume element; dA = area element; cv = control volume; and cs = control surface. Variables $\mathbf{N}$ and η can be vectors or scalars. This representation of Reynolds transport theorem can be used to write any conservation law with the application of different assumptions. For example, in the case of mass balance, $\eta = 1$, and in the case of momentum, $\eta = u\mathbf{i} + v\mathbf{j}$ in cartesian coordinates in which u and v are the velocity components in x and y directions.

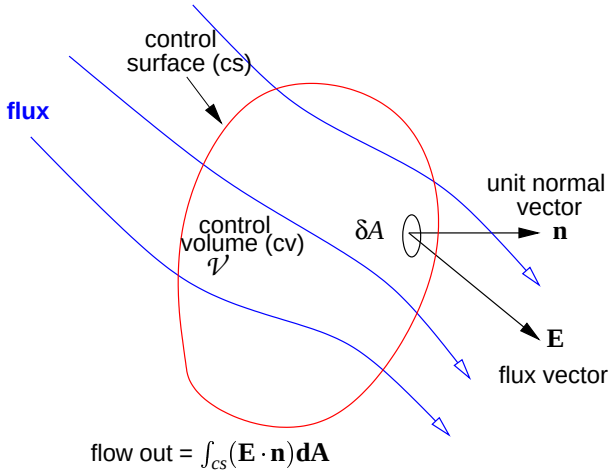

Figure 2.2: *An arbitrary control volume*

2.3.1 Mass Balance Equation

The mass balance equation in integral form can be written using $\eta = 1$ in Equation 2.1 as:

$$0 = \frac{\partial}{\partial t} \int_{cv} dV + \int_{cs} (\mathbf{E} \cdot \mathbf{n})\, dA \tag{2.2}$$

in which $\mathbf{E} = u\mathbf{i} + v\mathbf{j}$ and $\frac{D\mathbf{N}}{Dt} = 0$ because mass is conserved in a Newtonian fluid system.

In the HSE the small elemental control volumes are represented by triangular prisms or objects of any other shape, depending on the water body type and discretization used (Figure 2.3). The first term in Equation 2.2 represents storage in the control volumes or "waterbodies" and the second term in Equation 2.2 represents flux across control surfaces or "watermovers". The formulation of waterbodies and watermovers within the context of the solution of mass balance in its integral form are described in Sections 2.4 and 2.5.

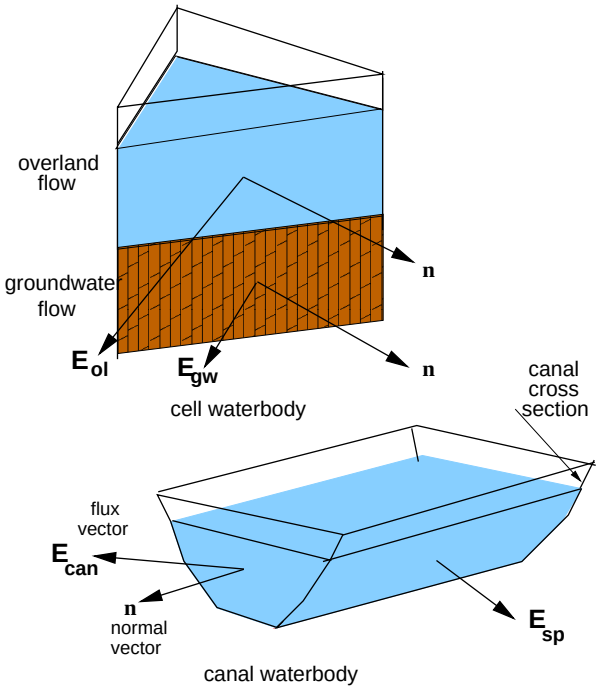

Figure 2.3: *Control volumes or waterbodies used in the HSE*

2.3.2 Momentum Equation

The equation of motion or the equation describing Newton's second law is the second vector equation necessary to describe shallow water flow. This equation is also referred to as the

momentum equation of the St. Venant equations. It is obtained by substituting η with $\mathbf{E} = [u, v]^T$ in the vector form of the Reynolds transport equations.

$$\mathbf{F} = \frac{\partial}{\partial t} \int_{cv} \mathbf{E}\rho \, d\mathcal{V} + \int_{cs} \mathbf{E}\rho(\mathbf{V} \cdot \mathbf{n}) \, dA \tag{2.3}$$

in which $\mathbf{V} = [u, v]^T$ = velocity vector for shallow water flow; $\mathbf{F}$ = force vector. The force vector is expressed as

$$\mathbf{F} = \begin{pmatrix} \rho g h S_x - \tau_{bx} \\ \rho g h S_y - \tau_{by} \end{pmatrix} \tag{2.4}$$

in which τ_{bx}, τ_{by} = components of bottom shear stress along x and y directions; S_x, S_y = water surface slopes in x and y directions. The bottom shear stresses can be explained using

$$\tau_{bx} = \frac{\rho g n_b^2 u |\mathbf{V}|}{h^{\frac{1}{3}}} \tag{2.5}$$

$$\tau_{by} = \frac{\rho g n_b^2 v |\mathbf{V}|}{h^{\frac{1}{3}}} \tag{2.6}$$

$$\tag{2.7}$$

in which h = water depth; n_b = Manning's roughness coefficient. The water surface slopes S_x and S_y are defined as

$$S_x = \frac{\partial H}{\partial x} \tag{2.8}$$

$$S_y = \frac{\partial H}{\partial y} \tag{2.9}$$

in which H = water level. The computation of Equation 2.3 within a numerical scheme can be complex. In RSM, all the terms of the right hand side representing various inertia terms are neglected for simplicity. The components of $\mathbf{F}$ resulting in simple equations are then absorbed into the equation of mass balance to form the diffusion flow equations.

A number of conditions have made it possible to use the diffusion flow assumption in south Florida under certain conditions. Lal (2001) showed that the assumption is challenged only in the deepest portions of the Everglades when disturbances of period less than four days are used. This calculation was carried out using the same conditions proposed by (Ponce et al., 1978). In other shallower areas, solutions with periodic components less than four hours can be simulated without violation of the same assumptions. Lal (2001) showed that a mesh size of two miles or larger is appropriate under the deep sections, based on numerical error considerations. Diffusion assumption can also becomes weak in deep canals of RSM for the same reason. Since only long term regional effects are of interest, some of the inertia effects giving short term dynamic response times can be irrelevant, as long as the accuracy of the long period solution components can be maintained.

2.4 Waterbodies Formulation

Control volumes in RSM are referred to as waterbodies. The first term on the right hand side of Equation 2.2, $\frac{\partial}{\partial t}\int_{cv} d\mathcal{V}$, represents the change in storage with time of all the waterbodies within the aggregated control volume. Calculation of the change in mass in the waterbody over arbitrary waterbodies is facilitated by the introduction of the stage-volume relationship, which describes the relationship between the volume of water in the waterbody and the water head.

2.4.1 Stage-Volume (SV) Relationships Describing Waterbodies

The stage-volume (SV) relationship is obtained by manipulating the control volume term of Equation 2.2 as follows:

$$\frac{\partial}{\partial t}\int_{cv} d\mathcal{V} = \int_{cv} \frac{d\mathcal{V}(H)}{dH}\frac{dH}{dt} \tag{2.10}$$

$$= \int_{cv} A_0 \frac{df_{sv}(H)}{dH}\frac{dH}{dt} \tag{2.11}$$

$$= \int_{cv} A(H)\frac{dH}{dt} \tag{2.12}$$

in which A_0 = plan area of the waterbody; $f_{sv}(H)$ = normalized stage-volume relationship that applies to any of the control volumes; $A_0 f_{sv}(H)$ = volume of water above a specified datum of the waterbody; and $A(H)$ = effective area of the waterbody and is defined as:

$$A(H) = A_0 \frac{\partial f_{sv}(H)}{\partial H} \tag{2.13}$$

The SV relationship is shown in Figure 2.4. It applies to 2-D overland flow, groundwater flow, canal flow and lake flow. As shown in Figure 2.4, the term $\frac{df_{sv}(H)}{dH}$ becomes 1 for overland flow and s_c for groundwater flow.

The stage-volume relationship functions make it possible to use detailed descriptions of local stage-storage characteristics in integrated models. This feature is necessary when the local topography is complex and in the case of special land surface characterizations in agricultural and urban areas. The SV relationship provides water levels when the volume in a waterbody is known and vice versa. In the case of canals, they are used to obtain the water level when the canal geometry is known. Local topography, storage coefficient, and other geometric information are used in the development of SV functions for 2-D cells. The SV functions are monotonically increasing functions that can be expressed as lookup tables developed using observed data. Some simple examples of $f_{sv}(H)$ are described below.

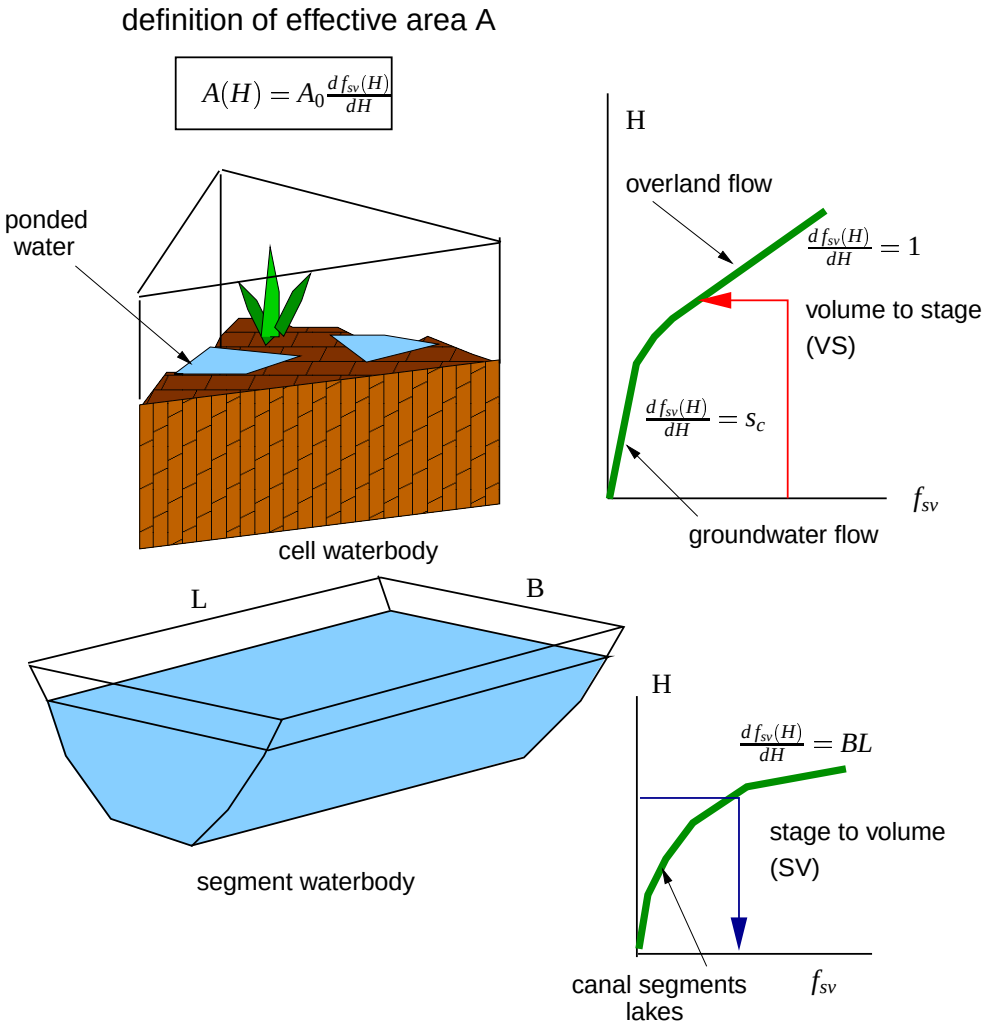

Figure 2.4: *Stage-volume relationship for cell and segment waterbodies*

2.4.2 Stage-Volume (SV) Relationship for Flat Ground

The stage-volume (SV) relationship function $f_{sv}(H)$ for a cell is used to obtain the volume of water in a control volume when the water head is known. This has to be a one-to-one relationship that has a unique inverse relationship called the VS converter described next. When the ground level is assumed horizontal, the SV relationship for a cell with a single layered aquifer is given by:

$$V = A_0 \, f_{sv}(H) = A_0 s_c (H - z_b) \quad \text{for} \quad H < z \tag{2.14}$$

$$V = A_0 \, f_{sv}(H) = A_0 s_c (z - z_b) + A_0 (H - z) \quad \text{for} \quad H \geq z \tag{2.15}$$

in which V = volume of water in control volume or waterbody; z_b = elevation at the bottom of the aquifer; z = elevation of the ground surface, and A_0 = cell area.

2.4.3 Inverse (VS) Relationship for Flat Ground

The inverse (VS) relationship $f_{vs}(V)$ is used every time the head is determined for a control volume using the volume of water in it. Since the expression for flat ground is piecewise linear, Equations 2.14 and 2.15 can be used to obtain the following relationships:

$$H = f_{vs}(\frac{V}{A_0}) = z + \left\{\frac{V}{A_0} - s_c(z - z_b)\right\} \quad \text{for} \quad V > A_0 s_c(z - z_b) \tag{2.16}$$

$$H = f_{vs}(\frac{V}{A_0}) = z_b \quad \text{for} \quad V < 0 \tag{2.17}$$

$$H = f_{vs}(\frac{V}{A_0}) = z + \frac{V}{A_0\ s_c} \quad \text{otherwise} \tag{2.18}$$

2.4.4 SV Relationship for a Canal Segment

For a canal with a rectangular cross section, the relationship $f_{sv}(H)$ between the water volume and the head is:

$$V = BL\ f_{sv}(H) = 0 \quad \text{for} \quad H < z_c \tag{2.19}$$

$$V = BL\ f_{sv}(H) = BL(H - z_c) \quad \text{for} \quad H \geq z_c \tag{2.20}$$

in which z_c = elevation of canal bottom; L = length of canal segment and B = canal width.

2.5 Watermovers Formulation

The surface flux integral term of the Reynolds transport theorem $\int_{cs} (\mathbf{E} \cdot \mathbf{n})\ dA$ contains the sum of all fluxes crossing the entire control surface. Because there are many types of control volumes with many types of flux functions surrounding a given waterbody, the surface integral is dissected and organized systematically for computational and functional reasons (Figure 2.5). The surface integration terms are organized according to the type of head dependency.

The surface integral is divided into a number of easily definable watermovers and source terms forming the total surface integral. Some terms in the calculation of flux across a control surface are gradient driven while others are not. The gradient-driven terms generally fill in the flow resistance matrix in the numerical solution. Terms that are not driven by head

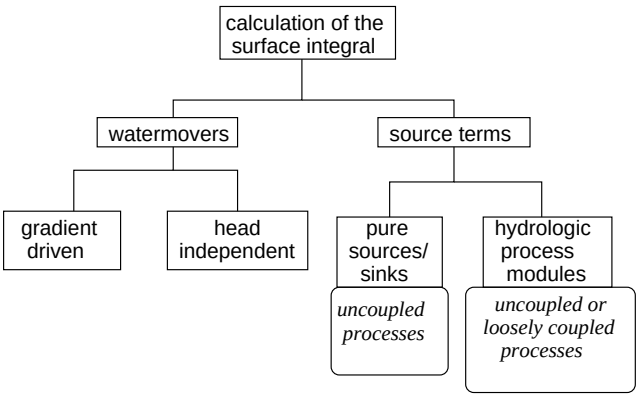

Figure 2.5: *Organization of surface integration terms*

gradient are sometimes referred to as the source and sink terms because traditionally they included rainfall, ET and other head independent terms. These terms include recharge, runoff, irrigation, pumping and a number of other processes. Some of the terms such as pumping are head independent. These terms are classified as pure sources and sinks. Hydrologic process modules (HPMs) can be uncoupled or loosely coupled with head.

The sum total of all the flows entering a single control volume i can be expressed as:

$$Q_i(\mathbf{H}) = \sum_{r=1}^{wm} (\mathbf{E} \cdot \mathbf{n})_r \, \Delta A_r = \sum_{r=1}^{wm} q_r(\mathbf{H}) + S_i(\mathbf{H}) \tag{2.21}$$

in which H = water head vector; $q_r(\mathbf{H})$ = discharge across gradient driven watermover r; $S_i(\mathbf{H})$ = the summation of non-gradient-driven watermovers; ΔA_r = flow area of cell wall r of a prismatic cell (see Figure 2.3) where $\Delta A_r = h\Delta l_r$; h = water depth; Δl_r = length of cell wall r; wm = number of watermovers contributing to the waterbody i; $\mathbf{n} = n_x\mathbf{i} + n_y\mathbf{j}$ = unit outward normal vector for the face r of the polygon; $\mathbf{E}$ = average flux rate across the control surface per unit length defined as $u\ \mathbf{i} + v\ \mathbf{j}$, which is also equal to $-K\nabla H$ for free surface diffusion flow or groundwater flow. The term $S_i(\mathbf{H})$ indicates the possibility of a head dependency.

The gradient-driven watermover is the basic abstraction needed to transfer water between any two waterbodies. Watermovers assist in the calculation of flow across control surfaces in canal flow, overland flow and all other kinds of flows such as structure flow. By design, gradient watermovers conserve mass. Some watermovers such as those for overland flow, groundwater flow and canal flow are created implicitly based on cell and canal network topology and geometry. Because only watermovers can move water between waterbodies, the model can track mass balance of the system at the highest level of abstraction. In the current diffusion flow formulation, discharge across a single watermover $q_r(\mathbf{H})$ between two

waterbodies shown in Figure 2.6 is expressed as:

$$q_r(\mathbf{H}) = k_0(\mathbf{H}) + k_1(\mathbf{H})H_1 + k_2(\mathbf{H})H_2 \tag{2.22}$$

in which k_0, k_1, k_2 = values obtained as a result of linearization of the function q_r; H = water head vector; H_1, H_2 = water levels of control volumes 1 and 2. Discharge functions $q_r(\mathbf{H})$ for various types of watermovers are described later in this section. Depending on the types of cells or waterbodies adjacent to a particular waterbody, a variety of watermovers may be needed to complete the surface integral around a given waterbody.

2.5.1 Overland Flow Watermover

Cordes and Putti (1996) showed the equivalence of a low-order mixed finite element method based on RT0 elements as described in Raviart and Thomas (1977) with a finite volume method for triangles under certain conditions. Because of the equivalence, it is possible to use an expression derived for the mixed finite element method to compute flow rates for the finite volume method.

In the equivalent finite volume method, water levels at circumcenters are used in the computation of flow across control surfaces. In the mixed finite element method, water levels in triangular prisms are assumed to vary linearly, and the water level at the centroid is the average water level.

If the Manning's equation is used to compute flow in cells m and n, defined in Figure 2.6, then for:

$$\begin{aligned} & \{H_m > H_n \quad \text{and} \quad h_m > 0 \quad \text{and} \quad H_m > z_n\} \\ \text{or} \quad & \{H_m < H_n \quad \text{and} \quad h_n > 0 \quad \text{and} \quad H_n > z_m\} \end{aligned}$$

$$\text{then} \quad T_{mn} = \frac{h_r^{\frac{5}{3}}}{n_r\sqrt{S_r}} \quad \text{for} \quad S_r > S_{tol} \tag{2.23}$$

$$T_{mn} = \frac{h_r^{\frac{5}{3}}}{n_r\sqrt{S_{tol}}} \quad \text{for} \quad S_r \leq S_{tol} \tag{2.24}$$

in which h_r and n_r are defined as:

$$h_r = 0.5(h_m + h_n) \tag{2.25}$$

$$n_r = 0.5(n_m + n_n) \tag{2.26}$$

H_m, H_n = heads at the circumcenters; h_m, h_n = water depths at the circumcenters; z_m, z_n = ground elevations of cells m and n; n_m, n_n = Manning's roughness coefficients of cells m and n; S_r = magnitude of the slope of the energy grade line and S_{tol} = a small slope below which the energy slope is not allowed to go in the calculation of T_{mn} to prevent a division by zero.

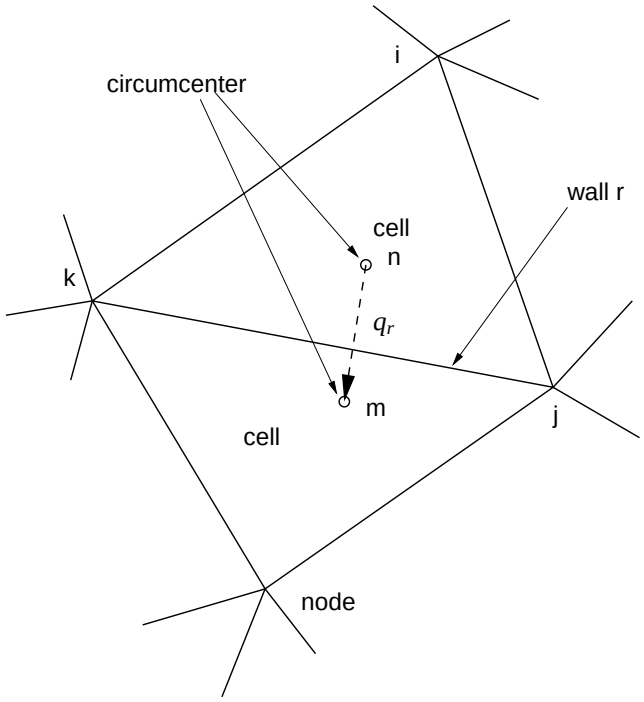

Figure 2.6: *Sample waterbodies with circumcenters m and n used to define variables*

A value of 10^{-13} to 10^{-7} is used in the Everglades because these slopes are below typically observed slopes except in deep pools of water. S_r is computed using

$$S_r = \sqrt{\frac{(\hat{H}_j - \hat{H}_k)^2}{\Delta l_r^2} + \frac{(H_m - H_n)^2}{\Delta d_{mn}^2}} \tag{2.27}$$

in which Δd_{mn} = distance between circumcenters of triangles m and n; Δl_r = length of wall r; $\hat{H}_j$ and $\hat{H}_k$ = the heads at nodes j and k, computed as weighted averages of surrounding heads. The cell areas are used as weights in the averaging. The conditions given for Equation 2.23 and Equation 2.24 make sure that water is available at the upstream cell, and that water doesn't flow upstream.

Since there are many watermovers across many waterbodies, the influence of each watermover towards every waterbody is organized in submatrices that will be added to a global flow resistance matrix. The submatrix is derived for each section of the control surface considering that the flow across each section r adds water to cell n and removes water from cell m. The flow rates q_m and q_n from waterbodies m and n can be related to heads H_m and H_n using:

$$\begin{pmatrix} q_m \\ q_n \end{pmatrix} = \begin{pmatrix} -K_{mn} & +K_{mn} \\ +K_{mn} & -K_{mn} \end{pmatrix} \cdot \begin{pmatrix} H_m \\ H_n \end{pmatrix} \tag{2.28}$$

which can also be expressed as:

$$\mathbf{q}(\mathbf{H}) = \mathbf{M}'(\mathbf{H}) \cdot \mathbf{H} \tag{2.29}$$

in which $\mathbf{M}'(\mathbf{H})$ = a submatrix of the total matrix $\mathbf{M}(\mathbf{H})$. This formulation is shown in Figure 2.7. The same information could be presented as part of pseudocode that is used in

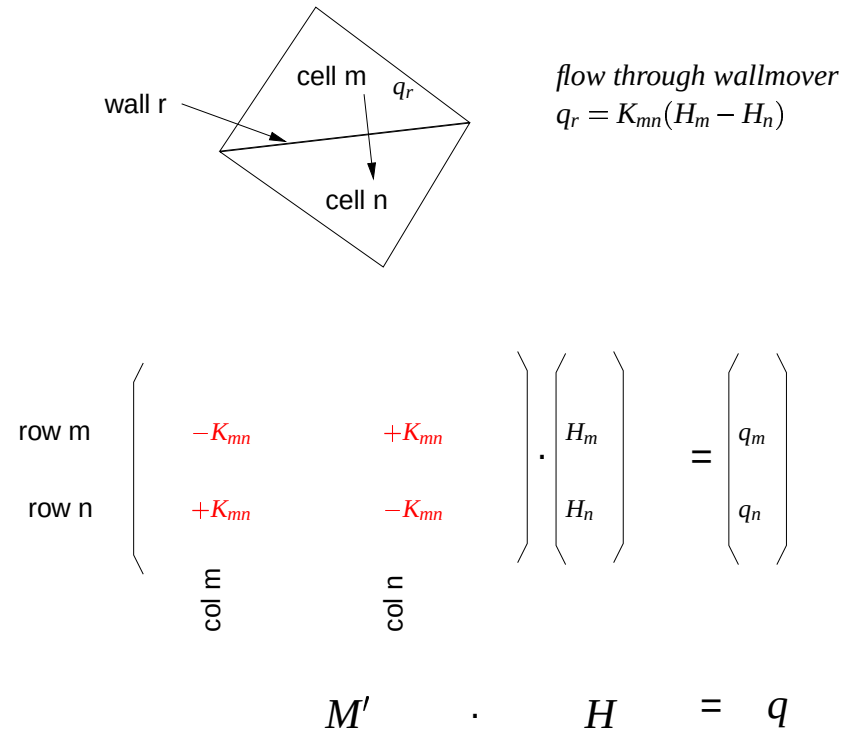

Figure 2.7: *Submatrix for a single watermover as part of total matrix*

the semi-implicit formulation. Flow from a cell m to n can be written as a modification of the following matrix elements:

$$M_{m,n} \rightarrow M_{m,n} + \frac{T_{mn}\Delta l_r}{\Delta d_{mn}} \tag{2.30}$$

$$M_{m,m} \rightarrow M_{m,m} - \frac{T_{mn}\Delta l_r}{\Delta d_{mn}} \tag{2.31}$$

$$M_{n,n} \rightarrow M_{n,n} - \frac{T_{mn}\Delta l_r}{\Delta d_{mn}} \tag{2.32}$$

$$M_{n,m} \rightarrow M_{n,m} + \frac{T_{mn}\Delta l_r}{\Delta d_{mn}} \tag{2.33}$$

The circumcenter-based method can be used only with acute-angled triangles (Raviart and Thomas, 1977; Cordes and Putti, 1996). When this method is used with obtuse angled

triangles, the circumcenter falls outside the triangle, and the numerical error tends to be large. With rectangular cells, the method becomes equivalent to the finite difference method.

2.5.1.1 Overland Flow Watermover for Mixed Flow

When the water levels are above ground in one or both of two adjacent cells, overland flow takes place between them. The discharge in the watermover q_r between two adjacent cells is computed using the circumcenter method derived for mixed finite elements (Lal, 1998c). For mixed flow types where two adjacent cells use different types of flow equations (e.g., Manning's and a lookup table), flow $(\mathbf{E}\cdot\mathbf{n})_r$ for control surface r in Equation 2.21 is computed using:

$$\begin{aligned} q_r &= (\mathbf{E}\cdot\mathbf{n})_r \qquad (2.34)\\ &= K_{mn}(H_m - H_n) = \Delta l\, T_r \frac{H_m - H_n}{\Delta d_{mn}} \begin{cases} \text{for} \quad H_m > H_n \quad \text{and} \quad H_m > z_m \quad \text{and} \quad H_m > z_n \\ \text{or} \quad H_n > H_m \quad \text{and} \quad H_n > z_n \quad \text{and} \quad H_n > z_m \end{cases} \end{aligned}$$

in which H_m, H_n = water levels in triangular cells m and n; d_{mn} = distance between circumcenters of triangles m and n; Δl = length of the wall; z_m, z_n = ground elevations of cells m and n; T_r = equivalent inter block transmissivity in the overland flow layer, computed based on the assumption that transmissivity varies linearly between circumcenters (Goode and Appel, 1992; McDonald and Harbaugh, 1984). Variable T_r is computed as:

$$T_r = \frac{T_m + T_n}{2} \quad \text{for} \quad 0.995 \le \frac{T_m}{T_n} \le 1.005 \qquad (2.35)$$

$$T_r = \frac{T_m - T_n}{\ln \frac{T_m}{T_n}} \quad \text{otherwise} \qquad (2.36)$$

T_m and T_n are the values for the cells defined in Equation B.9 (see Appendix B) for overland flow. Matrix elements filled up by the overland flow watermovers are described in Lal (1998b).

2.5.2 Groundwater Flow Watermover

When simulating saturated groundwater flow with confined and unconfined aquifers, transmissivity of the adjacent cells is computed first. The discharge in the watermover q_r is then computed using:

$$q_r = \Delta l\, \frac{H_m - H_n}{\left(\frac{l_m}{T_m} + \frac{l_n}{T_n}\right)} \qquad (2.37)$$

in which l_m, l_n = the distances from the circumcenters to the wall; T_m, T_n = transmissivities.

2.5.3 Canal Flow Watermover

Canal flow under the diffusion flow conditions is calculated using the following equation:

$$\begin{aligned} q_r &= (\mathbf{E}\cdot\mathbf{n})_r \\ &= K_{mn}(H_m - H_n) = T_r\frac{H_m - H_n}{\Delta d_{mn}} \begin{cases} \text{for} & H_m > H_n \quad \text{and} \quad H_m > z_m \quad \text{and} \quad H_m > z_n \\ \text{or} & H_n > H_m \quad \text{and} \quad H_n > z_n \quad \text{and} \quad H_n > z_m \end{cases} \end{aligned} \tag{2.38}$$

in which H_m, H_n = water levels in two canal segments m and n, as shown in Figure 2.8. When

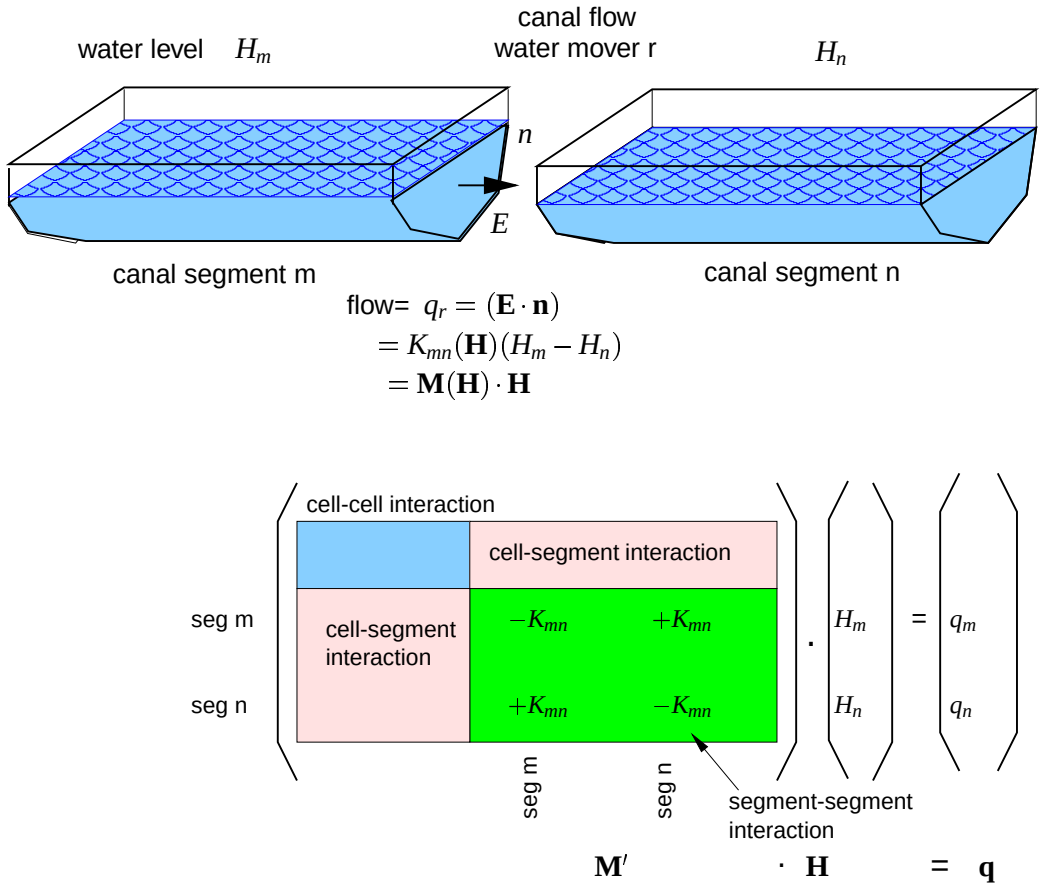

Figure 2.8: *Canal flow calculations*

simulating canal flow, a linearly varying conveyance is assumed between canal segments. The equation for discharge between two segments m and n is the same as Equation 2.35. The value of T_m for example, for segment m is

$$T_m = \frac{A_m}{l_m\sqrt{S_n}n_b}\left(\frac{A_m}{P_m}\right)^{\frac{5}{3}} \tag{2.39}$$

in which A_m = average canal cross sectional area of segment m; P_m = average wetted perimeter; n_b = average Manning roughness coefficient and l_m = length of a canal segment.

When simulating canal networks, each pair of segments of a canal joint is implicitly considered as a canal watermover. A canal joint with n limbs has $n(n-1)/2$ canal watermovers as a result. All these watermovers have to be considered before populating the matrix. Their summation computes the actual discharge.

2.5.4 Canal-Cell Watermover

There are two types of canal-cell watermovers, representing seepage between the canal and the cell and representing overbank flows between the canal and the cell. Seepage between a canal segment and a cell is described using a canal seepage watermover, where the seepage rate q_l per unit length of the canal is derived using Darcy's equation as follows:

$$q_l = k_m p \frac{\Delta H}{\delta} = \frac{k_m p}{\delta}(H_i - H_m) \tag{2.40}$$

in which k_m = sediment layer conductivity; p = perimeter of the canal subjected to seepage; δ = sediment thickness and ΔH = head drop across the sediment layer. Construction of the submatrix created for the watermover is shown in Figure 2.9.

2.5.5 Structure Flow Watermover

Structure flow watermovers are defined using linearized structure equations or lookup tables; A water control structure is a structure that can be used to impose management decisions onto the flow control. Linearization of structure equations is not always easy for most of the structures. Structure discharges are generally expressed as $q_s = q_s(H_u, H_d, G)$, in which H_u and H_d are upstream and downstream water levels and G = gate opening. Linearization of the structure equations is necessary before they are used in the implicit solution method. Such a linearization is accurate only in gradually varied flow.

Considering that $q_s = q_s(H_u, H_d, G)$ can be extremely nonlinear, differential equations with structure equations can be stiff and difficult to solve without special methods or small time steps. As an alternative, one and two-dimensional lookup tables and regression equations are also useful in describing structure flow.

2.5.6 Head Independent Watermovers Representing Sources and Sinks

Pumping into and out of a cell is conceptualized using head independent watermovers. In the flux calculation described in (Equation 2.21), this is described using the term S_i. These

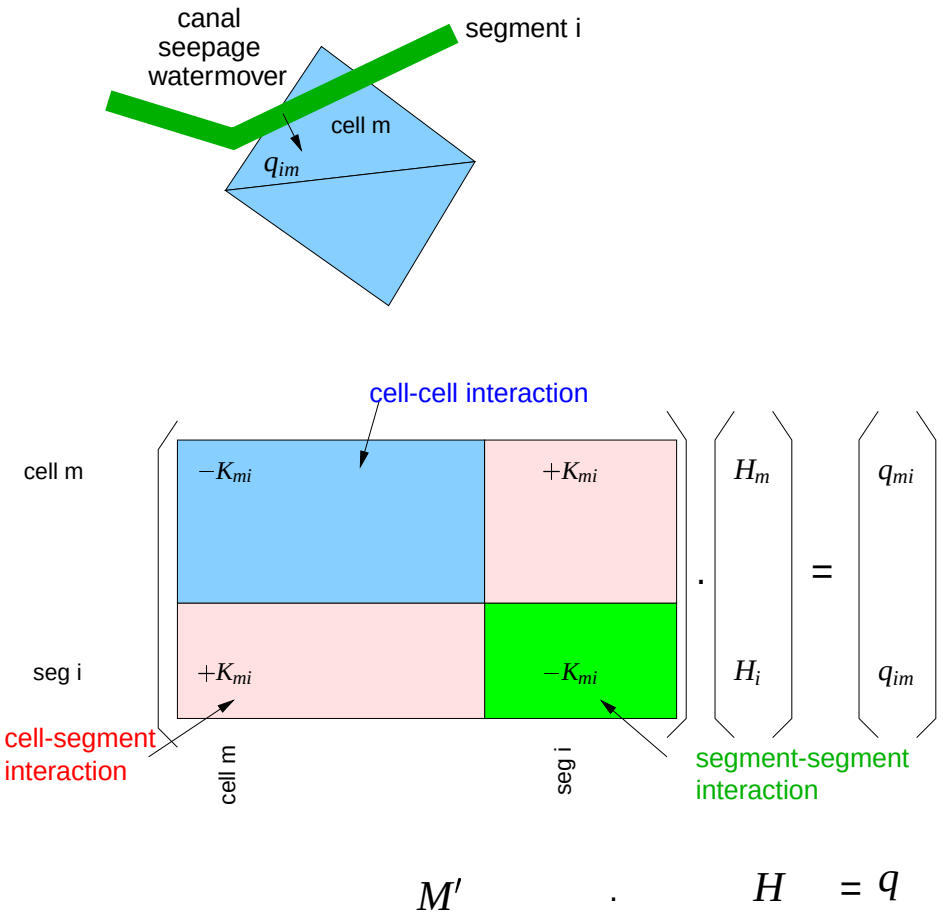

Figure 2.9: *Matrix elements for canal-aquifer interaction*

terms can also be considered as source and sink terms. If water is pumped at a known rate $p(t)$ into a cell i described by a time series data set, the source term for cell i is expressed as:

$$S_i = p(t) \tag{2.41}$$

The case of management-driven pumping or diversion, the hydrologic process modules (HPMs) take care of the calculation of $p(t)$. HPMs are described in greater detail in Section 2.6 and in Appendix C.5.

2.6 Hydrologic Process Module (HPM) Formulation

Hydrologic process modules are activated at the beginning of each model time step. They are designed to simulate the effects of local hydrology on the regional system. The local hydrology depends on the local land use, water use and water management practices. Different land use types have different hydrology, water storage properties and generate different recharge and, therefore, different hydrologic responses. Hydrologic Process Modules (HPMs) are used to separate the complexities of the natural and managed flow processes associated with local hydrology and simulate rainfall, ET, infiltration, percolation, seepage, unsaturated subsurface flow, irrigation, urban water use, stormwater detention and surface water management practices of the natural and managed landscapes from the regional system. In the simple form or the complex form, the HPMs are an integral part of the HSE within RSM. At a minimum they simulate precipitation and evapotranspiration to calculate recharge to the saturated flow in the regional solution.

Physical processes that take place at a local scale are generally rapid. As a result, reasonable assumptions can be made to simulate some of these processes within the control volume. The net effects of the local hydrologic processes are accumulated and applied on the regional system using HPMs.

The HPMs contain storage, routing and simple interchange mechanisms to simulate the processes mentioned above. The recharge R_{rchg}, irrigation Q_{irr} and runoff Q_{ro} are applied to the regional system using the S_i term described in Equation 2.21. They are computed separately for each cell with a new land use type. The equation for mass balance is used to compute recharge during each time step. This equation can be in a very simple form or a very complex form as follows:

$$\Delta S = P - ET - evap - R_{rchg} + Q_{irr} + Q_{ws} - R_{ro} - Q_{sew} - Q_{sep} - Q_{seep} - S_{det} \qquad (2.42)$$

in which ΔS = change in storage (water content) in HPM; P = precipitation; ET = actual evapotranspiration; evap = evaporation from interception, surface detention and bare soil; R_{rchg} = recharge; Q_{irr} = irrigation; Q_{ws} = urban water supply; R_{ro} = runoff; Q_{sew} = sewage discharge; Q_{sep} = water discharged to onsite disposal systems; Q_{seep} = water lost through seepage; and S_{det} = water stored in stormwater detention systems. Some of the optional terms may not be applicable to some of the processes.

In the HSE, computation of each term in Equation 2.42 is carried out within each HPM of each respective mesh cell. The source and sink terms from Equation 2.42 allow a variety of processes to be simulated in HPMs. These processes affect the storage of water and the distribution of water applied to the cell.

The HPMs are developed for various land use types, land management and water management practices. The HPM structure provides the capability to apply different hydrologic processes for the local hydrology of each cell. More details on HPMs can be found in Flaig

et al. (2005), which is provided in Appendix C.5.

2.6.1 Simple HPM

In the simplest case, the HPM processes rainfall and evapotranspiration (Figure 2.10). The ET rate is determined by a crop adjustment coefficient, $ET = K_c * PET$, in which K_c is a function of water table depth. Some examples of simple HPMs include:

- Natural Wetland System `<layer1nsm>`
- Five Unsaturated Soil Layer `<layer5>`
- Unsaturated Soil `<unsat>`
- No Action `<layerpc>`

2.6.2 Complex HPM

HPMs provide the opportunity to apply complex processes to the local hydrology. These processes include irrigation, stormwater detention, unsaturated water flow, and impervious land hydrology (Figure 2.11). These HPMs contain several parameters that describe surface water management practices and affect water storage as well as demand and discharge. Some examples of complex HPMs include:

- Precipitation Runoff Routing `<prr>`
- Agricultural Irrigation Requirements `<afsirs>`
- Drainage Collector Ditch `<pumpedditch>`
- Agricultural Impoundment `<agimp>`
- Multi-Basin Routing `<mbrcell>`
- Impervious Land `<imperv>`
- Consumptive Use `<cu>`
- Urban Detention `<urbandet>`

2.6.3 HPM Hubs

Hubs are used to combine a number of complex capabilities of HPMs. The HPM hub provides the capability of applying water supply demand and runoff to specific locations in the mesh and network for a group of cells (Figure 2.12). This capability is useful where there is a large urban development that is serviced by a single public water supply well (PWS) or has

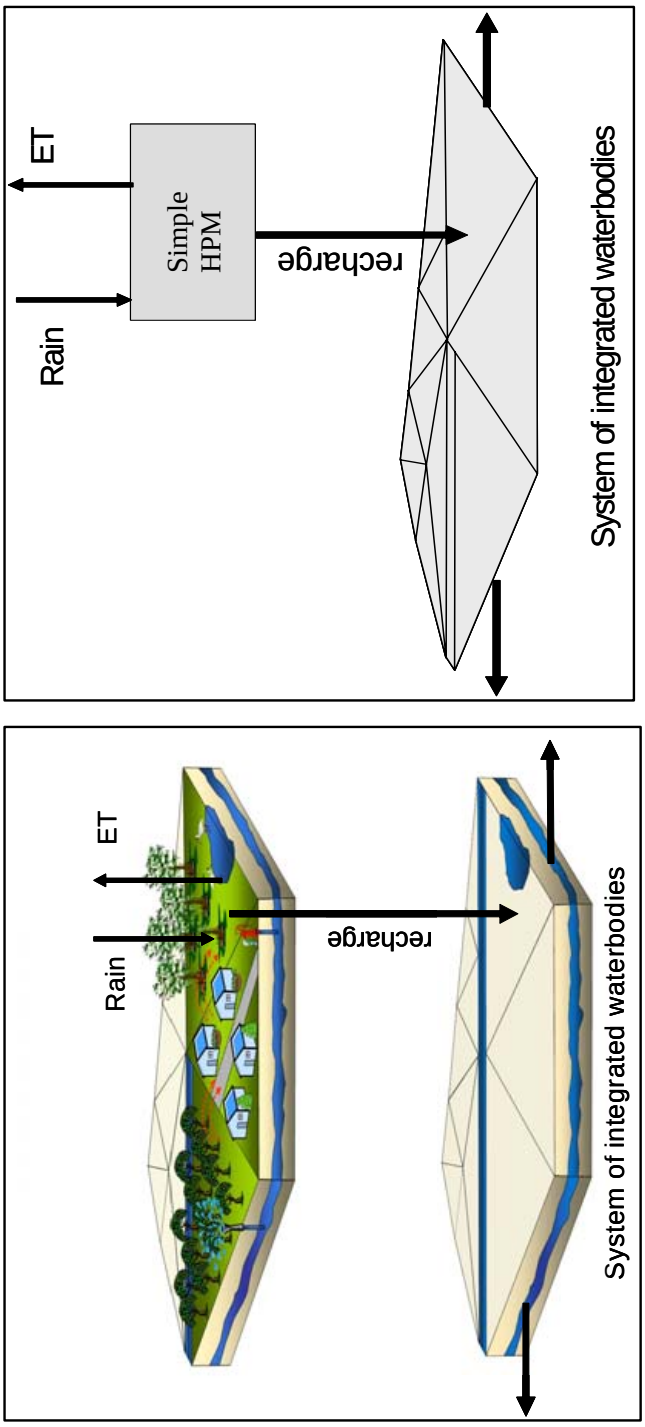

Figure 2.10: *Simple Hydrologic Process Module with no internal storage.*

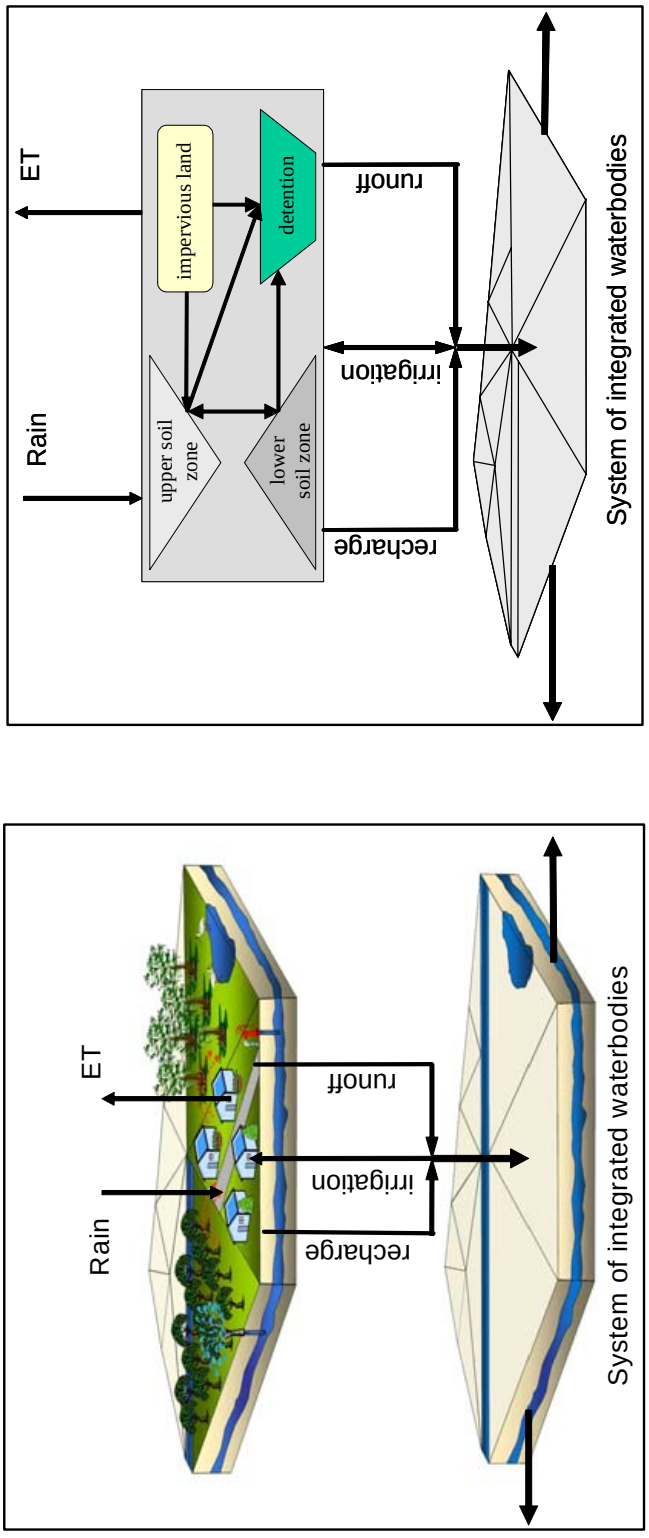

Figure 2.11: *Complex Hydrologic Process Module with multiple internal processes including soil water storage. The outflows are directed to the homecell in this example.*

a single runoff. The PWS may be located considerably distant from the hub. The runoff and irrigation from the HPM within a hub may be directed to any mesh cell or segment. The recharge from the hub is directed uniformly to the cells below the footprint of the Hub.

The Hub may consist of a single HPM type or a combination of HPM types. In a single HPM implementation, all of the land in the footprint of a hub is assigned to a single HPM type. It is also possible to assign several HPM types to the Hub based on the percent of the area of that land use type within the Hub. For example, an urban development Hub could consist of 20 percent impervious land, 40 percent pervious land, 30 percent golf course and 10 percent stormwater detention pond. The Hub allows runoff to be routed among the HPM types (i.e., runoff from impervious could be routed to pervious, then to the detention pond, and then off site). Similarly, the demand could be routed from offsite to the detention pond, and then to the golf course. The recharge to each homecell coincident with the Hub footprint would have the area-weighted average recharge of all landuse types in the Hub.

Although the volume of water calculated for runoff, recharge or water supply may be affected by the cell head, the HPMs are not a direct function of the cells heads and are not directly coupled to the cell heads.

2.7 Assembly of all Waterbodies

The equation of mass balance in integral form written for one control volume is:

$$\frac{\partial}{\partial t}\int_{cv} d\mathcal{V} = -\int_{cs} (\mathbf{E}\cdot\mathbf{n})\, dA \tag{2.43}$$

This can be written for all the finite volume cells in vector form as:

$$\mathbf{A}(\mathbf{H})\cdot\frac{d\mathbf{H}}{dt} = \mathbf{q_s}\cdot(\mathbf{H}) + \mathbf{S}(\mathbf{H}) \tag{2.44}$$

in which $\mathbf{H} = [H_1, H_2, \ldots H_m \ldots H_{wb}]^T$ = a vector containing average heads in all cells, segments and lakes in some recognizable order; $\mathbf{q_s}(\mathbf{H}) = [q_{s1}(\mathbf{H}), q_{s2}(\mathbf{H}), \ldots q_{s-wb}(\mathbf{H})]^T$; $q_{si}(\mathbf{H})$ = vector containing the summation of flow entering waterbody described in Equation 2.21; $\mathbf{S}(\mathbf{H})$ = the source term in vector form; $\mathbf{A}(\mathbf{H})$ = a diagonal matrix whose elements $A(m,m)$ are the effective cell areas A_m in the case of a cell m described in Equation 2.13; $\mathbf{S}(\mathbf{H})$ = vector containing all source terms or non-gradient driven fluxes. $\mathbf{q_s}(\mathbf{H})$ can be linearized using:

$$\mathbf{q_s}(\mathbf{H}) = \mathbf{M}(\mathbf{H})\cdot\mathbf{H} \tag{2.45}$$

in which $\mathbf{q_s}(\mathbf{H})$ is constructed by adding the subvectors $\mathbf{q}(\mathbf{H})$ in Equation 2.29; $\mathbf{M}(\mathbf{H})$ = global flow resistance matrix made up by summing submatrices $\mathbf{M'}(\mathbf{H})$. The computational procedure begins by populating matrix $\mathbf{M}$ and assembling flow resistance expressions across watermovers.

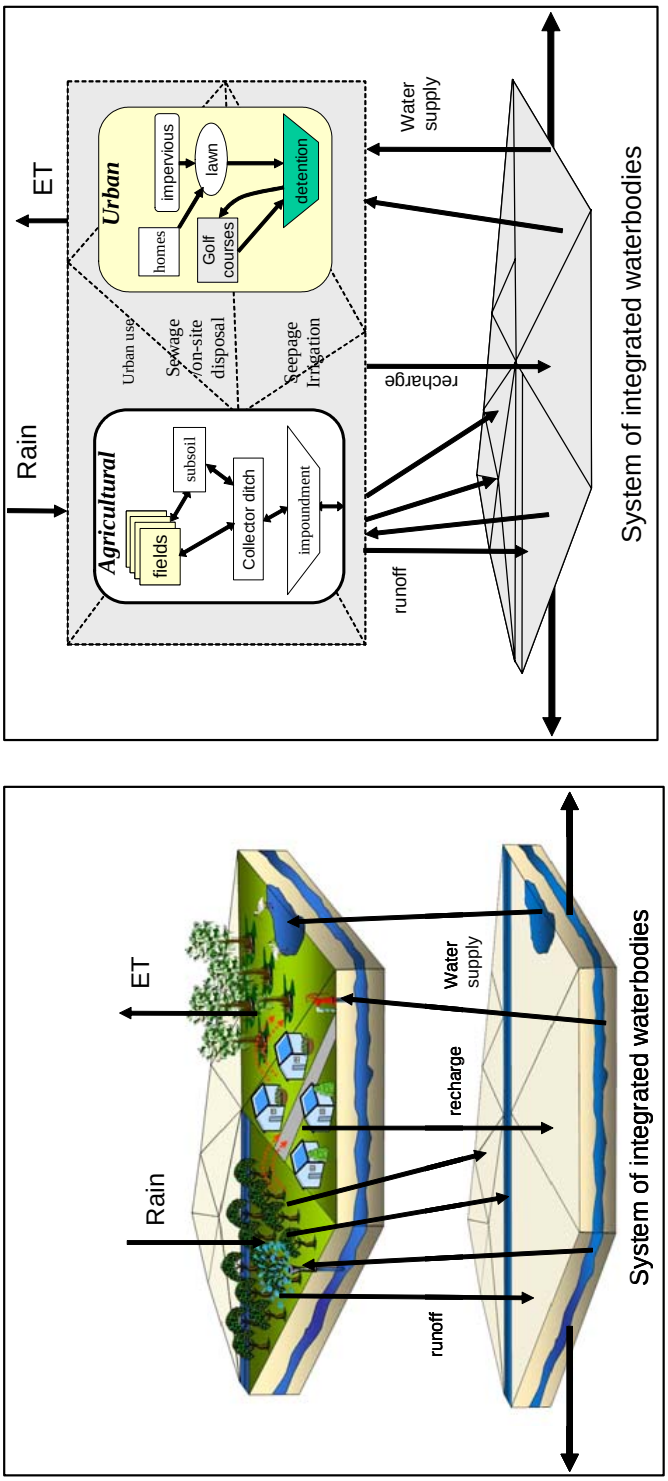

Figure 2.12: *Hub Hydrologic Process Module with multiple internal HPMs includes soil water storage and stormwater storage. The Hub may cover one or many mesh cells.*

2.8 Numerical Solution using the Weighted Implicit Method

The ordinary differential Equation 2.44 derived using the finite volume method is solved by using the following weighted finite difference formulation:

$$A_i\ H_i^{n+1} = A_i\ H_i^n + \Delta t[\alpha q_{si}^{n+1} + (1-\alpha)q_{si}^n] + \Delta t[\alpha S_i^{n+1} + (1-\alpha)S_i^n] \tag{2.46}$$

in which H_i^n = average surface water level in cell i at time step n; α = time weighting factor; $\alpha = 0$ and 1 for explicit and implicit problems, respectively. Using linearization in Equation 2.45, Equation 2.46 can be expressed as the following system of linear equations:

$$\begin{aligned}[\mathbf{A} - \alpha\Delta t\mathbf{M}^{n+1}] \cdot \Delta\mathbf{H} = \Delta t[\mathbf{M}^n] \cdot \mathbf{H}^n + \Delta t(1-\alpha)[\mathbf{M}^n - \mathbf{M}^{n+1}] \cdot \mathbf{H}^n \\ +\Delta t[\alpha\mathbf{S}^{n+1} + (1-\alpha)\mathbf{S}^n]\end{aligned} \tag{2.47}$$

Here, $\mathbf{q}_s^n = \mathbf{M}(\mathbf{H})^n \cdot \mathbf{H}^n$. The matrix $[\mathbf{A} - \alpha\Delta t\mathbf{M}^{n+1}]$ is symmetric. In many gradually varying problems $\mathbf{M}^{n+1}$ is replaced with $\mathbf{M}^n$ to simplify Equation 2.47 (Akan and Yen, 1981). Test runs show that this is a useful procedure for many problems. If this assumption is not made then $\mathbf{M}^{n+1}$ must be updated by using an iterative procedure within the time step, by first computing $\Delta\mathbf{H}$ using Equation 2.47 with the most recent estimates of $\mathbf{M}^{n+1}$, and next updating $\mathbf{H}^{n+1}$. Iterations are continued similarly by updating $\mathbf{M}^{n+1}$ and using Equation 2.47 until convergence. Akan and Yen (1981) show that only two to four iterations were required for convergence of the water level up to four significant digits. This type of iteration was not used in the current application. In other words, the second term on the right hand side of Equation 2.47 is neglected. Even without this assumption, this term gets cancelled when $\alpha = 1$. If $\mathbf{S}$ is independent or weakly dependent on $\mathbf{H}$, then the approximation $\mathbf{S}^n = \mathbf{S}^{n+1}$ is valid, and iterations within the same time step can be avoided.

Matrix $\mathbf{P}$ is sparse for large problems. For example, the element density is less than 1% for a one thousand cell discretization.

The solution of Equation 2.47 is sensitive to the α, values used;α is a time weighting factor. When $\alpha = 0$, $\Delta\mathbf{H}$ can be computed by using a simple matrix multiplication. An α of 0.5 gives higher accuracy similar to Crank-Nicholson type schemes. For most models, α is assumed to be in the range 0.6-0.8. For most integrated models, it is close to 1.0 when nonlinearities are severe and the model show signs of instability. Figure 2.13 shows a sketch of the space-time diagram in the computational domain of the RSM. The figure shows the space and time discretizations, and the types of interactions a single cell will have with its neighbors.

The implicit solution method takes into account the water balance in all the waterbodies during the time interval between times t^n and t^{n+1}. Knowing the volumes of water $\mathbf{V}(\mathbf{H}^n) = \mathbf{f_{sv}}(\mathbf{H}^n)$ at time step t^n and $\Delta\mathbf{H}$, it is possible to compute $\mathbf{V}^{n+1}$ using

$$\mathbf{V^{n+1}} = \mathbf{V^n} + \mathbf{A} \cdot \Delta\mathbf{H} \tag{2.48}$$

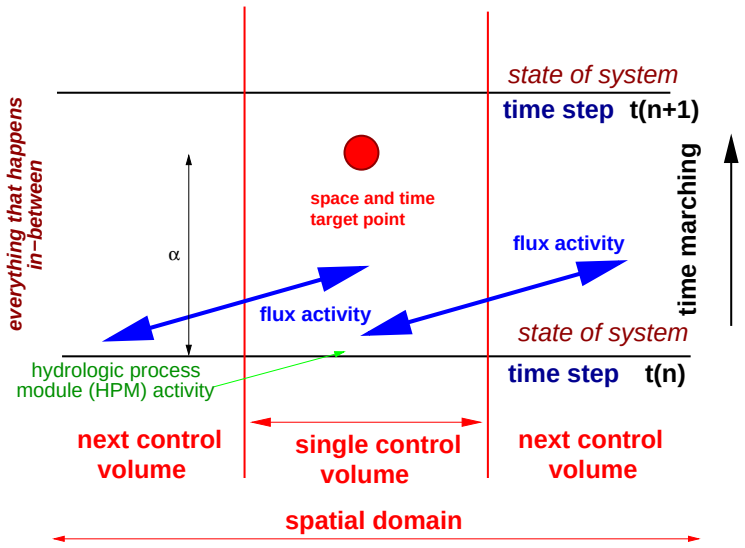

Figure 2.13: *Computational space-time space of RSM*

The new heads $\mathbf{H^{n+1}}$ at time step $n+1$ are computed using the storage-volume relationship $\mathbf{H^{n+1}} = \mathbf{f_{vs}}(\mathbf{V^{n+1}})$. Heads are used in the model only to compute the hydraulic driving forces in the watermovers. Except during this conversion, the model equations can be explained as a system of mass balance equations.

Figure 2.14 shows the basic steps involved in the initialization and the time progression within the RSM. The actual number of steps involved is much larger with many more initialization processes. The figure only shows the steps involved mainly for the finite volume calculations.

2.8.1 Average Water Velocity

The average water velocity in a cell is computed by using the following vector basis function developed for RT0 mixed elements of Raviart and Thomas (1977), and used by Cordes and Putti (1996):

$$\vec{v} = \frac{1}{2A\ h}\left[Q_{r1}\begin{pmatrix} x-\hat{x_1} \\ y-\hat{y_1}\end{pmatrix} + Q_{r2}\begin{pmatrix} x-\hat{x_2} \\ y-\hat{y_2}\end{pmatrix} + Q_{r3}\begin{pmatrix} x-\hat{x_3} \\ y-\hat{y_3}\end{pmatrix}\right] = -K\nabla H \qquad (2.49)$$

in which Q_{r1}, Q_{r2}, Q_{r3} = discharge rates across cell walls $r1, r2$ and $r3$ counting outward as positive; $(\hat{x_i}, \hat{y_i})$ = the coordinates of the nodes; (x, y) = coordinates of any point, including the circumcenter in the current case at which the head is computed. In the case of right-angled triangles, /citePutti:1996 showed that the mixed finite element method is equivalent

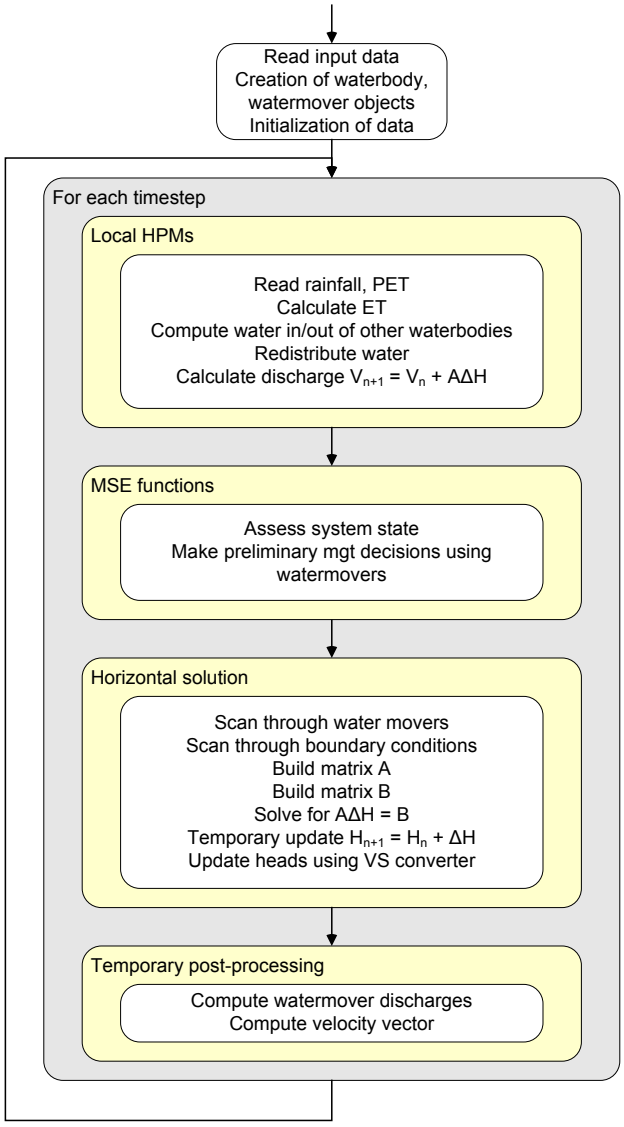

Figure 2.14: *A simplified flowchart of RSM computational steps*

to a finite difference method.

The HPMs are one set of process modules linked to the HSE. Other modules include Water Quality Process Modules (WQPM) and Ecological Process Modules (EPM). The WQPMs use the flow solution from the HSE to provide advective flow for the biogeochemial processes modeled in the WQPMs. EPMs are being developed to simulate landscape and habitat processes that use the hydrology from the HSE to drive functional changes in the environment.

Chapter 3

Management Simulation Engine Theory and Concepts

The HSE provides a highly efficient and flexible computation engine capable of simulating a diverse spectrum of hydrologic and hydraulic conditions. These capabilities include the simulation of coupled streamflow (canal) networks and ground/surface water flows, which can be passively controlled by free-flowing structures such as weirs, spillways, and culverts. However, in many real world applications, there is imposed a complex hierarchy of water resource operational policies dependent on actuarial imposition of flow constraints on actively controlled flow structures. To provide for simulation of such complex, highly interrelated (coupled) water resource management schemes within the framework of the RSM, a management module has been carefully designed and incorporated into the RSM.

The management module of the RSM is the Management Simulation Engine (MSE). The MSE consists of a multi-level hierarchical control scheme, which naturally encompasses the local control of hydraulic structures, as well as the coordinated sub-regional and regional control of multiple structures. MSE emphasizes the decoupling of hydrologic state information from the managerial decision algorithms, facilitating the interoperation and compatibility of diverse management algorithms and providing flexibility to adapt a model implementation to swiftly changing operational policies on the ground. The MSE is intended to allow a flexible, extensible expression of a wide variety of anthropogenic water resource control schemes integrated with the hydrologic state evaluations of the RSM. Synergy between the multilayer control hierarchy and decoupled hydrologic state and management information facilitates a water resource management feature set not typical of integrated hydrologic models.

The MSE design is based on the principle that operational and managerial decisions applied to water control structures can be viewed as information processing algorithms decoupled from the hydrologic state information on which they operate. Essentially, the HSE provides hydrologic and hydraulic state information, while external policies that dictate

managerial constraints and objectives are applied through MSE controllers and supervisors.

In cases where discrete spatiotemporal model inputs are sufficient for controller and supervisor algorithms, the MSE accepts inputs directly from HSE data monitors. However, in cases where integrated spatiotemporal state information, or aggregated state information based on specific pre-processing is required, the MSE is able to store and access information in the MSE Network.

The MSE network is an abstraction of reservoirs, streams and canals (waterbodies), together with a stream/canal flow network and water control structures (watermovers) dedicated to representing the managerial architecture of the model.

3.1 MSE Concepts

MSE is an integral component of the RSM, and provides two modes of functionality in the analysis and prediction of water control structure operational behaviors:

1. Simulate existing water resource policies through assessment of currently implemented management operational policies and rules in response to hydrologic forcing (e.g., rain, ET)
2. Develop alternative resource control strategies through the optimization of operational policies and rules

The first mode is a critical capability for the assessment of water control operations in response to historic, real-time, or forecast forcing conditions. The second mode forms an important analysis tool aimed at identification of alternative operational policies which must perform complex, multi-variate, resource allocation functions under the control of system boundary conditions and constraints. The MSE is formulated to address both of these needs by incorporating a variety of supervisory control algorithms including rule-based expert systems, finite state-machine processors, as well as a generic mathematical programming language interface, which provides access to a suite of state-of-the-art optimization algorithms (Park et al., 2005).

The MSE is therefore capable of addressing specific water resource allocation analysis, for example:

- Enable water resource reallocation in response to competing demands during a water shortage
- Diminish flow/containment problems during flood situations

- Consider downstream needs for water supply

From a functional perspective, the MSE is essentially an information filter tasked with the imposition of flow constraints on model water control structures. This is accomplished within the framework of the RSM in three coupled operations: data gathering, data processing and decision making, and decision application, as represented in Figure 3.1. An overview of each of these areas relevant to their implementation in the MSE is discussed in the following sections.

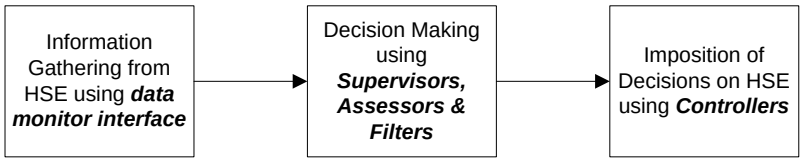

Figure 3.1: *Functions of the Management Simulation Engine*

3.2 Information Gathering from HSE

All hydrologic and hydraulic state information including water stages, flow values, rainfall, ET, hydrologic boundary conditions, or any other state variable used as input or computed as output by the HSE is available to the MSE and the assessors through the implementation of a uniform data monitor interface. The data monitor interface extends naturally to the MSE input/output variables. Therefore, the input state information available to a controller or a supervisor is not limited to water levels or flow values, but can include control information, decision variables, constraints or any other management variable from any other controller or supervisor in the model.

A central feature of the MSE, which enables decoupling of the hydrologic state information maintained by the HSE and the operational process information of the MSE, is the MSE network (Figure 3.2). This network is based on a standard graph theory representation of a flow network comprised of arcs and nodes (Ahuja et al., 1993; Ford and Fulkerson, 1962). The MSE network also provides a mathematical representation of a constrained, interconnected flow network, which facilitates the efficient graph theory solution of network connectivity and flow algorithms.

From the hydrologic perspective, the HSE canal network is composed of an interconnected network of segments, with each segment maintaining parameters relevant to aquifer-

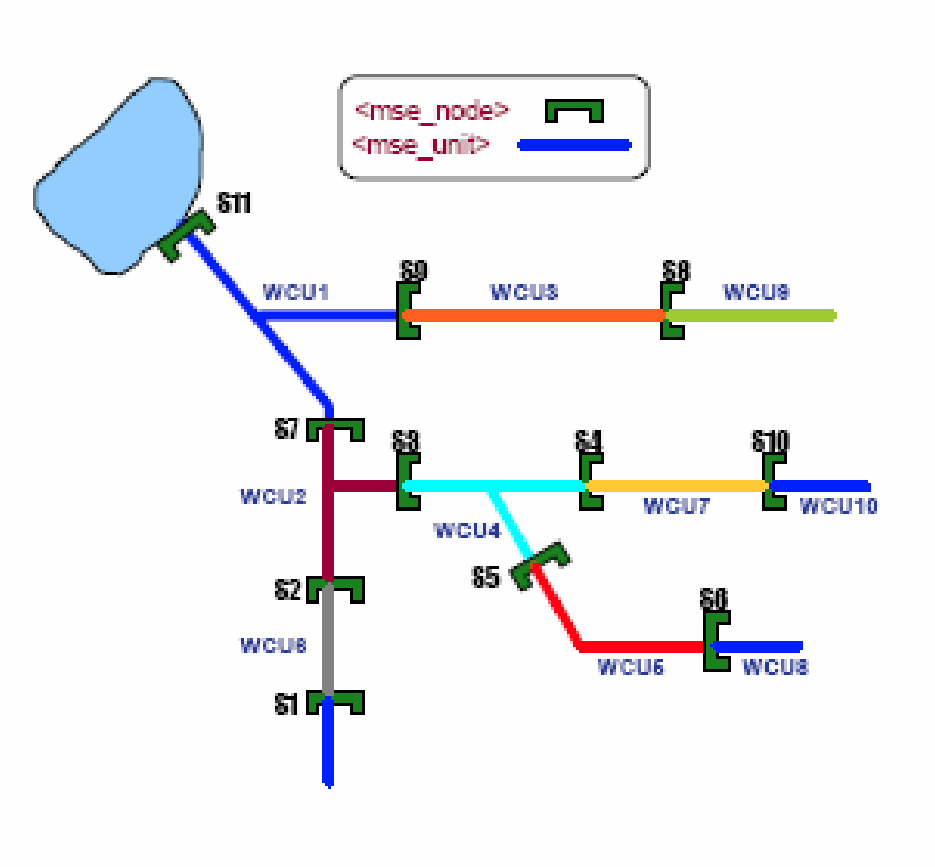

Figure 3.2: *The MSE network structure*

stream interaction, flow resistance, spatial coordinates and other physical properties (Figure 3.3). The spatial representation of HSE segments is typically dictated by topographic and physical parameters. From the water resource management viewpoint of the MSE, the important features of the flow network are its connectivity, flow capacities, flow regulation structures, and assessed state information relevant to managed sections of the network. The MSE network maintains a mapping between these two representations (Figure 3.4).

The primary data object in the MSE network is the water control unit (WCU). A WCU maps a collection of HSE canal segments that are operationally managed as a discrete entity to an arc in the MSE network. WCUs are created from associated collections of these HSE arcs. WCUs are typically bounded by hydraulic control structures, which are represented as nodes in the MSE network. Each WCU includes associative references to all inlet and outlet hydraulic flow nodes.

The MSE network data objects serve as state and process information repositories for management processes. They maintain assessed and filtered state information, provide pa-

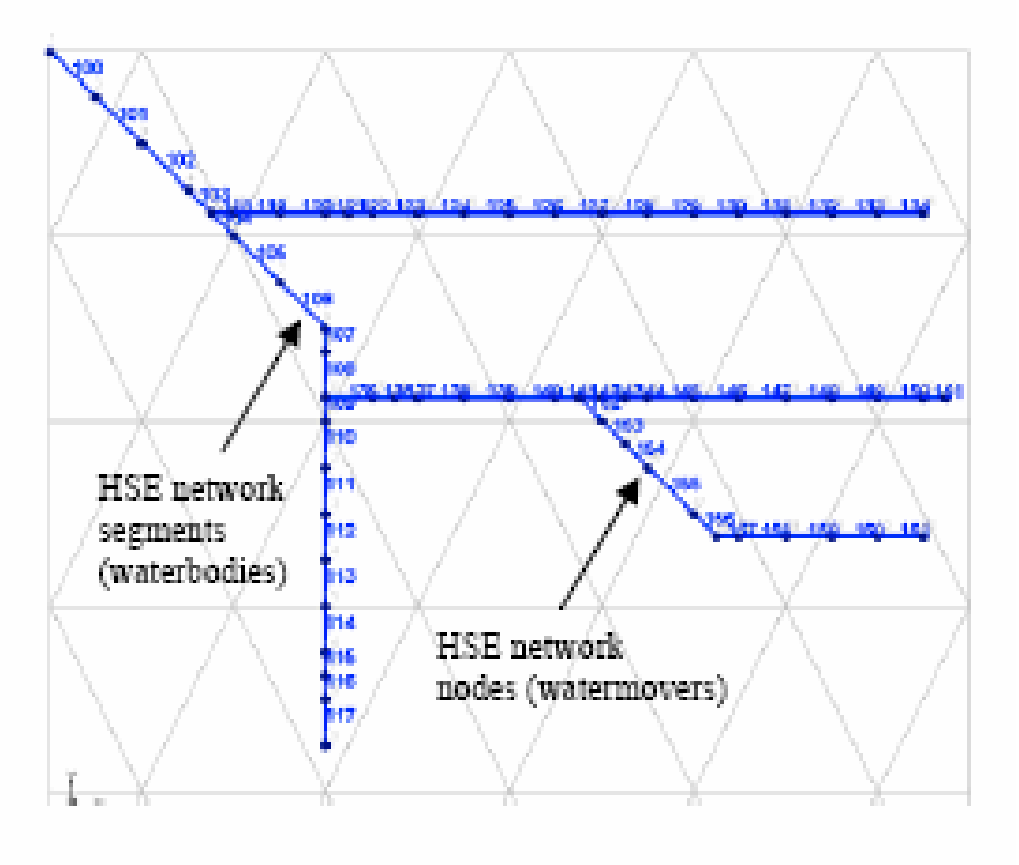

Figure 3.3: *The HSE network structure*

rameter storage relevant to a water control unit (WCU) or hydraulic structure managerial constraints and variables, and serve as an integrated data source for any MSE algorithm seeking current state information. Some variables stored in a structure (node) object include:

- current flow capacity of a physical structure
- maximum design flow capacity of a physical structure
- reference to hydraulic watermover(s) in HSE
- reference to structure controller(s) in MSE
- operational policy/rule water levels
- water supply
- water demands

The WCU objects incorporate:

- time-varying or seasonal stage maintenance levels
- flood control stage maintenance levels
- inlet flow
- outlet flow
- water volume

Each WCU in the MSE network is referenced by a unique label, and has an associative data storage object which dynamically allocates storage for assessment results. This allows multiple, independent assessments of the WCU state. For example, one assessment of WCU inlet structure flows might come from a graph algorithm, while another could be obtained from a LP model.

This abstraction from hydrologic objects to managerial objects condenses the network representation facilitating the organization and storage of relevant assessed state and process information. As an example, Figure 3.3 depicts an HSE canal network consisting of 63 nodes

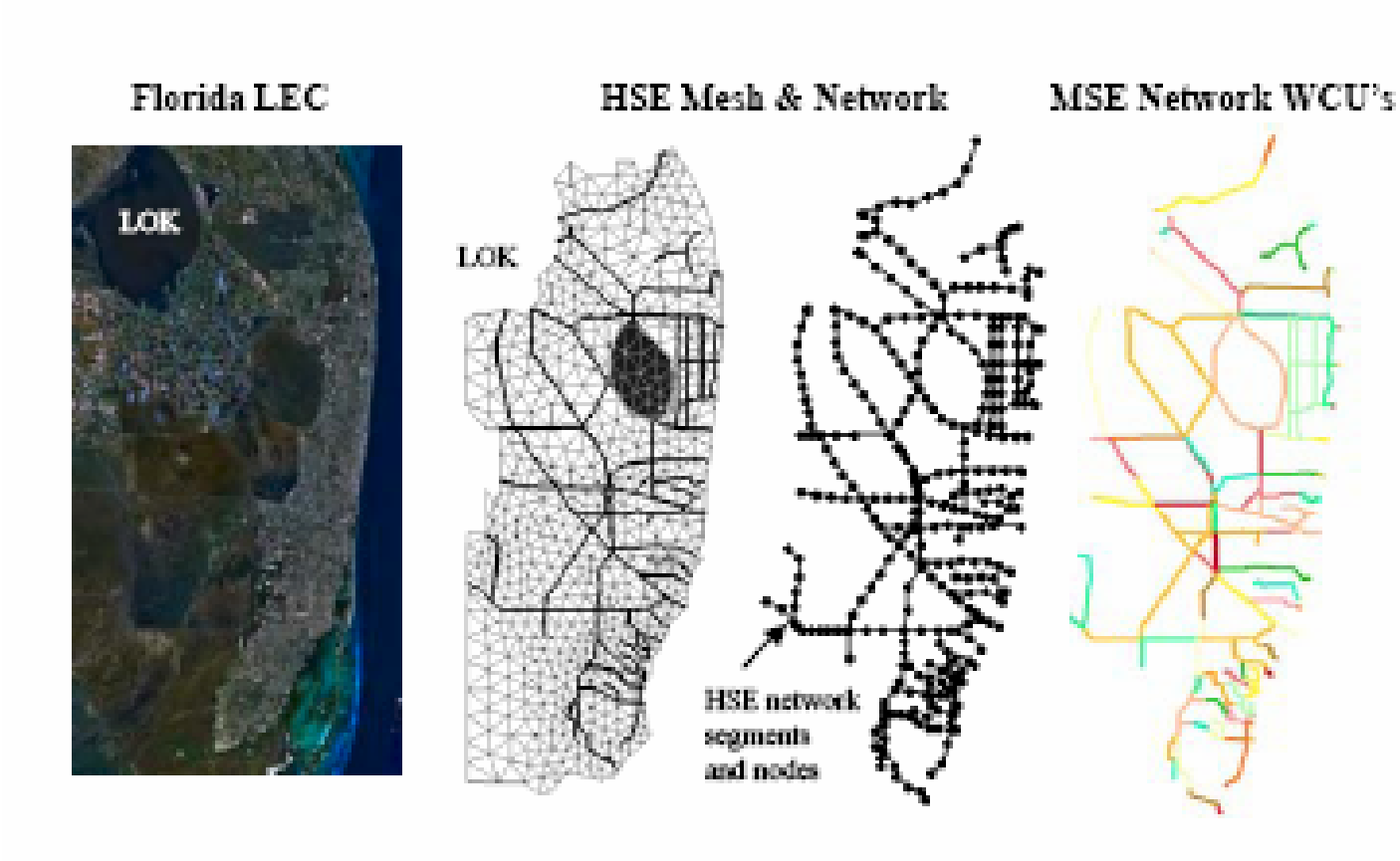

Figure 3.4: *Schematic comparison of HSE and M SE network structures*

and 62 segments. Some of the nodes correspond to locations of hydraulic control structures, though the association is not apparent from examination of the HSE network. Each canal segment has a unique identifier which allows the modeler or MSE processor to monitor state information of the segment. However, it may be appropriate to make water management decisions based on some assessed or filtered version of aggregated canal segment states.

Consider now an abstraction of the HSE network into 10 WCUs, regulated by 11 hydraulic structures, as shown in Figure 3.2. In the MSE network each line segment represents a WCU, while each node represents a hydraulic structure which regulates a WCU. The modeler or MSE processor is able to directly monitor information stored in any of these object data containers, information which has already been assessed and automatically stored in the appropriate WCU data object at each timestep.

As with other RSM model inputs, the WCU mapping from the HSE canal network is performed with an input XML entry.

3.3 Decision Making: Supervisors, Assessors

The MSE architecture is based on a multilayered hierarchy, with individual water control structures regulated by controllers while the regional coordination and interoperation of controllers is imposed by supervisors. Supervisors can change the functional behavior of controllers, completely switch control algorithms for a structure, or override the controller output based on integrated state information and/or rules. A schematic depiction of the HSE-MSE layered hierarchy is shown in Figure 3.5.

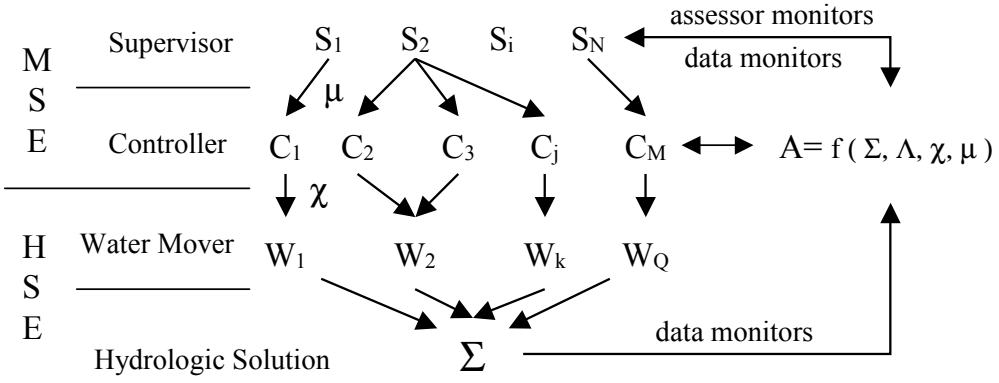

Figure 3.5: *RSM multilayer control hierarchy*

At the lowest layer is the hydrologic state information ($\sum$) computed by the HSE. This

information includes water stages, flow values, rainfall, ET, hydrologic boundary conditions, or any other state variable used as input or computed as output by the HSE. All such variables are made available to the MSE and assessors through the implementation of a uniform data monitor interface. This transparency of state and process information throughout the model is central to the efficient synthesis and processing of heterogeneous information required to simplify and naturally express complex water management policies.

The top level of the MSE is the supervisory layer. There is no limit on the number of supervisory algorithms, or constraint on the number of controllers that a supervisor may influence. Based on state and process information, which optionally may have been filtered or assessed, the function of a supervisor is to produce the supervisory control signal (μ) for a single, or collection of, hydraulic structure controllers. The supervisors are therefore able to comprehensively coordinate the global behavior of multiple independent or coupled hydraulic structures.

3.3.1 MSE Supervisors

An MSE supervisor is effectively a meta-controller, a controller of controllers. The addition of this supervisory layer considerably simplifies the control expression of multiple, coordinated hydraulic structures. In addition to the organizational simplification of control algorithms, the additional layer enables representation of management functions which are not realizable with a single control layer.

In relation to the controllers, which are multi-input single-output (MISO) processors, the supervisors are multi-input multi-output (MIMO) processors. Supervisors have the ability to change individual response characteristics of controllers, or, in the case of multiple controllers attached to a watermover, to dynamically select and activate a specific controller for any watermover. Specifically, the supervisory functions include:

- Comprehensive assessment of state and process information
- Controlling multiple parameters of multiple controllers
- Dynamic switching of multiple controllers
- Flow regulation override for controller(s)

Supervisors can therefore change the functional behavior of controllers, completely switch control algorithms for a structure, or override a controller output based on integrated state information and/or rules.

There is no practical limit on the number of supervisors allowed in a model, or on the number of controllers that a supervisor may affect. It is common to have a hybrid selection of different supervisors, each one regulating a specific sub-regional collection of hydraulic

structures. The ability to selectively tailor management control algorithms, as well as the flexibility to easily reconfigure them in a plug-and-play fashion lends considerable power to the implementation of diverse and complex operational management scenarios.

The current suite of supervisors includes:

- Fuzzy rule based
- GLPK Linear Programming (GNU Linear Programming Kit)
- Finite state machine (user defined)
- Graph flow algorithms
- Heuristic assessors to capture special operations for a particular modeled area

These supervisors are discussed in more detail in South Florida Water Management District (2005).

3.3.2 Assessors and Filters

In the RSM, state and process information can be functionally transformed by an independent set of filters, which can be viewed as information pre-processors. These processors are denoted as assessors and filters. For example, an assessor may perform statistical filtering such as spatiotemporal expectations, amplitude or time-delay modulation, or any other suitable data filtering operation. The MSE is then tasked with appropriately processing the assessed state information to produce water management control signals, which are applied to the hydraulic control structures to satisfy the desired constraints and objectives.

The role of assessors in the MSE is to perform data preprocessing required for operational control decisions. By decoupling the conditioning and filtering of state and process information from the decision making algorithms, the decision processors can be simplified and modularized. Therefore, an assessor is an information processor intended to provide specialized aggregation or differentiation of state variables particular to a managerial decision process. The suite of assessors provides for specialized quantification of hydrologic state variables freeing managerial algorithms from data preprocessing.

Related to the assessors are MSE filters. Filters are generic information processors implemented to perform simple, often redundant data filtering operations. The RSM implements a unified design approach and interface for monitors, filters, and assessors based on object-oriented design principles. As a result, the interfacing of these constructs from the users perspective is particularly simple and powerful. Assessor, filters and monitors can operate in a piped FIFO (first-in, first-out) fashion.

3.4 Imposition of Decisions on HSE: Controllers

3.4.1 MSE Controllers

The MSE controllers are the intermediary between the hydraulic structures (watermovers) and the regional-scale supervisory coordinators. The controllers can operate independently of the supervisors; in fact, they are not required at all for uncontrolled operation of a hydraulic structure (e.g., an uncontrolled spillway). The essential purpose of a controller is to regulate the maximum available flow through a structure to satisfy a local constraint. A controller may take as an input variable any state or process information which can be monitored within the RSM. Since the interface between a structure watermover and any controller is uniform, it is possible to change controllers dynamically with a supervisory command, or manually with a simple XML input change. The unitary interface also allows for the modeler to mix and match controllers in a particular model application so that the local control schemes are a hybridization of any of the available control algorithms.

At each model time step, once the controllers have computed their respective control values, these signals are applied as flow constraints to the structure watermovers in the HSE. Each watermover will compute a maximum flow capacity based on the hydrologic state conditions and hydraulic transfer function of the structure. The resultant controlled flow will be some fraction of the currently available maximum flow capacity. The current suite of controller modules includes:

- One- and two-dimensional rulecurves
- Piecewise linear transfer function
- Proportional Integral Derivative (PID) feedback control
- Sigmoid Activated Proportional Integral (PI) feedback control
- Fuzzy control
- User-defined finite state machine

The controllers available for a specific model implementation are specified in the controller section of the XML model input file. Documentation, specifications and example usage of controllers are specified in the RSM Management Simulation Engine User Manual (South Florida Water Management District, 2005) and Park (2005).

Bibliography

Abbott, M., J. Bathurst, J. Cunge, P. O'Connell, and R. Rasmussen (1986a). An introduction to the European Hydrological System, "System Hydrologique European", (SHE), 1: A structure of a physically based, distributed modeling system. *Journal of Hydrology 87*, 61–77.

Abbott, M., J. Bathurst, J. Cunge, P. O'Connell, and R. Rasmussen (1986b). An introduction to the European Hydrological System, "System Hydrologique European", (SHE), 2: History and philosophy of a physically based, distributed modeling system. *Journal of Hydrology 87*, 45–59.

Ahuja, R., T. Magnanti, and J. Orlin (1993). *Network Flows: Theory, Algorithms, and Applications*. Prentice Hall.

Akan, O. and B. C. Yen (1981, April). Diffusion-wave flood routing in channel networks. *ASCE Journal of Hydraulics Division 107*(6), 719–732.

Balay, S., W. Gropp, D. Kushik, L. McInnes, and B. Smith (2001). *(PETSC) Users Manual, ANL-95/11 - Revision 2.1.3*. Argonne, Illinois: Argonne National Laboratory.

Bosak, J. and T. Bray (1999, May). XML and the second generation web. *Scientific American*, 89–93. http://fox.rollins.edu/ tlairson/ecom/xmlsciam.html.

Brion, L., S. Senarath, and A. Lal (2000, Dec 11-15). Concepts and algorithms for an integrated surface water/groundwater model for natural areas and their applications. In *Greater Everglades Ecosystem Restoration (GEER) Conference*, Naples, Florida.

Brion, L., S. Senarath, A. M. W. Lal, and M. Belnap (2001, May 20-24). Application of the South Florida Regional Simulation Model in the Southern Everglades. In B. K. Panigrahi (Ed.), *Proceedings of the Specialty Symposium Held in Conjunction With the World Water and Environmental Resources Congress*, 1801 Alexander Bell Drive, Reston, Virginia 20191-4400, pp. p. 110. Environmental and Water Resources Institute of ASCE: American Society of Civil Engineers.

Chow, V., D. Maidment, and L. Mays (1988). *Applied Hydrology*. New York, NY: McGraw-Hill Book Company.

Cordes, C. and M. Putti (1996). Triangular mixed finite elements versus the finite volumes in groundwater modeling. In A. A. et al. (Ed.), *Int. Conf. Comp. Meth. Water Res. XII*, Southampton, London, pp. 61–68. Computational Mechanics.

Cunningham, K. J., J. L. Carlson, G. L. Wingard, E. Robinson, and M. A. Wacker (2004). Characterization of aquifer heterogenity using cyclostratigraphy and geophysical method in the upper part of the karstic Biscayne aquifer, southeastern Florida. Water Resources Investigations Report 03-4208, United States Geological Survey.

Fan, A. (1986). A routing model for the upper Kissimmee chain of lakes. Technical Publication 86-5, South Florida Water Management District, West Palm Beach, FL.

Flaig, E., R. VanZee, and W. Lal (2005). Hydrologic process modules of the regional simulation model: An overview. HSE White Paper.

Ford, L. and D. Fulkerson (1962). *Flows in Networks*. Princeton University Press.

Goode, D. and C. Appel (1992). Finite-difference interblock transmissivity for unconfined aquifers and for aquifers having smoothly varying transmissivity. Water-resources investigations report 92-4124, United States Geological Survey. 79 p.

Gupta, A., G. Karypis, and V. Kumar (1997). Highly scalable parallel algorithms for sparse matrix factorization. *IEEE Trans. Parallel Distrib. Syst. 8*(5), 502–520.

Hirsch, C. (1989). *Numerical Computation of Internal and External Flows, Computational Methods for Inviscid and Viscous Flows*. Wiley Series in Numerical Methods in Engineering. New York: Wiley.

Hromadka II, T., R. McCuen, and C. Yen (1987). Comparison of overland flow hydrograph models. *Journal of Hydrologic Research, ASCE 113*(11), 1422–1440.

HydroGeoLogic (2000). *MODFLOW-HMS: A Comprehensive MODFLOW-Based Hydrologic Modeling System: Software Documentation*. Herndon, Virginia: HydroGeoLogic, Inc.

Kadlec, R. H. and R. L. Knight (1996). *Treatment Wetlands*. Boca Raton, Florida: Lewis Publishers.

Lal, A. M. W. (1995). Calibration of riverbed roughness. *Journal of Hydraulic Engineering, ASCE 121*(9), 664–671. http://www.sfwmd.gov/org/pld/hsm/pubs/wlal/calib_jo.pdf.

Lal, A. M. W. (1998a, April). Performance comparison of overland flow algorithms. *Journal of Hydraulic Engineering, ASCE 124*(4), 342–349. http://www.sfwmd.gov/org/pld/hsm/pubs/wlal/alg_pap2.pdf.

Lal, A. M. W. (1998b, August 3-7). Simulation of overland and groundwater flow in the Everglades National Park. In *Proceedings of the International Water Resources Engineering Conference*, Memphis, Tennessee, pp. 610–615. http://www.sfwmd.gov/org/pld/hsm/pubs/wlal/abs_tenn1.pdf.

Lal, A. M. W. (1998c, September). Weighted implicit finite-volume model for overland flow. *Journal of Hydraulic Engineering, ASCE 124*(9), 941–950. http://www.sfwmd.gov/org/pld/hsm/pubs/wlal/poly.pdf.

Lal, A. M. W. (2000). Numerical errors in groundwater and overland flow models. *Water Resources Research 36*(5), 1237–1247. http://www.sfwmd.gov/org/pld/hsm/pubs/wlal/gw_err.pdf.

Lal, A. M. W. (2001, May 20-24). Selection of time step and grid size in modeling integrated stream-aquifer interaction. In *Proceedings of the World Environmental Congress*, Orlando, Florida. http://gwmftp.jacobs.com/Peer_Review/stream-aquifer.pdf.

Lal, A. M. W. (2005). Determination of aquifer parameters using generated water level disturbances. To be submitted to Water Resources Research.

Lal, A. M. W., R. VanZee, and M. Belnap (2005, April). Case study: Model to simulate regional flow in South Florida. *Journal of Hydraulic Engineering, ASCE 131*(4), 247–258. http://www.sfwmd.gov/org/pld/hsm/pubs/wlal/oodpaper.pdf.

Lin, S. (2003, spring). History of regional modeling in south florida. personal communication.

McDonald, M. and A. Harbaugh (1984). A modular three dimensional finite difference groundwater flow model. Technical report, United States Geological Survey, Reston, Virginia.

Menke, W. (1989). *Geophysical Data Analysis: Discrete Inverse Theory* (Revised Edition (textbook) ed.). New York: Academic Press, Inc.

Panton, R. (1984). *Incompressible flow*. New York, NY: John Wiley and Sons, Inc.

Park, J. (2005). Management Simulation Engine of the Regional Simulation Model: An overview. MSE White Paper, 50 p.

Park, J., J. Obeysekera, and R. VanZee (2005). Multilayer control hierarchy in an integrated hydrological model. *Journal of Water Resources Planning and Management, ASCE*. submitted.

Ponce, V. M., R. Li, and D. Simons (1978). Applicability of kinematic and diffusion models. *Journal of Hydrology 104*, 353–360.

Raviart, P. and J. Thomas (1977, May 15-19). A mixed finite element method for second order elliptic problems. In I. Galligani and E. Magenes (Eds.), *Mathematical aspects of the finite element method*, New Jersey. Springer-Verlag.

Schenk, O. and K. Gartner (2004, April). Solving unsymmetric sparse systems of linear equations with PARDISO. *Journal of Future Generation Computer Systems 20*(3), 475–487.

Schmidt, J. and L. Roig (1997). The adaptive hydrology (ADH) model: a flow and transport model for coupled surface water-groundwater analysis. In *XXVIIth Congress of the IAHR and ASCE*, San Francisco, California, pp. 367–372.

Senarath, S., R. Novoa, J. Barnes, and L. Brion (2001, fall). Simulating the flow dynamics in the southern everglades using a finite volume model. Abstract.

Shen, H., D. Zhao, G. Tabios III, K. Loftin, S. Sculley, and J. Chamberlain (1997). Application of RBFVM-2D model to Kissimmee River restoration in Florida State of USA. *Journal of Hydraulic Engineering, ASCE*, 474–479.

Solomantine, D. (1996). Object orientation in hydraulic modeling architecture. *Journal of Hydraulic Engineering, ASCE 10*(2), 125–135.

South Florida Water Management District (1999). *South Florida Water Management Model Primer 3.5.* 3301 Gun Club Road, West Palm Beach, FL 33406: South Florida Water Management District. http://www.sfwmd.gov/org/pld/hsm/models/sfwmm/.

South Florida Water Management District (2005). *Management Simulation Engine User Manual.* 3301 Gun Club Road, West Palm Beach, FL 33406: South Florida Water Management District.

Swain, E. and E. Wexler (1996). A coupled surface water and groundwater flow model (MODBRANCH) for simulation of stream-aquifer interaction. Techniques of water resources investigations of the USGS, United States Geological Survey, Government Printing Office, Washington D.C.

Tisdale, T. (1996). Object-oriented analysis of South Florida hydrologic systems. *Journal of Computing in Civil Engineering 10*(4), 318–326.

VanderKwaak, J. (1999). Numerical simulation of flow and chemical transport in integrated surface-subsurface hydrologic systems. Ph.D. thesis, University of Waterloo, 218 pp.

Walton, R., E. Wexler, and R. Chapman (1999). An integrated groundwater-open channel flow model (MODNET). Tech. report, West Consultants, Bellevue, Washington.

Yeh, G., H. Cheng, J. Cheng, H. Lin, and W. Martin (1998). A numerical model simulating water flow and contaminant and sediment transport in a watershed system of 1-D stream-river network, 2-D overland regime, and 3-D subsurface media (WASH123D: Version 1.0). Technical report CHL-98-19 prepared for the U.S. Environmental Protection Agency, United States Army Corps of Engineers, Waterways Experiment Station.

Zhao, D., H. Shen, G. Tabios III, J. Lai, and W. Tan (1994, July). Finite-volume two-dimensional unsteady-flow model for river basins. *Journal of Hydraulic Engineering, ASCE 120*, 863–883.

Appendix A

Regional Simulation Model Philosophy

A.1 Notes on the use of models

RSM is like many other computer models in that it is built around numerical methods that solve ordinary and partial differential equations. It is also similar to other models because of the way in which flow resistance equations are incorporated among regional equations to represent a wide variety of local and regional conditions. And similar to many other recent models, the RSM simulates both natural and anthropogenic conditions.

RSM is different from many other models in that (a) it is designed with object-oriented methods, (b) provides auxiliary tools (e.g., error analysis methods) for use during both model implementation and model application, and (c) separates operations management through the MSE component. A certain level of understanding of object-oriented methods, and the basic RSM object types such as waterbodies and watermovers are required before adding new objects to the model. Numerous articles written on model application, calibration, error analysis and analytical methods should also be consulted prior to the application of the HSE (see Appendix C).

RSM is also different from many other models because of the availability of numerous MSE components such as optimal controllers and linear programming (LP) algorithms. These options provide numerous operational alternatives to influence the HSE. One should be very careful in selecting the proper operational options and the interpretation of the results if a model application is to be successful (South Florida Water Management District, 2005). Considering these factors, an RSM application can be more challenging than the application of any other model.

Being able to run the model with a data set does not say anything about the validity or the accuracy of the dataset or the output. The following checks can be helpful in assuring

that the model results are relevant.

1. The input data collected has to be for a physically meaningful problem.
2. The problem should be one that can be solved with the governing equations used in the model.
3. The hydraulic problem has to be mathematically well posed. Only well posed problems can be solved using computational procedures for partial differential equations. Proper use of initial and boundary conditions are extremely important in setting up a well-posed problem. See Abbott (1982) or any other similar text for well-posedness.
4. Consider the fact that the model is built upon governing equations that are initial-boundary value problems. This means that the solution at any time and space depends on both initial and boundary conditions. On one hand if the dependency does not exist, the problem is not a well- posed problem, and the model results are meaningless. Similarly, if the model is based on faulty initial and boundary conditions, the results have to be considered suspect depending on the severity of the dependence.
5. Select the time and cell size for the discretization based on Lal (2000) (see Appendix C), Lal (2001) or any other similar study on numerical error analysis. The accuracy of the solution is limited by the conditions stipulated in these documents.
6. Follow acceptable calibration procedures, and check if the correlation coefficient and other indicators between the observed and simulated time series data is reasonable. Tools based on generalized inverse solution using Singular Value Decomposition (SVD), and conjugate gradient methods (Lal, 1995) are being created to calculate uncertainty and covariance matrices for models. These estimates can be used to evaluate model parameter uncertainty in a limited way (Menke, 1989).
7. If the model discharges are to be accurate, ensure that boundary condition discharges used as inputs to the model are accurate as well (i.e., calibrate to flows).
8. Check if the overall mass balance conditions in the model are within reasonable (<10%) limits. This still does not guarantee that there are no local numerical errors.

If *at least one* of the above conditions is violated, the model is not usable under general conditions. The model may however be usable for certain regions on a limited basis if it can be scientifically justified.

During the interpretation of model results, one should consider that the regional results from the PDEs are valid only on areas larger than the size of the cells or the segments. If an imaginary Fourier sine component is used to describe this spatial extent, results are accurate only over areas covering multiple cells as described by Lal (2000) in Appendix C. For example, a model grid resolution of one by one mile, is adequate to resolve hydlorogic features that may extend as much as three to four miles. However, the opposite is not true.

A.2 Scope of the RSM

The scope of the RSM has broadened over the years to be much more than a new integrated hydrologic model or a replacement for the SFWMM. The model and the model development process both benefitted from years of model development experience in South Florida. RSM is designed to accomplish a number of philosophical goals including the following:

1. **Provide a common hydraulic and hydrologic base for a variety of other disciplines.** Many South Florida ecosystem studies use a variety of hydrologic models to understand the underlying hydrology. RSM provides a common hydrology solution that can be used in the comparison of certain ecosystem solutions.

2. **Open architecture.** RSM is designed with an open architecture in the model structure so that the model can grow and evolve as needed for a reasonable period of time without having to abandon the entire model. The RSM OO architecture also allows for an assortment of similar tools to be supported and maintained while legacy tools are discontinued or revitalized. New watermovers can be added, new management operations can be added, and entirely new capabilities can be plugged in to the system without impacting existing model functions.

3. **Open and broad participation.** The intent of open and broad participation is to allow for many developers from multiple agencies and disciplines to contribute to the development process. One of the primary goals in having a regional simulation model (RSM) is to promote scientific discipline under a single umbrella. This openness is intended to bring state-of-the-art science into the model. The RSM project allows a large number of scientists to come together and create tools that encapsulate the expertise of each of the disciplines at their best. The objective is to create a software suite that captures multiple areas of expertise under one software architecture. Since the model is developed with many common hydrologic components describing how the hydrology impacts various aspects of the ecosystem, the terms associated with describing the system have to be understood and clearly communicated between ecologists and engineers. This necessitates the development of a common terminology and a set of definitions that can eventually help in the advancement of science.

4. **Allow for alternative approaches to be tested using more than one method.** Solutions to some difficult modern day problems are non-unique. Many times there is more than one opinion about the same issue, and the old science is obsolete in the face of the new science. Since there is no "oversight authority" for science, there is potential for a "battle of the sciences" or the "lack of a science" when scientific methods are to be applied. RSM allows for alternative methods to be evaluated on a fair basis in some of the most difficult situations. For example, two different overland flow equations could be coded as separate watermovers, and their results compared to each other and

to observed data. If different watermovers successfully model system performance in different areas of the model, they can all be used where they are best suited.

5. **Avoiding problems arising from proprietary source code.** RSM is developed with the intention of minimizing problems that arise due to proprietary source code. Since the numerical solutions depend on the algorithms which are in the source code, not knowing the source code is the same as not knowing the method of solution. Model results depend on the algorithms and therefore algorithms have to be known in understanding and interpreting model results. RSM code is open to scrutiny, and benchmarks highlight the behavior of the model. Both benchmarks and the source code are key parts of the model documentation.

6. **Standardization of methods and communication protocols.** At present, different computer models are put together using a large variety of different nonstandard methods. Even if a certain amount of this is inevitable, the ability to compare results under certain known conditions is important during model applications. With the RSM model, an attempt is made to use standard and recognized methods so that this goal can be accomplished without difficulty (e.g., use standardized and recognized methods to estimate ET across disciplines). This also encourages model developers to adopt the same terminology used by hydrologists, ecologists, systems operators and other professionals. Each of the disciplines is also expected to bring a clear understanding of definitions, scope, acceptable methods of quantification, bounds and uncertainties to the results.

7. **Fair opportunities to participate.** Anyone willing to create software modules such as hydrologic process modules (HPMs), structure flow modules, or storage volume (SV) converters should be allowed and even encouraged to do so, as long as the need and the function are scientifically justified and resources are available.

8. **Non personal ownership of science or software.** Many of the developments in environmental sciences, ecology, hydrology and even computational methods are geared toward public service, and therefore essentially non-proprietary for most purposes. The primary developers believe in the open disclosure of the true author of a certain module, and the use of scientific method falling to the original authors.

Appendix B

Governing Equations Using the Traditional Approach

B.1 Partial differential equations governing overland flow

The partial differential equation (PDE) form of the governing equations are not directly used in the RSM. It is presented here mainly because these are the equations that are traditionally used to describe shallow water behavior. They are also useful in obtaining analytical solutions that are used to verify the accuracy of the model.

Partial differential equations governing overland flow provide a depth-averaged description of flow in shallow waterbodies. These equations are commonly referred to as Saint Venant equations. They consist of a continuity equation and momentum equations. The two dimensional continuity equation for shallow water flow is

$$\frac{\partial h}{\partial t} + \frac{\partial (hu)}{\partial x} + \frac{\partial (hv)}{\partial y} - R_{rchg} + W = 0 \tag{B.1}$$

u, v	velocities in x and y directions
h	water depth
R_{rchg}	source term per unit area
W	water pumped out of the system per unit area

In a simplistic way, R_{rchg} can be computed using

$$R_{rchg} = RF - ET - q_{int} \tag{B.2}$$

RF	rainfall intensity
ET	evapotranspiration rate
q_{int}	overbank or seepage flow

The equation (B.2) in its form is simplistic because it neglects complex interactions between the components. These aspects are dealt in local hydrologic modules that process the information as explained later.

The momentum equations used in the x and y directions are

$$\frac{\partial(hu)}{\partial t} + \frac{\partial(u^2h)}{\partial x} + \frac{\partial(uvh)}{\partial y} + hg\frac{\partial(h+z)}{\partial x} + ghS_{fx} = 0 \tag{B.3}$$

$$\frac{\partial(hv)}{\partial t} + \frac{\partial(uvh)}{\partial x} + \frac{\partial(v^2h)}{\partial y} + hg\frac{\partial(h+z)}{\partial y} + ghS_{fy} = 0 \tag{B.4}$$

in which S_{fx} and S_{fy} = components of friction slopes in x and y directions. The momentum equations can be combined with the continuity equation without the source term to produce the following vector momentum equation

$$\frac{\partial \mathbf{V}}{\partial t} + \nabla(\frac{1}{2}V^2 + gH) + g\mathbf{S_f} + \mathbf{V} \times \boldsymbol{\omega} = 0 \tag{B.5}$$

in which $\boldsymbol{\omega} = \nabla \times \mathbf{V}$; $\mathbf{V} = u\mathbf{i} + v\mathbf{j}$ = velocity vector; $\mathbf{S_f}$ = friction slope vector; $H = h + z$ = water level above the datum; z = bottom elevation above datum. The steps in obtaining the equation are presented by Panton (1984). Equation (B.5) can be integrated along a stream line to obtain the commonly used energy equation. The first term in (B.5) which is the local acceleration term and the second term which is the convective acceleration term are responsible for inertia effects. The first term is neglected in slowly varying flow to obtain diffusion flow equations. If flow is irrotational, $\mathbf{V} \times \boldsymbol{\omega} = 0$ and (B.5) reduces to

$$\nabla E = -\mathbf{S_f} \tag{B.6}$$

which can also be written in terms of the x and y components as $\frac{\partial E}{\partial x} = -S_{fx}$ and $\frac{\partial E}{\partial x} = -S_{fy}$ with $E = h + z + V^2/(2g) = H + V^2/(2g)$ being the energy head above the datum. Equation (B.6) without the velocity head in E is normally used as the foundation of diffusion flow formulations (Hromadka II et al., 1987).

A general form of the Manning equation written as $V = \frac{1}{n_b}h^{\gamma}S_f^{\lambda}$ in which n_b = Manning coefficient when $\gamma = 2/3$ and $\lambda = 1/2$; $V = \sqrt{v^2 + u^2}$ = magnitude of the velocity vector. This modified form allows the use of a variety of complex flow types such as the flow in wetlands Kadlec and Knight (1996). In diffusion flow $S_f = S_n$ is assumed, in which S_n = slope of the water surface (or the energy surface when E is used) computed as $\sqrt{(\frac{\partial H}{\partial x})^2 + (\frac{\partial H}{\partial y})^2}$. Akan and Yen (1981) and Hromadka II et al. (1987) used the following equation to compute

u and v:

$$u = -\frac{T(H)}{h}\frac{\partial H}{\partial x} \tag{B.7}$$

$$v = -\frac{T(H)}{h}\frac{\partial H}{\partial y} \tag{B.8}$$

$T(H)$ can be expressed using the Manning equation for $H > z$ as

$$T(H) = \frac{1}{n_b}(H - z)^{\gamma+1} S_n^{\lambda-1} \tag{B.9}$$

in which, $S_n = Max(S_n, \delta_n)$ when $\lambda < 1$ to avoid division by zero. A value of $\delta_s \approx 10^{-13} - 10^{-7}$ is useful for most South Florida applications. Lower values are more accurate if stability does not become a problem. A value of $\lambda \approx 1$ gives laminar-like flow. It is also possible to express $T(H)$ as

$$T(H) = C(H)|S_n|^{\lambda-1} \tag{B.10}$$

where the function $C(H)$ defined as conveyance can be expresses using lookup tables if necessary. In all cases, discharge per flow width $q(H)$ is expressed as

$$q(H) = T(H)S = C(H)S^{\lambda} \tag{B.11}$$

Variable $T(H)$ is useful in linearizing and simplifying the diffusion flow equation. The continuity equation (B.1) can now be expressed, using (B.8), as

$$s_c\frac{\partial H}{\partial t} = \frac{\partial}{\partial x}T(H)\frac{\partial H}{\partial x} + \frac{\partial}{\partial y}T(H)\frac{\partial H}{\partial y} + R_{rchg} - W \tag{B.12}$$

in which s_c = storage coefficient used in sub-surface flow. In the case of overland flow, $s_c = 1$. When the velocity head is included, H in (B.12) is replaced with E, as explained earlier. The equation can be solved for both overland flow and saturated groundwater flow using many of the methods used to solve parabolic equations. The model does not use the differential form of the governing equations in (B.12).

B.2 Partial differential equations governing single layer 2-D groundwater flow

For groundwater flow under assumptions of Darcy's law, the governing equation is given by (B.12) in which $T(H)$ becomes the transmissivity of the aquifer. For an unconfined aquifer, $T(H) = k_h(H - z_b)$ where z_b = elevation at the bottom of the aquifer and k_h = hydraulic conductivity of the aquifer. For groundwater flow, transmissivity $T(H)$ can be provided as a lookup table function if necessary because of the convenience provided by object oriented programming.

B.3 Boundary conditions for 2-D flow

Unless boundary conditions are specified at infinity as in the case of Theies problem, finite domain problems need boundary conditions. Boundary conditions for overland and ground water flow can be classified as external and internal type. External boundary conditions are the boundary conditions required at the physical boundaries of the model domain.

The type of boundary conditions to be used is determined by the type of the problem, requirements of well-posedness, and the availability of data. In many instances, the latter dominates in the decision to select the type of boundary condition. If the boundary conditions type selected is not the proper type, the resulting solution will lack in well-posedness, and the solution may not be unique. In some cases, the non-uniqueness is limited to the local boundary area only.

In the case of the complete solution of the Saint Venant equations under sub-critical flow, no-flow and open boundaries are the most commonly used types. No-flow or fixed land boundaries require one boundary condition. The commonly used no-flow condition requires that the flow or the velocity normal to the wall is zero. Even if full shallow water flow equations are not solved in the model, they are described to show the complete set of conditions that would otherwise be needed.

At open boundaries of 2-D shallow water water models, two boundary conditions are required at the inflow points and one at outflow point. Under ideal conditions, flows both inside and outside the boundary have to be simulated until both the heads and discharges match from both sides. However, the most commonly used boundary condition at inflows includes a zero tangential velocity and a water level time series. If a control point is located at the upstream end, the corresponding relationship has to be used instead. The two components of water velocities can also be used as at open boundaries as the two boundary conditions. The commonly used outflow boundary condition is a specified head boundary condition. However, if the outflow is located at a control point having a structure, it is common to have the rating curve as the boundary condition.

With overland flow simulated as diffusion flow, the governing equation used is nonlinear parabolic. The boundary conditions used for overland flow are therefore similar to those used with ground water flow. With diffusion flow or ground water flow, only one boundary condition is needed at any boundary. The most common types used for groundwater are the Dirichlet and Neuman types. There are other types such as the Cauchy type made by combining the first two types.

Dirichlet type: In this type of boundary condition, the head is specified as a function of time.

Neuman type: In this type of boundary condition, the flux normal to the bounfary is prescribed with time. Impervious boundary or a no-flow boundary is a special type of this

boundary condition in which case, the normal flux is zero.

Cauchy type: This is a mixed type boundary condition, and is applied when the aquifer is close to a waterbody, and is insulated with a semi-pervious layer.

Specified head and specified flow are the most commonly used external boundary condition types.

Internal boundary conditions control flow within a model that would otherwise have natural flow. Internal boundary conditions are the conditions introduced within the model domain as a result of structures, levees, and other flow control structures. The method of defining some of the boundary conditions are the same for both external and internal boundary conditions. Boundary conditions for the finite volume method can be assigned at cell centers or cell walls. In the end, however, they have to be expressed in terms of the water levels at the cells.

B.4 Partial differential equations governing flow in canals

Gradually varied 1-D unsteady flow is explained using the depth averaged equations commonly referred to as Saint Venant equations. In the current version of the model, the inertia terms are neglected to obtain the diffusion form of the Saint Venant equations. The first of the two equations is the continuity equation.

$$\frac{\partial A}{\partial t} + \frac{\partial Q}{\partial x} + q_{int} = 0 \tag{B.13}$$

in which, x is the distance measured along the canal; A = flow cross sectional area; Q = discharge through A; q_{int} = overland flow or groundwater flow entering into the canal per unit length. Rainfall and evapotranspiration are assumed to be taking place only in the 2-D overland flow area. The second of the two equations is the momentum equations.

$$\frac{\partial Q}{\partial t} + \frac{\partial}{\partial x}\left(\beta\frac{Q^2}{A}\right) + gA(\frac{\partial H}{\partial x} + S_f) = 0 \tag{B.14}$$

in which, S_f = friction slope in x direction; H = water level; β = momentum correction coefficient. After neglecting the first three terms contributing to inertia effects, the momentum equation in reduces to $\frac{\partial H}{\partial x} = -S_f$ in which, $H = h + z$ = water level above a datum; z = bottom elevation above datum. Friction slope S_f is related to the velocity using a general form of the Manning's equation is written as $V = \frac{1}{n}R^{\gamma}S_f^{\lambda}$ in which $R = A/P$ = hydraulic radius; P = wetted canal perimeter; n = Manning's coefficient when $\gamma = 2/3$ and $\lambda = 1/2$; S_f = friction slope. Akan and Yen (1981), Hromadka II et al. (1987), and others showed that flow can be expressed in the following form using Manning's equations.

$$Q = -T(H)\frac{\partial H}{\partial x} \tag{B.15}$$

in which, $T(H)$ can be expressed for the Manning's equation as

$$T(H) = \frac{1}{n} A R^{\gamma} S_n^{\lambda-1} \tag{B.16}$$

in which, $S_n = Max(S_n, \delta)$ when $\lambda < 1$. A value of $\delta \approx 1.0 \times 10^{-10}$ is used to avoid division by zero. $T(H)$ is useful in linearizing and simplifying the diffusion flow equation. The continuity equation Equation B.13 can now be expressed using Equation B.15 as

$$\frac{\partial A}{\partial t} = \frac{\partial}{\partial x} T(H) \frac{\partial H}{\partial x} + q_{ae} \tag{B.17}$$

This equation can be solved as a non-linear diffusion equation. The finite volume method is not directly based on this differential form of the governing equations.

Appendix C

Selected Publications for Further Reading

This set of publications is intended to serve as an introduction to the theory behind RSM.

1. *Weighted implicit finite-volume model for overland flow* (Lal, 1998c) (section C.1 starting on printed page 68)

2. *Numerical errors in groundwater and overland flow models* (Lal, 2000) (section C.2 starting on printed page 107)

3. *Case study: Model to simulate regional flow in South Florida* (Lal et al., 2005) (section C.3 starting on printed page 158)

4. *Determination of aquifer parameters using generated water level disturbances* (Lal, 2005) (section C.4 starting on printed page 203)

5. *Hydrologic process modules of the Regional Simulation Model: An overview* (Flaig et al., 2005)(section C.5 starting on printed page 247)

6. *Management simulation engine of the Regional Simulation Model: An overview* (Park, 2005)(section C.6 starting on printed page 249)

C.1 Weighted implicit finite-volume model for overland flow

A WEIGHTED IMPLICIT FINITE VOLUME MODEL FOR OVERLAND FLOW

A. M. Wasantha Lal, [1]**, M. ASCE**

A weighted implicit finite volume model is developed to simulate two dimensional diffusion flow in arbitrarily shaped areas. The model uses a mixture of unstructured triangles and quadrilaterals to discretize the domain, and a mixture of cell wall types to describe structures, levees, and flow functions that characterize two dimensional flow. The implicit formulation makes the model stable and run faster with very large time steps. The sparse system of linear equations that result from the implicit formulation is solved by using iterative solvers based on various pre-conditioned conjugate gradient methods. The model was tested under a variety of conditions. The results were compared to results from known models applied to axisymmetric and other test problems that had known solutions.

The model was successfully applied to the Oxbow section of the Kissimmee River in Florida, and the results were compared with results from physical and numerical modeling studies. This analysis indicated that the circumcenter-based flow function for walls that is used in the model gives overall superior results in all the cases considered. Results of the numerical experiments showed that the use of weighted implicit methods and iterative solvers provide modelers with improved flexibility and control of the overall accuracy and the run time. The method is to be used as an efficient solution method for local and regional modeling problems in South Florida.

INTRODUCTION

Simulation of overland flow is an important function of large scale hydrologic models. Many such models, including the NSM (Natural System Model) and the SFWMM (South Florida Water Management Model), which are used to simulate the hydrology of South Florida, are based on solving

[1]Lead Civil Engineer, South Florida Water Management District, 3301 Gun Club Rd., West Palm Beach, FL 33406

approximate forms of the St. Venant equations to simulate overland flow. An ideal model for the simulation of 2-D overland flow is expected to handle water bodies of arbitrary shape and may have to use a wide range of temporal and spatial features to meet accuracy requirements at different locations and times. Some of the historic developments related to this goal are described in the texts by Abbott (1979), Tan (1992), and Chaudhry (1993). The features that make models useful for practical applications include the ability to handle wetting and drying; the ability to simulate flow through structures such as weirs, gates and culverts; and the ability to handle tributary and slough inflows.

The earliest 2-D models to solve the St. Venant equations were based on various explicit finite difference methods and rectangular grids. Liggett and Woolhiser (1967), Chow and Ben-Zvi (1973), and Katopodes and Strelkoff (1978) developed some of the early models. More recently, complete equation models have been developed that are capable of handling the inertia terms better and can produce better results for dam-break types of dynamic problems. Fennema and Chaudhry (1990) and Garcia and Kahawita (1989) have developed two such models. Finite element and finite volume methods are useful when the flow domain is arbitrary and the discretization is non-uniform. Fenner (1975) and Akanbi and Katopodes (1988) developed models based on the finite element method, and Zhao et al. (1994) used a finite volume method for solving the complete equations. Most of the complete equation models that use irregular grids require a long time to run and are inefficient to use in large scale hydrologic applications, such as modeling of the Everglades, in which the inertia term is negligible. The challenge of maintaining both fine spatial resolution and low run times can be met by using diffusion flow models in which the inertia terms are neglected. In diffusion flow models one equation is solved for the water level, instead of the three coupled equations that form the St. Venant equations.

Ponce et al. (1978) established a theoretical range of applicability for diffusion flow models. Such models have been applied in the past by Xanthopoulos and Koutitas (1976) to simulate flood wave problems, by Akan and Yen (1981) to study channel confluence flow problems and by

Hromadka et al. (1985) to study dam failure problems. These studies showed that diffusion flow models can be used successfully to simulate a variety of natural flow conditions. Hromadka et al. (1987) also used a 2-D diffusion flow model to compare overland flow models. Diffusion flow models have been used successfully to simulate hydrologic conditions in the Everglades, using the NSM and the SFWMM models developed by the South Florida Water Management District (Fennema et al. 1994).

A finite volume method is useful for South Florida because many of the post-drainage features in the area take the shape of polygons bounded by levees and canals. It satisfies strict mass balance because of conservative property. The basic idea behind the finite volume method is to begin with the conservative form of the differential equation, integrate it over a finite volume, and use Gauss' theorem to convert results into surface integrals which can then be discretized (Hirsch, 1988). During the computation of these surface integrals along the cell walls, functions defining average wall fluxes are needed. Two types of functions are used in this paper, one which uses a line integral, and one which uses the circumcenters (centers of the circumscribing circles) of triangles. In the case of structures or any other flow features, these wall functions are replaced with appropriate functions. When a cell-centered finite volume method is used with rectangular grids, the finite volume method collapses to a finite difference method.

The ordinary differential equations resulting from the finite volume formulation can be solved by using a weighted implicit method. The weighting factor that is used in many 1-D models such as DAMBRK (Fread, 1973, 1988) provides control over accuracy and stability, and the weighting also makes it possible to produce solutions even under stiff conditions. The final solution of the finite volume method is the solution of a sparse system of linear equations at every time step. The availability of a variety of sparse solver methods and packages has made it possible to exercise control over the run time and accuracy.

Both direct and iterative methods are available to solve sparse systems. Iterative methods, such

as the preconditioned conjugate gradient method, are less susceptible to round-off error, and they are more efficient for large problems (Aziz and Settari, 1979). Some of the public domain sparse solvers available through the Internet include SLAP (Seager, 1988), Templates (Barrett, 1993) and IML++ (Dongarra, 1995). Numerous pre-conditioners are used with sparse solvers to speed convergence and sometimes to make the solution feasible. When flow conditions are nearly steady due to negligible disturbances from rainfall and other events, iterative solvers need very few iterations. This feature can make the current model run extremely fast except during unsteady events.

Hydrologic models applied to the South Florida landscape are expected to simulate both large-scale flow features in the Everglades and small-scale flow features in urban areas. They are expected to be capable of both long and short term simulations with relatively short run times. This paper describes the formulation, numerical testing, numerical error analysis, and the successful application of the model to a portion of the Kissimmee river. A number of additional tests were conducted to study the variation in numerical error with spatial and temporal discretizations. Results demonstrate the fast performance of the model when compared to explicit models. The results are also useful in selecting the spatial and temporal discretization for future applications of the model to other areas in South Florida. Some results shown at low resolutions give additional information about the behavior of numerical errors in the model output.

GOVERNING EQUATIONS

Overland flow is described by the depth-averaged flow equations commonly referred to as Saint Venant equations. These equations consist of a continuity equation and momentum equations. The two dimensional continuity equation for shallow water flow is

$$\frac{\partial h}{\partial t} + \frac{\partial (hu)}{\partial x} + \frac{\partial (hv)}{\partial y} - RF + IN + ET + q_{ea} = 0 \tag{1}$$

in which u and v are velocities in x and y directions; $h =$ water depth in units L; $RF =$ rainfall intensity; $IN =$ infiltration rate; $ET =$ evapotranspiration rate, all in units L/T; $q_{ea} =$ volume rate of overland flow entering or leaving canals, measured per unit cell area per unit time. The

momentum equations used in the x and y directions are

$$\frac{\partial(hu)}{\partial t}+\frac{\partial(u^2h)}{\partial x}+\frac{\partial(uvh)}{\partial y}+hg\frac{\partial(h+z)}{\partial x}+ghS_{fx}=0 \tag{2}$$

$$\frac{\partial(hv)}{\partial t}+\frac{\partial(uvh)}{\partial x}+\frac{\partial(v^2h)}{\partial y}+hg\frac{\partial(h+z)}{\partial y}+ghS_{fy}=0 \tag{3}$$

in which S_{fx} and $S_{fy}=$ components of friction slopes in x and y directions. The momentum equations can be combined with the continuity equation without the source term to produce the following vector momentum equation

$$\frac{\partial\mathbf{V}}{\partial t}+\nabla(\frac{1}{2}V^2+gH)+g\vec{S}_f+\mathbf{V}\times\omega=0 \tag{4}$$

in which $\omega=\nabla\times\mathbf{V}$; $\mathbf{V}=u\mathbf{i}+v\mathbf{j}=$ velocity vector; $\vec{S}_f=$ friction slope vector; $H=h+z=$ water level above the datum; $z=$ bottom elevation above datum. The steps in obtaining the equation are presented by Panton (1984). Equation (4) can be integrated along a stream line to obtain the commonly used energy equation. The first term in (4) which is the local acceleration term and the second term which is the convective acceleration term are responsible for inertia effects. The first term is neglected in slowly varying flow to obtain diffusion flow equations. If flow is irrotational, $\omega=0$ and (4) reduces to

$$\nabla E=-\vec{S}_f \tag{5}$$

which can also be written in terms of the x and y components as $\frac{\partial E}{\partial x}=-S_{fx}$ and $\frac{\partial E}{\partial x}=-S_{fy}$ with $E=h+z+V^2/(2g)=H+V^2/(2g)$ being the energy head above the datum. Equation (5) without the velocity head in E is normally used as the foundation of diffusion flow formulations, in which the water level H is used instead of the energy head E (Hromadka et al., 1987). Even if all of the equations that follow are expressed in terms of H, it can be shown that H in these equations can be replaced with E to give the necessary equations for conditions under which the velocity heads are important. This simple conversion is possible in slowly varying flow if $\frac{\partial}{\partial t}(V^2/2g)$ is small. Use of E instead of H helps to recover some of the lost inertia effects in slowly varying diffusion flow at converging and diverging boundaries. Unfortunately, diffusion flow models using the velocity head generate small oscillations in unsteady flow problems (Strelkoff et al., 1977), and it becomes

necessary to use H instead of E for such problems.

The friction slope $\vec{S}_f$ in (5) is computed using an equation for wetlands (Kadlec and Knight, 1996) or a general form of the Manning equation written as $V = \frac{1}{n_b} h^{\gamma} S_f^{\lambda}$ in which n_b = Manning coefficient when $\gamma = 2/3$ and $\lambda = 1/2$; $V = \sqrt{v^2 + u^2}$ = magnitude of the velocity vector. In diffusion flow $S_f = S_n$ is assumed, in which S_n = slope of the water surface (or the energy surface when E is used) computed as $\sqrt{(\frac{\partial H}{\partial x})^2 + (\frac{\partial H}{\partial y})^2}$. Akan and Yen (1981) and Hromadka et al. (1987) used the following equation to compute u and v:

$$u = -\frac{K}{h}\frac{\partial H}{\partial x}, \qquad v = -\frac{K}{h}\frac{\partial H}{\partial y} \tag{6}$$

K can be expressed for the Manning equation in general form as

$$K = \frac{1}{n_b} h^{\gamma+1} S_n^{\lambda-1} \quad \text{for} \quad \lambda \geq 1 \quad \text{and} \quad |S_n| > \delta_s \tag{7}$$

$$K = K_0 \quad \text{for} \quad \lambda < 1 \quad \text{and} \quad |S_n| \leq \delta_s \tag{8}$$

Term $K_0 = h^{\gamma+1}/(n_b \delta_s^{1-\lambda})$ provides continuity in function K, and gives a smoother flow profile for some problems, than $K_0 = 0$ used by Hromadka (1985). Depth $h = 0$ for dry cells. δ_s is used to bound K within finite limits; $\delta_s \approx 10^{-10}$ is used in the study for test cases in single precision. $\lambda \approx 1$ gives laminar-like flow. K is useful in linearizing and simplifying the diffusion flow equation. The continuity equation (1) can be expressed, using (6), as

$$\frac{\partial H}{\partial t} = \frac{\partial}{\partial x} K \frac{\partial H}{\partial x} + \frac{\partial}{\partial y} K \frac{\partial H}{\partial y} + S \tag{9}$$

in which $S = RF - IN - ET - q_{ea}$ is the source term. When the velocity head is included, H in (9) is replaced with E, as explained earlier. The equation can be solved for both surface flow and saturated groundwater flow using many of the methods used to solve parabolic equations.

The finite volume method

In the finite volume method (1) is expressed in the following integral form over an arbitrary control volume cv

$$\frac{\partial}{\partial t} \int_{cv} H \, dv + \int_{cv} \left[\frac{\partial}{\partial x}(hu) + \frac{\partial}{\partial y}(hv) - S \right] \, dv = 0 \tag{10}$$

in which dv = volume of element cv. The overall cv can be subdivided into cells. The Gauss divergence theorem can be used to simplify the second volume integral term of (10) and control it to a surface integral (Hirsch, 1988). Equation (10) for all the finite volume cells can be written in vector form as

$$\Delta\mathbf{A}\cdot\frac{d\mathbf{H}}{dt}=\mathbf{Q}(\mathbf{H})+\mathbf{S} \tag{11}$$

in which $\mathbf{H}=[H_1,H_2,\ldots H_m\ldots H_{nc}]^T$ is a vector containing the average heads in all the cells; $\mathbf{S}=$ the source term in vector form; $\Delta\mathbf{A}=$ a diagonal matrix whose element $\Delta\mathbf{A}(m,m)$ is equal to the cell area ΔA_m in the case of a cell m; **Q** and **S** are the net inflows and source terms to cells. The net inflow rate to a cell m is given by

$$Q_m(H)=\sum_{r=1}^{ns}(\bar{\mathbf{F}}\cdot\mathbf{n})_r\,\Delta l_r \tag{12}$$

$\Delta l_r=$ length of the side r of the ns sided polygon; $\mathbf{n}=n_x\mathbf{i}+n_y\mathbf{j}=$ unit outward normal vector for the face r of the polygon; $\bar{\mathbf{F}}=$ average flux rate across the wall per unit length defined as $hu\,\mathbf{i}+hv\,\mathbf{j}$, which is also equal to $-K\nabla H$ for free surface diffusion flow or ground water flow. Two alternative methods are used in the model to compute $\bar{\mathbf{F}}$ for overland flow. They are the line-integral-based method suggested by Hirsch (1988), and the circumcenter-based method suggested by Cordes and Putti (1996). In the case of flow over structures and levees, $Q_m(H)$ is computed using the appropriate structure equations instead of the above two methods. In the current cell-centered finite volume approach, H, ET, RF and IN are defined as cell average values.

The line-integral-based method for computing the wall flux

This method can be used with both triangular and quadrilateral cells. Using this method, the approximate flux $\bar{\mathbf{F}}_r$ for a wall r in (12) is computed by using fluxes at the nodes defining the wall. In Fig. 1,

$$\bar{\mathbf{F}}=0.5(\hat{\mathbf{F}}_j+\hat{\mathbf{F}}_k) \tag{13}$$

in which $\hat{\mathbf{F}}_j$ and $\hat{\mathbf{F}}_k$ are the fluxes at the nodes j and k computed using $-K\nabla H$. ∇H is computed using an integral equation around the nodes (Hirsch, 1988) such that

$$\int_v\nabla H\,da=\oint_s H\mathbf{n}dl \tag{14}$$

and dl = length of the sides of the polygon, referred to as the "shadow polygon", with cell centroids at vertices. Using (14), the flux $\hat{\mathbf{F}}_j$ for a node j can be expressed as

$$\hat{\mathbf{F}}_j = -K_j(\nabla\vec{H})_j = -\frac{K_j}{2\Delta\hat{A}_j}\left[-\sum_{p=1}^{np} H_p(y_{p+1}-y_{p-1})\mathbf{i} + \sum_{p=1}^{np} H_p(x_{p+1}-x_{p-1})\mathbf{j}\right] \tag{15}$$

in which $p = 1, 2, \ldots, np$ are the cell numbers around the node j forming the vertices of the shadow polygon; x_p, y_p are the coordinates of these vertices. In the equation, x_0, y_0 at $p = 1$ must be replaced by x_{np}, y_{np}, and x_{np+1}, y_{np+1} at $p = np$ must be replaced by x_1, y_1 to complete the integration correctly. Areas of the shadow polygons $\Delta\hat{A}_j$ are computed by using a similar line integration:

$$2\Delta\hat{A}_j = \sum_{p=1}^{np} x_p(y_{p+1}-y_{p-1}) \tag{16}$$

K_j are computed using (7) and (8). The nodal values of n_b and h in the equations are obtained by a weighted averaging of the values of surrounding cells. The respective cell areas are used as weights. The line integrals are computed counter clockwise as positive.

In the use of the weighted implicit implementation, $\mathbf{Q}(\mathbf{H}) = [Q_1, Q_2 \ldots Q_{nc}]^T$ of (11) is linearized as $\mathbf{M}\cdot\mathbf{H}$. The matrix $\mathbf{M}$ contains information about the connectivity among cells, geometry, and the roughness. The matrix $\mathbf{M}$ is assembled by computing the flow rates across all of the walls using (12), and adding or subtracting appropriate volumes from the cells. Consider the volume lost by donor m, crossing wall r defined by nodes j and k. Equations (12), (13) and the line integral around node j obtained using (15) makes the following modification to $\mathbf{M}$:

$$M_{m,p} \rightarrow M_{m,p} - \frac{K_j\,\Delta l_r}{4\Delta\hat{A}_j}\left[-n_{xr}(y_{p+1}-y_{p-1}) + n_{yr}(x_{p+1}-x_{p-1})\right],\ p = 1, \ldots, np \tag{17}$$

n_{xr}, n_{yr} = components of $\mathbf{n}$ for wall r; Δl_r = length of wall r. A similar expression is needed for node k. Flow into the receiver cell n also requires two similar expressions with negative signs placed on (n_{xr}, n_{yr}).

The circumcenter-based method for computing wall flux

Cordes and Putti (1996) showed the equivalence of a low-order mixed finite element method based on RT0 elements (Raviart and Thomas, 1977) with a finite volume method for triangles under

certain conditions. Because of the equivalence, it is possible to use an expression derived for the mixed finite element method to compute flow rates for the finite volume method. In the equivalent finite volume method, water levels at circumcenters are used in the computation of flow across walls. In the mixed finite element method, water levels in triangles are assumed to vary linearly, and the water level at the centroid is the average water level. Using Figure 2 as the definition sketch, $(\hat{\mathbf{F}} \cdot \mathbf{n})_r$ for wall r in (12) is computed as

$$(\hat{\mathbf{F}} \cdot \mathbf{n})_r = \Delta l_r K_r \frac{H_m - H_n}{\Delta d_{mn}} \tag{18}$$

in which $\Delta d_{mn} =$ distance between circumcenters of triangles m and n; H_m, H_n are the heads at the circumcenters. K_r is computed using (7) or (8). The depth and the bed roughness needed to compute K_r are obtained by weighted averaging the depth and bed roughness of cells m and n. S_n is computed using

$$S_n = \sqrt{\frac{(\hat{H}_j - \hat{H}_k)^2}{\Delta l_r^2} + \frac{(H_m - H_n)^2}{\Delta d_{mn}^2}} \tag{19}$$

in which $\hat{H}_j$ and $\hat{H}_k$ are the heads at nodes j and k, computed as weighted averages of surrounding heads. The cell areas are used as weights in the averaging. In the semi-implicit formulation the computation of flow from cell n to m involves the modification of the following matrix element as it receives water in cell m:

$$M_{m,n} \rightarrow M_{m,n} + \frac{K_r \Delta l_r}{\Delta d_{mn}}, \qquad M_{m,m} \rightarrow M_{m,m} - \frac{K_r \Delta l_r}{\Delta d_{mn}} \tag{20}$$

Elements $M_{n,m}$, $M_{n,n}$ are modified similarly due to water losses from the donor cell n. The circumcenter-based method can be used only with acute-angled triangles. When this method is used with obtuse angled triangles, the circumcenter falls outside the triangle, and the numerical error tends to be large. With rectangles the method becomes equivalent to the finite difference method.

The average water velocity in a cell is computed by using the following vector basis function developed for RT0 mixed elements of Raviart and Thomas (1977), and used by Cordes and Putti,

(1996):

$$\vec{v} = \frac{1}{2A\,h}\left[Q_{s1}\begin{pmatrix} x-\hat{x_1} \\ y-\hat{y_1} \end{pmatrix} + Q_{s2}\begin{pmatrix} x-\hat{x_2} \\ y-\hat{y_2} \end{pmatrix} + Q_{s3}\begin{pmatrix} x-\hat{x_3} \\ y-\hat{y_3} \end{pmatrix} \right] = -K\nabla H \qquad (21)$$

Here, Q_{s1}, Q_{s2}, Q_{s3} = discharge rates across cell walls $s1, s2$ and $s3$ counting outwards as positive; $(\hat{x_i}, \hat{y_i})$ = the coordinates of the nodes; (x, y) = coordinates of any point, including the circumcenter in the current case at which the head is computed. In the case of right-angled triangles, Putti (1996) showed that the mixed finite element method is equivalent to a finite difference method.

Flow through structures and levees

When the model is used to simulate structure flows, the specific cell walls are replaced with structure type walls, and flow rates of $Q_s(H)$ are used in (12) instead of $\mathbf{F}.\mathbf{n}$ to compute structure flows. Linearization of structure flow equations can be done either prior to the run using regression methods, or during the run using data from previous calls to the routine. $Q_s(H)$ is computed as a function of adjacent water levels, gate openings, and other physical parameters. Assuming that the variation of Q_s versus ΔH $(\Delta H = H_m - H_n)$ is linear during two consecutive time steps, a structure equation can be developed using the information collected during the time steps p and $p-1$ as

$$\begin{aligned} Q_s(\Delta H) &= Q_s^p + K_s(\Delta H - \Delta H^p) \quad \text{for} \quad \Delta H^p \neq \Delta H^{p-1} \qquad (22) \\ Q_s(\Delta H) &= Q_s^p \quad \text{otherwise} \end{aligned}$$

in which $K_s = (Q_s^p - Q_s^{p-1})/(\Delta H^p - \Delta H^{p-1})$; p = the time step count. If only the information at time step p is used, (22) reduces to $Q_s(\Delta H) = K_s\,\Delta H$, and the right hand side of the system of equations need not be modified. The introduction of a structure between cells m and n modifies $\mathbf{M}$ as $M_{m,n} \rightarrow M_{m,n} + K_s$, $M_{m,m} \rightarrow M_{m,m} - K_s$, $M_{n,m} \rightarrow M_{n,m} + K_s$, and $M_{n,n} \rightarrow M_{n,n} - K_s$ as in (20). In the computations it was assumed that the head loss due to bed friction is negligible when compared to head loss across structures. If iterations are carried out within a time step, the linearization will not introduce errors in the solution. Since rapid flow variations are not expected in diffusion flow, the linearization gives good results even for structures having nonlinear flow relations.

When there is a structure or a levee type cell wall, the two-dimensional flows in adjacent cells are affected and become more nearly one dimensional. The following equation, based on the Manning equation, is applied between cells across a wall under this condition:

$$Q_{1d} = K_n \Delta H = \frac{h^{\gamma+1} \Delta l_r}{n_b \Delta d} \left(\frac{\Delta H}{\Delta d} \right)^{\lambda-1} \Delta H \tag{23}$$

Here, n_b, h are averaged between cells; $\Delta d =$ distance between the cell centroids. Centroids are used to represent cell locations in restricted spaces or closer to structures and dry cells where free 2-D flow cannot be assumed, and slope S_n of the water surface profile cannot be determined accurately. For these cells K_n is computed by assuming that the water surface slope S_n in the Manning equation is approximately equal to $\frac{\Delta H}{\Delta d}$.

Boundary conditions

One boundary condition is needed at each boundary with diffusion flow. Specified head and specified flow are the most commonly used types. The no-flow type boundary is implemented simply by making $\overline{\mathbf{F}} = \mathbf{0}$ in (12). The matrix $\mathbf{M}$ needs no modification under no-flow conditions. In the case of a known inflow rate Q_I into a cell i through the boundary or due to pumping activity, row i of source term $\mathbf{S}$ in (11) must be modified as

$$S_i \rightarrow S_i + Q_I \tag{24}$$

Source term quantities such as rainfall, ET and infiltration are summed similarly for cell i.

If the flow domain is connected to an external reservoir as the boundary condition, and if the reservoir water level is H_0, the equation for flow rate into the domain Q_o is linearized as $Q_o = K_o(H_o - H_i)$, in which K_o is similar to the structure constant K_s in (22) and H_o and H_i are water levels of the water body and the cell. The modifications for matrix $\mathbf{M}$ and vector $\mathbf{S}$ are $M_{i,i} \rightarrow M_{i,i} - K_o$, and $S_i \rightarrow S_i + K_o H_o$. Implementation of head boundary conditions is explained later.

Formulation of the weighted implicit method

The ordinary differential equations (11) derived using the finite volume method are solved by using

the following weighted finite difference formulation

$$\Delta A_i\, H_i^{n+1} = \Delta A_i\, H_i^n + \Delta t[\alpha Q_i^{n+1} + (1-\alpha) Q_i^n] + \Delta t[\alpha S_i^{n+1} + (1-\alpha) S_i^n] \tag{25}$$

in which H_i^n = average surface water level in cell i at time step n; α = time weighting factor; $\alpha = 0$ and 1 for explicit and implicit problems. Using linearization, (25) can be expressed as the following system of linear equations:

$$[\Delta \mathbf{A} - \alpha \Delta t \mathbf{M}^{n+1}].\Delta \mathbf{H} = \Delta t[\mathbf{M}^n].\mathbf{H}^n + \Delta t(1-\alpha)[\mathbf{M}^n - \mathbf{M}^{n+1}].\mathbf{H}^n + \Delta t[\alpha \mathbf{S}^{n+1} + (1-\alpha)\mathbf{S}^n] \tag{26}$$

Here, $\mathbf{Q}^n = \mathbf{M}^n.\mathbf{H}^n$. The solution $\blacksquare\mathbf{H}$ is used to update the heads using $\mathbf{H}^{n+1} = \mathbf{H}^n + \blacksquare\mathbf{H}$. The matrix $\mathbf{P} = [\Delta \mathbf{A} - \alpha \Delta t \mathbf{M}^{n+1}]$ is so far symmetric. In many gradually varying problems $\mathbf{M}^{n+1}$ is replaced with $\mathbf{M}^n$ to simplify (26) (Akan and Yen, 1981). Test runs show that this is a useful procedure for many problems. If this assumption is not made then $\mathbf{M}^{n+1}$ must be updated by using an iterative procedure within the time step, by first computing $\Delta\mathbf{H}$ using (26) with the most recent estimates of $\mathbf{M}^{n+1}$, and next updating $\mathbf{H}^{n+1}$. Iterations are continued similarly by updating $\mathbf{M}^{n+1}$ and using (26) until convergence. Examples used in the paper need only 2-4 iterations for the convergence of the water level up to 4 significant digits. This type of iteration was not used in the current application.

Imposition of a head boundary condition to a cell i as $H_i = H_B$ is carried out by reconfiguring row i of $\mathbf{P}$. The entire row i is modified by using

$$\begin{aligned} P_{i,j} &= 0 \qquad \text{for} \quad j = 1,2,\ldots nc, \quad j \neq i \\ P_{i,j} &= 1 \qquad \text{for} \quad j = 1,2,\ldots nc, \quad j = i \\ S_i &= H_B - H_i^n \end{aligned} \tag{27}$$

Matrix $\mathbf{P}$ is sparse for large problems. The element density is less than 1% for a 1000 cell discretization. When $\alpha = 0$, $\Delta\mathbf{H}$ in (26) can be computed by using a simple matrix multiplication. $\alpha = 0.5$ gives higher accuracy as in the case of Crank Nicholson type schemes. With rectangular grids the finite volume method gives the finite difference solution.

Solution of the linear equations

The number of equations in the system of linear equations in (26) is equal to the number of cells, *nc*. If the cells are non-uniform and the physical properties are non-homogeneous, the problem may become stiff and the matrix $\blacksquare\mathbf{A} - \alpha\Delta t\mathbf{M}$ may become ill-conditioned. However, many fast efficient iterative sparse solvers that can handle ill-conditioned matrices have recently become available. The current model was tested with the SLAP solver (Seager, 1988) and the PetSc solver (Smith, 1995). Both solvers use iterative conjugate gradient methods and preconditioners. Preconditioners are useful in improving the convergence rate and the solvability. Without preconditioning, the number of iterations increases with the condition number. The condition number of a matrix is the ratio of the largest and smallest eigenvalues. If the system of equations becomes difficult to solve with the choicen sparse solver, Δt can be reduced until $\mathbf{A} - \alpha\Delta t\mathbf{M}$ becomes well-conditioned. The need to re-run the code due to non-convergence can sometimes be avoided by reusing **M** with a smaller Δt.

Active research is under way to develop faster sparse solvers. A feature available with faster packages gives one the ability to solve equations at each time step as a sequential process and incrementally improve the solution by starting from the solution for the previous time step. Without such methods the same or nearly the same equations may still have to be solved repeatedly at steady or near-steady conditions, wasting computer resources. Many of the new features in solvers can make the model run much faster during such events by carrying out the minimum required updating from one time step to the next and using only a few iterations, depending on the extent of transient flow activities.

NUMERICAL TESTS

The model was tested for accuracy by applying it to a number of test problems with known solutions. The first test was used to check the ability of the finite volume method to solve diffusion equations accurately. The second test was carried out with 2-D diffusion type overland flow. The remaining tests were designed to carry out a numerical error and stability analysis.

Test 1

A groundwater example from Wang (1982) was used for the first test. In the test a pumping well was positioned at the center of a 4000 m $\times$ 4000 m square confined aquifer having a constant transmissivity ($K\times$ aquifer depth) of 300 m^2/day and a storage coefficient of 0.002. A uniform initial water level of 10 m and a constant pumping rate of 2000 m^3/s were assumed. The triangular discretization used with the model is the same as that shown later in Fig. 5 with 238 cells, except that the linear dimensions are scaled down to fit the area into the 4000 m $\times$ 4000 m square. The MODFLOW model (McDonald and Harbaugh, 1984) was set up to simulate the same flow conditions using a 40×40 square grid with 1600 cells. Figure 3a shows the water level contours at the end of 30 days, obtained by using the circumcenter-based finite volume method. Figure 3b shows the same contours obtained by using the MODFLOW model. Drawdown curves at a number of monitoring points are shown in Fig. 4. The finite volume method using the line-integral-based flow function failed to produce convex water level contours near the well, and the results are not shown. The test shows that the circumcenter-based finite volume method with only 238 cells can produce relatively accurate solutions. The test also shows that the circumcenter-based method gives better results than the line-integral-based method for locally converging flow.

Test 2

An axisymmetric overland flow problem was used in the second test. The flow characteristics of this test are somewhat similar to the flow characteristics of the Everglades. The test bed has dimensions 161 km $\times$ 161 km (100 miles $\times$ 100 miles) and a flat bottom. The initial condition is

$$H = \left[0.4575 + 0.1525\cos\left(\frac{\pi r}{r_{max}}\right)\right] m \quad \text{for} \quad r \le r_{max} \tag{28}$$

$$H = 0.305\, m \quad \text{otherwise} \tag{29}$$

in which $r =$ distance from the domain center; $r_{max} = 32188$ m. The Manning roughness is assumed as 1.0; RF, IN and ET are neglected. An axisymmetric diffusion flow model was developed based on the following axisymmetric continuity equation to obtain an extremely accurate solution for the problem using a fine resolution

$$\frac{\partial(hr)}{\partial t} + \frac{\partial(uhr)}{\partial r} = 0. \tag{30}$$

This solution was used in computing small numerical errors in the finite volume model under

different resolutions. A model, similar to the 1-D model by Akan and Yen (1981) after a few modifications, was used to solve (30) accurately. The test was a 12 day simulation of the water level using both the axisymmetric model and the finite volume model. In the test, $\Delta r = 80.47$ m and $\Delta t = 1$ min were used with the axisymmetric model to obtain the water level in the problem accurate enough to compute numerical errors in other models. The error at the center was used for comparison purposes because the error is largest at this point. The water level computed accurately at the center is 0.442105 m. The expected circular shape of the solution was also used to test accuracy of the finite volume models.

The finite volume model using the circumcenter-based approach was used with discretizations of different refinements to recreate the results of the axisymmetric model. The results, obtained using a discretization of 238 cells and 135 nodes and a time step of 3 hrs, are shown in Fig. 5. The SLAP 2.0 sparse solver package (Seager, 1988) was used to solve the linear equations, and convergence was assumed when the largest change in the solution vector $\varepsilon_\infty < 0.3 \times 10^{-4} m$. Other parameter values used were $\alpha = 0.5$ and $\delta_s = 1.0 \times 10^{-10}$ (in equations (7) and (8)). The figure shows the grid used, and the contour plot of water levels after 12 days. The water level at the center of the circular patch, and at cells at radial distances of r =11885 m and $r = 31000$ m was monitored during the simulation. Figure 6 shows the general agreement of water levels at all the monitoring points, using both the axisymmetric model and the finite volume model. Figure 6 also shows the solution at $r = 0$ obtained using a finite volume model running with a time step of 3 hrs, and a higher resolution obtained using 1536 cells. As seen in the figure, the finite volume solution very closely matches with the axisymmetric solution at this high resolution.

Numerical error and stability

The accuracy of results obtained from a numerical model depends on the spatial and temporal discretizations. If a model is used to simulate flow features of a certain wave length, the resolution of the mesh should be sufficient to capture that wave length. A description of the variation of the numerical error with the spatial and temporal resolutions is provided by Lal (1998). To understand the behavior of the numerical error in the current finite volume model, triangular meshes of dif-

ferent levels of discretization were used in the simulation of the flow pattern used in the previous test case. The GMS software package (1995) was used to generate meshes for this test. An estimate of the numerical error was obtained for comparison purposes by presenting the numerical error at $r = 0$ after 12 days as a percentage of the depth at $t = 0$. Numerical error was computed by using the previously mentioned axisymmetric solution as the true solution because it has an error term much smaller than the error studied. Table 1 shows a summary of test results for the center, obtained by using circumcenter-based methods. Run times shown are for a SUN Sparc 20 (speed 90 MHz, 4.1 Mflops/s measured with the linpack benchmark test, Dongarra, 1993). The iterations shown are the iterations inside the SLAP2.0 solver indicating the computational effort. In the table Δx was computed as $\sqrt{\Delta A_c}$ in which ΔA_c is the average area of a triangular cell. ϕ is obtained as $k\Delta x$, in which k is the wave number of the water surface profile simulated in the model $= 2\pi/(\text{wavelength})$. Term π/ϕ gives an estimate of the spatial resolution, measured as the average number of spatial divisions within half the wave length of a sinusoidal water surface profile. β is the non-dimensional time step size, which is based on the analysis of Lal (1998):

$$\beta = \frac{h^{\frac{5}{3}}}{n_b\sqrt{S_n}}\frac{\Delta t}{\Delta x^2} \tag{31}$$

$\beta < 0.25$ for explicit finite difference methods. Test 0 corresponds to the test shown in Figures 5 and 6 for 238 cells. Results of test 12 with 1536 cells is also shown in Fig 6. Table 1 shows that the solution of the finite volume model approaches the axisymmetric solution as the spatial and temporal resolutions both get finer. This is true when the model is using the line-integral-based method too. Table 1 also shows that the run time decreases and the number of iterations per time step increases when the time step is increased.

A test was conducted to check the stability of the model under explicit conditions ($\alpha = 0$). Experimentation with different time steps showed that Δt at the points of incipient instability of the tests was approximately 52 hrs, 4.3 hrs and 3.5 hrs respectively with 116, 376 and 1536 cell configurations listed in Table 1. These time steps correspond to approximate β values of 0.06, 0.02 and 0.05 respectively. Incipient instability was assumed when dynamic oscillations were visible at the center of the solution. These results confirm, for example, that the tests 8-11 in Table 1, ob-

tained for $\alpha = 0.5$, would have been unstable under explicit conditions. The approximate stability limit $\beta \approx 0.05$ is useful in selecting the time step for explicit model runs. Nonlinear instability was not studied during the test.

Numerical tests were conducted to determine the convergence behavior of the finite volume code and the influence of δ_s in (8) on the performance of the code. Tests showed that the number of iterations increased when δ_s was decreased to very low values, because some of the K values in the matrix became very large (Lal et al., 1997), and the matrix became more unconditional and ultimately unsolvable as a result. The solution errors at the center after 12 hrs were 1 mm, 21 mm, and 88 mm as δ_s was changed to 10^{-6}, 10^{-5} and 10^{-4} respectively. A large δ_s causes the model to use (8) instead of (7) more often. $\delta_s = 10^{-10}$ was used in the axisymmetric flow test, and $\delta_s = 10^{-4}$ was used in the Kissimmee study that is explained later.

Different sparse solver options in the SLAP 2.0 package were tested while running test 0 referred to in Table 1. The purpose of the test was to investigate the performance of different solvers and pre-conditions. In the SLAP 2.0 package the incomplete LU decomposition with conjugate gradient (CG) solver, incomplete LU biconjugate gradient solver, and the incomplete LU biconjugate gradient solver with LU decomposition were reliable, and used the least number of iterations. The last option was used in the test. The number of solver iterations changed with the solver type and δ_s which affects the condition number of the matrix. With large time steps the SLAP 2.0 solver converged only when large α values are used. The recently developed PetSc solver (Smith et al., 1995) was found to be much more reliable and fast for larger problems.

Application to the Kissimmee River

The model was applied to the an experimental area near weir no. 2 of the Kissimmee River Basin, Florida, using the same discretization and the bed roughness used by Zhao et al. (1994). In the application by Zhao et al. the unsteady flow model RBFVM-2D was used over the test area shown in Fig. 7, which is approximately 1402 m $\times$ 1036 m. In the figure a flood canal passes from the

North to the South (left to right in the figure), and a one-notch weir is located near the upstream end near C1 to divert part of the flow into the river oxbow. The Manning coefficients of the flood plain, main channel and the river oxbow are 0.03, 0.025 and 0.04 respectively. The number of nodes and cells in the mixed grid used by the RBFVM-2D model and the line-integral-based finite volume model are 347 and 327 respectively. The same numbers in the case of the circumcenter-based method are 347 and 634 respectively. For the circumcenter-based method the quadrilaterals were divided into triangles. The results of the problem for an inflow of 221 m^3/s at the upstream boundary and a stage of 13.57 m at the downstream boundary are shown in Fig 7, after running the model until a reasonably steady state is reached. The results were obtained after including the velocity head $V^2/(2g)$ in (5). When the same simulation was repeated with the omission of the velocity head, the water level at C1 dropped by 1 cm. Water levels at other locations remained practically unchanged. Figure 7 shows contours of water levels, and the water level monitoring points. The elliptical patch of contours in the figure shows a small dry area. Figure 8 shows the velocity vectors drawn at the circumcenters using (21). The apparent overlap of arrows in the plot is due to the near right-angled triangles in the grid, which make the circumcenters nearly overlap. Figure 9 shows the results of the same test obtained using the line-integral-based method.

Comparison of water levels and water velocities in Table 2 shows that the water levels obtained with the current model agree with the physical model results and the RBFVM-2D model results at many locations. However velocities at O2, representing a narrow canal segment of the Oxbow, that were obtained by using diffusion flow models did not agree with other velocities. Comparison of the circumcenter-based method with the line-integral-based method show that both methods produced similar flow patterns in the Kissimmee application, unlike in the test cases with a locally convergent or divergent flow fields in which the line-integral-based method produced unacceptable local results. This occurred because the averaged $\bar{\mathbf{F}}$ in (13) does not provide a very accurate estimate of discharges across walls in acute angled triangles. Certain velocities near the boundary are not shown in Table 2 because line integrals could not be computed with this method without a closed path of integration.

With the Kissimmee application it was also found that the line-integral-based method required approximately 50 iterations when using 20 s time steps and the SLAP conjugate gradient method using LU decomposition preconditioner. The circumcenter method required approximately 200 iterations for the same case. The run time for the current model is a small fraction of the run time of explicit models such as RBFVM2D requiring 1-2 s time steps. The PetSc solver (Smith, 1995) with a new C++ version of the current model can reduce the number of iterations to less than 5 with even larger time steps, and make the model run much faster. With the development of better and faster external sparse solvers using parallel processing and other methods, large scale application of the model to South Florida continues to become less expensive, just with the upgrading of the solver.

SUMMARY AND CONCLUSIONS

An implicit finite volume model was developed to simulate diffusion flow across arbitrarily shaped landscapes. Tests were conducted to verify the model results by comparing them with results from the MODFLOW model and an axisymmetric model. The model was also applied to a variety of test problems, using a range of spatial and temporal discretizations to study the behavior of numerical errors. Results show that numerical errors tend to become smaller with finer discretizations, thus confirming the numerical consistency condition. The explicit option ($\alpha = 0.0$) showed incipient instability when the non-dimensional time step β exceeds approximately 0.05. The implicit option was stable for large values of β. Results show that, by selecting a spatial resolution (π/ϕ) of more than about 3 divisions per half sine wave, numerical errors for the test problems can be reduced to less that 1%.

The model used different wall types to represent structure flows, no flows, and 2-D flows. Flow across 2-D walls were computed by using a line-integral-based method and a circumcenter-based method. Results show that the circumcenter-based method produced better results under all the conditions tested, and that the line-integral-based methods produced local errors when used

with triangular discretizations to simulate locally convergent or divergent flow patterns. The line-integral-based method becomes the choice when polygons, not triangles, are used in the discretization. This method also needed fewer iterations inside the solver when used with test problems. Application of both methods to the Kissimmee River shows that the results agree with the results of the physical model and the RBFVM-2D model. The same application showed that, while the RBFVM-2D model needed 1-2 s time steps, the current model could be run faster with time steps over 10 times as large, even with older solvers, and many more times faster with modern solvers.

The structure of the current finite volume model allows new wall flow function types to be added to the existing circumcenter and line integral types, and new structure types to be added in the same way. This feature is useful for future extensions of the model into more complicated areas of South Florida and the Everglades. Increasingly powerful sparse solvers can continue to speed computations in the future and make it possible to simulate flows with much finer spatial resolutions and larger time steps otherwise possible, as demonstrated in the examples.

ACKNOWLEDGEMENTS

The writer wishes to thank Mark Belnap, Randy Van Zee, and Jayantha Obeysekara for providing valuable ideas during different stages of model development. Review of the manuscript by Todd Tisdale, Joel VanArmen, Steve Lin, Brion Lehar, Sashi Nair, Mark Wilsnack, and other members of the Hydrologic Systems Modeling group of the South Florida Water Management District was extremely useful.

APPENDIX I. REFERENCES

Abbott, M. B. (1979). *Computational hydraulics*, Ashgate Publishing Co., Brookfield, USA.

Akan, A. O., and Yen, B. C. (1981). "Diffusion-wave flood routing in channel networks", *J. Hydr. Div.,* ASCE, 107(6), 719-731.

Akanbi, A. A., and Katopodes, N. D. (1988). "Models for flood propagation on initially dry land", *J. Hydr. Engrg.,* ASCE, 114(7), 686-706.

Aziz, K. and Settari, A. (1979). *Petroleum Reservoir Simulation*, Elsevier Publishing Co., NY.

Barrett, R., Berry, M., Chan, T., Demmel, J., Donato, J., Dongarra, J., Eijkhout, V., Pozo, R., Romine, C., and van der Vorst, H. (1993). "Templates for the solution of linear systems: building blocks for iterative methods", *SIAM Publications, 1993*, distributed through `ftp netlib2.cs.utk.edu`.

Chaudhry, M. F. (1993). *Open-Channel Flow*, Prentice-Hall, NY.

Chow, V. T., and Ben-Zvi, A. (1973). "Hydrodynamic modeling of two-dimensional water flow", *J. Hydr. Div., ASCE,* 99(11), 2023-2040.

Cordes, C., and Putti, M. (1996). "Triangular mixed finite elements versus the finite volumes in groundwater modeling", Int. Conf. Comp. Meth. Water Res. XII, A. A. Aldama et al., editors, *Computational Mechanics*, Southampton, London, p 61-68.

Dongarra, J. (1993). "Performance of various computers using standard linear equation software", Computer Science Dept., Univ. of Tennessee, CS-89-85.

Dongarra, J., Lumsdaine, A., Pozo, R., and Remington, K. (1995). "IML++ v. 1.1. Iterative methods library", *National Institute of Standards and Technology Report, February 1995*, University of Tennessee, TN.

Fennema, R. J., and Chaudhry, M. H. (1990). "Explicit methods for 2D transient free-surface flows", *J. Hydr. Engrg.,* ASCE, 116(8), 1013-1034.

Fennema, R. J., Neidrauer, C. J., Johnson, R. A., McVicor, T. K., Perkins, W. A. (1994). "A computer model to simulate natural everglades hydrology", *Everglades, The Ecosystem and its Restoration,* Eds. Davis, S. M. and Ogden, J. C., St. Lucie Press, FL, 249-289.

Fenner, R. T. (1975). *Finite element method for engineers*, MacMillan, London.

Fread, D. L. (1973). ”Effects of time step in implicit dynamic routing”, *Water Resources Bulletin*, AWRA, 9(2), 338-350.

Fread, D. L. (1988). ”The NWS DAMBRK Model”, *National Weather Service*, NOAA, Silver Springs, MD.

Garcia, R. and Kahawita, R. A. (1986). ”Numerical solution of the St. Venant equations with the McCormack finite difference scheme.”, *Int. J. Numerical Methods in Fluids*, Vol. 6, 507-527.

GMS Department of Defence Groundwater Modeling System. (1995). Computer Graphics Laboratory, Bringham Young University, UT.

Hirsch, C. (1988). ”Numerical computation of internal and external flows”, *John Wiley & Sons,* New York.

Hromadka, II, T. V. and Lai, C. (1985). ”Solving the two-dimensional diffusion flow equations”, *Proc. of the specialty conf. sponsored by the Hyd. Div. of the ASCE,* lake Buena Vista, FL, Aug 12-17, 555-561.

Hromadka II, T. V., McCuen, R. H., and Yen, C. C. (1987). ”Comparison of overland flow hydrograph models”, *J. of Hydr. Res.*, ASCE, 113(11), 1422-1440.

Kadlec, R. H. and Knight, R. L. (1996). *Treatment wetlands*, Lewis Publishers, Boca Raton, FL, 197-207.

Katopodes, N. D., and Strelkoff, R., ”Computing two-dimensional dam break flood waves”, *J. Hydr. Div., ASCE,* 104(9), 1269-1288.

Lal, Wasantha, A. M. (1998). ”Performance comparison of overland flow algorithms”, *J. of Hydr. Engrg.,* ASCE, 124(4).

Lal, Wasantha, A. M., Belnap, M. (1997). ”A users guide to HSE, the hydrologic simulation engine of the South Florida Regional Simulation Model”, South Florida Water Management District, West Palm Beach, FL.

Liggett, J. A. and Woolhiser, D. A. (1967). "Difference solutions of the shallow-water equation" *J. Eng. Mech. Div.*, ASCE, 93(2), 39-71.

McDonald, M. and Harbaugh, A. (1984). "A modular three dimensional finite difference ground-water flow model", *US Geological Survey*, Reston, VA.

Ponce, V. M., Li, Ruh-Ming, Simons, D. B. (1978). "Applicability of Kinematic and diffusion models", *J. Hydr. Engrg.,* ASCE, 104(3), 353-360.

Panton, R. L. (1984). "Incompressible Flow", *John & Wiley Sons*, NY, 315-316

Raviart, P. A. and Thomas, J. M. (1977). "A mixed finite element method for second order elliptic problems", in Galligani, I., and Magenes, E., editors, *Mathematical aspects of the finite element method*, Springer-Verlag, New York.

Seager, M. L. (1988). "SLAP, Sparse linear algebra package 2.0", based on the report "Routines for solving large sparse linear systems", *Lawrence Livermore National lab*, Livermore Computing Center, January 1986 Tentacle pp 15-21.

Smith, B. F., McInne, L. C. and Gropp, W. D. (1995). *PETSc 2.0 user manual*, Tech Rep. ANL-95/11, Argonne National Lab.

Strelkoff, T., Schamber, D., and Katopodes, N. (1977). "Comparative analysis of routing techniques for the flood wave from a ruptured dam", *Proceedings of Dam-Break Flood-Routing-Model Workshop held in Bethesda, MD*, held on Oct., 18-20, 1977. Sponsored by Water Resources Council. U. S. Dept. of Commerce, NTIS, PB-275 437, pp 227-291.

Tan, Weyyan. (1992). *Shallow water hydrodynamics*, Elsevier Publishing Co., NY.

Wang, Herbert. (1982). *Introduction to groundwater modeling*, W. H. Freeman Co. NY.

Xanthopoulos, T. and Koutitas, C. (1976). "Numerical simulation of a two-dimensional flood wave propagation due to dam failure", *Journal of Hydraulic Research*, 14 (4), 321-331.

Zhao, D. H., Shen, H. W., Tabios III, G. Q., Lai, J. S., and Tan, W. Y., (1994) "Finite-volume two-Dimensional unsteady-flow model for river basins", *J. Hydr. Engg.,* ASCE, 120(7), 863-883.

DEFINITION OF VARIABLES

Variable	Definition
E	energy head (m).
$\bar{\mathbf{F}}_r$	average flux vector across the wall r.
$\hat{\mathbf{F}}_k$	flux vector at a node k.
g	gravitational acceleration.
$\mathbf{H}$	average water levels of all the cells, in vector form (m).
$\hat{H}$	water levels at the nodes (m).
h	depth of water (m).
K	hydraulic conductivity (m/s).
$\mathbf{M}$	matrix obtained after linearizing $\mathbf{Q}$.
$\mathbf{n}$	unit normal to a wall.
n_b	Manning roughness coefficient.
$\mathbf{Q}(\mathbf{H})$	inflow into all the cells, in vector form.
Q_s	flow rate across a structure.
$\mathbf{S}$	source or sink terms for all the cells, in a vector form.
$\vec{S}_f$	friction slope vector.
S_n	slope of the water surface or the energy surface.
$\mathbf{V}$	flow velocity vector.
u, v	x and y components of flow velocity (m/s).
x,y	space coordinates (m).
$\hat{x}$,$\hat{y}$	nodal coordinates.
z	ground elevation above datum (m).
$\Delta\mathbf{A}$	a diagonal matrix with the cell areas at the diagonals.
ΔA_i	area of cell i

Variable	Definition
$\Delta\hat{A}_i$	area of shadow cell i
Δd_{mn}	distance between circumcenters of triangles m and n.
Δl_r	length of wall r.
δ_s	slope below which only an approximate Manning eq. is used.
Δt	time step (s).

Table 1: Solutions of the test problems using various discretizations. Results of test 0 with non-homogeneous cells are shown in Figs 5 and 6. CPU is an abbreviation for central processing unit time.

Test	No. elem.	No. nodes	CPU (s)	No. iter.	Δx (m)	Δt (s)	h_{end} (m)	π/ϕ	β	ε %
1	116	69	2.4	18	14939	51840	0.4488	2.15	0.016	1.09
2	116	69	8.8	12	14939	10368	0.4484	2.15	0.003	1.03
3	116	69	16.4	11	14939	5184	0.4484	2.15	0.002	1.02
4	376	209	6.0	40	8298	207360	0.4450	3.88	0.212	0.48
5	376	209	25.1	19	8298	20736	0.4446	3.88	0.021	0.40
6	376	209	43.6	17	8298	10368	0.4444	3.88	0.011	0.38
7	376	209	78.8	13	8298	5184	0.4444	3.88	0.005	0.37
8	1536	809	60.1	104	4105	518400	0.4540	7.84	2.166	1.96
9	1536	809	75.3	78	4105	207360	0.4449	7.84	0.866	0.48
10	1536	809	98.3	67	4105	103680	0.4450	7.84	0.433	0.48
11	1536	809	258.0	35	4105	20736	0.4439	7.84	0.087	0.29
12	1536	809	436.0	27	4105	10368	0.4437	7.84	0.043	0.27
0	238	135	27.7	1	10429	5184	0.4390		0.50	0.49

Table 2: Comparison of physical model results with the results of the finite volume models using circumcenter-based walls and line-integral-based walls. Results of the finite RBFVM-2D model by Zhao et al. (1994) are also shown.

Gage	Physical model		RBFVM-2D model		Circum. meth.		Line int. Meth.	
	Velocity m/s	Stage m	Velocity m/s	Stage m	Velocity m/s	Stage m	Velocity m/s	Stage m
C1	0.30	13.87	0.29	13.78	0.24	13.87	–	13.85
C3	0.23	13.57	0.21	13.60	0.26	13.66	–	13.62
C4	0.23	13.57	0.25	13.60	0.25	13.61	0.28	13.61
C5	0.23	13.57	0.29	13.57	0.25	13.60	0.29	13.59
C6	0.23	13.57	0.31	13.58	0.27	13.57	0.27	13.58
C7	0.29	13.57	0.33	13.69	0.21	13.57	–	13.57
O1	0.85	13.67	0.67	13.69	0.98	13.77	0.70	13.73
O2	0.49	13.67	0.44	13.64	0.06	13.60	0.14	13.64

LIST OF FIGURES

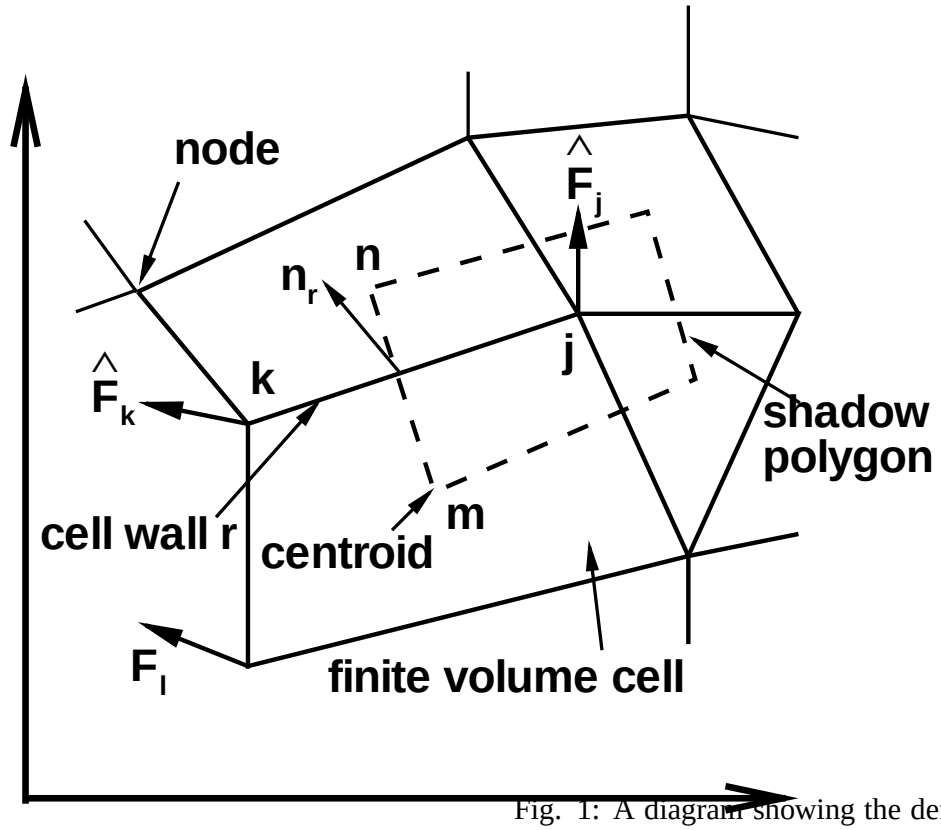

Fig. 1: A diagram showing the definition of variables used in the line integral method.

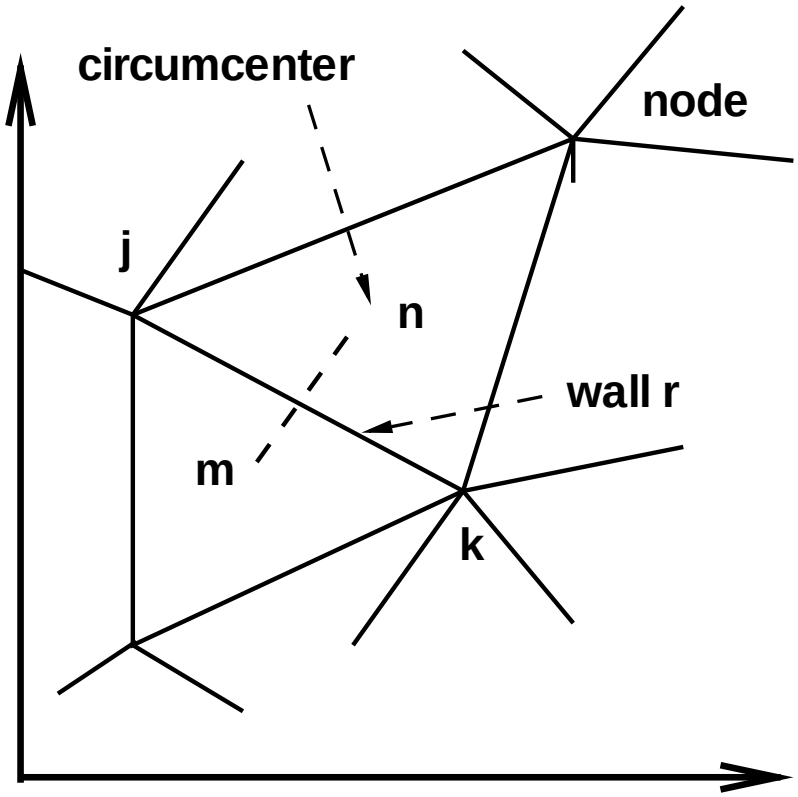

Fig. 2: A diagram showing the definition of variables used in the circumcenter method.

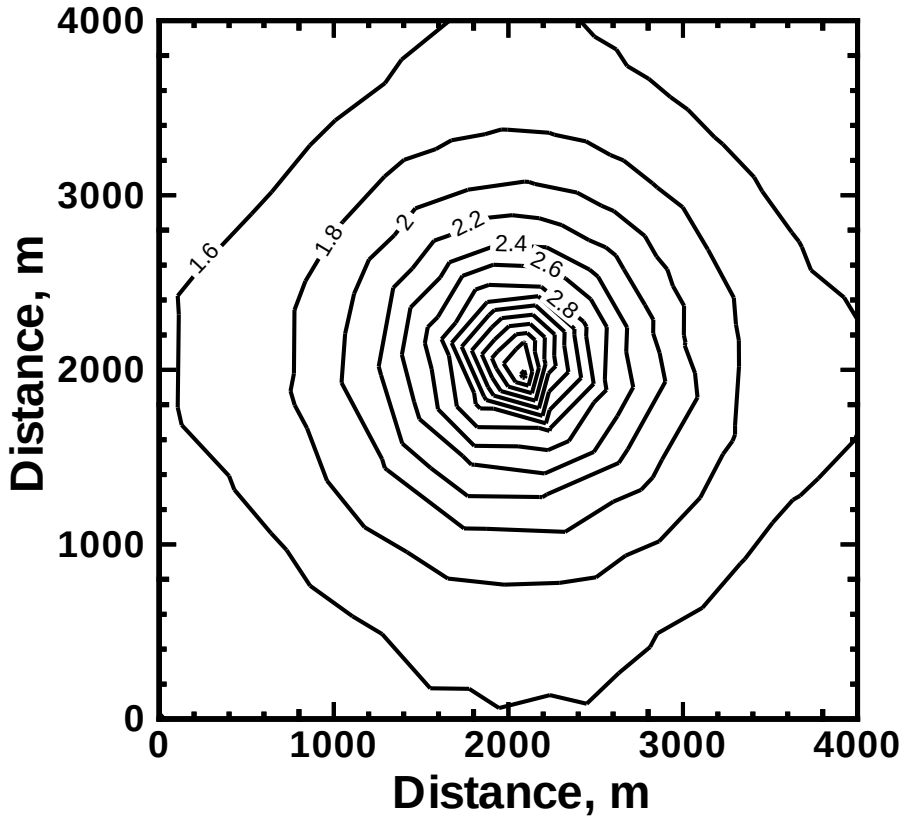

Fig. 3 a: Drawdown contours obtained using the finite volume model.

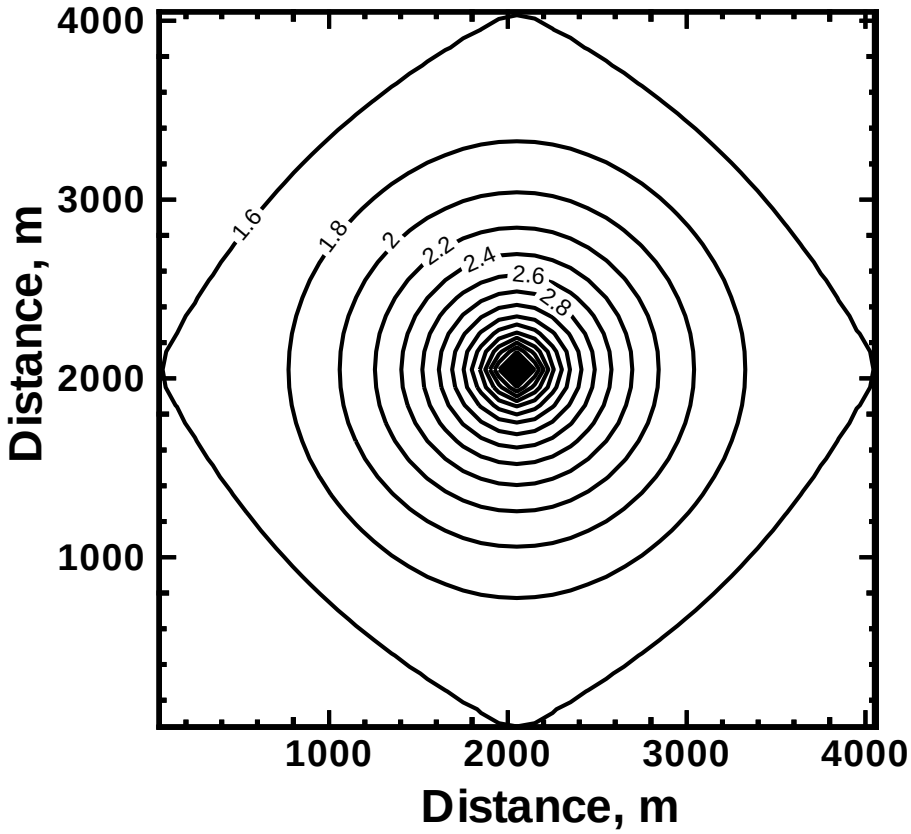

Fig. 3 b: Drawdown contours obtained using the MODFLOW model.

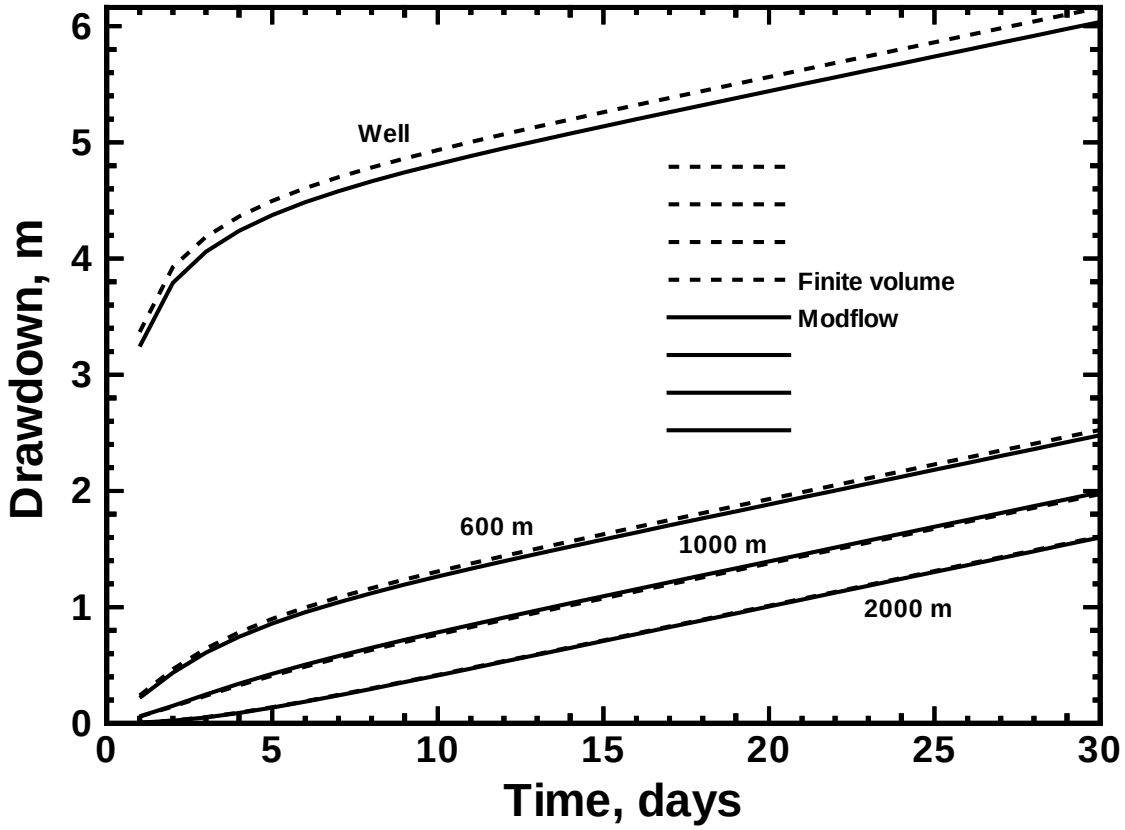

Fig. 4: Variation of drawdown with time at different distances.

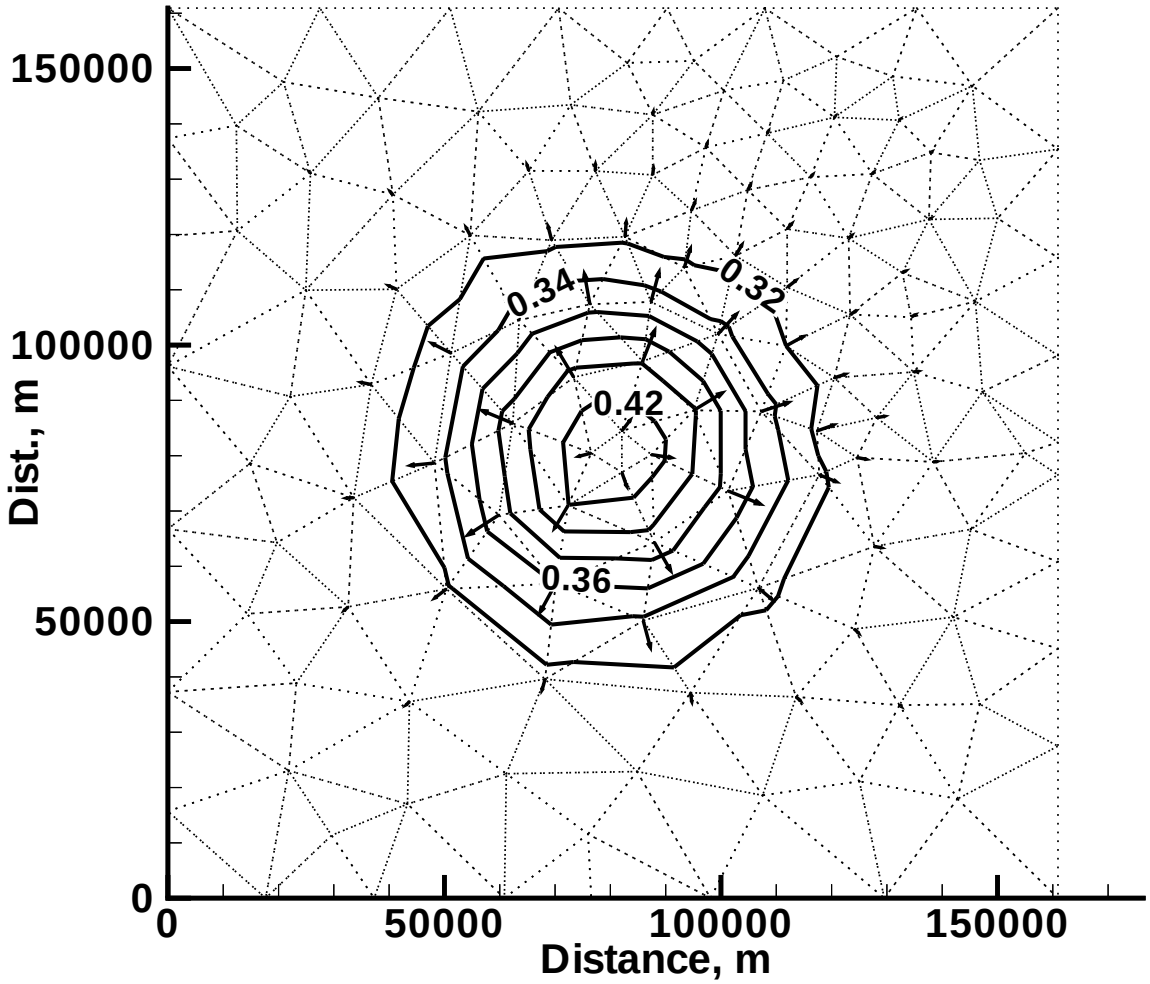

Fig. 5: A contour plot of the water levels in the axisymmetric test problem.

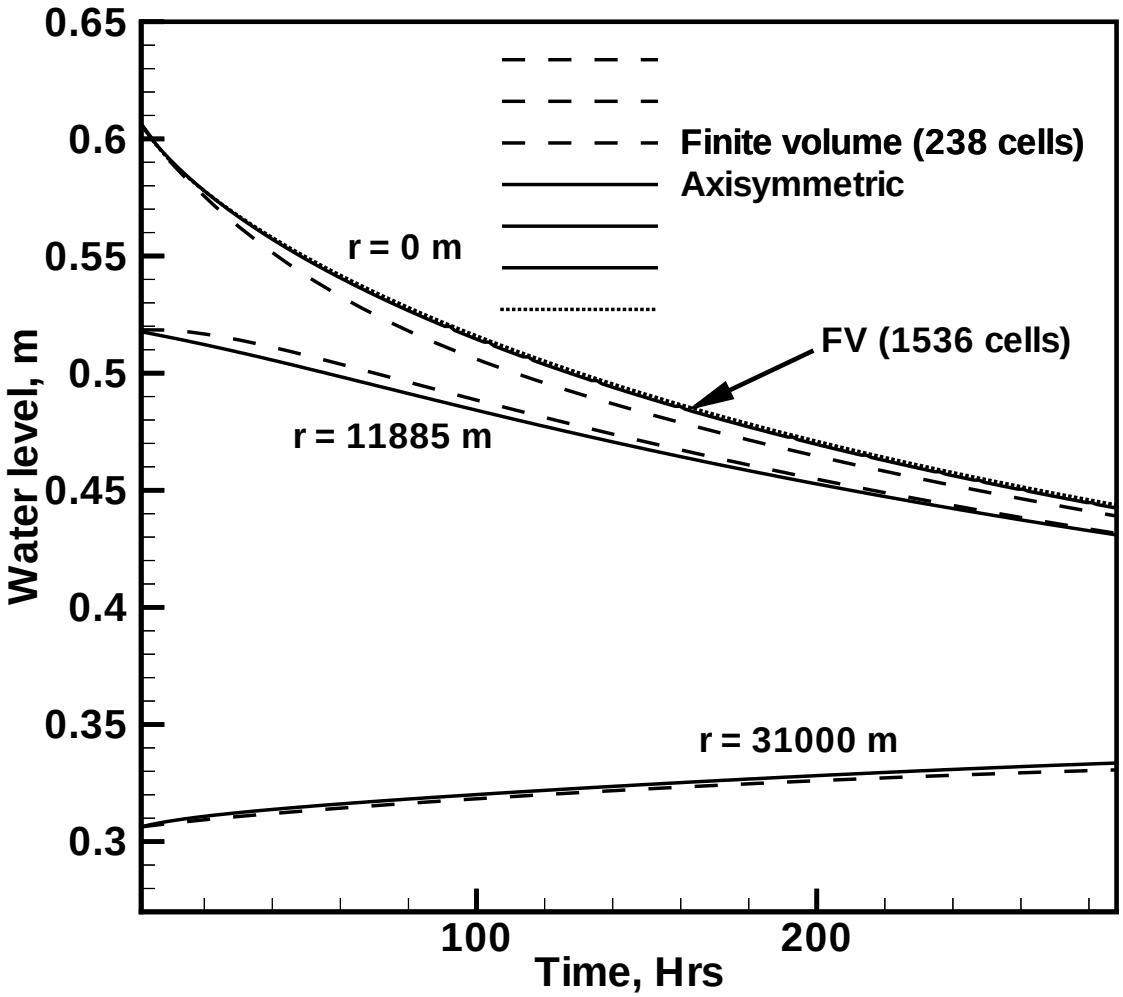

Fig. 6: Variation of the water level with time in the axisymmetric test problem.

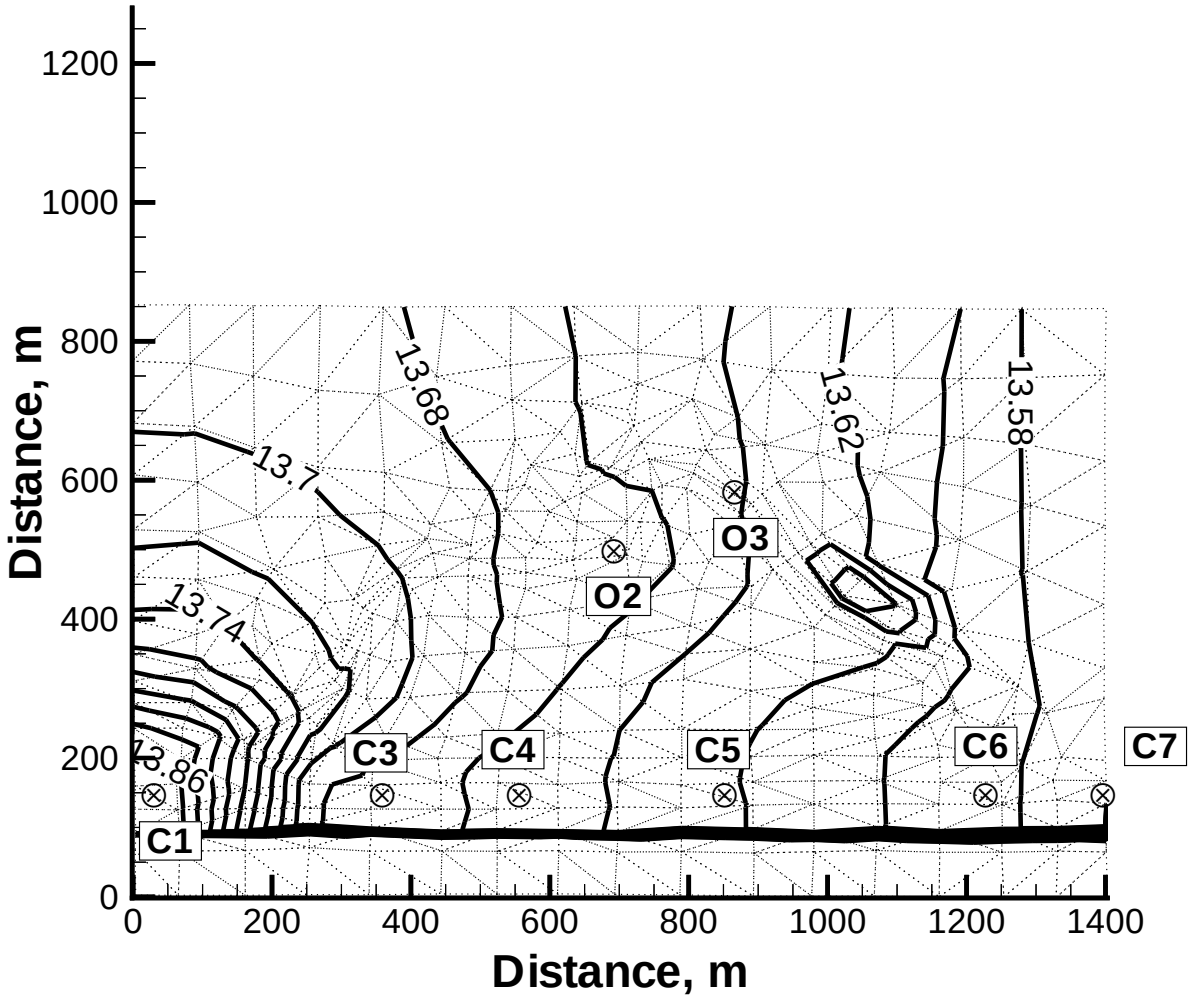

Fig. 7: A contour plot of the water levels in the Kissimmee river, obtained using the circumcenter method

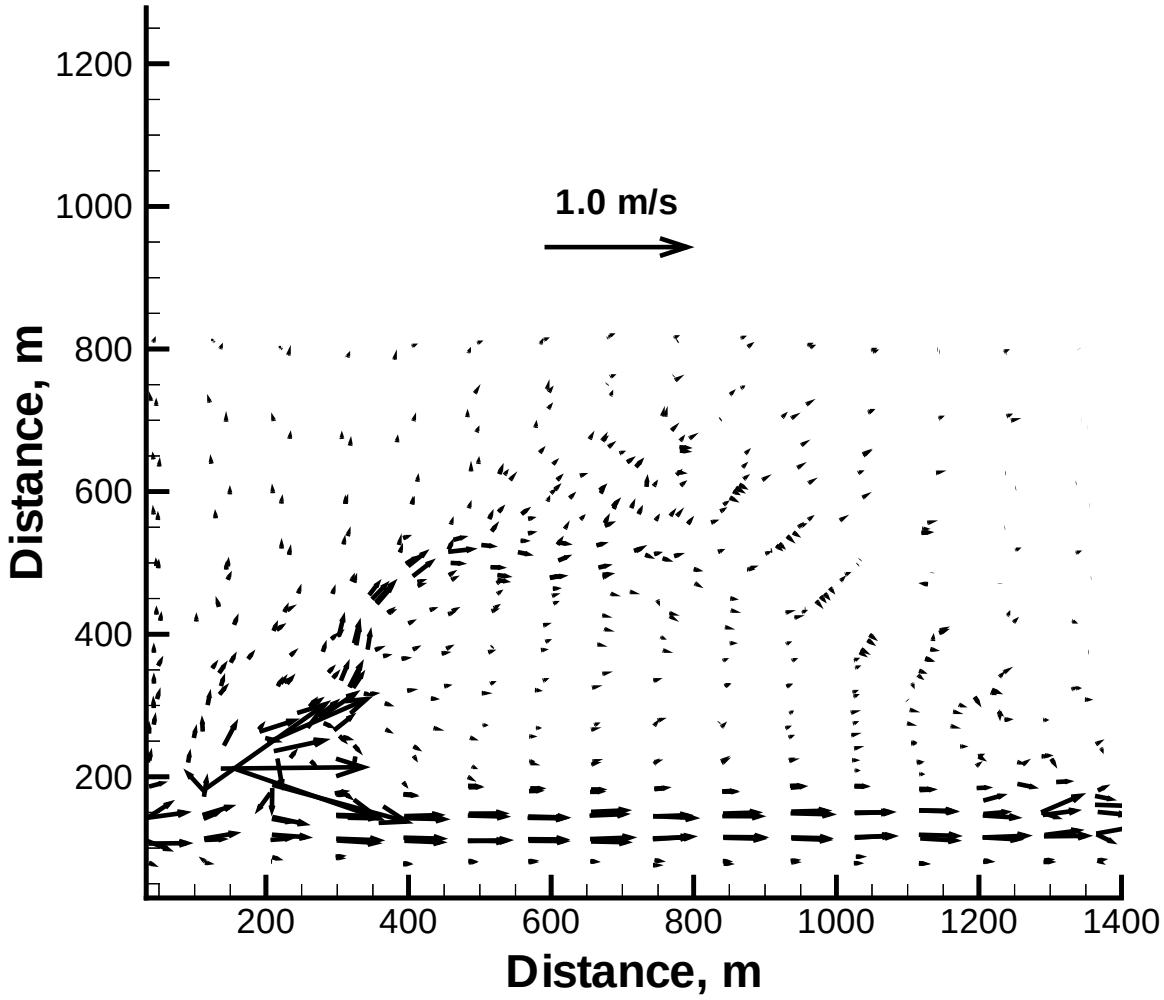

Fig. 8: A vector plot of the water velocities in the Kissimmee river obtained using the circumcenter-based walls.

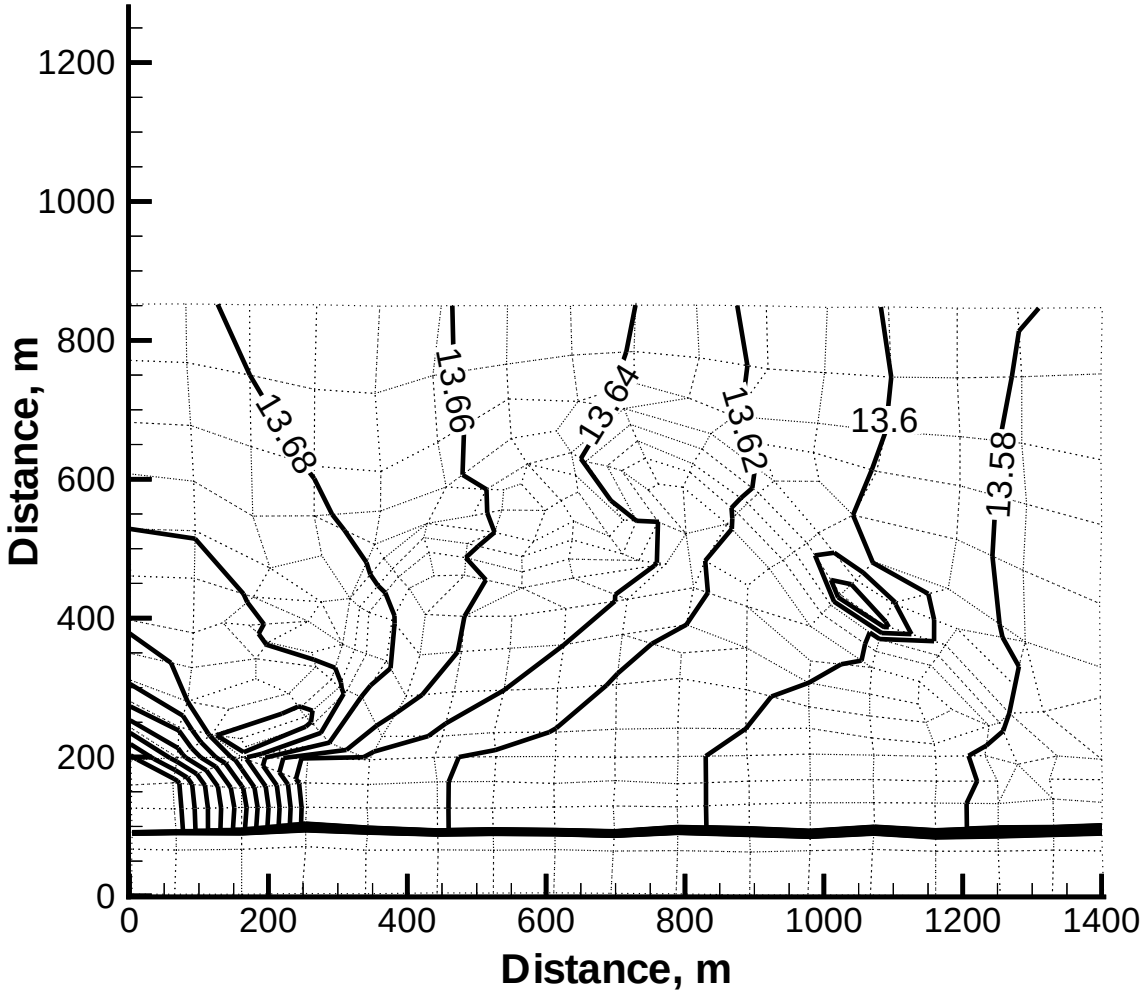

Fig. 9: A contour plot of the water levels in the Kissimmee river, obtained using the line-integral-based walls.

C.2 Numerical errors in groundwater and overland flow models

NUMERICAL ERRORS IN GROUNDWATER AND OVERLAND FLOW MODELS

A. M. Wasantha Lal

Lead Engineer

South Florida Water Management District

3301 Gun Club Road

West Palm Beach, FL 33406

ABSTRACT

Numerical error estimates are useful to evaluate the applicability of overland and groundwater flow models, and verify the validity of their results. In this paper, methods of estimating numerical errors are developed, and then applied to evaluate the numerical accuracy of the South Florida Water Management Model SFWMM. Analytical expressions for errors generated during the propagation of disturbances due to well pumping, boundary water-level changes and rainfall are obtained for steady and transient conditions using Fourier analysis of the linearized governing equations. Different situations under which truncation errors are introduced into models, and their variation with the spatial and temporal discretization are discussed. Numerical experiments are carried out with the MODFLOW model, and a number of implicit and explicit models to verify the results. Dimensionless parameters are used in the expressions so that the results can be used to determine discretization errors in in any existing or new finite difference model of regional or local scale.

INTRODUCTION

The number of computer models used to simulate various overland flow and groundwater flow conditions has increased recently due to the increased need to analyze environmental, agricultural and developmental issues. In South Florida, models of different scales are used for planning, management and regulation of water resources. Regional models are used mostly to address issues related to planning and management of water resources, while medium and small scale models, with county-wide and local coverages, are used for regulatory and permitting applications. The multi-agency efforts to implement the restoration of the Everglades have also increased the interest in, and requirement for various modeling efforts. As a result of the multiple and overlapping use of models, the need to understand, and properly apply and interpret the results of these models has increased greatly. The current study is aimed at understanding the relationships among spatial and temporal discretizations, and numerical errors of groundwater and surface water models. Both steady and unsteady cases are investigated for a variety of applications used in South Florida.

Most groundwater and overland flow models are based on applying a numerical method to solve a parabolic partial differential equation that is sometimes referred to as the diffusion equation. Diffusion flow models of varying resolutions are used to examine hydrologic processes at different scales. Numerical models of any scale contain uncertainties due to inaccuracies in the inputs, parameters, and algorithms. Input uncertainty is due to inaccurate or inadequate spatial and temporal input data such as rainfall, and evapotranspiration. This cause of uncertainty can be reduced by improving the data quality and the density of the data collection network. Parameter

uncertainty is mainly due to inaccurate values of spatially varying physical characteristics. This error can be reduced somewhat by calibration (Neuman, 1973, Willis and Yeh, 1987, Lal, 1995). Numerical errors are considered to be the source of algorithm uncertainty discussed in the present paper. Various unconditionally stable numerical methods using implicit or other methods have made it possible for modelers to use almost any discretization with computer models. Unlike explicit methods, where there is some error control because of the stability condition, implicit models such as MODFLOW need guidelines to select discretizations so that the error is known and controlled.

Richtmyer and Morton (1967) have compiled many of the basic developments behind consistency, convergence and stability of parabolic and other problems. In many of the early applications, the primary method of numerical error control is to use a discretization that satisfies the stability conditions derived using Von Neuman and other methods. Error analysis of partial differential equations generally provides an order-of-magnitude estimate. Error control is commonly used when solving initial value problems that involve ordinary differential equations, as in the Runge-Kutta-Fehlberg method and the Adams variable step-size predictor-corrector method (Burden and Fairs, 1985). Anderson and Woessner (1991) suggested that empirical methods based on model convergence should be applied to control numerical errors in MODFLOW applications. Hirsch (1989) used a method for error analysis based on linearization and Fourier Analysis. This method, which is similar to the Von Neuman method for stability analysis, has been used for diffusion and other equations. Lal (1998) used the same method with additional expressions derived for compu-

tational time to evaluate and compare the computational performances of various numerical models used to solve diffusion equations. The subject of error analysis and output evaluation has become increasingly important because the space and time discretizations used in some model applications are arbitrarily chosen. The use of unconditionally stable implicit methods has also complicated the use of the stability condition as an error control. The current study extends the ideas of Fourier analysis used by Hirsch (1989) and Lal (1998a) to develop expressions for numerical errors of many groundwater flow and overland flow models.

Numerical errors are introduced when the solution to the governing partial differential equations is represented by discrete values in the model, and when these discrete values are used in numerical computations in the finite difference method. Numerical errors introduced in the representation of data and during computations are discussed in the present paper. Stresses and errors due to conditions common in South Florida such as variable water levels in canals, variable pumping rates in wells, and variable rainfall are analyzed separately. The principle of superposition makes it possible to combine these cases. The error analysis is conducted for an arbitrary Fourier component and the steady state. The results are presented in dimensionless forms and verified using MODFLOW and other models. The results can be used in a wide variety of practical problems to determine numerical error. An application of the method is presented to demonstrate the evaluation of an overland flow model and a groundwater flow model for South Florida.

NUMERICAL SOLUTION OF THE DIFFUSION EQUATION

Two dimensional groundwater flow and overland flow can be explained using the following gov-

erning equation. For overland flow, the equation is derived by neglecting the inertia terms in the St Venant equations. (Hromadka and Lai, 1985, Lal, 1998).

$$s_c \frac{\partial H}{\partial t} = \frac{\partial}{\partial x}\left(K \frac{\partial H}{\partial x}\right) + \frac{\partial}{\partial y}\left(K \frac{\partial H}{\partial y}\right) + S \tag{1}$$

in which, $H = h + z =$ water level or water head; $S =$ source and sink terms representing rainfall, evapotranspiration and infiltration. For overland flow, $h =$ water depth; $K = \frac{h^{\frac{5}{3}}}{n_b \sqrt{S_n}}$ when the Manning's equation is used; $n_b =$ Manning's coefficient; $S_n =$ water surface slope and $s_c = 1$. For groundwater flow, $s_c =$ storage coefficient; $K =$ transmissivity of the aquifer, assuming an isotropic material; $K \approx k_c \bar{h}$ for unconfined flow in which $\bar{h} =$ water depth of the saturated layer and $k_c =$ hydraulic conductivity. The flow vector is computed using

$$\vec{Q} = K \vec{\nabla} H \tag{2}$$

in which, $\vec{Q} =$ flow vector giving flow rate per unit width. When a weighted implicit finite volume formulation is used, (1) can be expressed for an arbitrary cell as (Lal, 1998)

$$H_{i,j}^{n+1} = H_{i,j}^{n} + \alpha\, Q_{net}(H^{n+1}) \frac{\Delta t}{s_c \Delta A} + (1-\alpha)\, Q_{net}(H^{n}) \frac{\Delta t}{s_c \Delta A} + \frac{\bar{S} \Delta t}{\Delta A} \tag{3}$$

in which $\Delta A =$ area of the cell; $Q_{net} =$ net inflow to the cell; $\alpha =$ weighting factor for semi-implicit schemes; $n =$ time step; $\bar{S} =$ weighted average source term for the area during the time step. For the rectangular grid used in the study, $Q_{net}(H)$ is given by

$$Q_{net}(H) = K_{i+\frac{1}{2},j}(H_{i+1,j} - H_{i,j}) + K_{i-\frac{1}{2},j}(H_{i-1,j} - H_{i,j})$$
$$+K_{i,j+\frac{1}{2}}(H_{i,j+1} - H_{i,j}) + K_{i,j-\frac{1}{2}}(H_{i,j-1} - H_{i,j}) \quad (4)$$

Explicit and the implicit methods are obtained by using $\alpha = 0$ and 1.0 with (3) and (4).

NUMERICAL ERROR ANALYSIS

Numerical errors are present in computer models because of the use of discrete values to represent continuous functions explaining flow conditions, and the use of numerical methods to approximately solve the governing equations. Texts by Richtmyer and Morton (1967) and Sod (1985) are two of the early and recent books that describe the general methods of Fourier analysis and complex analysis used in analyzing numerical methods, and in analyzing errors in the current paper. Hirsch (1989) described the adaptation of some of these methods of stability analysis to error analysis.

In this paper, errors are considered to be introduced in three different ways even if they can all be classified as truncation errors.

(A) Errors are introduced when the initial and boundary condition data are recorded and provided to the model as discrete values in time and space. Due to this type of error in ”representation”, spectral components in the solution with frequencies or wave numbers above a certain value are either completely truncated, or not represented accurately.

(B) Errors are introduced if the internal discretization of the model is not sufficient to carry the

solution over the entire time and space domain. For example, even if the time step is sufficient to describe a boundary disturbance, if the spatial discretization is inadequate at any point in its path, the solution may not propagate accurately.

(C) Numerical errors are also introduced when computations are carried out using the Fourier components that are left over and did not vanish due to reasons given in (A) and (B). Computer models are based on numerical approximations for derivatives, etc. They use finite differences and other methods for these approximations. The truncation errors resulting from these approximations are considered here, and are computed using Fourier analysis.

Higher frequency components in the solution are subjected to these errors more than the lower frequency components. They will be quantified using an arbitrary Fourier component of the solution. Assuming that a component can be described using its wave number k ($k = 2\pi/$ wavelength) or frequency f ($f = 2\pi/$ period), the following approximate expressions were obtained for time or space discretization errors (A) and (B) of 1-D and 2-D problems. A Monte Carlo method was used to determine these errors by representing a large number of different 1-D and 2-D wave shapes with random wave numbers and random phase shifts using a uniform grid, and estimating the maximum errors between the true solution and the linearly interpolated grid–based solution.

$$\phi = 0.5\sqrt{\varepsilon_d} \quad \text{or} \quad \varepsilon_d = 4.0\,\phi^2 \quad \text{for 1-D} \tag{5}$$

$$\phi = 0.35\sqrt{\varepsilon_d} \quad \text{or} \quad \varepsilon_d = 7.8\,\phi^2 \quad \text{for 2-D} \tag{6}$$

in which, ε_d = maximum percentage discretization error. The spatial discretization error ε_d exists even with the smallest time steps possible. $\phi = k\Delta x$ is the dimensionless form of Δx. The same

equation applies for time discretizations when ϕ is replaced with ψ in which $\psi = f\Delta t$. Quantity ϕ was also used by Hirsch (1989) to make Δx dimensionless. ε_d only depends on the geometrical shape of the wave form. For 1-D problems, 1% and 5% errors in discretization, for example, correspond to ϕ or ψ equal to 0.5 and 1.1 respectively. For 2-D problems, they correspond to ϕ or ψ equal to 0.35 and 0.80 respectively. An easier way to visualize ϕ or ψ is to consider that approximately $\frac{\pi}{\phi}$ grid spaces or discretizations are needed to describe half the wave length of a sine wave. It can be seen that approximately six grid spaces are needed over the length of half a sine wave to represent it so that the maximum error is $< 1\%$. Three discretizations per half sine wave or $\phi = 1.05$ makes the maximum error $< 4.5\%$. Equation (6) can also be obtained using actual model runs (Lal, 1998a).

The error explained in (B) can be understood by realizing that k and f of a single Fourier component are related as a result of the governing equations. The relationship between f and k can be obtained for diffusion flow using solutions of the form $H = H_0 e^{I(kx - ft)}$ and $H = H_0 e^{I(kx+ky-ft)}$ respectively for 1-D and 2-D problems in which $I = \sqrt{-1}$. In the case of 2-D problems, k is assumed to be the same in both x and y directions for simplicity. Substituting the above forms of the solution in the governing equations, it can be shown that wave number k of a sinusoidal water level variation in a semi-infinite aquifer is related to the disturbing frequency f by

$$f = d\frac{K}{s_c}k^2 \tag{7}$$

in which, $d = 1$ and 2 for 1-D and 2-D problems respectively. For a problem with a constant disturbance $H = H_0 \sin(ft)$ maintained at the boundary, the same solution is true with $d = 2$ and 4 for

1-D and 2-D problems.

Computational errors

To estimate computational errors (C), the behavior of the numerical scheme in response to an arbitrary i th harmonic with a wave number $k_i = \frac{i\pi}{N}$ is compared with the behavior of the governing equation with respect to the same harmonic. In the equation, $N = L/\Delta x$ in which L is the length of the domain in x direction. A grid spacing of Δx would allow a minimum wave length $\lambda_{min} \approx 2\Delta x$ and a maximum wave length $\lambda_{max} \approx 2L$. In the analysis, a term ϕ_i defined as $\phi_i = k_i \Delta x$ is used to represent the i th harmonic in dimensionless form (Hirsch, 1989). The subscript is often removed for simplicity. A term $\psi = f\Delta t$ can be defined similarly to represent a harmonic in the time domain, in which the frequency $f = 2\pi/T_p$, and $T_p =$ wave period. ϕ is used as the dimensionless variable to describe the spatial discretization.

For numerical methods based on finite differences, an analytical expression can be derived for the numerical error (Hirsch, 1989, Lal, 1998).

$$\varepsilon = 1 - |G| \tag{8}$$

in which, $\varepsilon =$ magnitude of the analytically computed numerical error per time step as a fraction of the amplitude; $G =$ ratio of amplitudes of numerical and analytical solutions, or the amplification factor of the numerical method.

$$G = \frac{1 - 4d(1-\alpha)\beta \sin^2(\phi/2)}{1 + 4d\alpha\beta \sin^2(\phi/2)} \frac{1}{e^{-d\beta\phi^2}} \tag{9}$$

$\beta = \frac{K\Delta t}{s_c \Delta x^2}$ = non-dimensional form of Δt; $d = 1, 2$ for one and two dimensional problems with

square grids. Equation (8) which is derived assuming the analytical solution (7) (Hirsch, 1989) can be expanded to give

$$\varepsilon = \pm\frac{d^2\beta^2\phi^4}{2} + \frac{d\beta\phi^4}{12} + \ldots = \pm\frac{d^2k^4K^2\Delta t^2}{2\,s_c^2} + \frac{dKk^4\Delta t\Delta x^2}{12\,s_c} + \ldots \tag{10}$$

in which $+$ and $-$ signs correspond to implicit and explicit models respectively. The cumulative numerical error after many time steps, ε_T, depends on the number of time steps n_t, and the error at each time step ε. Error ε_T is bounded by $n_t\varepsilon$, in which $n_t = T/\Delta t$. This bound is obtained by assuming that the errors are additive. In the sine cycle, these errors are additive for half the cycle and subtractive for the other half. The bound is

$$\varepsilon_T \approx \frac{\varepsilon}{\beta\phi^2}\frac{TKk^2}{s_c} = \frac{\varepsilon}{d\beta\phi^2} fT \tag{11}$$

where, $k =$ wave number of the harmonic; $T =$ maximum duration over which a given harmonic stays in the computational domain and accumulates errors. Examples shown below demonstrate how fT is computed. In the problem of a water level variation driven by a stationary rainfall pattern, $fT = \pi/4$ because the error is largest after a quarter cycle. In the problem of a water level disturbance at the boundary of a semi-infinite aquifer, the disturbance travels at a speed of f/k, and covers a distance X in time T making $fT = kX$. It can be shown using (16) described later that the absolute error in this problem is maximum when $fT = 1$. Similarly it can be shown that $fT < 3$ for most practical applications for which error $< 5\%$.

Equation (11) can be simplified by using a truncated Taylor series expansion. For explicit,

implicit and semi-explicit 1-D and 2-D finite difference models,

$$\varepsilon_T \quad \text{(expl/impl 1-D)} \quad \approx \quad \frac{fT\phi^2}{2}(\mp\beta - \frac{1}{6}) \tag{12}$$

$$\varepsilon_T \quad \text{(semi-impl 1-D)} \quad \approx \quad fT\left[\frac{\phi^2}{12} - \frac{\phi^4}{12}(\beta^2 - \frac{1}{30})\right] \tag{13}$$

$$\varepsilon_T \quad \text{(expl/impl 2-D)} \quad \approx \quad fT\phi^2(\pm\beta - \frac{1}{12}) \tag{14}$$

$$\varepsilon_T \quad \text{(semi-impl 2-D)} \quad \approx \quad fT\left[-\frac{\phi^2}{6} + \frac{2\phi^4}{3}(\beta^2 + \frac{1}{120})\right] \tag{15}$$

The positive and negative signs apply for the explicit and implicit methods respectively. Semi-implicit methods use $\alpha = 0.5$. Explicit 1-D and 2-D models additionally require $\beta < 0.5$ and $\beta < 0.25$ respectively for stability. Numerical experiments will later show that offsets of β such as $1/6$ and $1/12$ in (12) and (13) can be neglected especially with implicit methods using relatively large β. The above equations also show that semi-implicit methods are second order accurate in time because β is to the second power.

PROPAGATION OF ERRORS

When the water level in a canal, tidal bay or the ocean varies, a disturbance in head is created which travels away from the source of the disturbance. Water level changes due to such stresses constitute an important part of the solution in many models. To understand numerical errors in such solutions, propagation of a sinusoidal disturbance $H = H_0 \sin(ft)$ in a semi-infinite aquifer is studied in 1-D. It can be shown that the analytical solution for head in such a semi-infinite medium is

$$H(x,t) = H_0 e^{-kx} \sin(ft - kx) \tag{16}$$

in which, $f = 2Kk^2/s_c$ according to (7). The analytical solution for discharge is given by

$$Q(x,t) = \sqrt{2}KkH_0 e^{-kx} \sin\left(kx - ft - \frac{\pi}{4}\right) \tag{17}$$

Equation (16) shows that the amplitude H becomes less than 1%, 5% and 37% of the starting amplitude H_0 when $fT = kX > 5$, 3 and 1 respectively in which T and X are described earlier as the time or the distance of evolution over which errors accumulate. These values show that the waveforms become negligible after traveling about one cycle. Instead of the fixed percentages such as 1% or 5%, if the decayed amplitude is expressed as a fraction α_d of the original amplitude in (16), the ratio of the amplitudes of $H(x,t)$ and H_0 or $\exp(-kx) = \alpha_d$ can be used to express the exact solution (7) as

$$\frac{s_c X^2}{KT_p} = \frac{(\ln \alpha_d)^2}{\pi} \quad \text{or} \tag{18}$$

$$\frac{KT}{s_c L_p^2} = -\frac{\ln \alpha_d}{8\pi^2} \tag{19}$$

in which, $T_p =$ period of the wave; $L_p =$ wave length. These equations are similar to the equations derived by Townley (1995) and used by Haitjema (1995) for transient state analysis. They can be used to determine the length and the time scales of a disturbance in a porous medium when the disturbance has a period T_p or a wave length L_p. The numerical error at a distance x from the point of disturbance is computed using (11) and $fT = kX$ as discussed earlier.

$$\varepsilon_T(x) = \frac{k\varepsilon}{\beta\phi^2} x \tag{20}$$

This equation shows that as a percentage, the numerical error increases linearly with x. Since water level fluctuations decrease exponentially, the absolute error first increases and then decreases with

the distance, giving a maximum ε_T of approximately $0.37\phi^2\beta$, at $fT = kX = 1$.

In order to verify the accuracy of the analytical estimates for numerical error, ε values were computed for a 1-D semi-infinite problem using both analytical and numerical methods. The numerical experiment involved studying the decay of the amplitude of a sinusoidal boundary disturbance with distance. The error in the amplitude of the numerical model ε_T was determined by subtracting the analytical amplitude from the amplitude obtained for the numerical model. Equations (16) and (17) were used to compute analytical amplitudes. The graph of ε_T against x is obtained by subtracting the analytical amplitude envelope from the model amplitude envelope. To obtain the model amplitude envelope, over 1000 cycles of sine waves were passed through the domain first until a sufficiently steady initial initial condition is reached. Then, the envelope was determined by sending over 200 sine waves until a fairly steady envelope curve is formed. Figure 1 shows one such amplitude envelope for the MODFLOW model ($\phi = 0.8$, $\beta = 0.78$) and its graph of ε_T versus number of grids points from the boundary, when the total number of equally spaced grid points is 100. Errors at the sine wave peaks (maximums) and troughs (minimums) are both shown. The graph of ε_T versus x is approximately straight near the boundary, and has a gradient $k\varepsilon/(\beta\phi^2)$ according to (20). Model values of ε can be obtained for various computer models using this gradient. Each of the numerical experiments leads to one point in the ε versus β plot. Since dimensionless parameters are used, the actual physical dimensions and physical constants used in the tests are not important. The analytical plot of ε versus β was obtained using (8). Explicit, semi-implicit and the fully implicit MODFLOW models values were obtained using $\alpha = 0.0$, 0.5

and 1.0 with $d = 1$.

Figures 2, 3 and 4 show the ε values observed in the ADI, explicit and the MODFLOW(PCG2) models respectively and the corresponding analytical values. A range of ϕ values such as 0.2, 0.4 and 0.8 were used in the experiments. All the figures show that the analytical and numerical plots of ε agree very closely, implying that the analytical expressions derived for numerical error are accurate for the models investigated. These results are similar to the results shown by Lal (1998a) obtained using a water level subsidence experiment. Figure 3 shows that the error measured as the (numerical value – analytical value) is small when $\beta \approx 0.16$, and becomes negative when $\beta < 0.16$. The dashed line in Figure 3 shows that the approximate form of the analytical solution in (12) based on a truncated Taylor series is also relatively accurate. The behavior of error with β and ϕ for a problem with a triangular mesh is demonstrated in the paper by Lal (1998b).

NUMERICAL ERRORS OF FLOW VELOCITY AND DISCHARGE

In overland flow and groundwater flow models based on the diffusion equations, discharge across two neighboring cells is

$$Q^n_{i+1/2,j} = K\frac{H^n_{i+1,j} - H^n_{i,j}}{\Delta x} \tag{21}$$

in which, $H^n_{i,j}$ and $H^n_{i+1,j}$ are the heads of the cells; $Q^n_{i+\frac{1}{2},j}$ = flow rate betweens cells per unit width. In order to compute the numerical error in the flow, a solution for a Fourier component of the form $H^n_i = H^n_0 \exp(I\phi i)$ is substituted in (21) to obtain $Q^n_{i+1/2} = 2KH^n_0 I \sin(\phi/2)/\Delta x$. Using an analytical solution of the form $H(x,t) = H_0 \exp(-Kk^2 t)\exp(Ikx)$ for which the numerical solution is H^n_i, the governing equation can be used to obtain the analytical flow rate as $Q(x,t) = KkIH(x,t)$. The ratio between numerical and analytical amplitudes of $Q^n_{i+1/2}$ and $Q(x,t)$ can now be used to compute the numerical error as $\varepsilon_Q = 1 - 2|G|\sin(\phi/2)/\phi$ in which $|G|$ in (8) is computed as $H^n_i/H(x,t)$. ε_Q can be related to ε for small ϕ using the approximate relationship

$$\varepsilon_Q \approx \varepsilon\frac{2\sin(\frac{\phi}{2})}{\phi} \tag{22}$$

in which ε_Q = numerical error in discharge for one time step, as a fraction of the analytical discharge for the specific Fourier component. Numerical errors in flow velocity and discharge are given by the same expression. Comparison of (8) with (22) shows that the error in the head and the discharge are approximately the same, with the former slightly higher.

The accuracy of (22) can be verified in the same way it was done for the head, by simulating the propagation of sinusoidal disturbances in head, and observing the decay of the amplitudes of the sinusoidal discharge rate with distance. This method is similar to the method used for errors in

head. The method is started by first running a model for a long period of time, passing over 10000 cycles of waves until a fairly steady wave shape is established as the initial condition. Errors are computed by assuming the analytical solution (17) to be exact. The gradient of the error versus distance curve is used as before to compute ε_Q for the model. Figure 5 shows a plot of ε_Q with β for a fully implicit model ($\alpha = 1$) when $\phi = 0.5$, 1.0, and 1.5. According to the figure, the analytical estimates of error compare well with the values observed in the models.

NUMERICAL ERRORS NEAR WELLS UNDER VARIABLE PUMPING RATES

Numerical errors of model results are large close to groundwater wells because of the extreme curvature in the solution. The Thiem equation provides an approximate but efficient method to compute water levels very close to a well when the water level of the cell is known (Anderson and Woessner, 1991). Numerical error at and near a cell containing a well subjected to a variable pumping rate is investigated in this section. The results are useful in selecting the optimal discretization for new models, and in evaluating the output of existing models. All the formulas are derived for an arbitrary Fourier component of the pumping rate time series. The well is assumed to be circular, and situated at the center of a square cell to simplify the derivations. Even if some of these assumptions may not be true in the actual application, results of the study are useful in understanding the behavior of numerical errors near wells.

The following equation governing groundwater flow around a well is used for the analysis.

$$s_c \frac{\partial H}{\partial t} = \frac{K}{r} \frac{\partial}{\partial r} \left(r \frac{\partial H}{\partial r} \right) \tag{23}$$

Consider a solution in the form $H = R(r)T(t)$ in which $T(t) = \exp(Ift)$. Using separation of

variables, (23) can be reduced to

$$r^2\frac{d^2R}{dr^2}+r\frac{dR}{dr}-\frac{IfRr^2s_c}{K}=0 \tag{24}$$

Using a characteristic length $\lambda=\sqrt{K/(fs_c)}$, radius r can be made dimensionless as $\hat{r}=r/\lambda$. Similarly, t can be made dimensionless using $\hat{t}=ft$. The general solution of (24) that is also finite at $\hat{r}\rightarrow\infty$ can be expressed as

$$H(\hat{r},\hat{t})=cK_o(\hat{r})\exp(I\hat{t}) \tag{25}$$

in which $K_o(\hat{r})$ is a modified Bessel function; $c=$ a constant that has to be determined for the specific problem with specific boundary conditions. Consider a well of radius r_w pumped with a sinusoidal pumping rate $Q(t)=Q_0\sin(\hat{t})$. The constant c can be determined by assuming that $Q(t)=$ flow rate at $\hat{r}=\hat{r}_w$ of the solution in (25) in which $\hat{r}_w=$ dimensionless well radius. This assumption is valid for most wells in South Florida where the storage capacity of the well is negligible. Substituting c into (25), it is possible to obtain the analytical solution of the pumping problem as

$$H(\hat{r},\hat{t})=\frac{s_cQ_0K_o(\hat{r})}{2\pi K\hat{r}_wK_1(\hat{r}_w)}\sin(\hat{t})\quad\text{for}\quad\hat{r}>\hat{r}_w \tag{26}$$

In the case of extremely small diameter wells, $\hat{r}_wK_1(\hat{r}_w)\rightarrow 1$ as $\hat{r}_w\rightarrow 0$, and (26) becomes

$$H(\hat{r},\hat{t})=\frac{s_cQ_0K_o(\hat{r})}{2\pi K}\sin(\hat{t}) \tag{27}$$

Equation 26 shows that the amplitude decays rapidly with distance as exhibited by the behavior of K_o. Equation 26 is used as the exact solution when computing the numerical error in a square finite difference cell. Table 1 shows the variation of the portion $K_0(\hat{r})/(\hat{r}_wK_1(\hat{r}_w))$ of (26) as an indicator of this amplitude. The table shows the influence of the well; for example, when $\hat{r}>2.75$

and $\hat{r}_w$ =0.5 or less, the amplitude of the water level fluctuation will decay to less than 5%. When $\hat{r}_w$ =0.1, then $\hat{r} > 1.95$ for the amplitude to decay to 5%.

In order to determine the numerical error in a model when used to simulate pumping, a $\Delta x \times \Delta x$ square cell containing the well is simulated by approximating it as an axisymmetric problem. The square cell is approximated as a circular area of an equivalent radius. The head at this radius is considered as the model head for that cell. The equivalent problem is solved by assuming the solution to be in the form (25) with a value of c to be determined using a water balance equation. Integral form of the continuity equation for the cell is as shown below, in which the first term is the pumping rate, the second term is the seepage rate through the cell wall, and the third term is the rate of change of total water volume in the cell.

$$-Q(t) + 2\pi r_c K \left(\frac{\partial H}{\partial r}\right)_{r=r_c} \approx \int_{r=0}^{r_a} 2\pi r s_c \frac{\partial H}{\partial t}\, dr \tag{28}$$

in which a radius $r_c = a_c \Delta x$ is used to compute the approximate seepage rate into the $\Delta x \times \Delta x$ cell. Anderson and Woessner (1991) used r_c as the radius of a well at which the drawdown for pumping rate $Q(t)$ is given by the numerical solution based on a grid spacing Δx. The radius $r_a = a_a \Delta x =$ radius at which the square cell area is equal to the area of the circle. The value of a_c is 0.208 (Anderson and Woessner, 1991), and the value of a_a is 0.564 because $\Delta x^2 = \pi r_a^2$. The pumping rate is assumed as $Q(t) = Q_0 \sin(ft)$. The value of c obtained by substituting (25) into (28) is used in (25) to obtain the head in the numerical model as

$$H_c(\hat{r},\hat{t}) = \frac{s_c Q_0 K_o(\hat{r}) \sin(\hat{t} - \hat{t}_o)}{2\pi K \hat{r}_c K_1(\hat{r}_c) \sqrt{\left[1 + \left(\frac{M_o(\hat{r}_a)}{\hat{r}_c K_1(\hat{r}_c)}\right)^2\right]}} \quad \text{for} \quad \hat{r} \geq \hat{r}_c \tag{29}$$

in which, $M_o(r_a)$ is defined as

$$M_o(\hat{r}_a) = \int_0^{\hat{r}_a} \hat{r} K_o(\hat{r})\, d\hat{r} \tag{30}$$

$\hat{t}_0 =$ a time lag error which is not investigated further in the current study. Value of $H = H_c$ obtained at $\hat{r} = \hat{r}_c$ in (29) is considered as the numerical value of the cell containing the well. The exact solution is given by (26) at a radius $\hat{r} = \hat{r}_c = 0.208\Delta x$. They differ in amplitude and phase. The difference in amplitude is used to compute the approximate numerical error by first computing the ratio C_c between the amplitudes of the numerical and exact solutions. The approximate error in amplitude is $\varepsilon_w = 100(1 - C_c)$, compared to a well of effective radius r_c. Using (29) and (26), C_c can be expressed as

$$C_c = \frac{1}{\sqrt{\left[1 + \left(\frac{M_o(\hat{r}_a)}{\hat{r}_c K_1(\hat{r}_c)}\right)^2\right]}} \tag{31}$$

To compute the numerical values of ε_w, $\hat{r}_c = a_c \Delta x \sqrt{(fs_c/K)}$ and $\hat{r}_a = a_a \Delta x \sqrt{(fs_c/K)}$ are used with $a_c = 0.208$ and $a_a = 0.564$. Table 2 shows the values of ε_w obtained for various values of $\Delta x \sqrt{(fs_c/K)}$. It shows that the amplitudes of head in the numerical model are less than or equal to exact values. Table 2 also shows that when $\Delta x \sqrt{(fs_c/K)}$ is larger than about 1.4, the error in the cell containing the well is more than 5%. When $\Delta x \sqrt{(fs_c/K)} > 5$,the error is larger than 43%, and the cell size is comparatively larger than the radius of influence of the well. The dynamics of water level fluctuation in the well at this point are dominated by the storage of water in the cell. Error ε_w is the smallest numerical error possible as time step $\Delta t \to 0$. Linear superposition can be used to compute the effects of multiple wells with steady and unsteady dumping rates.

In order to verify these results, a test is carried out with a 50 X 50 cell MODFLOW model with 2000 m square cells in a confined aquifer of $K/s_c = 500$, using a sinusoidal pumping rate of a variable pumping frequency f at the middle. About 200 pumping cycles were used first to obtain an initial condition for the test. About 200 more cycles were used to obtain the maximum amplitude in head for for a given frequency. The time step was selected so that $\psi < 0.08$, and therefore the time step is too small to cause significant errors. Table 3 shows the ε_w values obtained using the MODFLOW model, and the corresponding analytical values obtained using (31). It shows that the values agree well, and that the method can be used successfully to compute numerical errors in amplitude near groundwater wells. The results, which do not depend on actual dimensions, also indirectly confirm that the values of $a_c = 0.208$ and $a_a = 0.564$ used are sufficiently accurate. Errors in the numerical model can be larger because of errors of $O(\Delta t)$ and boundary effects. Errors further away from the well can be as large as the fraction of the amplitude. These errors can be determined approximately using (11).

NUMERICAL ERRORS UNDER STEADY STATE

Numerical errors under steady state due to disturbances caused by the source term can be determined by using methods similar to those used under unsteady conditions. Since steady state solutions are boundary dependent, a source term $S(x,y) = 2E_0Kk^2 \exp(Ikx)\ \exp(Iky)$ is used to create a solution of (1) far away from the boundaries that can be solved both analytically and numerically. Such a source term can be introduced using a variable rainfall distribution. The analytical solution of the problem can be shown to be of the form $H(x,y) = E_0 \exp(Ikx) \exp(Iky)$. To obtain the numerical solution, consider an arbitrary Fourier component $H_{i,j} = E \exp(I\phi i)\ \exp(I\phi j)$. Substituting

this component in the finite difference form of the governing equations, and computing the ratio of amplitudes of numerical and analytical forms, an estimate for the percentage error in amplitude can be estimated as

$$\varepsilon_s = 100\left(1 - \frac{\phi^2}{4\sin^2(\frac{\phi}{2})}\right) \approx -100\left(\frac{\phi^2}{12} + \frac{\phi^4}{240} + \ldots\right) \tag{32}$$

in which, $\varepsilon_s =$ steady state error as a percentage of the solution amplitude. The equation shows for example that ε_s exceeds 5% when ϕ exceeds 0.763. The corresponding values for 1% and 10% are 0.345 and 1.064 respectively. Equation (32) can be verified by making steady state runs for conditions with steady source terms having sinusoidal intensity variations. Model runs showed that the error equation can be verified up to 4 decimal places of precision.

NUMERICAL ERRORS NEAR WELLS UNDER STEADY STATE

Numerical errors are large near wells because of the curvature in the solution. The Thiem equation is used to compute the head distribution analytically when the water level in the cell containing the well is known. Thiem equation is expressed as

$$Q = 2\pi K \frac{H_2 - H_1}{\ln(r_2/r_1)} \tag{33}$$

in which, $Q =$ pumping rate; subscripts 1 and 2 represent the well and the cell value respectively. $r_2 = 0.208\,\Delta x$ is used with square grids.

In order to represent numerical errors in dimensionless form, all the errors are normalized against the drawdown of the cell containing the well or the ”center cell”. The well is assumed to be positioned at the center of the square cell. The problem of determining the discretization then

becomes a problem in geometry, in which the error in drawdown is expressed in terms of $r_I/\Delta x$, in which r_I is the radial distance to a reference elevation or the radius of influence. The radius of influence can be computed using a number of empirical and semi-empirical equations outlined in the text by Bear (1972). For different values of $r_I/\Delta x$, the numerical error in the drawdowns of different cells including the cell containing the well can be obtained using numerical model runs. The drawdowns of different cells are measured with respect to a point at a radial distance r_I, and the errors are computed assuming that the drawdowns computed using (33) are exact. All errors are presented as percentages of the drawdown of the center cell, which is assumed to be equivalent to a well of diameter $0.208\Delta x$. A $50\times$ 50 cell grid was used to run the numerical model. Figure 6 shows the variation of the error obtained for cells at various distances. Three levels of discretization given by $r_I/\Delta x = 6$ and 14 along the axis and 7 along a diagonal are shown in the plots. All the plots in log scale follow an approximately linear behavior. If $r_I/\Delta x$ is less than about 7, the discretization is very coarse, and only a few points are available to make a plot in Figure 6 making such a plot less reliable. The percentage error in the figure can be expressed approximately using

$$\varepsilon = 2.07\exp\left(-0.726\frac{r}{\Delta x}\right), \quad \Delta x \leq r < r_I \tag{34}$$

in which, $\varepsilon =$ error as a percentage of the drawdown in the center cell. The same equation can be written to express the absolute error as

$$H_\varepsilon = 2.07\left(\frac{Q}{2\pi T}\right)\log\left(\frac{r_I}{\Delta x}\right)\exp\left(-0.726\frac{r}{\Delta x}\right) \quad \Delta x \leq r < r_I \tag{35}$$

These equations can also be used to obtain Δx for a model if the maximum error allowed at a distance r from the well is known. Superposition is possible with errors as with heads in the case of

multiple wells.

NUMERICAL ERRORS IN THE SOURCE TERM

Rainfall and evapotranspiration are considered as source terms in the equation governing overland and groundwater flow. The source term is a major contributor to stress, mainly in regional models when far away boundaries have only a limited dynamic influence. Stresses introduced through the source term create water level variations that are subject to errors during computations associated with the source term as well as other terms. A spatially and temporally varying rainfall pattern is used to study errors in the source term.

It can be shown that a solution in the complex form $H = H_0 \sin(Ikx + Iky - I f_I t)$ satisfies the governing equation (1) if the source term describing rainfall excess (rainfall - evapotranspiration) is expressed as $S = s_c H_0 \sqrt{(f_I^2 + f_k^2)} \cos(kx + ky - f_I t - \gamma))$ in which $k =$ the wave number; $f_I =$ frequency describing the rainfall pattern; $f_k = dKk^2$, $\gamma = \tan^{-1}(f_I / f_k)$. The above equation for H is used to obtain the analytical solution when computing numerical errors during the following experiments.

An analytical expression for the numerical error created by the source term is obtained by isolating the source term, determining the error generated by it, and combining with the error generated by the diffusion term. A solution of the form $H_0 \sin(f_I t)$ satisfies the truncated form of (1) without the second derivative terms when $S = s_c f_I H_0 \cos(f_I t)$. Consider the following weighted

implicit finite difference equation for the truncated equation.

$$H_i^{n+1} = H_i^n + \frac{\Delta t}{s_c}(\alpha S_i^{n+1} + (1-\alpha)S_i^n) \tag{36}$$

Numerical error in (36) can be computed by comparing the analytical solution corresponding to H_i^{n+1}, or $H_i(t+\Delta t)$, which is $H_0 \sin(f_I t + f_I \Delta t)$, with the numerical solution obtained by substituting $S_i^n = s_c f_I H_i \cos(f_I t)$ in (36). After algebraic manipulations, ε_I, the maximum numerical error introduced through the source term as a fraction of the amplitude can be expressed as a percentage of the amplitude as

$$\varepsilon_I = \sqrt{\psi_I^2 - 2\psi_I \sin\psi_I + 4\sin^2(\frac{\psi_I}{2})[1-\alpha(1-\alpha)\psi_I^2]} \tag{37}$$

in which, $\psi_I = f_I \Delta t$. For fully explicit and implicit methods, the expression reduces to

$$\varepsilon_I = \sqrt{\psi_I^2 - 2\psi_I \sin\psi_I + 4\sin^2(\frac{\psi_I}{2})} \approx \frac{\psi_I^2}{2} - \frac{\psi_I^4}{72} + \ldots \tag{38}$$

The ψ_I values corresponding to 1%, 5% and 10% errors are 0.448, 0.673 and 0.802 respectively. With central differencing, these numbers become 1.073, 1.413 and 1.593 respectively. The numerical error as a result of both the source term and the diffusion term is assumed to be

$$\varepsilon_r = \sqrt{\varepsilon^2 + \varepsilon_I^2} \tag{39}$$

in which ε is the error in one time step due to the diffusion terms alone, computed earlier using (8).

The accuracy of ε_r in (39) is tested by simulating the stress induced by two one dimensional rainfall patterns $N = N_0 \sin(kx - f_I t))$ traveling in opposite directions. The value of β required to estimate ε is computed using $\beta = \psi_k/\phi^2$ in which, $\psi_k = f_k \Delta t$ and $f_k = Kk^2/s_c$. Figure 7 shows

the variation of the numerical error for a fully implicit 1-D model under such source induced flow conditions. Results are shown for two sets of ϕ and β values. Up to 20 cycles of spatial waves were simulated in the experiment using 100 grid points. Over 4000 time cycles were used to create the initial condition before the experiment was carried out as before. The figure shows that the numerical and analytical estimates agree approximately.

APPLICATION TO AN EXISTING MODEL IN SOUTH FLORIDA

A number of hydrologic models are used in South Florida to solve problems of various space and time scales. These models are based on the same governing equations, and have many similar characteristics. The South Florida Water Management Model (SFWMM) (SFWMD, 1997, Fennema, et al., 1994) developed by the South Florida Water Management District (SFWMD) is one of the regional models used in the area. SFWMM is a physically based overland and groundwater flow model. It simulates flow over a very large part of South Florida. The model uses a 3.2 km (2 mile) square grid, and a 6 hr. time step. Time series data for the boundary conditions and the source term are provided at 1 day time steps. In order to evaluate the validity of the diffusion flow assumption in the model, first consider somewhat extreme values of water depth $h = 1$ m, and slope $S_0 = 2\text{–}5\times10^{-5}$ in the Central and Southern Everglades during wet periods. These values can be used to compute the wave period of the shortest Fourier component that can be simulated, using $T_p = 30\sqrt{(h/g)}/S_0 \approx 4$ days, as suggested by Ponce (1978). This equation is based on a maximum amplitude error of 5%. The equation shows that the diffusion assumption is valid unless events of shorter duration are simulated. If however the slopes are large, and the depths are low as in certain areas of the Everglades, the model can simulate events of shorter duration using finer

discretizations.

The 3.2 km (2 mi) grid and the 6 hr time step in the SFWMM can represent various Fourier components in the solution with various accuracies. Table 4 shows errors of representation described in type (A) or (B) for different Fourier components, computed using (5) and (6). It shows that the SFWMM can represent Fourier components of wavelength as small as 18 km and period as small as 5.7 days with an accuracy of 5%. Using a typical high value of $K = 250\ m^2/s$ for overland flow obtained using $h \approx 1\ m$, $S_0 \approx 2 \times 10^{-5}$ and $n_b \approx 1$ for the deep portions of the Everglades, a Fourier component of wave length 18 km in space can be shown to be associated with a wave period of 2.5 days in time according to $f = 2Kk^2$. The time step required to represent a Fourier component of period 2.5 days with a maximum error of 5% is approximately 0.4 days. In the case of groundwater, assuming a typical high value of $K = 8\ m^2/s$ found near the Lower East Coast of South Florida, Fourier components of period 77 days and larger can be represented using the same spatial grid. Data presented at 14 day intervals are sufficient to describe stresses of this period. Any high frequency component in the groundwater flow generated by daily data is not supported by the spatial grid.

In order to compute the numerical error due to water level changes at internal and external boundaries, consider a water level fluctuation of amplitude 1 m and period 6 days near a canal as an example. The amplitude at a distance of 6.4 km or two cells is computed by first obtaining k using $f = 2Kk^2$ as $1.557 \times 10^{-4} s^{-1}$ and then using (16). The amplitude at the distance is

$1.0 \times e^{-kx} = 0.37$ m. Assuming that $\phi = k\Delta x = 0.5$, β can be shown to be 0.52. Since $\beta > 0.25$, it can be seen that an explicit model is unstable under the conditions. For an implicit model, the error is approximately $(1/2)kx\phi^2\beta$ or 6.5% of the amplitude, and the absolute error is 6.5% of 0.37 m or 24 mm. The percentage error in discharge for this case is also approximately 6.5%. The error is largest when $fT = 1$, or at a distance of 7 km.

The error due to rain driven water level fluctuations is proportional to the rainfall intensity. In South Florida, this is one of the largest driving forces of hydrology, and also the largest potential source of error in models. For a stationary rainfall intensity pattern described by a period of 12 days and a wave length of 18 km for example, $\psi_I = f_I\Delta t = 0.524$, and the error $\varepsilon_I = 13.6\%$ according to (37). For the stresses induced by this rainfall, $\phi = 1.1$, and $\beta = 0.52$ which gives $\varepsilon_T = 6.7\%$ when using $fT = \pi/4$ and (12). The total numerical error due to both source term and diffusion term computations as a result of rain driven flow can now be computed using (39) to give 15.2%. If the wave length of the rainfall density pattern is 18 km or less, the rainfall data has to be collected with a spatial resolution of 3.2 km to maintain a $<5\%$ error in the input data interpretation. When rainfall data is collected at a lower resolution, the model will contain only the corresponding lower frequency components. In South Florida, short duration small scale rainfall events account for a large part of the total rain, and have to be represented accurately if these components are to be represented accurately in models.

To demonstrate the accuracy of the SFWMM in simulating water levels near a pumping well,

use Table 2 and select $\Delta x\sqrt{(fs_c/K)} < 1.4$ for the error in the center cell to be less than 5%. With 3.2 km cells and $K = 8\ m^2/s$ for groundwater, this corresponds to a pumping cycle of period > 48 days. This example shows that heads computed near a well have large errors except in cases where the pumping rates change very slowly. Table 1 shows that the amplitude decays to less than 0.5% after 5 cells. The steady state error is less that 1.1% of the steady state drawdown of the center cell.

The numerical error in the final model output is a combination of errors in various steady and unsteady state stress components. When the numerical error is needed at a given point in the model, the first step is to find the sources of the stresses, and their spatial and temporal characteristics. When they are found, the principle of superposition can be used to find the errors due to each of the stresses. In many parts of the Everglades, stresses are mainly due to rain and canal level fluctuations that result from the operation of pumps and water control structures.

SUMMARY AND CONCLUSIONS

The study shows that numerical errors resulting from spatial and temporal discretizations can be explained using dimensionless variables ϕ and β respectively. The results shows that the error generally increases with both ϕ and β. For a given spatial discretization ϕ, it can be shown that the error cannot be reduced below a certain value unless ϕ is also reduced. Similarly, the error for a given β cannot be reduced unless ϕ too is reduced. Using $\phi < 1.1$ and $\psi < 1.1$ in the case of 1-D, errors of spatial and temporal discretization can generally be kept below 5%. Using numerical experiments with explicit models and implicit models such as MODFLOW, and using variable boundary water levels, variable rainfall patterns and variable well pumping rates, it was possible

to show that numerical errors in a variety of finite difference models can be computed using the proposed analytical equations. Test results also show that the analytical error estimates obtained for steady state problems with a steady rainfall pattern are accurate. Numerical errors other than amplitude errors resulting from material heterogeneities, discontinuities, or boundary effects are not considered in the study.

In the case of the experiment using a variable boundary water level, the results show that the maximum error as a percentage of the amplitude increases linearly with distance from the boundary. The results also show that the maximum error in the discharge behaves similarly. By using a steady water head profile generated by a steady rainfall pattern, it was possible to show that $\varepsilon_s > 5\%$ if $\phi > 0.763$. By using rainfall patterns changing with time, it was also possible to show that the error ε_I in computations involving the source term is $>5\%$ when $\psi_I > 0.673$ where ψ_I describes the temporal discretization of the rainfall. Using pumping experiments carried out at a cell in the MODFLOW model, it was shown that the numerical value of the amplitude in the cell containing the well decreases with increasing cell size, and the error $> 5\%$ when $\Delta x > 1.4\sqrt{(K/fs_c)}$. Results using a steady state pumping problem show that the error in the drawdown of the cell containing the well when $r_w = 0.208\Delta x$ is about 1%, and reduces rapidly with radial distance. A summary of some of the practically useful equations obtained during the study are shown in Appendix A. The study shows that sufficient spatial discretizations and matching temporal discretizations must be used if a given Fourier component is to be represented accurately in a model.

ACKNOWLEDGMENTS

The writer thanks Mark Belnap for the MODFLOW runs, and Joel VanArmen for reading and reorganizing the manuscript. Review comments by Jayantha Obeysekera, Todd Tisdale, Victor Kelson, Randy Van Zee, Ken Tarboton and Matt Hinton of the Hydrologic Systems Modeling group of the South Florida Water Management District were extremely useful. The writer specially thanks Dr. Richard Cooley, and other reviewers of Water Resources Research for the review and the excellent suggestions.

APPENDIX A

A Summary of practically useful equations

Table A.1: Practically useful formulas in approximate form. In the equations, f = frequency of the disturbance in water level; K = transmissivity of the aquifer.

Equation	Reference
$X\sqrt{(fs_c/K)} = 4.3$	X is the distance at which a 1-D disturbance of frequency f would decay to 5% of the amplitude.
$\Delta x = 1.1\sqrt{K/fs_c}$	Δx gives the spatial discretization needed to represent a water surface profile with 5% accuracy. The profile is created by a disturbance of frequency f.
$\Delta x = 0.5\sqrt{K\varepsilon_d/fs_c}$	Δx needed to represent the same spatial discretization with a ε_d % accuracy.
$K\Delta t/\Delta x^2 s_c = 0.14$	Δt gives the time step needed if the numerical error is limited to 5% of the disturbing amplitude.

$\Delta x\sqrt{(fs_c/K)} < 1.4$	Δx gives the size of a square cell needed to solve the amplitude of a well fluctuation with a maximum error of 5%.
$\Delta x\sqrt{(fs_c/K)} = 5$	gives a practically useful upper bound of Δx that can be used to model a pumping well (error $< 40\%$).
$r\sqrt{(fs_c/K)} = 2.75$	r is the radius at which the amplitude of a well with $\hat{r}_w = 0.5$ decays to 5% of the amplitude of the well.
$\varepsilon = 2.07\exp(-0.726r/\Delta x)$	ε gives the numerical error of a steady state well as a percentage of the drawdown.

APPENDIX B

Definition of variables

Variable	Definition
A	area simulated by the model (m^2).
f_I	frequency of the rainfall pattern.
g	gravitational acceleration.
h	water depth, (m).
H	water level or water head (m).
H_ε	error in the steady state solution near a well.
K	transmissivity of aquifer for groundwater flow; $h^{\frac{5}{3}}/(n_b\sqrt{S_n})$ for overland flow, m^2/s.
K_0, K_1	modified Bessel functions of type 0 and 1.
r	radial distance from the center of a well.
$\hat{r}$	$= r\sqrt{(fs_c/K)} =$ dimensionless r.
$\hat{r}_w$	well radius in dimensionaless form.
S	source term representing rainfall and evapotranspiration.
s_c	storage coefficient
T	time during which a harmonic in the solution evolves, (s).
x, y	distances along x, y coordinate axes, (m).
X	distances at which a disturbance is measured, (m)
α	time weighting factor in the weighted implicit scheme.

Variable	Definition
β	$K\Delta t/(s_c\Delta x^2)$, dimensionless time step.
ΔA	area of a cell, (m^2).
Δx	size of a square cell.
ε	maximum local numerical error per one time step as a fraction of the local amplitude.
ε_Q	numerical error in discharge as a percentage of discharge.
ε_s	numerical error due to computations associated with the source term, as a fraction of the local amplitude.
ε_T	maximum local numerical error as a fraction of the local amplitude.
ϕ	dimensionless spatial discretization defined as $k\Delta x$.
ψ	a dimensionless time discretization defined as $f\Delta t$.
ψ_I	a dimensionless time discretization defined as $f_I\Delta t$.

REFERENCES

Anderson, M. P. and Woessner, W. W. (1991). "Applied groundwater modeling, simulation of flow and convective transport", *Academic Press, Inc.*, New York.

Bear, J. (1979) "Hydraulics of Groundwater", *McGraw Hill*, New York.

Burden, R. L. and Fairs, J. D. (1985). *Numerical analysis*, Third Edition, Prindle, Weber & Schmidt, Boston, MA.

Dongarra, J. J. (1998). "Performance of various computers using standard linear equation software", *Computer Science Dept. University of Tennessee*, Report CS-89-85, Knoxville, TN.

Feng, Ke, and Molz, F. J. (1997). "A 2-D diffusion based wetland model", *Journal of Hydrology*, 196(1997), 230-250.

Fennema, R. J., Neidrauer, C. J., Johnson, R. A., MacVicor, T. K., Perkins, W. A. (1994). "A computer model to simulate natural Everglades hydrology", *Everglades, The Ecosystem and its restoration*, Eds. Davis, S. M. and Ogden, J. C., St. Lucie Press, FL, 249-289.

Fitz, H. C., DeBellevue, E. B., Costanza R., Boumans, R., Maxwell, T., Wainger, L. and Sklar, F. H. 91996). "Development of a general ecosystem model for a range of scales and ecosystems", *Ecological Modeling*, vol 88, 263-295.

Haitjema, H. M. (1995). "Analytic element modeling of groundwater flow", *Academic Press*, New York.

Hirsch, C. (1989). *Numerical computation of external and internal flows*, John Wiley & Sons, Inc., New York, N.Y.

Hromadka II, T. V., and Lai, Chintu, (1985). "Solving the two-dimensional diffusion flow

model", *Proc. of the Specialty Conf. sponsored by the Hydraulics Div. of ASCE,* Lake Buena Vista, FL, Aug 12-17.

Lal, A. M. W. (1995). "Calibration of riverbed roughness", *J. Hydr. Div.,* ASCE, 121(9), 664-670.

Lal, A. M. W. (1998a). "Performance comparison of overland flow algorithms", *J. Hydr. Div.,* ASCE, 124(4), 342-349.

Lal, A. M. W. (1998b). "A weighted implicit finite volume model for overland flow", *J. Hydr. Div.,* ASCE, 124(9).

McDonald, M. and Harbough, A. (1988). "A modular three dimensional finite difference groundwater flow model", Report 06-A1, *US Geological Survey, Reston, VA*.

Neuman, S. P. (1973). "Calibration of distributed parameter groundwater flow models viewed as a multiple objective decision process under uncertainty", *Water Resources Research,* 9(4), 1006-1021.

Richtmyer, R. D. and Morton, K. W. (1967). *Difference methods for initial value problems,* Second Edition, J. Wiley and Sons, New York, NY.

SFWMD, (1997). "Documentation of the South Florida Water Management Model", Draft Document, South Florida Water Management District, West Palm Beach, FL.

Sod, G. A. (1985). Numerical methods in fluid dynamics, *Cambridge University Press,* Cambridge, UK.

Strack, O. D. L. (1989). Groundwater mechanics, *Prentice Hall,* NJ. Townley, L. R. (1995). "The response of aquifers to periodic forcing", *Advances in Water Resources,* vol 18, 125-146.

Willis R. and Yeh, W. W. G. (1987). Groundwater systems planning and management, *Prentice-Hall,* NJ.

FIGURE CAPTIONS

Figure 1: Variation of numerical error and amplitude with distance from the boundary for the MODFLOW model.

Figure 2: Variation of numerical error with spatial and temporal resolutions for the ADI method. Lines show analytical values and symbols show values observed in the model.

Figure 3: Variation of numerical error with spatial and temporal resolution for the explicit method. Lines show analytical values and symbols show values observed in the model.

Figure 4: Variation of numerical error with spatial and temporal resolutions for the MODFLOW model. Lines show analytical values and symbols show values observed in the model.

Figure 5: Variation of error in discharge for a fully implicit model. Lines show analytical values and symbols show values observed in the model.

Figure 6: Variation of steady state numerical error with radial distance.

Figure 7: Variation of error in the source term with ψ_I. Lines show analytical values and symbols show values observed in the model.

Table 1: Amplitudes of water level fluctuations given by (26) for various well radii $\hat{r}_w = a_c \Delta x \sqrt{(f s_c / K)}$ representing various discretizations. Values of $K_0(\hat{r})/(\hat{r}_w K_1(\hat{r}_w))$ are shown in the table. $a_c = 0.208$.

	$\hat{r}$							
$\hat{r}_w$	0.01	0.05	0.1	0.5	1.0	2.0	5.0	10.0
0.01	4.722	3.115	2.428	0.925	0.421	0.114	0.004	1.8×10^{-5}
0.05		3.128	2.438	0.929	0.422	0.114	0.004	1.8×10^{-5}
0.1			2.463	0.938	0.427	0.115	0.004	1.8×10^{-5}
0.5				1.116	0.508	0.137	0.004	2.0×10^{-5}
2.0						0.407	0.013	6.0×10^{-5}

Table 2: Variation of ε_w, the error in the amplitude of the cell containing a well as a percentage of its exact amplitude, with dimensionless Δx for a square grid. C_c, the ratio between amplitudes is also shown.

$\Delta x\sqrt{(fs_c/K)}$	0.01	0.02	0.05	0.1	0.2	0.5
C_c	1.0000	0.9999	0.9997	0.9990	0.9967	0.9844
ε_w (%)	$4.200\ 10^{-7}$	$5.130\ 10^{-5}$	$1.351\ 10^{-4}$	$1.508\ 10^{-3}$	$1.564\ 10^{-2}$	0.289

$\Delta x\sqrt{(fs_c/K)}$	1	2	5	10	20
C_c	0.9523	0.8886	0.5640	0.2563	$4.3228\ 10^{-2}$
ε_w (%)	2.13	11.1	43.6	74.4	95.7

Table 3: Comparison of values of ε_w obtained analytically and using the MODFLOW model.

$\Delta x\sqrt{(fs_c/K)}$	0.54	1.53	6.10	8.63
ε_w (analytical)	0.4%	6%	52%	68%
ε_w (MODFLOW)	4%	5%	71%	82%
ϕ	0.27	0.76	3.05	4.31

Table 4: Characteristics of various 1-D and 2-D Fourier components that can be represented by using a 3.2 km (2 mile) grid cell and a 1 day time step.

Wave length (1-D) (km)	41	18	13	6	4	19
Wave length (2-D) (km)	57	25	18	8	5	27
Max. error (%)	1%	5%	10%	50%	100%	4.5%

Wave period (Days)	12.8	5.7	4.1	1.8	1.3	6
Max. error (%)	1%	5%	10%	50%	100%	4.5%

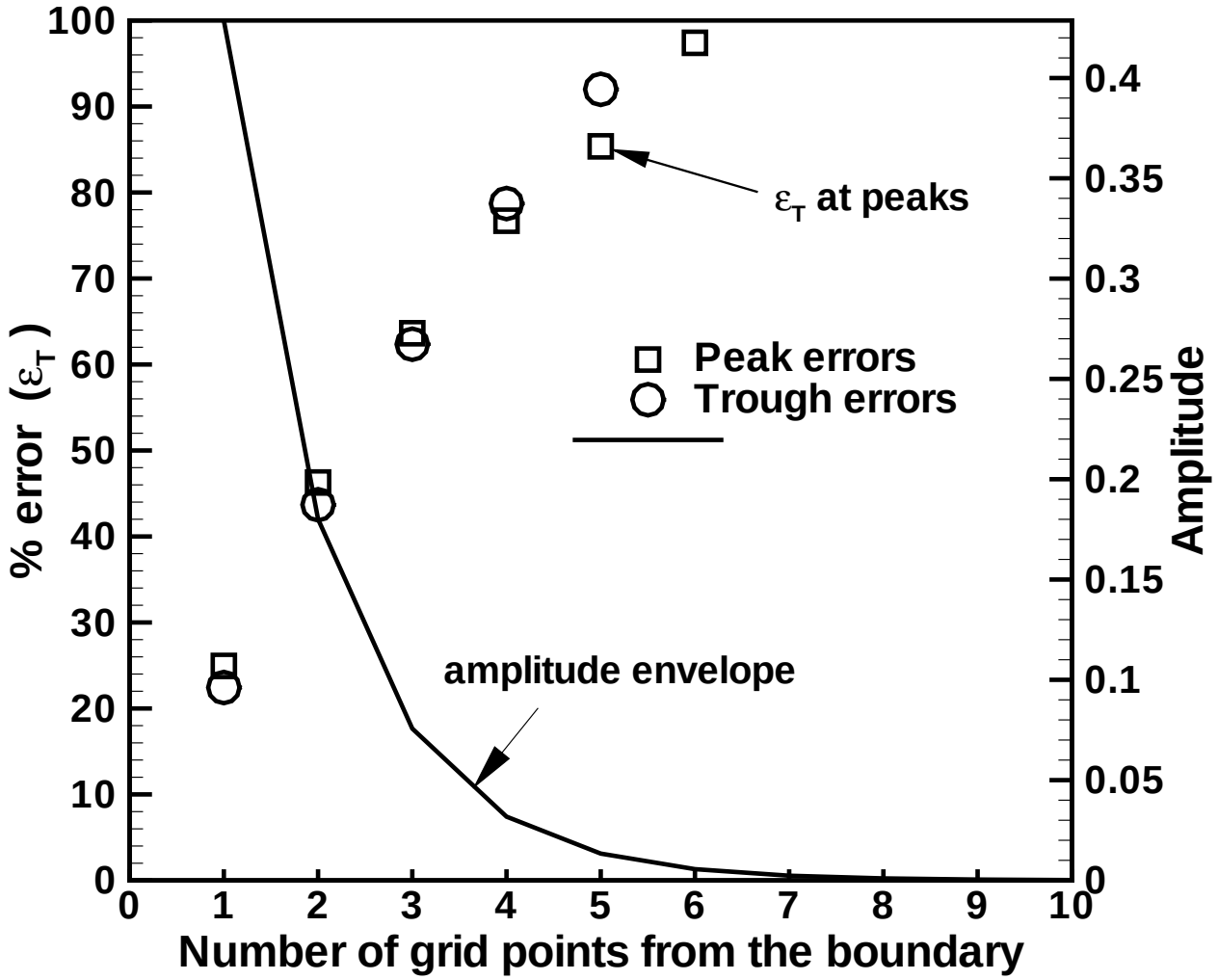

Figure 1: Variation of numerical error and amplitude with distance from the boundary for the MODFLOW model.

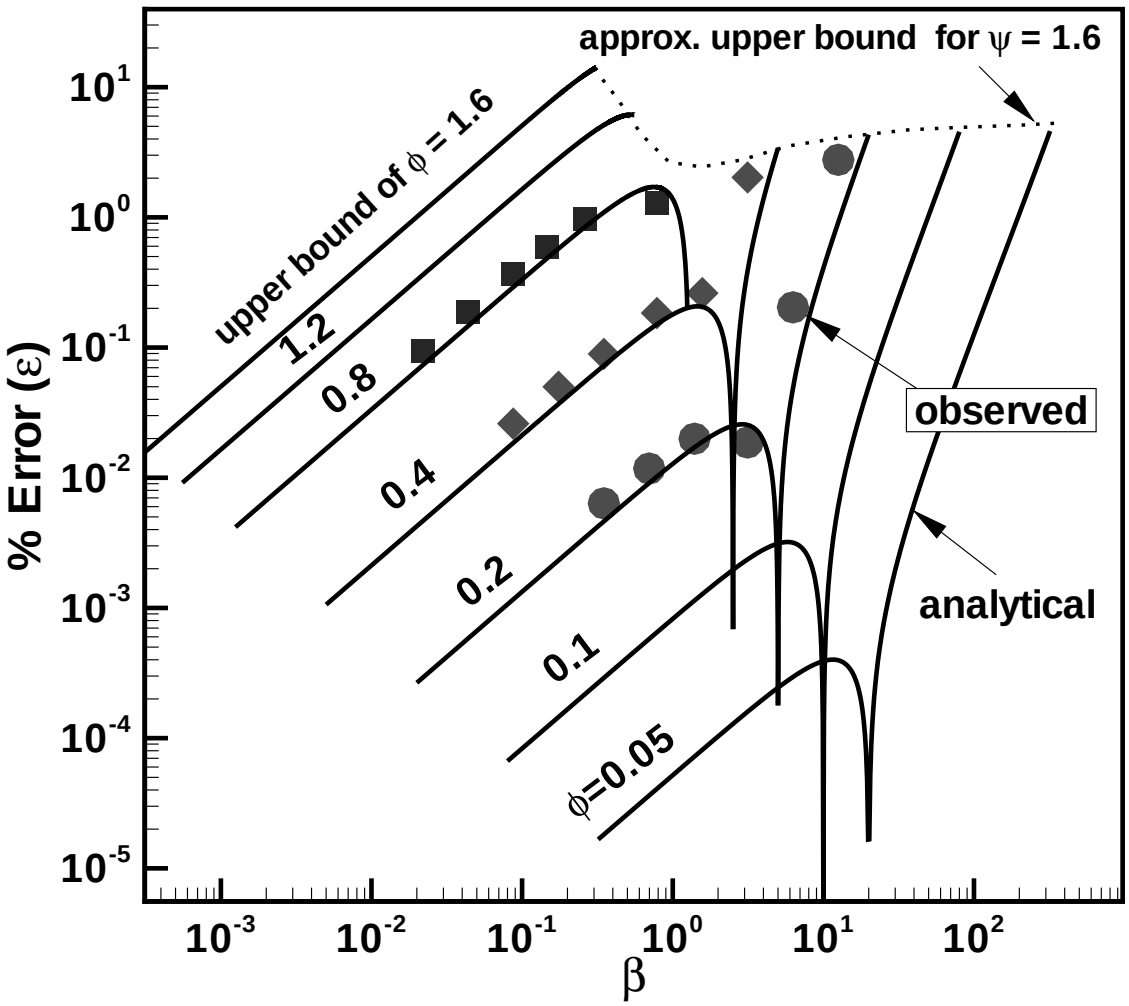

Figure 2: Variation of numerical error with spatial and temporal resolutions for the ADI method. Lines show analytical values and symbols show values observed in the model.

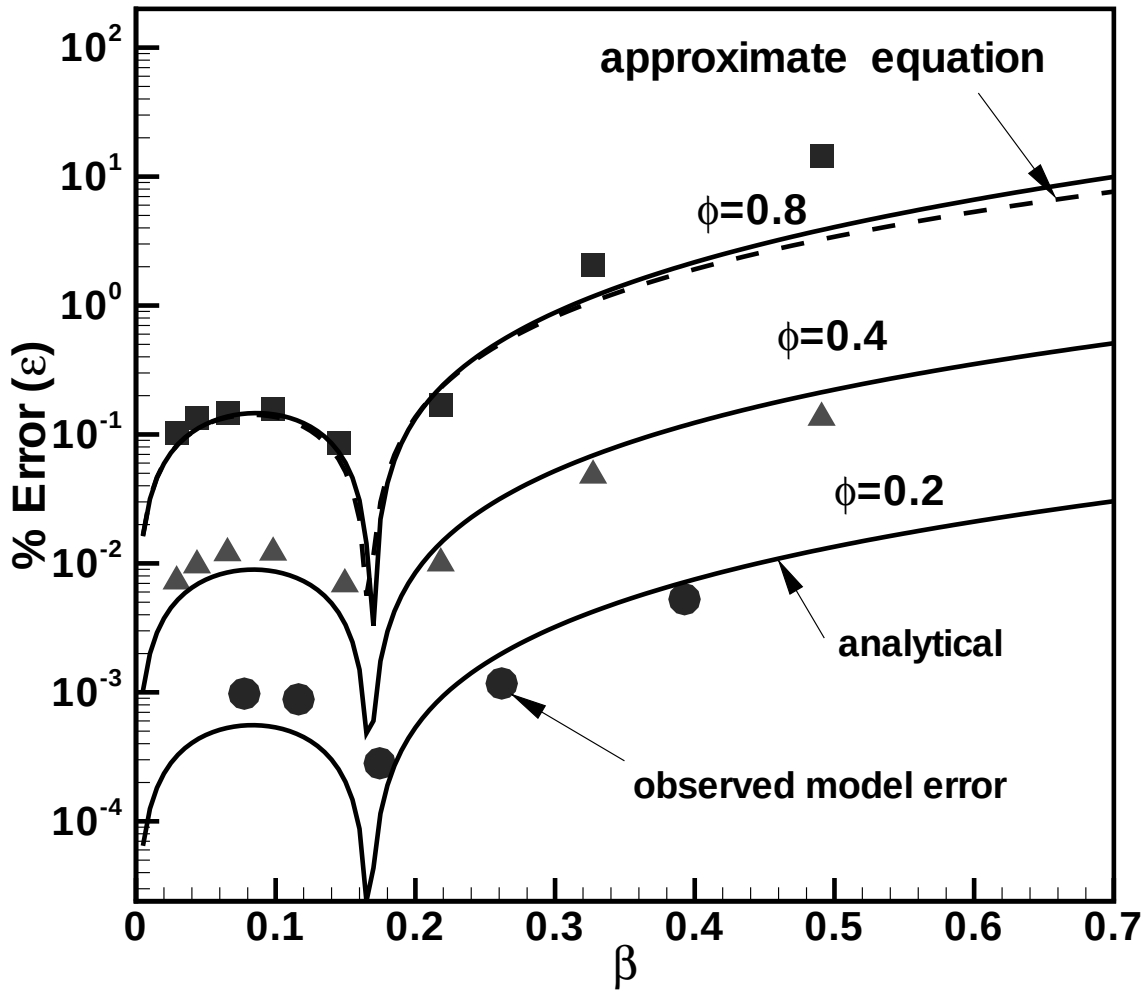

Figure 3: Variation of numerical error with spatial and temporal resolution for the explicit method. Lines show analytical values and symbols show values observed in the model.

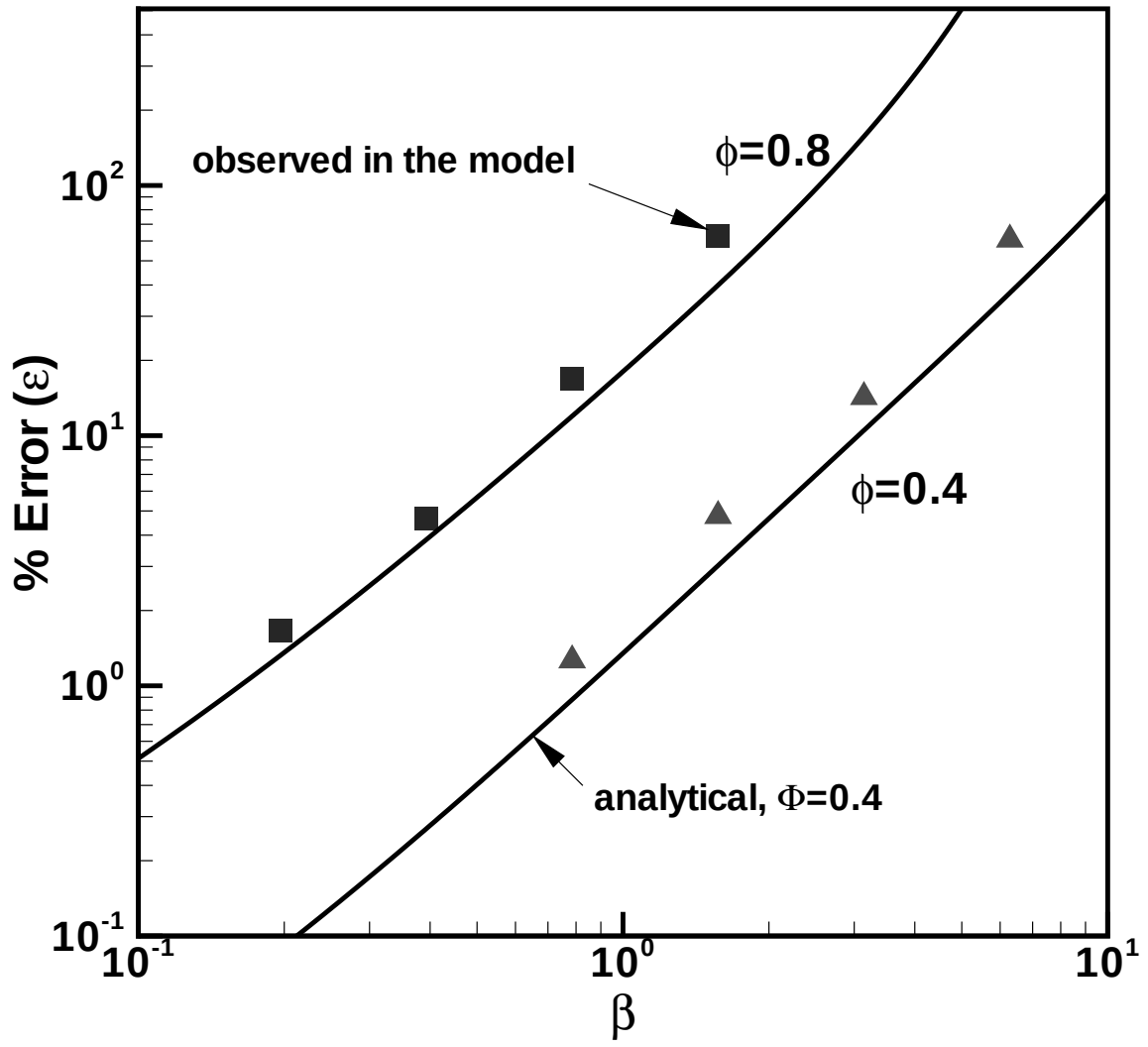

Figure 4: Variation of numerical error with spatial and temporal resolutions for the MODFLOW model. Lines show analytical values and symbols show values observed in the model.

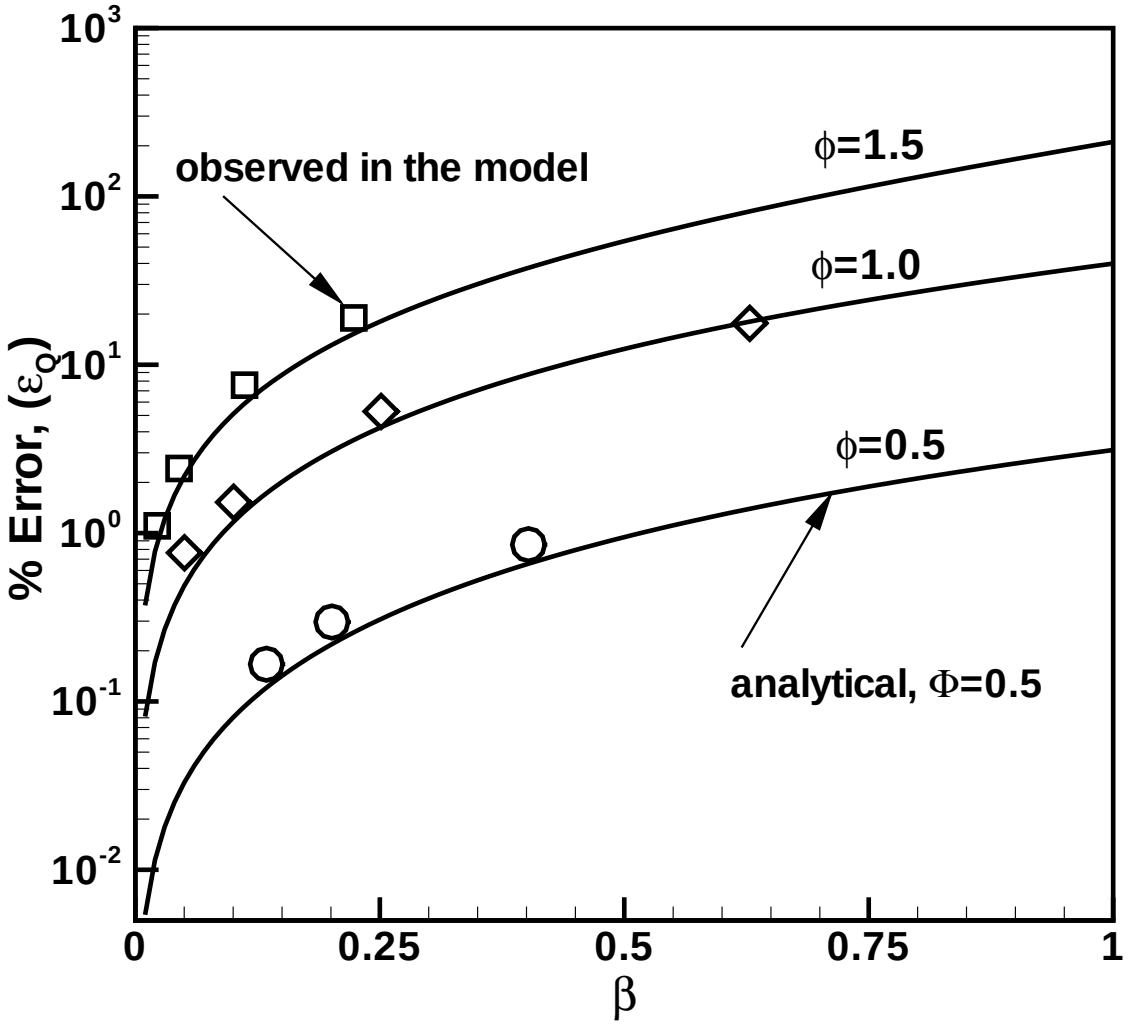

Figure 5: Variation of error in discharge for a fully implicit model. Lines show analytical values and symbols show values observed in the model.

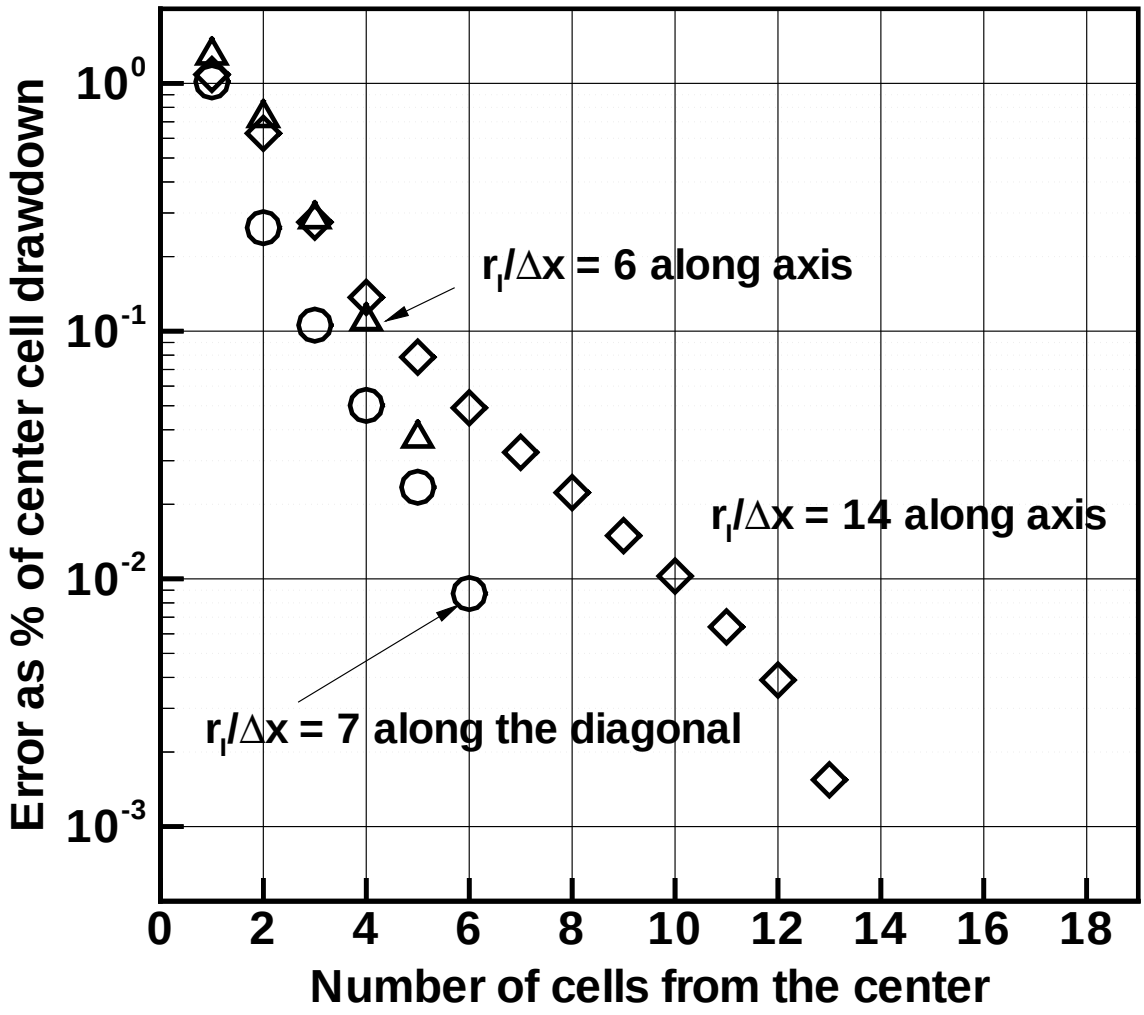

Figure 6: Variation of steady state numerical error with radial distance.

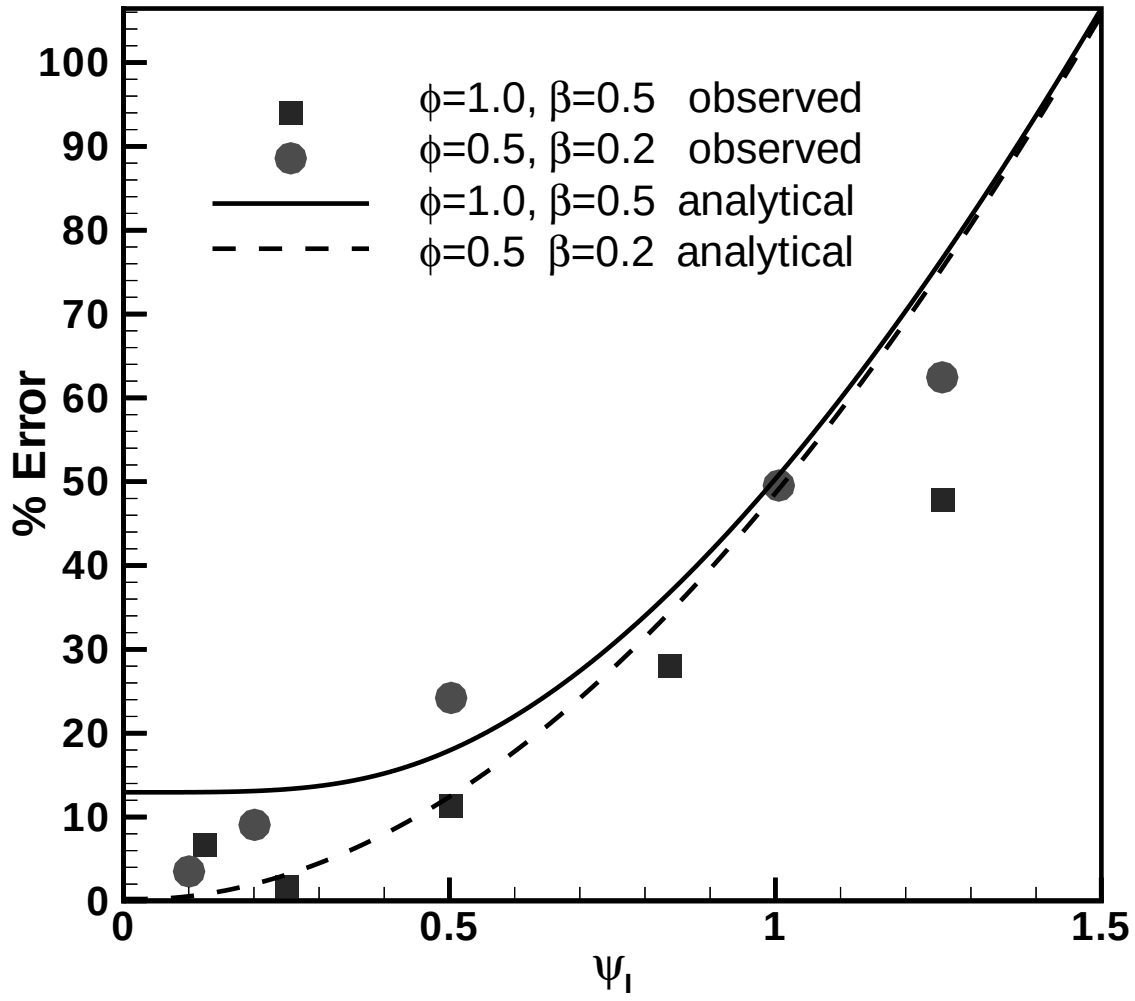

Figure 7: Variation of error in the source term with ψ_I. Lines show analytical values and symbols show values observed in the model.

C.3 Case study: Model to simulate regional flow in South Florida

CASE STUDY: A MODEL TO SIMULATE REGIONAL FLOW IN SOUTH FLORIDA

A. M. Wasantha Lal, Randy Van Zee, [1] **Mark Belnap** [2]

South Florida is a complex regional hydrologic system that consists of thousands of miles of networked canals, sloughs, highly pervious aquifers, open areas subjected to overland flow and sheet flow, agricultural areas and rapidly growing urban areas. This region faces equally complex problems related to water supply, flood control and water quality management. Advanced computational methods and super fast computers alone have limited success in solving modern day problems such as these because the challenge is to model the complexity of the hydrologic system, while maintaining computational efficiency and acceptable levels of numerical errors. A new, physically based hydrologic model for South Florida called the Regional Simulation Model (RSM) is presented here. The RSM is based on object oriented design methods, advanced computational techniques, XML (extensible markup language) and GIS (geographic information system).

The RSM uses a finite volume (FV) method to simulate 2-D surface and groundwater flow. It is capable of working with unstructured triangular and rectangular mesh discretizations. The discretized control volumes for 2-D flow, canal flow and lake flow are treated as abstract ”water bodies” that are connected by abstract ”water movers”. The numerical procedure is designed to work with these and many other abstractions. An object oriented (OO) code design is used to provide robust and highly extensible software architecture. A weighted implicit numerical method is used to keep the model fully integrated and stable. A limited error analysis was carried out and the

[1]Lead Engineer and Supervising Engineer, Hydrologic Systems Modeling, South Florida Water Management District, 3301 Gun Club Rd., West Palm Beach, FL 33406,

[2]Senior Engineer, formally at Hydrologic Systems Modeling, now at NTT/Verio, 1203 North Research Way, Orem, UT 84097.

results were compared with analytical error estimates. The paper describes an application of the model to the L-8 basin in South Florida and the strength of this approach in developing models over complex areas.

INTRODUCTION

South Florida is a very complex hydrologic system. Its complexity is mainly due to the considerable groundwater and surface-water interaction, spatial variability in land use, hundreds of flow control structures, extensive wetlands systems, adjacent urban areas, influence of Lake Okeechobee, and the unique flow characteristics of the Everglades and the water conservation areas. Even if the computing power is continuously increasing every year, the complexity of the hydrologic system and the water management issues in South Florida have been increasing at an even faster rate. Consequently, more efficient computational methods, more flexible computer codes, better code development environments, and better code maintenance procedures are needed to keep pace with these growing demands. The need for clean code design, participation by multiple developers from a variety of disciplines, and regular use of test cases to routinely check code integrity has become critical. Application of a number of new technologies described below has contributed to resolve some of these problems.

The first technological contribution came from recent developments in information technology and the use of object oriented (OO) code design methods. The use of extensible markup language XML (Bosak and Bray, 1999), geographic information system (GIS) technology and database support has allowed us to achieve a level of code flexibility and data integration that did not exist before. Object oriented methods have been used in the past for hydraulic model design by Solomontine (1996), Tisdale (1996), and many others. Although OO design may have been previously considered to be outside the expertise of many hydrologists, the increased complexity of the hydrologic processes involved, and the need to incorporate methods developed by professionals from many disciplines such as biology, hydrogeology and ecology have changed this view. The strong dependencies between hydrology, nutrient transport and ecology have created a need to integrate various approaches and therefore to integrate computer codes. Simple models that ad-

dress issues within one discipline at a time have become inadequate for studying complex systems. However, the improved use of GIS support tools, OO code design and XML language have made it possible to model complex systems, and organize and present large amounts of complex data.

The second technological contribution came from developments in computational methods. Use of unstructured meshes of variable size to simulate 2-D integrated overland and groundwater flow in irregular shaped domains has become common. Full and partial integration with canal networks and lakes is now possible. In the past two decades, a number of physically based, distributed-parameter models have emerged with such features. The early models include MODBRANCH by Swain and Wexler, (1996), MODNET by Walton et al. (1999), Mike SHE based on Abbott, et al., (1986a and b), WASH123 by Yeh et al. (1998), MODFLOW-HMS by HydroGeoLogic (2000), and models by VanderKwaak (1999), Schmidt and Roig (1997), and Lal (1998a). The computational engines of these models are based on solving a form of the shallow water equation for surface flow and either the variably saturated Richards' Equation or the fully saturated groundwater flow equation. Inertia terms in the shallow water equations were neglected, and the solution to the governing equations was obtained using a single global matrix. A number of features are available in these models to simulate structures, urban areas and agricultural areas. The choice of features depends on the intended application of the model.

Some developments in numerical error analysis by Hirsch (1989) and Lal (2000) also helped in the selection of optimal discretizations for integrated models. Results of error analysis are useful in developing model meshes that produce more accurate solutions and avoid large errors and incipient instabilities. Large-scale integration using implicit methods is practically impossible without understanding numerical error and instability. Because of unconditional stability, implicit models can be run with practically any time step regardless of whether the solution is accurate or not.

The third contribution came from a new generation of computer packages that can be used to solve large sparse systems of equations efficiently. It is now possible to develop implicit finite

volume algorithms and solve many complex equations simultaneously without iterating between various model components. Modern solvers such as PETSC (Balay, et al. 2001) support parallel processing, and have a variety of built-in tools and options to achieve fast model runs. These solvers are easy to use because details such as matrix storage methods are hidden from the user. The current model uses the software package PETSC (Balay, et al. 2001) to solve the matrices.

The most commonly used integrated model in South Florida is the South Florida Water Management Model, SFWMM (SFWMD, 1999). This model has been adopted to simulate regional hydrology and water management practices since the late 1970's. It simulates the water resources system from Lake Okeechobee in the north to Florida Bay in the south, covering an area of 7600 square miles with a mesh of 3.22 km by 3.22 km (2 mile by 2 mile) cells. The model simulates the major components of the hydrologic cycle including rainfall, evapotranspiration, overland and groundwater flows, canal flow, canal seepage, levee seepage and well pumping. It incorporates current or proposed water management protocols and operational rules. The success of the model has resulted in an increased demand for its use along with a growth of its size and complexity beyond what was originally intended. The code gradually became very complex, difficult to understand, improve, and expand. This was the primary factor that motivated the launching of a "new generation" regional simulation model (RSM). Unlike the SFWMM that was written in FORTRAN, the RSM code is being developed using an Object Oriented (OO) design and the C++ language. These choices were made so that the code design can allow for easy modification, growth, and participation of multiple developers.

The RSM is functionally a combination of a hydrologic simulation engine (HSE), which executes the flow simulations, and a management simulation engine (MSE) that can represent structure and pump operations. The HSE has been used to simulate flow in the Kissimmee River by Lal, (1998a), and in the Everglades National Park by Lal, et al., (1998c), and Brion, et al. (2000 and 2001). The accuracy of the model was verified using the MODFLOW model and an analytical solution for stream-aquifer interaction (Lal, 2001). This paper describes the model formulation and the object oriented design of the HSE. This model makes it possible to fully integrate the

components of the system, and allow for expansion using new hydraulic components, land use types, micro-hydrological features, canals, reservoirs, and other aspects of the system. An error analysis was carried out to determine the relationship of the numerical error to the size of the triangular cells and the time step. The results of this analysis can be useful in the design of spatial and temporal discretizations to minimize numerical error.

The paper includes an HSE application example that simulates the hydrology in the L-8 basin of South Florida. The L-8 basin is a relatively simple basin in South Florida; however, it has some of the complexities of the regional hydrologic system. Many of these complexities apply to conditions outside South Florida as well. The results of the simulation example are used to demonstrate why this approach was chosen to develop the new regional simulation model (RSM) for South Florida.

GOVERNING EQUATIONS

The governing equations for the integrated overland-groundwater-canal-lake flow system consist of mass balance or continuity equations and equations of motion. For overland and canal flow, non-inertia form of the Saint Venant equation is used as the governing equation. All the governing equations written in conservative form are finally assembled together in the implicit implementation of the finite volume method.

Overland and groundwater flow

The 2-D continuity equation from St Venant equations for unsteady overland flow and unsteady saturated groundwater flow in a single layered aquifer can be expressed using

$$s_c \frac{\partial h}{\partial t} + \frac{\partial (uh)}{\partial x} + \frac{\partial (vh)}{\partial y} - R_{rchg} + W = 0 \tag{1}$$

in which, u and v are the flow velocities in the x and y directions; $h =$ water depth for overland flow and saturated aquifer thickness for groundwater flow; $R_{rchg} =$ net contribution of the recharge from local hydrology into the regional system; $W =$ source or sink terms, for example, due to pumping wells measured in units of volume rate per unit area or L/T; $s_c =$ storage coefficient; $s_c = 1$ for overland flow. The term R_{rchg} is also measured in units L/T, and is computed for discretized cells referred to as pseudo cells designed to capture the recharge from local hydrology. A number of

pseudo cell models are described later.

When inertia terms are neglected, the momentum equation reduces to the diffusion flow equation. Diffusion flow assumption is valid for overland flow when inertia terms are small. Akan and Yen, (1981), and Hromadka, et al. (1988) and many others have used diffusion flow models for many practical applications. Ponce, et al. (1978) found the condition of applicability for these models as $T_p S_0 \sqrt{g/h} > 30$ in which $T_p =$ period of the smallest sinusoidal disturbance in the solution; $S_0 =$ bed slope. Lal (2000) found that this condition applies for most regional flows in South Florida with $T_p > 4$ days. It can be shown that the momentum equations under the diffusion flow assumption and the equations describing Darcy's law can be written as

$$u = -\frac{T(H)}{h}\frac{\partial H}{\partial x}, \quad v = -\frac{T(H)}{h}\frac{\partial H}{\partial y} \tag{2}$$

in which, $u, v =$ average flow velocities in x and y directions; $H =$ water head. For overland flow, $H = h + z$; $h =$ water depth; $z =$ ground elevation. For groundwater flow, $h =$ saturated aquifer thickness; $T =$ transmissivity of the aquifer. For both overland and groundwater flows, $T(H)$ can be expressed as a function of the state variable H. For single layered groundwater flow, $T = k_h(H - z_b)$ in which, $z_b =$ elevation of aquifer bottom; $k_h =$ hydraulic conductivity of the aquifer. For overland flow, $T = C(H)\,|S_n|^{\lambda-1}$ in which $C(H)$ is defined as the conveyance where $S_n =$ magnitude of the maximum water surface slope which is approximately equal to S_f, the energy slope under the diffusion flow assumption (Akan and Yen, 1981). Variable $\lambda =$ an empirical constant described later. The purpose of keeping generic functions for $T(H)$ and $C(H)$ is to use object oriented design methods and allow for the implementation of a variety of flow behaviors. These functions can represent constants, analytic functions or lookup tables based on field experiments. Abstract representations of $T(H)$ and $C(H)$ can be used to describe complex flows through wetlands. A power function that can describe many flow resistance equations including the Manning equation, the laminar flow equation, and a number of other wetland equations is $V_n = (1/n_b)h^{\gamma}S_n^{\lambda}$ in which, $V_n =$ average flow velocity. This equation can be used to derive an expression for T as

$$T(H) = \frac{h^{\gamma+1}|S_n|^{\lambda-1}}{n_b} \tag{3}$$

in which $S_n = Max(S_n, \delta_n)$ is used when $\lambda < 1$ to prevent division by zero at $S_n = 0$. The discharge per unit width can be described now as $q(H) = T(H)S = C(H)\,|S|^{\lambda-1}S$. The variable $\delta_n = 10^{-13} - 10^{-7}$ is used in the flat terrains of South Florida. A large value of δ_n allows more flat areas of the system to be solved by an approximate form of the Manning equation and prevent instability. Equation (3) can also be used in wetlands by selecting the parameters suggested by Kadlec and Knight (1996). For the Manning equation, $\gamma = 2/3$; $\lambda = 1/2$; $n_b =$ Manning constant. Comprehensive flow equations for shallow streams have recently been developed by Katul (2002) and Lopez and Garcia (2001). The abstract base class for $C(H)$ allows for such functions to be seamlessly accommodated in to the model.

Canal flow

The 1-D St Venant equations are used to describe gradually varied unsteady canal flow. The continuity equation for canal flow in conservative form is

$$\frac{\partial A_c}{\partial t} + \frac{\partial Q}{\partial n} - R_{canal} + W = 0 \tag{4}$$

in which, $A_c =$ cross sectional area of the canal; $Q =$ discharge rate; $n =$ distance along the canal; $R_{canal} =$ volume rate at which water is entering the canal due to seepage and other sources per unit length (L^2/T); $W =$ source and sink terms due to pumps. When diffusion flow is assumed and inertia terms are neglected, gravity and friction terms left in the momentum equation give $Q = C(R)/\sqrt{|S_n|}S_n = A_c R^{2/3}/(\sqrt{|S_n|}n_b)S_n$ in which $R =$ hydraulic radius; $S_n =$ water surface slope; $S_n = S_f =$ friction slope as assumed by Akan and Yen (1981). The purpose of writing the equation in this form is to create a generic function $C(R)$ for conveyance that is not limited to use the Manning equation. Discharge Q can now be expressed as

$$Q = -T_c \frac{\partial H_c}{\partial n} \tag{5}$$

in which, $H_c =$ canal water level; $T_c = A_c R^{2/3}/(n_b\sqrt{|S_n|})$; $C(R) = A_c R^{2/3}/n_b$ when the Manning equation is used. Slope S_n is computed using $Max(S_n, \delta_n)$ with $\delta_n = 10^{-13} - 10^{-7}$ as described earlier.

Lake flow

The equation governing mass balance in a lake is

$$A_l \frac{\partial H_l}{\partial t} - R_{lake} + W = 0 \tag{6}$$

in which, $A_l =$ lake area; $H_l =$ water level; $R_{lake} =$ net volume rate at which water is entering the lake water body due to leakage. The governing equations written in conservative form are used in the implicit implementation of the finite volume method.

Recharge from the local hydrologic system

The local hydrology in a regional system depends on the local land use type along with all its management practices. Different land use types generate different recharges and therefore different hydrologic responses. The recharge R_{rchg} described in (1) therefore has to be computed separately for each cell with a new land use type. The computations take into account ET, rainfall, soil moisture effects, urban detention, local drainage effects, agricultural practices, and local management practices depending on the land use type. The equation of mass balance is used to compute recharge as

$$R_{rchg} = P - E + I - \frac{dU_s}{dt} - \frac{dD}{dt} \tag{7}$$

in which, $R_{rchg} =$ recharge rate (m/s) computed as a volume rate per unit cell area entering into the cell; $P =$ precipitation rate; $E =$ evapotranspiration rate; $I =$ water entering the cell during irrigation and other similar functions; $U_s =$ unsaturated moisture depth; $D =$ detention volume converted to depth. The rates $\frac{dU_s}{dt}$ and $\frac{dD}{dt}$ if used, depend on infiltration and percolation rates of the local cell. In the model, these complex computations are carried out within the pseudo cell (object) of each respective cell. Pseudo cells are developed for various land use types, permitting conditions or management practices. More information about pseudo cells is provided under the object design.

THE IMPLICIT FINITE VOLUME METHOD

Governing equations for overland flow, groundwater flow, canal flow, lake flow and other types of flow are based on conservation laws and can be solved using the finite volume method. Equations in conservative form are written as

$$\frac{\partial U}{\partial t} + \frac{\partial F(U)}{\partial x} + \frac{\partial G(U)}{\partial y} + S(U) = 0 \tag{8}$$

in which, U is a conservative variable representing H, H_c, or H_l; variables $F(U)$ and $G(U)$ are the x and y components of flux in 2-D flow and $S(U) = -R_{rchg} + W =$ summation of source/sink terms. The finite volume formulation is applied to all 2-D, 1-D and lake related regional flows. The numerical model is developed for generic control volumes and is applied to all water bodies on an equal basis regardless of whether they are 2-D cells, canal segments or lakes.

The finite volume formulation for the governing equation (8) is derived by integrating over an arbitrary control volume or water body Ω.

$$\frac{\partial}{\partial t}\int_{\Omega} U \, d\Omega + \int_{S} (\mathbf{E}.\mathbf{n}) \, dA + \int_{\Omega} S \, d\Omega = 0 \tag{9}$$

in which, $\mathbf{E} = [F, G]^T =$ flux rate across the wall and $\mathbf{n} =$ a unit vector normal to the wall. The first term of (9) represents the rate of change of water volumes in water bodies such as cells, canal segments and lakes. The second term is obtained using the Gauss' theorem and contains the sum of fluxes crossing the control surfaces of the water bodies. This term contains all flow exchanges among the water bodies. Any mechanism that is capable of moving water between any two water bodies is defined as an abstract water mover. Water bodies and water movers are two of the basic building blocks of the model. They eventually become abstract base classes in the OO design. These abstractions are capable of growing and evolving into various model objects as the model evolves.

In the model, equation (9) is solved for average water heads H, H_c or H_l of all the water bodies simultaneously. In the finite volume formulation, (9) reduces to the following system of differential equations which is solved simultaneously to simulate the integrated system.

$$\Delta\mathbf{A}(\mathbf{H})\frac{d\mathbf{H}}{dt} = \mathbf{Q}(\mathbf{H}) + \mathbf{S} \tag{10}$$

in which, $\mathbf{H} =$ a vector containing the water heads of all 2-D cells, canal segments, and lakes together. The first term of (10) is derived from the first term of (9) which is equal to $\frac{\partial \mathbf{V}}{\partial t}$ in which $\mathbf{V} =$ volumes of water contained in water bodies. In the attempt to describe $\mathbf{V}$ as a function of $\mathbf{H}$, a new function $f_{sv}(H)$ referred to as the stage-volume (SV) relationship function is introduced. It

holds behaviors very important to flat terrains of South Florida and helps to determine water levels accurately. For each water body $i = 1, 2, \ldots$ the function takes the form $V_i = f_{sv}(H_i)$. The slope of this function is defined as

$$\Delta A_i(H_i) = \frac{\partial f_{sv}(H_i)}{\partial H_i} \tag{11}$$

in which, $\Delta A_i(H_i)$ are the effective plan areas of water bodies i. For 2-D open water flow, these are the cell areas. For groundwater, these are s_c times cell areas. $\Delta\mathbf{A}(\mathbf{H})$ in (10) is the diagonal matrix whose elements (i,i) are $\Delta A_i(H_i)$. The reverse relationship of the SV relationship is defined as $H_i = f_{vs}(V_i)$. Both forward and reverse functions are used in the model to conserve mass during the mapping between V_i and H_i.

The term $\mathbf{Q}(\mathbf{H})$ of (10) gives the net inflow rate to each water body due to the action of all the water movers in vector form. In order to solve this coupled nonlinear system (10), water mover equations are linearized prior to assembly as a large system of linear equations. The linearized form for any water mover is

$$Q_r(\mathbf{H}) = k_0 + k_i H_i + k_j H_j \tag{12}$$

in which $Q_r(\mathbf{H})$ = discharge rate through the water mover r. The water mover r moves water from water body i to water body j. Linearization is performed to determine values of k_0, k_i and k_j using partial differentiation or approximate methods depending on the type of the water mover. They are used to build the resistance matrix $\mathbf{M}(\mathbf{H})$ that can be viewed as a result of the linearization of $\mathbf{Q}(\mathbf{H})$ as $\mathbf{Q}(\mathbf{H}) = \mathbf{M}(\mathbf{H}).\mathbf{H}$. The ordinary differential equations (10) with linearized $\mathbf{Q}(\mathbf{H})$ are solved using a weighted implicit method. Lal (1998a) used the following system of equations to solve (10).

$$[\Delta\mathbf{A} - \alpha\Delta t\mathbf{M}^{n+1}].\Delta\mathbf{H} = \Delta t[\mathbf{M}^n].\mathbf{H}^n + \Delta t[\alpha\mathbf{S}^{n+1} + (1-\alpha)\mathbf{S}^n] \tag{13}$$

in which, α = time weighting factor, assumed to be in the range 0.6-0.8 for most integrated models and close to 1.0 when nonlinearities are severe and the model show signs of instability. This equation takes into account the water balance of all the water bodies during the time interval between times t^n and t^{n+1}. Knowing the volumes of water $\mathbf{V}(\mathbf{H^n}) = \mathbf{f_{sv}}(\mathbf{H^n})$ at time step t^n and

ΔH, it is possible to compute $\mathbf{V}^{n+1}$ using

$$\mathbf{V^{n+1}} = \mathbf{V^{n}} + \Delta\mathbf{A}.\Delta\mathbf{H} \tag{14}$$

The new heads $\mathbf{H^{n+1}}$ at time step $n+1$ can now be computed using the storage-volume relationship $\mathbf{H^{n+1}} = \mathbf{f_{vs}}(\mathbf{V^{n+1}})$. Heads are used in the model only to compute the hydraulic driving forces in the water movers. Except during this conversion, the model equations can be explained as a system of mass balance equations.

When water budgets for the model are needed, the volumes of water passing between water bodies, $Q_r(\bar{H})\Delta t$ are computed first using (12). In this expression, the heads $\bar{\mathbf{H}}$ used are defined to be at a time $t^n + \alpha\Delta t$ and are computed as $\bar{\mathbf{H}} = \mathbf{H}^n + \alpha\Delta\mathbf{H}$. The water balance in any water body i can be verified for accuracy by comparing the change in water volume in the water body $\Delta A_i(H_i^{n+1} - H_i^n)$ with the summation of water mover discharges $Q_r(\bar{H})\Delta t$.

THE OBJECT DESIGN

The process of abstraction and determining the relationship between abstractions form the basis for OO design. The basic abstractions used in the RSM model include: (i) ”water bodies” that represent discretized cell elements, canal segments and lakes which store water; (ii) ”water movers” that represent the only mechanisms to move water between water bodies; (iii) ”stage-volume relationship functions” (SV) that map between the stages and the volumes in water bodies and (iv) ”pseudo cells” that capture the local hydrologic function in the water bodies and compute their recharge. The entire hydrologic system can be decomposed into these and other abstract types such as transmissivity and conveyance functions $T(H)$ and $C(H)$. Figure 1 shows some of the basic building blocks of the model. These abstractions allow a single numerical scheme to be used for the governing equations describing all flow types.

Abstract data types or classes in the model can be related to other classes through inheritance. A ”subclass” or a ”derived class” of a water body base class for example, can be a discretized overland flow cell, canal segment or a lake. They all inherit properties of the base class. Inheritance makes it possible to use polymorphism in OO modeling and allows functions to behave correctly

depending on the object type. Polymorphism also allows water bodies to transform into canals, cells and lakes while water movers can transform into canal flow, overland flow and structure flow. Special methods associated with these objects fill the proper elements in the matrix. Four of the abstract classes used in the model are described below.

Water bodies

The water body is the basic abstraction that collects water conservatively. Water body objects represent control volumes of the finite volume method, and provide a protected status for conservative variables such as water mass and solute mass. Cell elements, canal segments and lakes become polymorphic water bodies. The head of the water body when needed is computed by calling the stage-volume relationship function of the water body described as $H_i = f_{vs}(V_i), \quad i = 1,2,\ldots$ The first terms of (9) and (10) represent change of volume in water bodies. Figures 1 and 2 show examples of water bodies. Figure 3 shows part of a class diagram for water bodies which was written using the convention of Rumbaugh, et al. (1991).

Water movers

The water mover is the basic abstraction needed to transfer water between any two complex water bodies. It represents the flux term in the finite volume method, and transfer flow across control surfaces as in canal flow, overland flow and all other kinds of flow such as structure flow. By design, they conserve mass. Some water movers such as those for overland flow, groundwater flow and canal flow are created based on cell and canal network geometry. Water movers such as structure water movers are added as needed using input data. When new structure types are needed, they are added only as water movers. All water mover objects are placed in object containers to be accessed easily using the C++ Standard Template Library (STL) features (Stroustrup, 2000). Figures 1 and 2 show sketches of sample water movers. Figure 3 shows part of a class diagram for water movers. Since only water movers can move water between water bodies, the model can track mass balance of the system at the highest level of abstraction.

Overland flow water mover

When the water levels are above ground in adjacent cells, overland flow takes place. The discharge in the water mover Q_r between two adjacent cells as described in (12) is computed using

the circumcenter method derived for mixed finite elements (Lal, 1998a).

$$Q_r = \Delta l \; T_r \frac{H_m - H_n}{\Delta d_{mn}} \begin{cases} \text{for} \quad H_m > H_n \quad \text{and} \quad H_m > z_m \quad \text{and} \quad H_m > z_n \\ \text{or} \quad H_n > H_m \quad \text{and} \quad H_n > z_n \quad \text{and} \quad H_n > z_m \end{cases} \tag{15}$$

in which, H_m, H_n = water levels in triangular cells m and n; d_{mn} = distance between circumcenters of triangles m and n; Δl = length of the wall; z_m, z_n = ground elevations of cells m and n; T_r = equivalent inter block transmissivity in the overland flow layer, computed based on the assumption that transmissivity varies linearly between circumcenters (Goode and Appel 1992, and McDonald and Harbough 1988). Variable T_r is computed as

$$T_r = \frac{T_m + T_n}{2} \quad \text{for} \quad 0.995 \leq \frac{T_m}{T_n} \leq 1.005 \tag{16}$$

$$T_r = \frac{T_m - T_n}{\ln \frac{T_m}{T_n}} \quad \text{otherwise} \tag{17}$$

T_m and T_n are the values for the cells defined in (2) for overland flow. Matrix elements filled up by the overland flow water movers are described in the paper by Lal (1998a).

Groundwater flow water mover

When simulating groundwater flow, transmissivity is assumed as constant inside a cell. The discharge in the water mover Q_r is computed using

$$Q_r = \Delta l \; \frac{H_m - H_n}{\left(\frac{l_m}{T_m} + \frac{l_n}{T_n}\right)} \tag{18}$$

in which, l_m and l_n are the distances from the circumcenters to the wall; T_m and T_n are transmissivities described in (2).

Canal flow water mover

When simulating canal flow, a linearly varying conveyance is assumed between canal segments. The equation for discharge between two segments m and n is the same as (15). The value of T_m for example, for segment m is

$$T_m = \frac{A_m}{l_m \sqrt{S_n} n_b} \left(\frac{A_m}{P_m}\right)^{\frac{5}{3}} \tag{19}$$

in which, A_m = average canal cross sectional area of segment m; P_m = average wetted perimeter; n_b = average Manning roughness coefficient and l_m = length of a canal segment. When simulating

canal networks, each pair of segments of a canal joint is considered as a canal water mover. A canal joint with n limbs has $n(n-1)/2$ canal water movers as a result. All these movers have to be considered before populating the matrix. Their summation computes the actual discharge.

Canal seepage water mover

Seepage between a canal segment and a cell is described using a canal seepage water mover. The seepage rate q_l per unit length of the canal is derived using Darcy's equation.

$$q_l = k_m p \frac{\Delta H}{\delta} \tag{20}$$

in which, $k_m =$ sediment layer conductivity; $p =$ perimeter of the canal subjected to seepage; $\delta =$ sediment thickness and $\Delta H =$ head drop across the sediment layer.

Canal overbank flow also occurs between a canal segment and a segment, but only when the cell has overland flow. The water mover used for this type of exchange is based on a simple broad-crested weir.

Structure flow water mover

Linearization of structure equations to fit to the format of (12) is not always easy for most of the structures. Consider a structure whose discharge can be expressed as $Q_s = Q_s(H_u, H_d, G)$ in which H_u, H_d are upstream and downstream water levels and $G =$ gate opening. One of the simpler methods uses a previous call to function $Q(H_u, H_d, G)$ to obtain the following approximate linearization.

$$Q(H_u, H_d) = \frac{Q(H_u^n, H_d^n, G^n)}{H_u^n - H_d^n}(H_u - H_d) \tag{21}$$

in which the superscript n represents values from previous time steps. This linearization is accurate only in gradually varied flow, and works for a limited number of cases. Considering that $Q_s = Q_s(H_u, H_d, G)$ can be extremely nonlinear, differential equations with structure equations can be stiff and difficult to solve without special methods or small time steps. One and two-dimensional lookup tables and regression equations are also useful in describing structure flow.

Stage-volume (SV) relationships

Stage-volume relationship functions make it possible to use local stage-storage characteristics in

integrated models. This feature is useful when the local topography is complex as in the case of ridge-and-slough formations in the Everglades, or as in the case of special land surface characterizations in agricultural and urban areas. The SV relationships can provide accurate water levels when the volume in a water body is known and vice versa. In the case of canals, they are used to obtain the water level when the canal properties are known. Local topography, storage coefficient, and other geometric information are used in the development of SV functions for 2-D cells. They can be complex functions or lookup tables based on experimental data. Some simple examples of $f_{sv}(H)$ are described below.

SV relationship function $f_{sv}(H)$ for a cell with a horizontal ground surface

When the ground level is assumed horizontal, the SV relationship for a cell with a single layered aquifer is given by

$$V = f_{sv}(H) \quad = \quad As_c(H - z_b) \quad \text{for} \quad H < z \tag{22}$$

$$V = f_{sv}(H) \quad = \quad As_c(z - z_b) + A(H - z) \quad \text{for} \quad H \geq z \tag{23}$$

in which, $z_b =$ elevation at the bottom of the aquifer; $z =$ elevation of the ground and $A =$ cell area.

Inverse relationship $f_{vs}(V)$ for a cells with a horizontal ground surface

Since the expression for flat ground is linear, (22) and (23) can be used to obtain the following relationships.

$$H = f_{vs}(V) \quad = \quad z + \left\{ \frac{V}{A} - s_c(z - z_b) \right\} \quad \text{for} \quad V > As_c(z - z_b) \tag{24}$$

$$H = f_{vs}(V) \quad = \quad z_b \quad \text{for} \quad V < 0 \tag{25}$$

$$H = f_{vs}(V) \quad = \quad z + \frac{V}{A\, s_c} \quad \text{otherwise} \tag{26}$$

SV relationship $f_{sv}(H)$ for a canal segment with a rectangular section

For a canal with a rectangular cross section, the relationship is

$$V = f_{sv}(H) \quad = \quad 0 \quad \text{for} \quad H < z_c \tag{27}$$

$$V = f_{sv}(H) \quad = \quad BL(H - z_c) \quad \text{for} \quad H \geq z_c \tag{28}$$

in which, $z_c =$ elevation of canal bottom; $L =$ length of canal segment and $B =$ canal width. The inverse relationships of most of the functions are complex and are not described here. However

they have to be monotonic.

Pseudo cells

The hydrologic system of South Florida covers areas with many types of land use. Most areas along the east coast are heavily urbanized, while some of the areas in the south are natural and wetland type. Areas south of Lake Okeechobee are mostly agricultural. Pseudo cells are used to separate the complexities of the unsaturated subsurface flow accounting, irrigation practices, urban detention and routing practices of the natural and managed systems from the regional system. Contribution of recharge from the local system to the regional system is computed using the mass balance condition given in (7). Pseudo cells contain storage, routing and simple management based interchange mechanisms to simulate infiltration, percolation, seepage, and urban drainage among other things. The AFSIRS model (Smajstria 1990), CASCADE model (SFWMD, 2001), NAM model (DHI, 1998) and a few other models are available as pseudo cell models for HSE. The simplest pseudo cell is one for open water where the equation for recharge (7) becomes

$$R = P - E \tag{29}$$

Boundary conditions

When solving 1-D and 2-D diffusion flow equations, only one boundary condition of discharge type or water level type is needed at each boundary. General head, uniform flow, and lookup table type boundary conditions are very useful with diffusion flow. These and other 2-D boundary condition types are described in the paper by Lal (1998a).

Some of the boundary conditions are simple enough that they can be applied to general water bodies. The flow boundary condition for a water body is one of them. It specifies the flow rate to a water body as

$$Q_i(t) = Q_B(t) \tag{30}$$

in which, $Q_i(t) =$ inflow rate to water body i and $Q_B(t) =$ specified inflow rate. Similarly, the head boundary condition for a water body states that the water level can be assigned to a constant value

or a time series value. For a water body i, it is stated as

$$H_i(t) = H_B(t) \tag{31}$$

in which $H_i(t) =$ the head at water body i at time t and $H_B(t) =$ assigned value. One problem of the head bc is that it reorganizes the entire matrix and resets data in the contributing water movers. To avoid this, the head boundary condition can be applied to cell walls instead of cells and canal joints instead of canal segments. To apply a head bc at a cell wall, a certain discharge q_i is added to the cell i to bring about a change in wall head to $H_B(t)$. The discharge to be added is

$$q_i = \frac{T(H)l}{l_c}(H_B(t) - H_i) \tag{32}$$

in which, $T(H) =$ transmissivity; $H_i =$ cell head; $l =$ wall length and $l_c =$ distance from the wall to the circumcenter. The general head boundary condition is also useful under certain groundwater conditions. It is described using the equation

$$q_i = K_G\, l(H_B(t) - H_w) \tag{33}$$

in which, $K_G =$ specified conductance value in m/s; $H_w =$ wall boundary head. The uniform flow boundary condition is similar, and relates slope to flow rate q_i as

$$q_i = T(H)S_b \tag{34}$$

in which $S_b =$ slope of uniform flow associated with the water body.

Operation of structures and pumps

Some structures and pumps in the model are operated to achieve certain performance goals in the hydrologic system. The operations are based on rules assigned by water managers. Some of the operations are manual and others are automatic. Some operational rules are very complex because they have evolved over time based on historic events, human needs, and prior experiences of the water managers. The complex operational rules and logical directives applied to the structures and pumps are implemented as on/off type or proportional type functions on structures and pumps.

The purpose of operating structures and pumps is to achieve a desired performance in the system at the desired time. Some performances and conditions are mandated by legislation. A

number of the performance measures used for South Florida are described in a comprehensive review study report (USACOE, 1999). Currently many of the operations are rule-based, and not necessarily optimal. However optimization can be used in the future to determine decision variables in the system. The methods available include optimal control methods (Gelb, 1974), linear programming (Loucks, et al., 1981), and optimization by simulation. These methods are built into the MSE section of the model. The methods currently used are described in the South Florida Water Management Model documentation (SFWMD, 2001).

Water budgets

In a compartmentalized landscape such as South Florida, determination of the water budget within a hydrologic basin or a compartment can be very important for many water managers. Water bodies and water movers are ideally suited to carry out water budget computations because they track the volume of water contained in and passing through them using the abstract base class design. Each water body has an attached list of water movers that can report the discharges. The discharge computation for the water movers is carried out using (12) and the updated values of head and k. An example showing the water budgets of two arbitrary water bodies is presented in Table 2. In the table, the lists of water movers attached to each water body, and the discharges in them are shown.

Model errors

Even if mass balance errors in the finite volume method are small as shown in Table 2, other computational errors can be large depending on the discretization. Improper selection of spatial and temporal discretizations can make a model implementation ineffective in producing solutions of certain necessary scales. Recent studies show that proper discretization can be based on rules derived using analytical equations for numerical error (Lal 2000). These rules, along with rules regarding the applicability of the diffusion approximation of St Venant equations, and rules to control nonlinear instability are important in making sure that solutions to integrated models are accurate and oscillation free.

Numerical error analysis methods are presented partly to demonstrate their use in model verification, and partly to demonstrate how the methods can be used in model error control. The

experiment involves a 1-D sinusoidal boundary disturbance in a 2-D groundwater domain. The experiment demonstrates that numerical errors of the model agree with the analytical estimates of error. The experiment also demonstrates how to calculate numerical errors for a model when spatial and temporal discretizations are known. During numerical experiments it can be shown that error behavior with near-isometric triangular cells is similar to the error behavior with rectangular cells. This allows the use of a dimensionless spatial discretization $\phi = k\sqrt{\Delta A}$ for triangles instead of $\phi = k\Delta x$ for rectangles in which $k =$ wave number of the disturbance and $\Delta A =$ cell area. For the experiment, a confined groundwater domain is created in a 10 $km \times 10$ km area and populated with 3200 approximately isometric triangles. A 1-D sinusoidal head disturbance is then introduced into the domain by applying it on one of the boundaries. Water heads at different distances away from the wall are then monitored over long periods. These heads are compared with their analytical estimate to obtain observed errors in the amplitude. The observed errors are then compared with analytical error estimates (Lal 2000).

To demonstrate analytical error estimation, the analytical solution for 1-D groundwater flow is first expressed as

$$H(x,t) = H_o e^{-kx} \sin(ft - kx) \tag{35}$$

in which, $f =$ frequency of the boundary disturbance in radians per second; $H_o =$ amplitude of the disturbance; $x =$ distance from the boundary and $k = \sqrt{fs_c/(2T)}$. The analytical solution for the numerical error for this problem is (Lal, 2000).

$$\varepsilon_T(x) = \frac{k\varepsilon}{\beta\phi^2}x = \frac{2k\varepsilon}{\psi}x \tag{36}$$

in which, $\varepsilon_T(x) =$ maximum error over the duration as a fraction of the amplitude at a distance x; $\Delta t =$ time step; $\psi = f\Delta t = (2\pi/T_p)\Delta t =$ dimensionless time step and $\varepsilon =$ maximum error per time step as a fraction of the amplitude; $\beta = T\ \Delta t/(s_c\ \Delta A)$ in which β is a useful dimensionless parameter which has to be less than 0.5 for the stability of the explicit method when solving the 1-D groundwater flow equation. It can be shown by substitution that $\beta = \psi/(2\phi^2)$ for this problem. Analytical values of ε (or ε_{anal}) can be obtained as a function of β and ψ or ϕ and ψ (Lal, 2000). Figure 5 is a contour plot of the same.

In order to show that values of ε measured in the numerical model (referred here as ε_{obs}) compare well with analytical values of ε (referred here as ε_{anal}), values of ε_{obs} are obtained first. To do this, $\varepsilon_T(x)$ of (36) are plotted against x for a number of model runs and (36) is fitted to determine the slope. Figure 4 shows one such plot when the period $T_p = 8.6$ hrs or $f = 2\pi/T_p = 2.029 \times 10^{-4}\, s^{-1}$, $\Delta t = 30$ min, $\sqrt{\Delta A} = 152$ m for the mesh, $T = 20.0 m^2/s$ (for an arbitrary porous medium) and $s_c = 0.2$ confirming that the error behavior is linear as shown in (36). Using the slope of the graph $2k\varepsilon/\psi = 8.65 \times 10^{-5}$, the value of ε (or ε_{obs} in this case) can be obtained as 1.53% using $k = \sqrt{fs_c/(2T)} = 0.001007$, and $\psi = 0.365$. The analytical value $\varepsilon_{anal} = 1.57\%$ can be obtained using the method by Lal (2000) or Fig 5 with $\phi = k\sqrt{\Delta A} = 0.153$ and $\psi = 0.365$. The observed value of ε_{obs} for the model is shown as a dot in Figure 5 compares well with the analytical values in contours. Table 1 shows the summary of the model runs shown in Figure 5.

The analytical values of ε_{anal} in Figure 5 can be used to predict model errors in any future model when the cell size ΔA and the time step are known, and when the stress comes from a similar forcing function. To derive an equation for maximum absolute error anywhere in the domain ε_{abs} in units of length, (35) and (36) can be used.

$$\varepsilon_{abs} = \frac{2H_0\varepsilon}{e\psi} \tag{37}$$

where $e = 2.718$. The maximum error is negative, and occurs at a distance $x = 1/k$ from the boundary during the peak and the trough of the cycle. The steps involved in computing the error are: (a) compute $f = 2\pi/T_p$ knowing the period of the water level disturbance; (b) compute $\psi = f\Delta t$; (c) compute $k = \sqrt{fs_c/(2T)}$; (d) compute $\phi = k\sqrt{\Delta A}$; (e) use Figure 5 to read ε for the ϕ and ψ; (f) compute ε_{abs} using (37). For the problem with $T_p = 8.6$ hrs described earlier, the error is $2.0 \times 0.0157/(2.718 \times 0.365) = 3.2\%$ of the disturbing amplitude according to (37). If this error is too large, finer discretizations have to be selected.

Once the discretization is known, error analysis can be used to determine the cutoff frequency and wave number of the solution. A time step of 30 min for example can only represent solutions of period larger than $2\pi\Delta t/\psi = 2\pi \times 0.5/0.5 = 6.3\, hrs.$ with 1% accuracy (Lal, 2000).

The smallest spatial feature for this solution is $2\pi \times 152/0.5 = 600\ m$ long. The second important consideration in selecting a discretization is run time, which is proportional to $k^4/(\psi\phi^2)$ or $f^2/(\psi\phi^2)$ in which k or f describes the level of spatial and temporal detail needed to be simulated by the model (Lal, 1998a).

MODEL VERIFICATION AND APPLICATIONS

The computational methods used in the RSM model have been verified in the past using a number of methods (Lal, 1998a). The most rigorous verification of the model was carried out using an analytical solution for the problem of stream-aquifer interaction (Lal 2001). In the test, sinusoidal water level disturbances of varying frequency were used to disturb a canal interacting with an aquifer. The decay and the delay of the solution for water levels in the system were obtained using the current model and the analytical method. A wide range of parameter values were used in the test. The results of the test plotted using dimensionless variables show that the numerical solution agrees with the analytical result. The error analysis described in the previous section is also useful as a verification method.

The earliest application of the FORTRAN version of the model with 2-D overland and groundwater capabilities was on the Kissimmee River (Lal 1998a). The C++ version of the model with 2-D capabilities was used to simulate flows in the Everglades National Park by Lal, et al. (1998c). The current application uses the fully integrated model in C++. The L-8 basin of South Florida was selected to demonstrate the complexity of the problem, while keeping the presentation simple. Many of the hydrologic components and issues related to the L-8 basin are typical for South Florida. Although it is usually not easy to isolate individual basins in the South Florida hydrologic system, the L-8 basin is relatively isolated and therefore somewhat easy to study. Figure 6 shows a site map of the L-8 basin. The details listed below will demonstrate how even the simplest basins can have a large amount of critical information to consider. As it can be seen, many of the complexities are due to human influences.

A brief description of the L-8 application

The L-8 basin is located within an area approximately 100 km x 100 km in size, near the northern

boundary of Palm Beach County, FL. It is delineated by artificial levees, and consists of natural, agricultural and urban areas adjacent to each other. The basin is bounded by the L-8 canal and the M-canals on the south, the Pratt and Whittney Complex and the Indian Trail Drainage District on the east, and the Lake Okeechobee on the west. It includes the Corbett and Dupuis Wildlife areas to the north, parts of the Village of Royal Palm Beach (VRPB) to the east, an agricultural area covering citrus to the south, and an agricultural area to the north. Water supply needs of the system include the agricultural demand in the north drawn from the L-8 canal, irrigation withdrawals along the M-canal and water withdrawals from M canal for the City of Palm Beach Utilities Department. Eastward water movement along the M-0 canal is due to the pump station on the canal. The capacity of the L-8 canal is about 14 m^3/s when its water level is about 4.6 m above sea level. The capacity of the M-canal is about 8.5 m^3/s. The M-1 canal drains some of the water in the Village of Royal Palm Beach to C-51 canal.

The L-8 canal is connected to Lake Okeechobee at culvert S10-A at the north end. During the simulation period, excess runoff from L-8 is routed to the lake by gravity during flooding. At the southern end, L-8 is connected to the structure complex S-5A, which is capable of sending water to the south, L-8 canal or the C-51 canal and then the ocean depending on a number of conditions. The model uses a head boundary condition at culvert S10-A and a discharge boundary condition near the structure S5-A. The L-8 canal and all the other canals are fully integrated with the 2-D flow domain except near S5-A where the canal runs by itself. Most of the 2-D domain covered in the model is assumed to have no-flow boundaries. The boundary condition near the agricultural area south of S10-A is a constant wall head type, set to 4.3 m.

A number of levees restrict overland flow in the basin. The levee along the L-8 canal is the most prominent, and prevents water in the Dupuis and Corbett wildlife areas from directly entering into the L-8 canal. There are four water control structures and bleeders located in the levee to maintain the water levels in the 5.2-5.8 m range and release the excess to L-8. A second levee, marked as FPL road on the map, runs from north to South between the Dupuis and Corbett areas preventing overland flow between them. A third levee prevents overland flow from the northeastern

quarter entering the VRPB except through a culvert structure. The remaining canal sections in the southwestern quarter are assumed to be without levees and are therefore subjected to both stream-aquifer and stream-overland flow interactions.

The operation of the 720-acre impoundment by the Indian Trail Water Conservation District (ITWCD) is used to demonstrate how one of the water management operations are simulated in the model. The impoundment is used during floods to maintain low water levels in areas draining to M-0 canal. The ITWCD operates pumps sending water into the impoundment when the flood levels at the M-0 canal exceed critical levels. The pump capacity is 31 m^3/s. The outflow from the impoundment passes through three outflow structures with 1.4 m discharge pipes and a 6.4 m invert elevation. The discharges in the pumps can be characterized approximately using a 1-D lookup table in XML similar to the following. The following is also a self explanatory example of the use of XML in data entry.

```
<single_control wmID="3" id1="10034" id2="354"
    control="10034" revflow = "yes"
    label="Pump at the impoundment" >
        5.0   0.0
        5.1   6.3
        5.3  12.6
        5.9  25.2
        6.1  31.0
</single_control >
```

The lookup table moves water from a water body with ID=10034 which is the canal segment in M-0 to water body with ID=354 which is a cell in the impoundment starting at a water level of 5.0 m. Pumping is controlled by water level in the water body 10034. When the water level of the control is 5.9 m, the discharge rate is 25.2 m^3/s as shown in the lookup table. The identification tag of the water mover is 3, which is used when assigning an operational logic. The operational

logic is written at a separate section of the model called the management simulation engine (MSE) not described here.

The total simulation period used is between 1992-1995, while 1994 is used for calibration. The time step selected is 1 day because of data availability. The area is discretized using 1027 cells and 49 canal segments. Figures 6 and 7 show the discretizations. Daily rainfall and potential evapo-transpiration (PET) are provided to the model in a 3.22 km X 3.22 km square mesh. The first seven months of the simulation are used for initialization. Figure 7 shows the water levels and the water velocity vectors one year after the simulation has begun. The figure shows the drainage patterns in the L-8 basin and the confluence of flow into the area where the structures are located. The flow is prevented from moving into Dupuis because of the levee between Dupuis and Corbett. Figure 8 shows water levels at gages marked DUPUIS1 and DUPUIS2 in the northern part of the basin. Figure 9 shows that water levels in the basin very close to the canal are influenced by the canal levels. The correlation coefficients for DUPUIS1-4 gages calculated according to Flavelle (1992) are 0.80, 0.81, 0.85 and 0.88 and the standard error estimates are 0.03 m, 0.03 m, 0.15 m and 0.13 m respectively. All the water levels indicate that the model is capable of representing the system reasonably under the natural stresses of the rain and imposed stresses of the L-8 canal. Figure 10 shows the simulated and computed discharges in the L-8 canal for the same period.

The finite volume method and the object oriented code design are responsible for some of the water budget functions of the code. These capabilities are illustrated using water budgets of two water bodies for one day of the simulation period. Table 1 shows the water budgets of cell 192 and segment 10008 on December 31, 1992. The tables were created using the list of water mover objects attached to the water bodies. This computation was easy because of the finite volume method, and the fact that water budget calculations are assigned to abstract base classes of water bodies and water movers. The example illustrates the complexity of the system and how it is managed using the new tool.

Current and future applications

One of the functions of RSM in South Florida is to serve as a regional hydrologic model for many

disciplines. Since RSM provides support to accommodate complex site-specific conditions using features such as pseudo cells, SV relations, transmisivity functions and conveyance functions, it is possible to design many complex model applications without making code changes. Scientists familiar with complex local conditions and management rules can develop pseudo cell models describing local agricultural practices, permitted rules and other informations, and the model can populate various areas with these pseudo cell objects. Current applications of the methods discussed in the paper include the Water Conservation Area 1 (16292 cells), South West Florida, (40000 cells), Loxahatchee river watershed (7247 cells), Welter, (2002), Southern Everglades (52817 cells) in Florida, and the Kala-Oya basin in Sri Lanka (3200 cells), Lal et al., (2004).

SUMMARY AND CONCLUSIONS

An implicit finite volume method, a high-speed sparse solver, and the object oriented design approach contributed to the development of a fully integrated regional hydrologic model. A number of abstractions such as the water body, water mover, storage-volume (SV) relationship and pseudo cells were used to accommodate the complex hydrologic features of the system seamlessly into one simple computational algorithm. An object oriented design provided an unlimited capability for the model to expand. The implicit method helped to make it stable.

The model was applied to a small but complex hydrologic basin in South Florida to demonstrate how different hydrologic components with different land use types could be incorporated into one model application. Results show that the model is capable of simulating the water levels and discharges observed in the field. Results also show that the model can provide consistent water budget information for model components.

The limited error analysis shows that the numerical errors of the model results agree with the error estimates computed using analytical methods developed by Lal (2000). Analytical estimates of numerical error are extremely useful in designing suitable model discretizations with known numerical error limits.

Table 1: Model runs used in the comparison of analytical and observed errors

T_p	Δt	$T \quad m^2/s$	$k \quad m^{-1}$	ϕ	ψ	β	ε_{anal}	ε_{obs}
8.6 hrs	0.5 hrs	20.0	0.00101	0.153	0.365	7.791	1.53%	1.56%
8.6 hrs	0.5 hrs	2.0	0.00318	0.484	0.365	0.779	1.81%	1.57%
5.1 hrs	0.5 hrs	20.0	0.00131	0.199	0.616	7.791	4.1%	9.0%
20.0 days	1.0 day	2.0	0.00043	0.0648	0.314	37.39	1.13%	1.12%

Table 2: Sample water budgets for two water bodies on Dec 31 st, 1992 in m^3/day

Water Body	Attached water movers	Inflow vol
Cell 192	Overland from Cell 191	0.00
	Overland from 94	0.00
	Groundwater from cell 191	6.56
	Groundwater from cell 193	3178.24
	Groundwater from cell 94	-44.39
	Seepage from seg 10008	-4722.00
	Change in storage	-1268.68
	Mass balance error	2.2×10^{-5}
Segment 10008	Flow from seg 10007	-63347.40
	Flow from seg 10009	51222.50
	Flow in weir	0.00
	Flow in bleeder	0.00
	Overbank fl. from cell 191	6436.07
	Seepage from cell 191	4722.06
	Seepage from cell 96	65.60
	Seepage from cell 94	35.96
	Seepage from ell 95	13.61
	Change in storage	-861.50
	Mass balance error	-8.3×10^{-5}

REFERENCES

Abbott, M.B., Bathurst, J.C., Cunge J. A., O'Connell, P.E. and Rasmussen, R., (1986a). An introduction to the European Hydrological System System Hydrologique European, (SHE), 1: History and philosophy of a physically based, distributed modeling system, *Journal of Hydrology*, 87, pp 45-59.

Abbott, M.B., Bathurst, J.C., Cunge J. A., O'Connell, P.E. and Rasmussen, R., (1986b). An introduction to the European Hydrological System, "System Hydrologique European", (SHE), 2: A structure of a physically-based distributed modeling system, *Journal of Hydrology*, 87, pp 61-77.

Akan, O., Yen, B. C., (1981). "Diffusion flow routing in channel networks", *J. Hydraul. Div., ASCE*, 107(6), 719-732.

Balay, S., Gropp, W. D., Kushik, D., and McInnes, L. C., Smith, B. (2001). *(PETSC) Users Manual, ANL-95/11 - Revision 2.1.3,* Argonne National Lab, IL.

Bosak, J. and Bray, T. (1999). "XML and the second generation web", *Scientific American*, May, 1999.

Brion, L. Senarat, S. U. S., and Lal, A. M. W. (2000). "Concepts and algorithms for an integrated surface water/groundwater model for natural areas and their applications", *Greater Everglades Ecosystem Restoration (GEER) Conference*, Naples, FL, December 11-15, 2000.

Brion, L., Senarat, S. U. S., Lal, A. M. W., and Belnap, M. (2001). "Application of the South Florida Regional Simulation Model in the Everglades", *Proceedings, ASCE Specialty Symposium: Integrated Surface and Groundwater Management*, Orlando, FL, May 20-24.

Danish Hydraulic Institute, DHI, (1998). "Users manual and technical references for MIKE-11", Denmark.

Flavelle, P. (1992). "A quantitative measure of model validation and its potential use for regulatory purposes" *Advances in water resources*, 15, 5-13.

Gelb, A. (1974). *Applied Optimal Control*, MIT Press, Cambridge, MA.

Hirsch, C. (1989). *Numerical computation of external and internal flow*, John Wiley, New York.

Hromadka, T. V., McCuen, R. H. and Yen, C. C. (1988). ”Comparison of overland flow hydrograph models”, *Journal of Hydraulic Engineering*, 113(11), 1422-1440.

HydroGeoLogic, (2000). *MODFLOW-HSM: A Comprehensive MODFLOW-Based Hydrologic Modeling System: Software Documentation*, HydroGeoLogic Inc., Herndon VA.

Kadlec, R. H., and Knight, R. L. (1996). *Treatment wetlands*, Lewis Publishers, Boca Raton, Fla.

Katul, G. (2002). ”A mixing layer flow theory for flow resistance in shallow streams”, *Water Resour. Res.,* 38(11), 1250.

Lal, A. M. W. (1998a). ”Weighted implicit finite-volume model for overland flow”, *J. Hydr. Engrg., ASCE*, 124(9), 941-950.

Lal, A. M. W. (1998b). ”Performance comparison of overland flow algorithms”, *J. Hydr. Engrg., ASCE,* 124(4), 342-349.

Lal, A. M. W., Belnap, M., and Van Zee, R. (1998c). ”Simulation of overland and ground water flow in the Everglades National Park”, *Proc., Int. Water Resour. Engrg. Conf., ASCE, Reston, VA*, 610-615.

Lal, A. M. W. (2000). ”Numerical errors in groundwater and overland flow models”, *Water Resources Research*, 36(5), 1237-1247.

Lal, A. M. W. (2001). ”Modification of canal flow due to stream-aquifer interaction”, *J. Hydraul. Eng.,* 127(7), 567-576.

Lal, A. M. W. (2004), Van Zee, R., Welter, D., Liyamagama, B. S. and Shelton, P. D. ”An integrated river basin model to investigate upland and sub-surface hydrology of the Kala-Oya basin”, *Proc. Tenth Asian Congress of Fluid Mechanics*, May 17-21, Peradeniya, Sri Lanka.

Lopez, F. and Garcia, M. (2001). ”Mean flow and turbulent structure of open-channel flow through non-emergent vegetation”, *J. Hydraul. Eng.,* 127(5), 392-402.

Loucks, D. P., Stedinger, J. and Haith, G. (1981). *Water Resources Systems Planning and Analysis*, Prentice Hall, NJ.

McDonald, M. and Harbough, A. (1988). A modular three-dimensional finite difference groundwater flow model, *Tech. Water Resour. Invest: 06-A1*, U. S. Geol. Surv., Reston, VA.

Ponce, V. M., Li, R-M, Simons, D. B. (1978). "Applicability of kinematic and diffusion models", *J. Hydr. Engrg., ASCE*, 104(3), 353-360.

Rumbaugh, J., Blaha, M., Premerlani, W., Eddy, F., and Lorensen, W. (1991). *Object-oriented modeling and design*, Prentice Hall, Englewood, NJ.

Schmidt, J.H., and Roig L.C. 1997 "The Adaptive Hydrology (ADH) Model: a Flow and Transport Model for Coupled Surface Water-Groundwater Analysis" *XXVIIth Congress of the IAHR and ASCE*, San Francisco, California, 367-372.

Smajstria, A. G. (1990). *Technical Manual, Agricultural Field Scale Irrigation Requirements Simulation (AFSIRS) Model*, Agricultural Engineering Department, University of Florida, Gainsville, FL.

Solomantine, D. P. (1996). "Object orientation in hydraulic modeling architecture", *J. Hydraul. Eng.,* 10(2), 125-135.

South Florida Water Management District, SFWMD (1999). *A primer to the South Florida Water Management Model, SFWMM*, version 3.5, South Florida Water Management District, April, 1999.

South Florida Water Management District, SFWMD (2001). *Users guide for the routing model CASCADE 2001, version 1.0*, South Florida Water Management District, August 2001.

Stroustrup, B. (2000). *The C++ programming language*, Addision Wesley, NJ.

Swain, E. D., and Wexler, E. J. (1996). "A coupled surface water and groundwater flow model (MODBRANCH) for simulation of stream-aquifer interaction", *Techniques of water resources investigations of the USGS*, US Geological Survey, Government Printing Office, Washington, D.C.

Tisdale, T. (1996). "Object-oriented analysis of south Florida hydrologic systems", *Journal of Computing in Civil Engineering*, 10(4), 318-326.

USACOE, (1999). *Central and Southern Florida Project Comprehensive Review Study* Final Inte-

grated Feasibility Report, US Army Corps of Engineers, Jacksonville, also available at www.evergladesplan.o

VanderKwaak, J.E., (1999), *Numerical simulation of flow and chemical transport in integrated surface-subsurface hydrologic systems*, Ph.D. theses, University of Waterloo, p 218.

Walton, R., Wexler, E. J., and Chapman, R. S. (1999). "An integrated groundwater-open channel flow model (MODNET)", *Tech. Report,* West Consultants, Bellevue, Wash.

Welter, D. (2002). *Loxahatchee National Wildlife Refuge RSM model*, Technical Report, South Florida Water Management District.

Yeh, G. T., Cheng, H. P., Cheng, J. R. Lin, H. C. and Martin, W. D. 1998 "A numerical model simulating water flow and contaminant and sediment transport in a watershed systems of 1-D stream-river network, 2-D overland regime, and 3-D subsurface media (WASH123D: Version 1.0)", US Army Corps of Engineers, Waterways Experiment Station, *Technical Report CHL-98-19 prepared for the US Environmental Protection Agency.*

ACKNOWLEGEMENT

The author wishes to thank Joel Von Armen, Todd Tisdale and Joe Park of the South Florida Water Management District for reviewing the manuscript and suggesting many technical and editorial problems. The author also acknowledges David Welter and Clay Brown for the close teamwork that made this work possible. Jayantha Obeysekera was the director of the Hydrologic Systems Modeling Division at the time.

APPENDIX II: NOTATION

The following symbols were used in the paper.

A_c	cross sectional area of a canal
A_l	lake area
B	width of a canal segment
$C(H)$	conveyance of overland flow
f	frequency defined as radians per second
$f_{sv}(H)$	stage-volume relationship function converting head to a volume
H	water head
$\mathbf{H}^n$	heads of water bodies at time step n
k	wave number defined as 2π/ wave length.
$\mathbf{M}$	resistance matrix
n_b	Manning coefficient
S	water surface slope
R	hydraulic radius of the canal
R_{rchg}	net contribution to recharge from local hydrology to the regional system
s_c	storage coefficient of the soil
$T(H)$	transmissivity of the aquifer
t	time
U, F, G	conservative variables in the equations of mass balance.
$\mathbf{V}$	volumes of water contained in the water bodies.
W	source and sink terms in the continuity equation
x, y	Cartesian coordinates
z_m	ground elevation of cell m
α	time weighting factor
$\Delta\mathbf{A}$	diagonal matrix of effective areas.

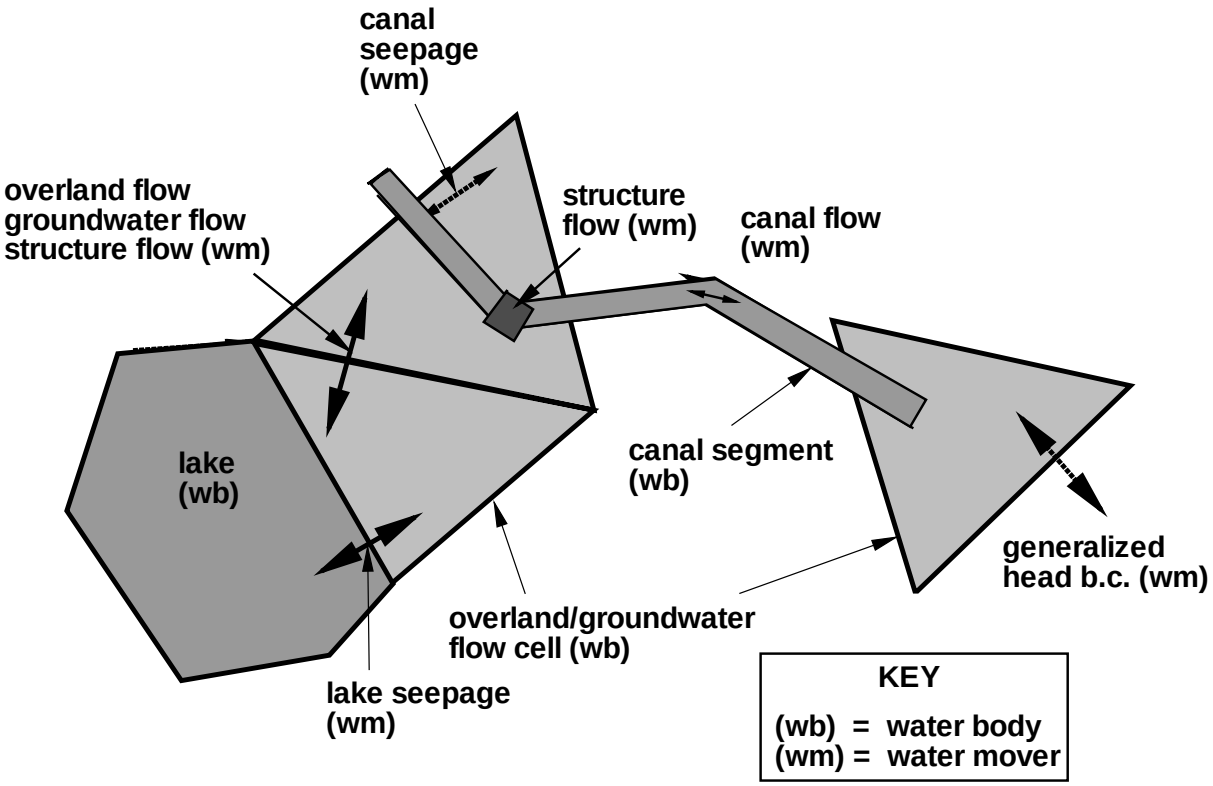

Figure 1: Objects used in the model

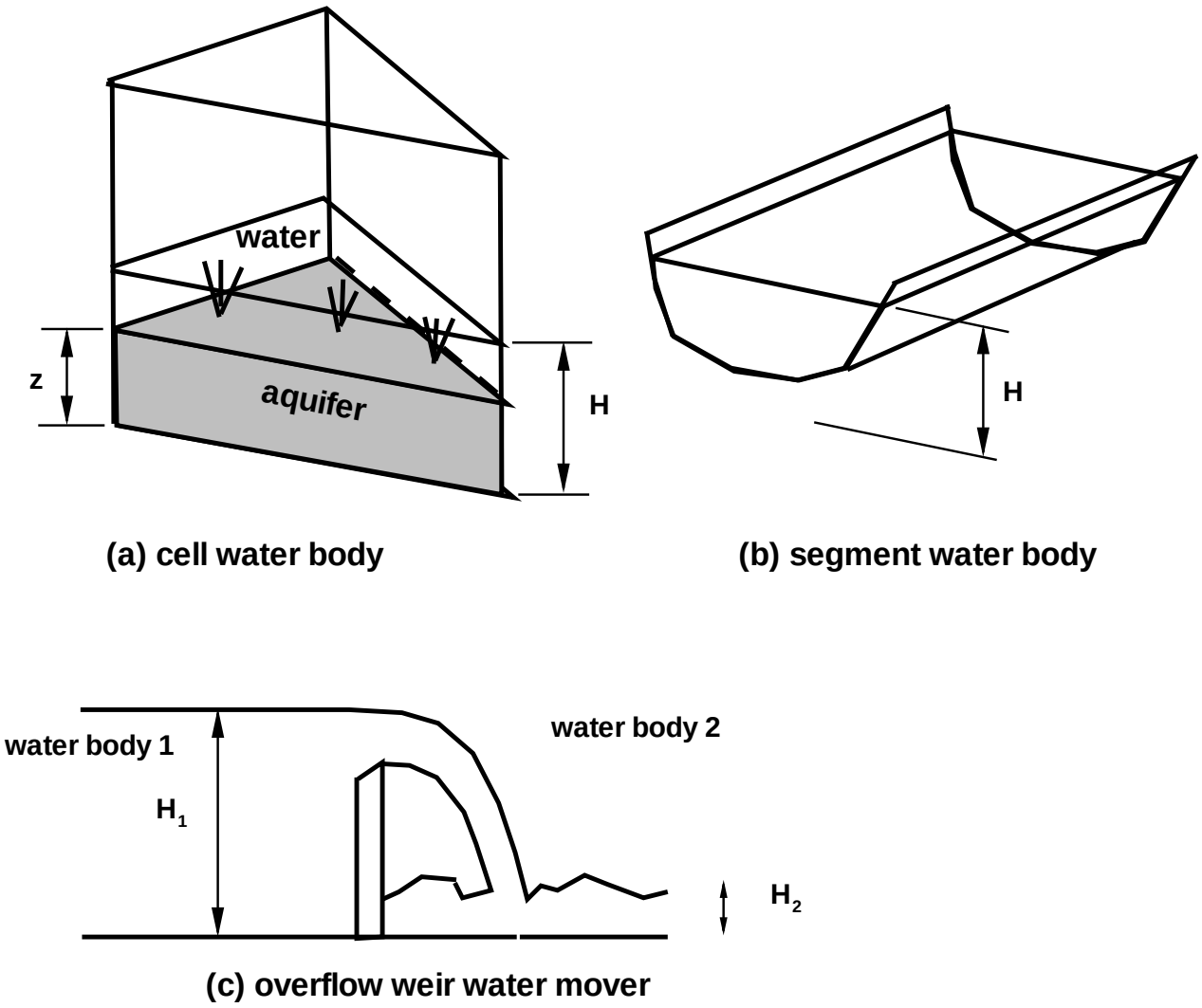

Figure 2: Examples of water bodies and a water mover

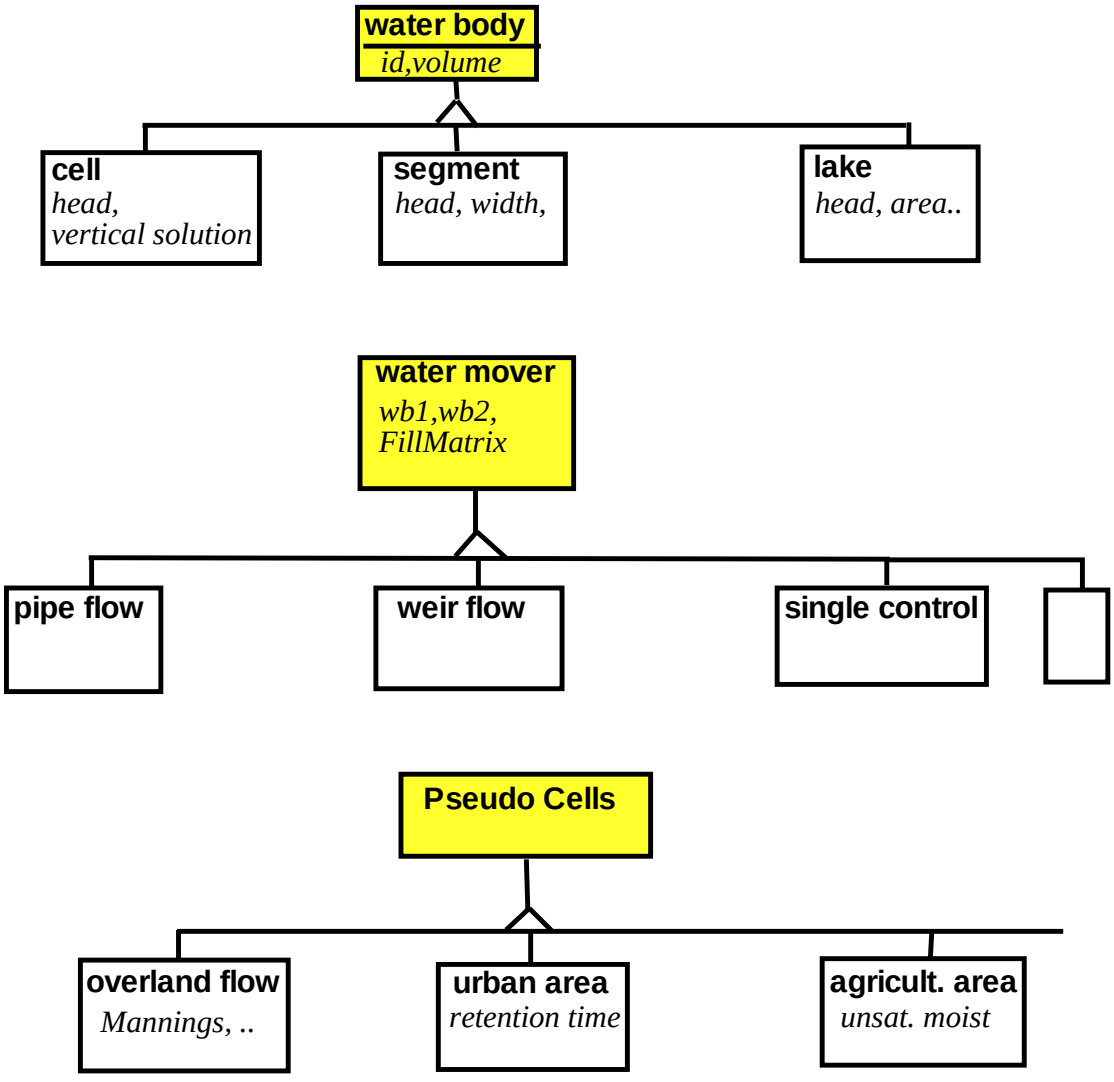

Figure 3: Class diagrams showing the basic building blocks of the model

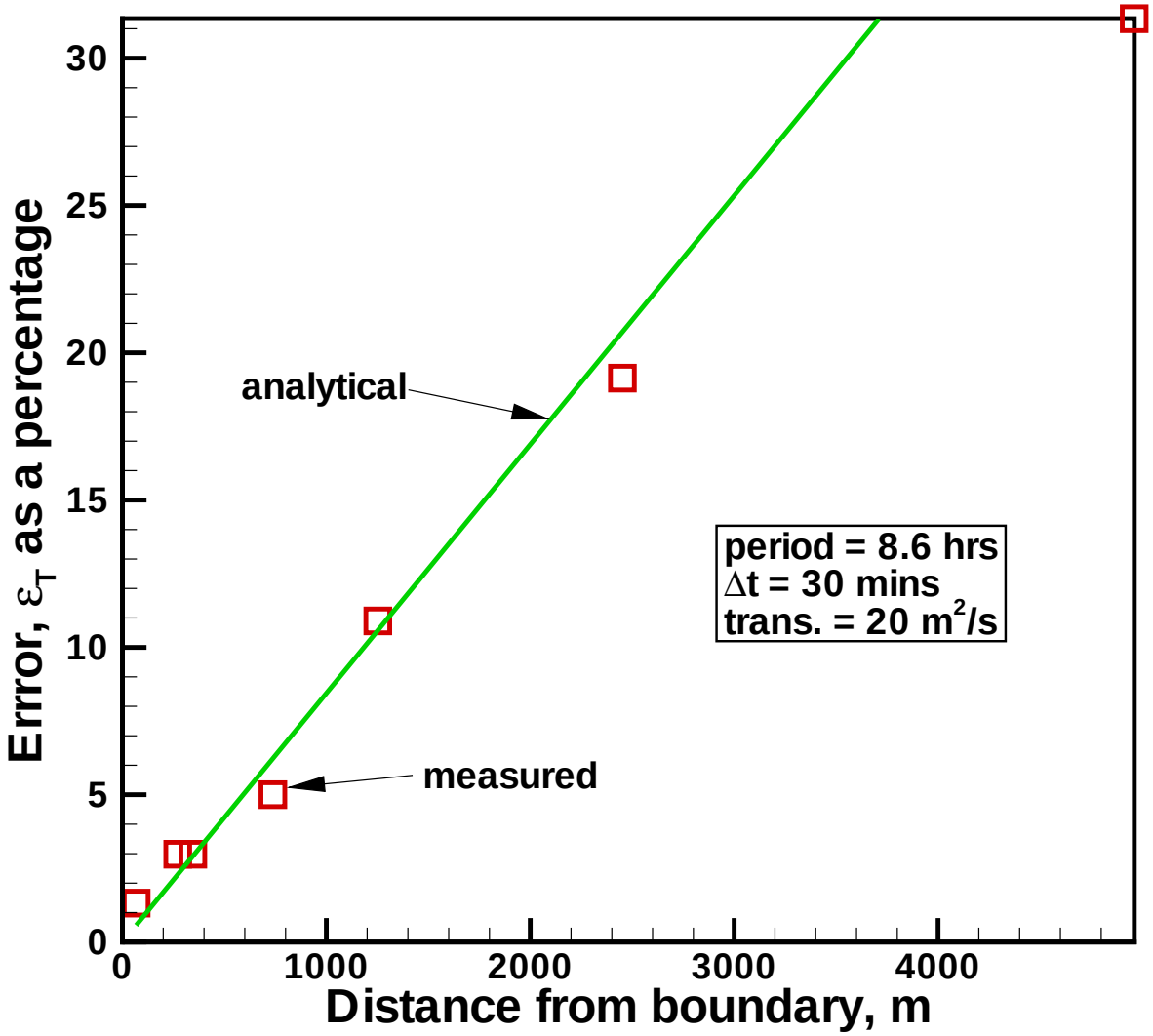

Figure 4: Variation of percentage error with distance

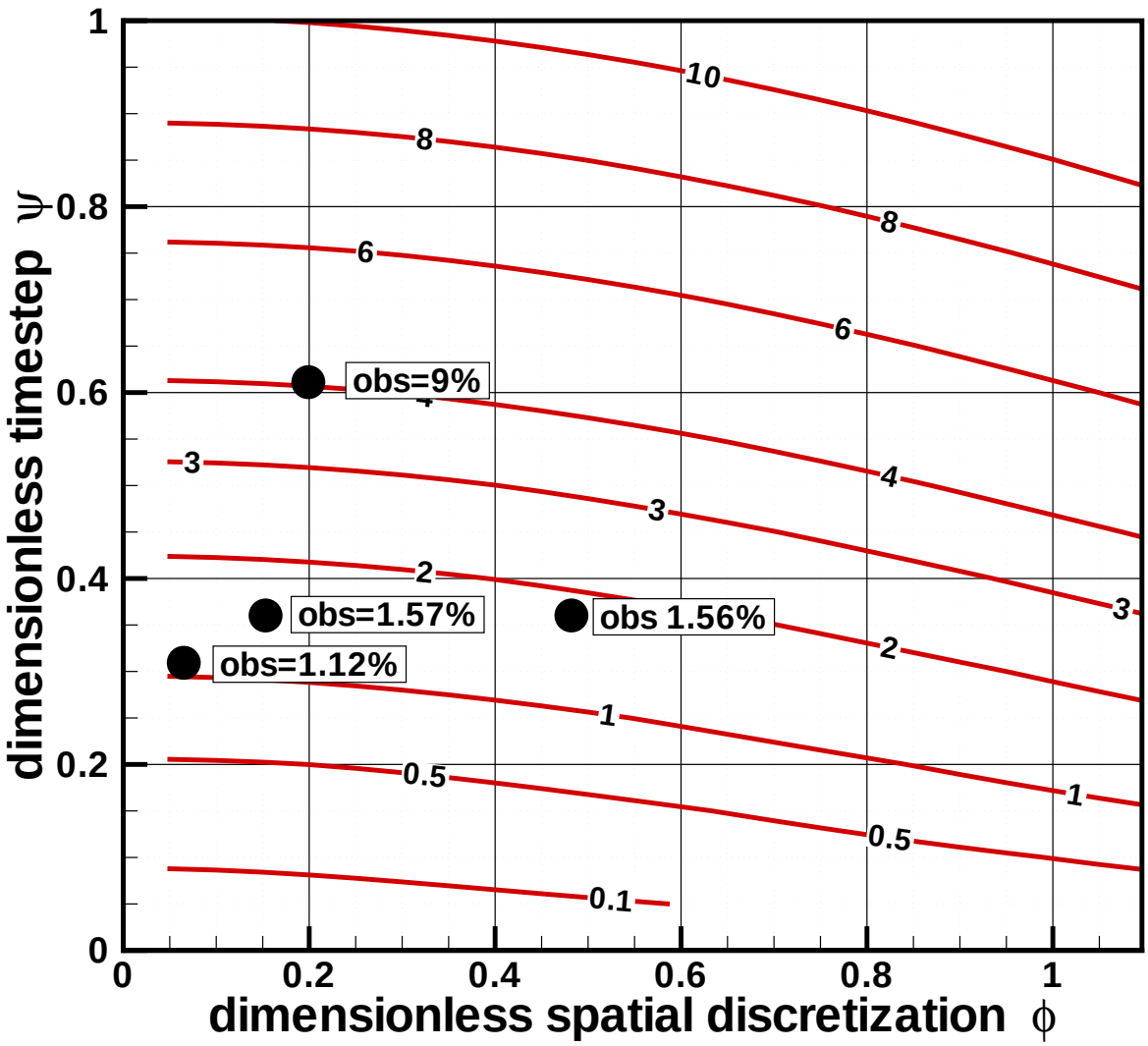

Figure 5: Contours of ε (%) against ϕ and ψ

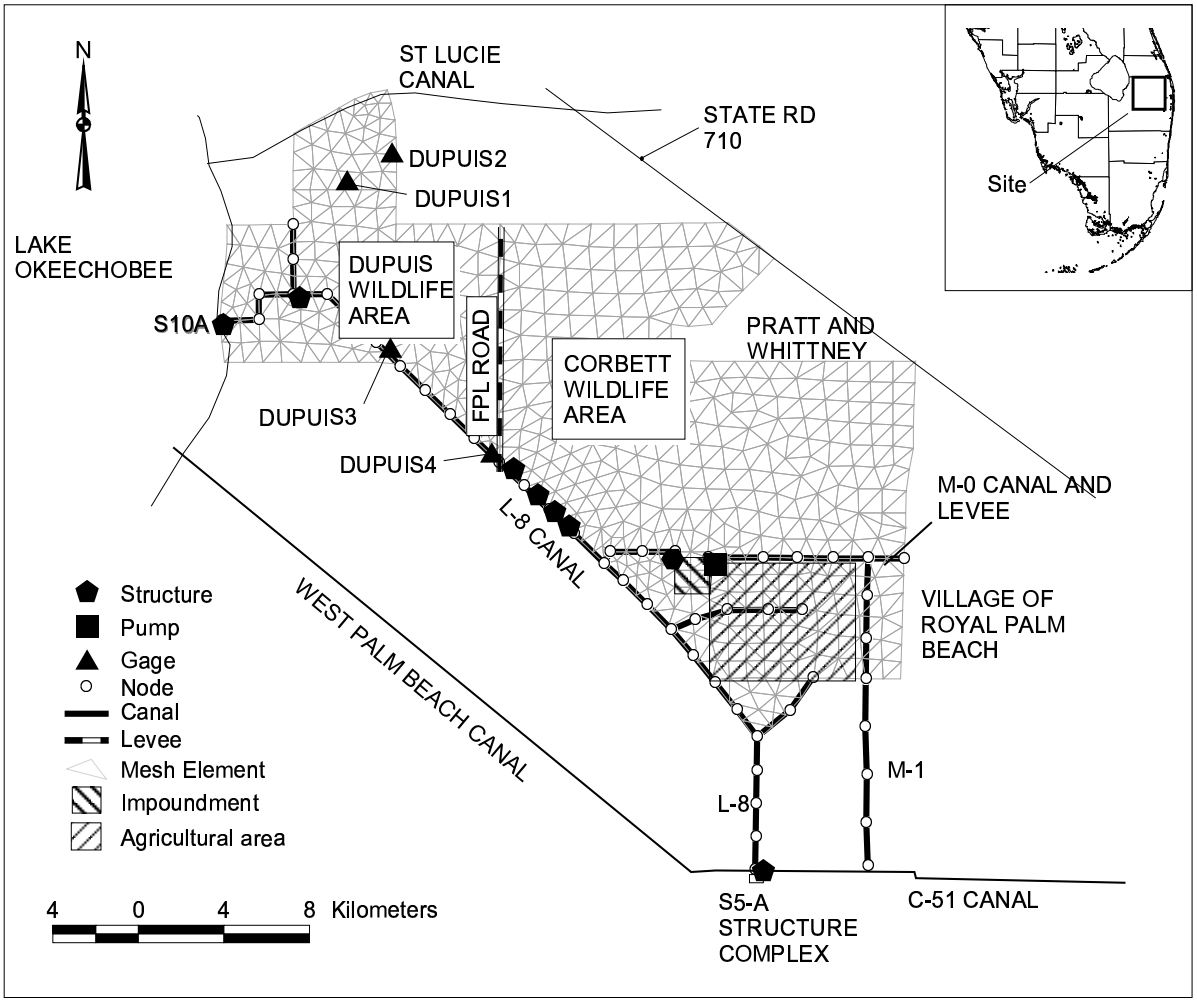

Figure 6: A site map of the L-8 basin

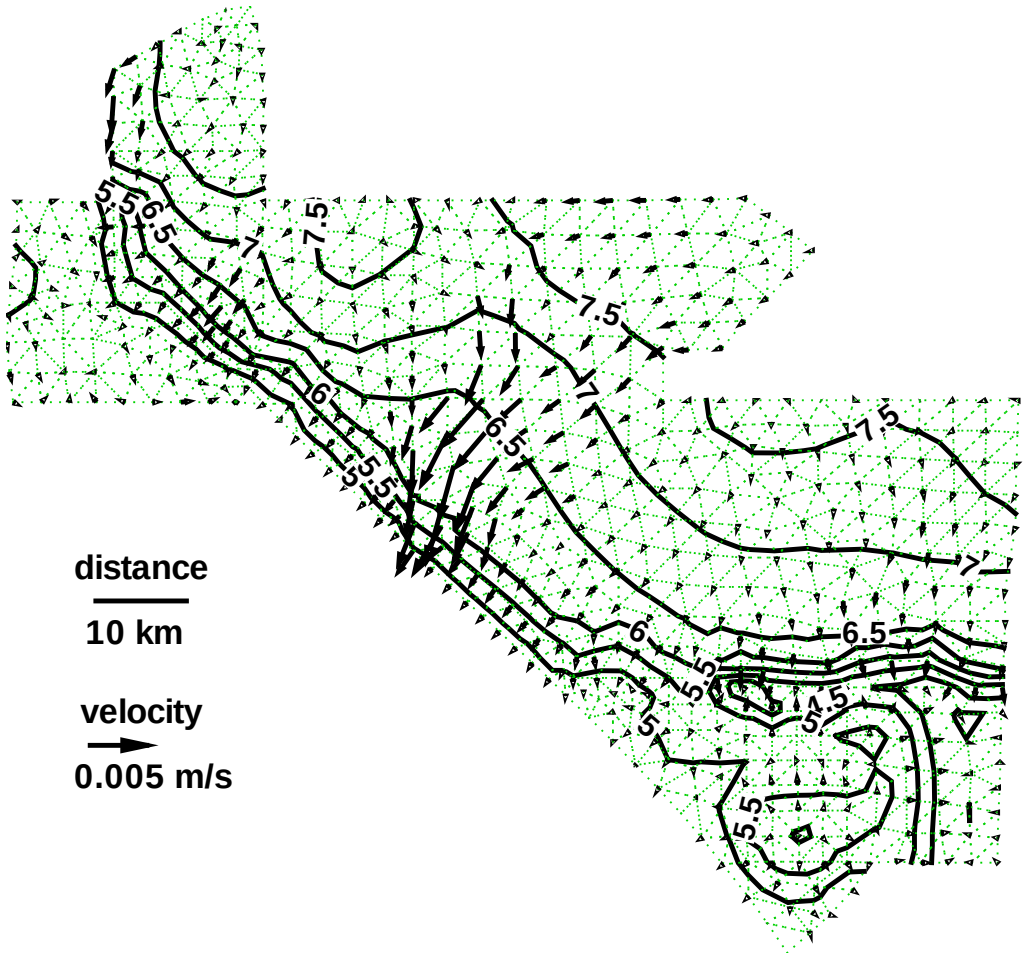

Figure 7: Water levels and flow velocities of L-8 in January, 1993

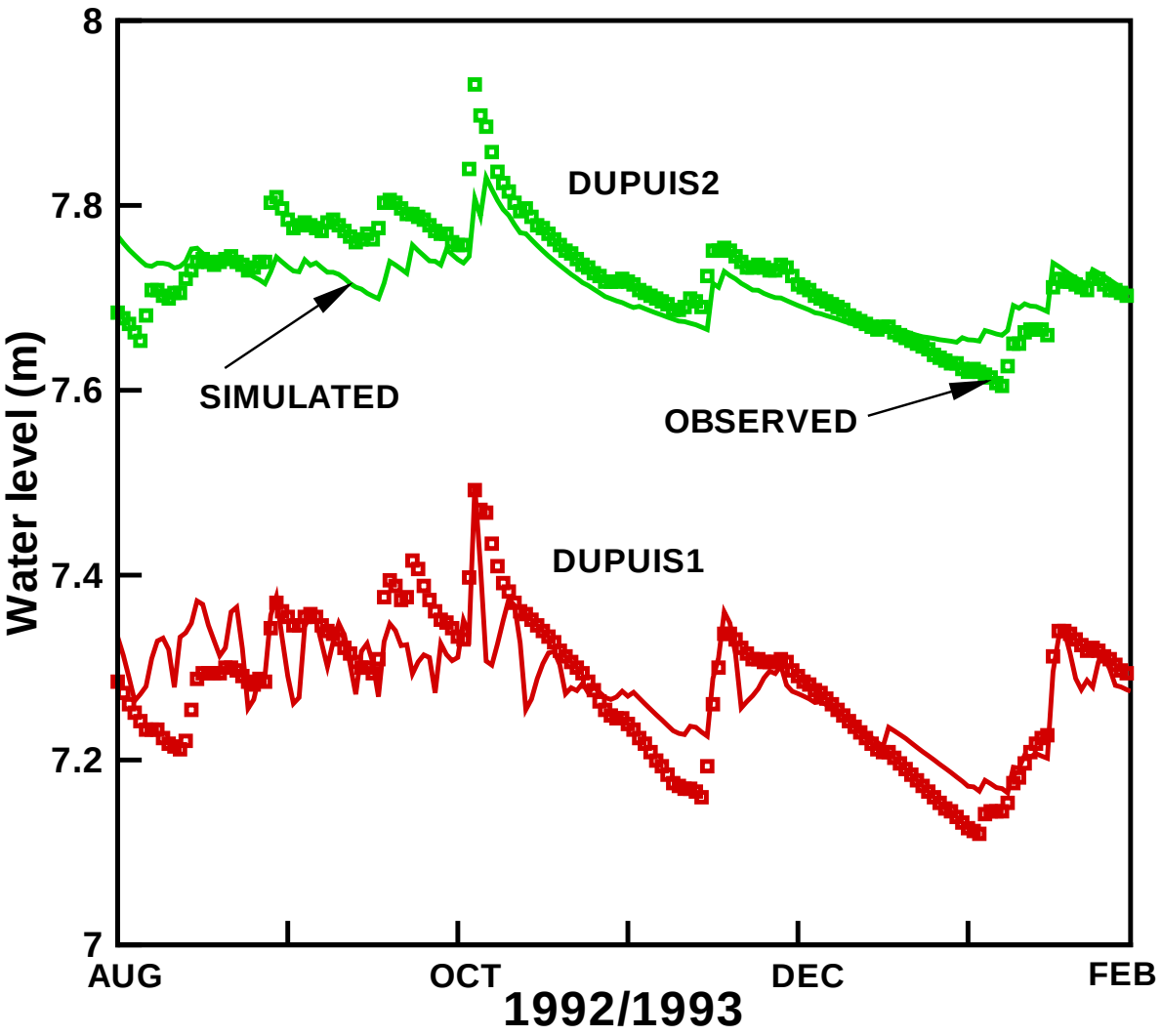

Figure 8: Water levels in Dupuis gages 1 and 2

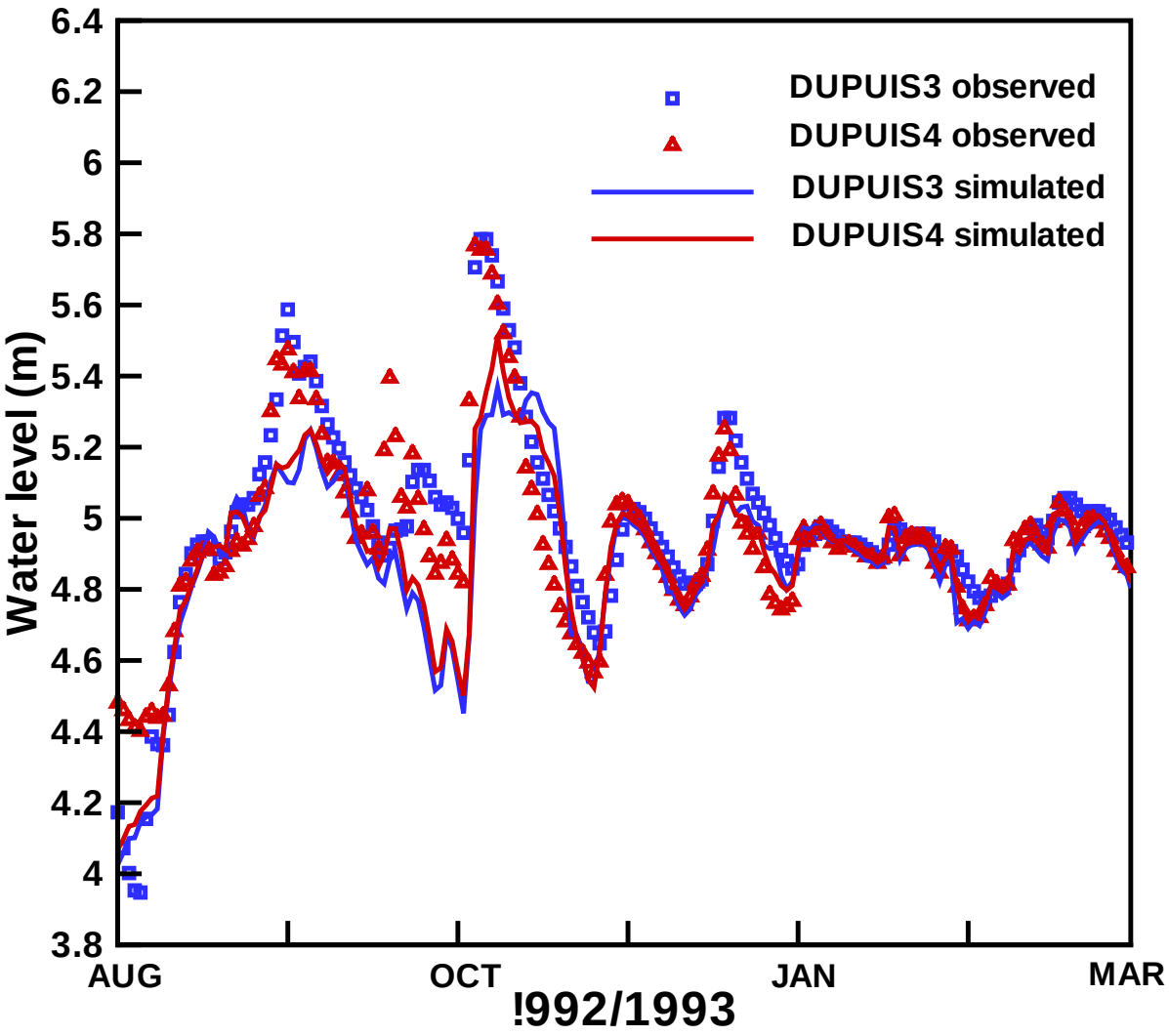

Figure 9: Water levels in Dupuis gages 3 and 4

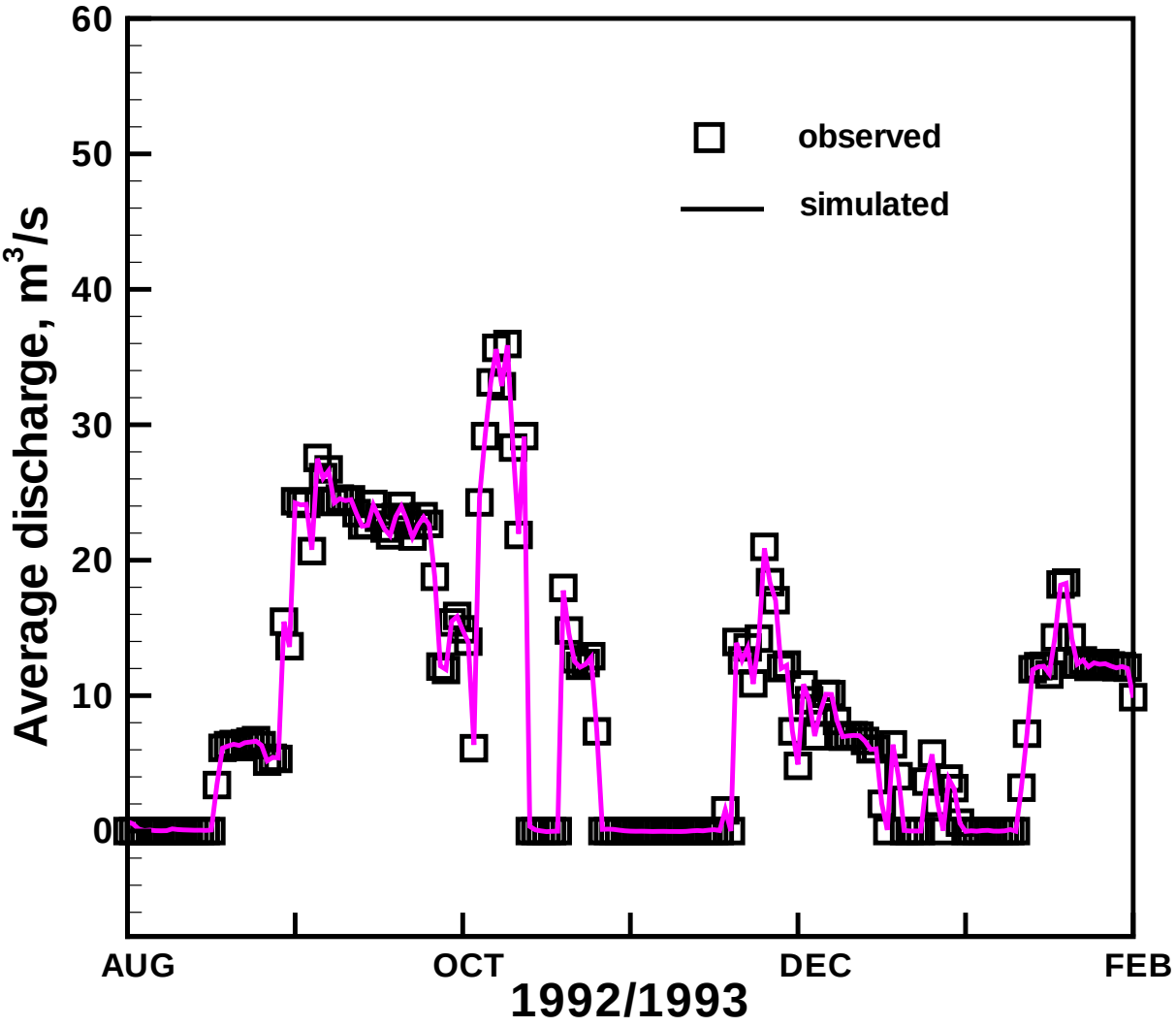

Figure 10: Discharges at S-10A

KEYWORDS

integrated hydrologic model, implicit finite volume method, South Florida regional simulation model, error analysis

C.4 Determination of aquifer parameters using generated water level disturbances

DETERMINATION OF AQUIFER PARAMATERS USING GENERATED WATER LEVEL DISTURBANCES

A. M. Wasantha Lal [1]

A method was developed to determine bulk values of aquifer and sediment parameters in a coupled canal-aquifer system using generated sinusoidal water level disturbance. The method is based on analytical solutions to canal-aquifer interaction derived in terms of dimensionless parameters. Numerical models were used to verify the behavior of the solutions in selected test problems. The method was applied to determine physical parameters of the L-31W canal in Miami-Dade County, Florida near the Everglades explicitly both in dimensionless and dimensional forms. The physical parameters were derived using data collected from a field experiment that was carried out using operational control features of the regional water management system.

Results of the analysis show that various dimensionless parameter groups determine dynamic behaviors of both confined and unconfined aquifers during canal-aquifer interaction. Which seepage process dominates in the system depends on the range of a particular dimensionless parameter. The analytical relationships developed in the paper are useful for calculating parameters in large regional systems where the historical data are noisy or questionable. These relationships make it possible to use measured stresses applied to the system in order to create recognizable signatures that can be used with relationships between the input and output signals to determine the parameters. Sinusoidal stresses were used in the current test, and the resulting parameter values are expressed in both dimensionless and dimensional forms.

[1]Lead Engineer and Supervising Engineer, Model Development Division, South Florida Water Management District, 3301 Gun Club Rd., West Palm Beach, FL 33406

INTRODUCTION

Quantification and control of groundwater flow and canal seepage in South Florida have become important concerns because of the role they play in management of the hydrology. Water management involves resolving problems created by competing and conflicting needs to access or control water. In this region, too much water is present during wet periods which must be routed away to tides or storage areas to be used during dry periods. During dry periods water is needed to meet demands in the agricultural and urban areas, satisfy environmental needs, control salinity in coastal areas, and restore natural areas such as the Everglades. Management of natural wetlands that are located next to urban and agricultural areas is an extremely difficult task considering that the water levels maintained for various land use types are different and the underlying limestone-based aquifer is extremely porous. The hydrologic system in southern Florida is complex due to the presense of canals that allow for the conveyance of water in and out of Lake Okeechobee, dikes and levees that create regional impoundments (water conservation areas), urban areas and natural areas. Any future restoration of natural areas could be accomplished only by ensuring that water supply and flood control needs in the urban and agricultural areas are not affected. In order to achieve all these goals, a good understanding of surface water flow, groundwater flow, and stream-aquifer interaction in canals is needed along with accurate estimates of underlying physical parameters. In the specific case of study site L-31W shown in Figure 1, determination of groundwater flow and canal seepage parameters is important in necessary in order to understand and control groundwater flow and canal seepage out of the Everglades National Park (ENP), minimize impacts of urban well fields, and manage freshwater base flow to Biscayne Bay. This manuscript describes a field test that can be used to determine aquifer parameters, and an analytical solution that can be used to calibrate aquifer and canal seepage parameters.

In South Florida, calibration of regional parameters is not a simple process because the physical system itself is not simple and the state variables of the system depend heavily on complicated operational rules. A typical water level or discharge time series in South Florida shows primarily the effects of rainfall and evapotranspiration (ET) stresses over with the effects of local and regional stresses due to structure and pump operations by public water supply users, industrial

users and agricultural users superimposed. Under these conditions, a calibration based on optimization or manual methods also has a limited use, partly because of the noise generated during the operations. Some of the calibration methods fail when the level noise in the historical data due to unmeasured natural and operational stresses are extremely high. One reason for the difficulty of calibrating such a system is the lack of understanding of the cause and effect relationships of hydrologic stresses and hydrologic responses.

The problem of parameter estimation of integrated models is complicated for other reasons as well. Since many integrated models are under-determined, it is difficult to obtain high parameter resolutions and low parameter errors when the data is noisy and the data collection network is sparse (Lal, 1998). Many of the numerical models for integrated systems are under determined because of the overuse of physical parameters. Even when the values of some of the parameter groups can be determined, resolution of the individual physical parameters can be difficult at times. In the case of the calibration of groundwater flow for example, hydraulic head data can be used to determine aquifer diffusivity, but not individual parameters for transmissivity and storativity. A second condition such as a steady state or a known discharge, is required to solve this problem. The result of using poorly calibrated or resolved parameters is large output uncertainty. When this happens, use of a model is limited to the locations where good data is available for the calibration.

Field testing is often used in the past on a number of occasions to determine aquifer parameters. Many of the field testing methods make use of analytical or numerical models. A comprehensive list of analytical equations that can be used to determine aquifer parameters is listed in the text by Bruggeman (1999). The method developed by Carr and Van Der Camp (1969) is one of the earliest that is similar to the current application. In its application, the amplitude and the phase lag of tidally induced water levels were used to obtain aquifer characteristics. Pinder, et al. (1969) developed a method to determine aquifer diffusivity using aquifer response behavior under fluctuating river stages. Since analytical equations used for this method cannot be solved explicitly, best fit methods were needed to obtain diffusivity from this test. Recent work on canal-aquifer interaction by Zlotnik and Huang (1999) also involved analytical expressions for dynamic aquifer

response in the case of shallow penetrating streams with bed sediments. Additionally, Motz (2002) also obtained a solution for a leaky confined aquifer using a 1-D dynamic solution for a canal cross section. All these solutions were for sudden changes in canal levels. Lal (2001) obtained a solution for the canal-aquifer interaction problem assuming diffusion flow along the canal with sinusoidal water level changes. As a result of the solution, it was possible to identify dimensionless parameters important to the variation of water levels along the canal. Recent additions to methods capable of determining aquifer diffusivity include analytical methods developed by Swamee and Singh (2003) and Singh (2004). These approaches however require the use of optimization methods to determine parameters.

In the specific case of southeast Florida, understanding the Hydrogeology has been challenging from the beginning. The difficulties have been described by many investigators from earlier times as in the case of Klein, et al., (1977) to more recent times as in the case of Miller (1997). Many including Fish and Stewart (1991) have described the difficulty of characterizing the aquifer as confined or unconfined, and the difficulty of describing some of the properties. Recent investigators on the heterogeneity include Cunningham, et al. (2003). Under these difficult conditions, canal drawdown experiments in conjunction with flow meter experiments have been used in the past to determine aquifer parameters. Since conducting pump tests in southeast Florida has been found to be a futile task, most drawdown tests make use of steady state solutions to determine canal aquifer parameters. Chin (1991) for example developed an analytical method to determine aquifer transmissivity after considering the clogging effects of bottom sediments. This method has been tested in the L-31N canal. In this test, a term ”reach transmissivity” defined as the flow out of a canal per unit length per unit head drop is used to measure the composite aquifer and sediment resistance to seepage. Genereaux and Guardiaro (1998) also conducted a drawdown test based on steady state equations to determine aquifer and canal resistance properties in the L-31W canal. Most tests, based on a steady state assumption only provide a limited set of parameters related to canal-aquifer interaction.

In this study, analytical solutions for simulating the dynamics of fully coupled canal-aquifer

interaction at a canal cross section are developed. It is assumed that the system is disturbed through changes in the canal stage. The analytical expressions are used to understand important seepage characteristics and estimate aquifer parameters. The analysis is first carried out for a single Fourier component of a general solution in order to simplify it. The results of the analysis show the existence of a number of basic dimensionless parameter groups influencing the solution. Some of these groups were previously listed by Lal (2001). Furthermore, since this study is based on water level variations along the canal, it is difficult to focus on cross-section based behaviors. In the current study focusing on a cross section, the dimensionless parameter groups influencing the solution include (a) a parameter group related to aquifer diffusivity; (b) a parameter group explaining vertical leakance in the case of a confined aquifer; (c) a parameter group explaining canal sediment resistance; (d) a parameter group explaining canal and aquifer storages and aquifer transmissivity. These dimensionless parameter groups determine the propagation behavior in the aquifer and the water levels at any point in the system. Extreme behaviors such as the hydraulic cutoff between the stream and the aquifer are functions of these parameter groups.

Field tests were conducted in the L-31W canal, which is part of the managed south Florida conveyance system. During the test, periodic discharge disturbances of known magnitude were generated using pumps and structure facilities. Water level disturbance data collected during the test from various points in the system were used to calculate the phase and the amplitude of the disturbance. Explicit relationships between the wave characteristics and parameters were used to determine the parameter values for sinusoidal stresses. A dry period was preferred for the test due to the low noise level and the absence of ponding. A low noise level in the data was important as a way to reduce parameter uncertainty. The period of the wave was selected so that only the targeted zone adjacent to the canal was stressed.

Analytical expressions relating parameters to the stress-response relationships are useful when studying both physical and numerical systems. These analytical expressions can be used to solve a number of problems in system identification especially when there is excessive data noise and a lack of knowledge of cause-effect relationships between the stress and the response. In the current

experiment, both the stress and the response are sinusoidal and the calculations of parameters are based on measured amplitude and phase. Experiments such as this suggest that it is possible to determine targetted parameters of the system, or understand the effect of targetted parameters whether the system is physical or numerical. Understanding and calibrating numerical models is a novel use of these analytical expressions.

There are advantages and disadvantages associated with the test. It is generally environmentally nondestructive, and the effects are local. It is easier therefore to obtain approval of a test from regulating agencies, even when testing is conducted close to a sensitive area. The flexibility to select the frequency and the amplitude allows for control of the tested area. High frequency disturbances are useful for investigations close to th canal, and low frequency disturbances are useful for far field investigations. In both cases, the overall resolvability of the parameters is limited by data noise. The disadvantages of the test are mainly due to the difficulty of creating sinusoidal water level or discharge disturbances in canals using limited operational facilities. Disturbances that have square wave shapes are also useful, but the analyses are complex. The test assumes the absence of ponded water over the aquifer and the differences in water levels along the canal to be small compared with the amplitude. The test is proposed to many areas of South Florida where the canal segments are relatively short or the water level differences along the canal are small.

THEORETICAL CONSIDERATIONS

In this section, analytical expressions describing the dynamic behavior of canal-aquifer interaction are derived. The derivation is carried out for a canal cross section as shown in Figure 2 assuming that the canal is fully coupled with the aquifer, and the seepage is impeded by a possible canal sediment layer. Even if the analysis is carried out for a leaky confined aquifer, the results are applicable to both leaky and non-leaky confined aquifers as well as unconfined aquifers when the coefficient of leakage or leakance of the confining layer is set to zero. The water level is assumed to be flat, and therefore the results are applicable to many short canal segments in south Florida with structures at both ends. This assumption is valid when the water level differences along a canal are small compared to the water level changes in the canal over a test cycle. The following

analysis is aimed at obtaining expressions for aquifer parameters in terms of the amplitude and the phase of the water level at different points in the aquifer.

Influence of diffusivity and vertical leakiness on the propagation behavior of confined aquifers

The one dimensional governing equation for a leaky confined aquifer is used to derive expressions for two parameters; the aquifer diffusivity and the coefficient of leakage of the confining layer. The governing equation for groundwater flow in a semi-confined aquifer is (Bear, 1979)

$$s_c \frac{\partial H}{\partial t} - R = \frac{\partial}{\partial x}\left(T \frac{\partial H}{\partial x}\right) + \frac{k_v}{\delta_v}(h(t) - H) \tag{1}$$

in which $R =$ recharge per unit length; $T =$ aquifer transmissivity; $H =$ water head in the leaky confined aquifer; $h(t) =$ water head outside the leaky confined aquifer; $\delta_v/k_v =$ coefficient of leakage or leakance of the semi-pervious confining layer. In unconfined aquifers, transmissivity can be approximated as $T \approx K\bar{d}$ where $K =$ hydraulic conductivity; $\bar{d} =$ average aquifer depth. For fully confined and unconfined aquifers, the term with k_v/δ_v is absent. The analysis of (1) is based on a single Fourier component of the solution described as

$$\mathbf{H} = H_0 e^{If t - \mathbf{k}x} \tag{2}$$

where $f = 2\pi/P =$ angular frequency of the perpetual disturbance imposed on the systemas; $P =$ period of the disturbance; $\mathbf{k} = k_1 + k_2 I$ where $k_1 =$ amplitude decay constant; $k_2 =$ wave number and $I = \sqrt{-1}$. All complex numbers are in boldface.

Values of k_1 and k_2 are key to the determination of aquifer parameters such as diffusivity (Carr and Van Der Camp, 1969). They are determined experimentally using linear plots of log amplitude and phase lag with distance at different points in the path of propagation. The linear equations used for this purpose are derived using (2) which can also be stated as $H_2 = H_0 e^{-k_1 x} \sin(ft - k_2 x)$. The linear equations are:

$$-\ln\left(\frac{|\mathbf{H_2}|}{|\mathbf{H_0}|}\right) = k_1\, x - \ln(\alpha_s) \tag{3}$$

$$\varphi = k_2\, x + \varphi_s \tag{4}$$

in which, $H_0 = |\mathbf{H_0}| =$ amplitude of the water level at the canal; $H_2 =$ amplitude of the water level at a distance x from the canal; $\alpha_s =$ ratio of the amplitude of the water level just outside the canal

sediment layer to the amplitude in the canal; $\varphi =$ phase lag between the water level in the canal and a point at a distance x from the canal; $\varphi_s =$ sudden change in the phase due to canal sediment. The graphs of $-\ln(|\mathbf{H_2}|/|\mathbf{H_0}|$ vs x and φ versus x for a homogeneous medium are straight lines with slopes k_1 and k_2 respectively. Both α_s and φ_s can be calculated from the intercepts. If there is no sediment layer, the intercept would be zero. Any nonlinearity in the curve indicates inhomogenuity of the aquifer with local slopes reflecting local parameters.

In the case of fully confined aquifers, $k_1 = k_2 = k_0$ (Carr and Van Der Camp, 1969). When the aquifer is semi-confined, k_1 and k_2 deviate from each other. The amount of deviation of k_1 and k_2 from a base value of k_0 for non-leaky aquifers can be used to obtain the coefficient of leakage itself. In order to calculate an expression for measuring the coefficient of leakage, (2) is substituted in the governing equation (1), and the result $\mathbf{k^2} = 2(I+\eta)k_0^2$ is solved to give $\mathbf{k} = k_0 n(\eta)\exp(I\kappa)$ in which.

$$n(\eta) = \sqrt{2}(1+\eta)^{\frac{1}{4}} \tag{5}$$

$$\kappa(\eta) = \tan^{-1}\frac{1}{(\sqrt{1+\eta^2}+\eta)} \tag{6}$$

$$k_0 = \sqrt{\frac{s_c f}{2T}} \tag{7}$$

$$\eta = \frac{1}{s_c f}\frac{k_v}{\delta_v} \tag{8}$$

When expressed as real and imaginary components of $\mathbf{k}$,

$$k_1 = k_0\sqrt{\left(\sqrt{1+\eta^2}-\eta\right)}(\sqrt{1+\eta^2}+\eta) \tag{9}$$

$$k_2 = k_0\sqrt{\left(\sqrt{1+\eta^2}-\eta\right)} \tag{10}$$

The dimensionless parameter η in (8) describes the leakiness of a confined aquifer. The equations show that $k_1 = k_2 = k_0$ for confined aquifers, and $k_1 > k_2$ when the confined aquifer becomes leaky. If k_1 and k_2 are significantly different, the implication is the presence of a leaky semi-confining layer. In this case (9) and (10) can be used to determine η by first calculating $r_k = k_1/k_2 = \eta + \sqrt{1+\eta^2}$ and then using $\eta = 0.5(r_k^2-1)/r_k$. Parameter k_0 is then computed using

$k_0 = \sqrt{(k_1^2 + k_2^2)}/n$. For unconfined aquifers or fully confined aquifers with no leakiness, $\eta = 0$, $n(\eta) = n = \sqrt{2}$, and $k_1 = k_2 = k_0$. If there are enough data and the slopes k_1 and k_2, along with their intercepts vary from place to place in the aquifer, the values can be used to create a map of aquifer properties can be plotted on a map to show the heterogenuity.

If the aquifer is leaky confined, $k_1 > k_2$ implying that disturbances decay faster and travel slower. If for example a difference between k_1 and k_2 of more than 5% is considered detectable and significant, the condition for a confined aquifer becoming leaky can be expressed as $\eta > 0.05$. Similarly, if the difference is more than 25%, then $\eta > 0.25$. When the leakiness is extremely large and k_2 reduces to a very low value such as 5% of its original value, the corresponding $\eta \approx 200$. The disturbances decay very rapidly under this condition. The governing equation (1) with an extremely large leakage term is not practically useful.

Numerical experiment to verify the analysis

A numerical experiment was carried out using the MODFLOW model (McDonald and Harbough, 1988) to test the validity of equations (9) and (10). In the experiment, real and imaginary components of **k** obtained using the analytical expressions and the MODFLOW model were plotted separately as shown in Figure 3. For the MODFLOW model, a 1-D two layer groundwater problem was set up with 200 cells of 100 m length. The confined layer was assigned a transmissivity value of $2.777 \times 10^{-4}\ m^2/s$ and a storage coefficient of 0.001. A sinusoidal pumping rate with a period of $P = 48$ Hrs or $f = 3.636 \times 10^{-5}\ s^{-1}$ was used with an amplitude of $1.0\ m^3/s$. Water levels at distances of 100 m, 200m, and 300 m were observed at every 1.0 Hr time step. The model was run with values of k_v/δ_v ranging between $5.5 \times 10^{-12}\ s^{-1}$ and $1.0 \times 10^{-7}\ s^{-1}$. The amplitude and the phase of the observed water level disturbance were calculated using the least square method as described later. The amplitudes were used to calculate k_1 using (2) giving $k_1 = \ln(H_2/H_1)/(x_2 - x_1)$ where H_1 and H_2 are the amplitudes at observation stations 1 and 2 at distances x_2 and x_1 from the canal. Phase measures were used to calculate k_2 using $k_2 = \phi_2 - \phi_1/(x_2 - x_1)$ where ϕ_1 and ϕ_1 are the phase values at stations 1 and 2. The value of k_0 was computed as descried earlier as 8.09 $\times 10^{-3}\ m^{-1}$. Figure 3 shows that the values of k_1/k_0 and k_2/k_0 obtained using the MODFLOW

model agree with the analytical solution. The figure also shows how the speed of propagation decreases and attenuation increases with increasing leakiness.

Analytical relationship for water levels across the sediment layer

If the intercepts in (3) and (4) are not zero, values of α_s and φ_s obtained from these intercepts can be used to calculate the parameters related to the canal sediment layer. The following mass balance condition is used to obtain equations relating the intercepts to the parameters.

$$-T\frac{\partial H_1}{\partial x}|_{x=0} = p\left(\frac{k_s}{\delta_s}\right)(H_0 - H_1) \tag{11}$$

where $p =$ wetted perimeter along which seepage occurs; $k_s =$ hydraulic conductivity of the sediment layer; $\delta_s =$ thickness of the sediment layer; $k_s/\delta_s =$ leakage coefficient of the canal sediment layer. Figure 2 shows a definition sketch. If there is heterogeneity of sediment properties at the bottom or the sides, a composite value of pk_s/δ_s has to used. Assuming the solution in the canal is described as $\mathbf{H_0} = H_0 e^{Ift}$, and the solution in the aquifer just outside the sediment layer is described as $\mathbf{H_1} = H_1 e^{Ift - I\varphi_s}$, the following can be obtained using (11) after simplification.

$$T\mathbf{k}\mathbf{H_1} = p\frac{k_s}{\delta_s}(\mathbf{H_0} - \mathbf{H_1}) \tag{12}$$

After substituting for $\mathbf{k}$ from previous section, this reduces to

$$\left[\frac{n(\eta)}{\sigma}e^{\kappa I} + 1\right]\mathbf{H_1} = \mathbf{H_0}e^{-I\varphi_s} \tag{13}$$

where $\sigma =$ dimensionless sediment conductance parameter defined as (Lal, 2001)

$$\sigma = \frac{p}{Tk_0}\frac{k_s}{\delta_s} = p\frac{k_s}{\delta_s}\sqrt{\frac{2}{fs_cT}} \tag{14}$$

Equation (13) can be used to express the relationship between $\mathbf{H_1}$ and $\mathbf{H_0}$ as

$$\mathbf{H_1} = \frac{\sigma\, e^{-I\varphi_s}}{\sqrt{n^2 + 2n\sigma\cos\kappa + \sigma^2}}\mathbf{H_0} \tag{15}$$

Equation 15 shows that the amplitude $\mathbf{H_0}$ is reduced due to the sediment layer by a factor α_s given by

$$\alpha_s(\sigma,\eta) = \frac{\sigma}{\sqrt{n^2 + 2n\sigma\cos\kappa + \sigma^2}} \tag{16}$$

and the phase lag due to the sediment layer is

$$\varphi_s(\sigma,\eta) = \sin^{-1}\frac{n\,\sin\kappa}{\sqrt{n^2+2n\sigma\cos\kappa+\sigma^2}} \tag{17}$$

If the aquifer is unconfined or non-leaky confined, $n=\sqrt{2}$ and the reduction of amplitude due to the canal sediment layer alone can be shown to be varying with σ as described in Figure 4. According to this figure, the canal is at a completely cutoff state (5% connection) when $\sigma < 0.073$ and a completely connected state (95% connection) when $\sigma > 19.5$. Table 1 shows a summary of this and other dimensionless parameters.

Relationship between a flow pulse and the resulting head response

The following mass balance equation for a unit length of the canal is used to obtain a relationship for the change in water level in a canal for a given inflow.

$$q + 2T\frac{\partial H_1}{\partial x} = B\frac{\partial H_0}{\partial t} \tag{18}$$

in which, $q=$ discharge into the canal per unit length; $H_0=$ water level in the canal; $B=$ width of the canal. Substituting the sinusoidal form of the solution discussed earlier for water level, and using $\mathbf{q} = q_0 e^{Ift+I\theta}$ for discharge rates, the following expression can be obtained after using (15) to explain the relationship between H_1 and H_0.

$$\frac{q_0}{fB}e^{-I\varphi_s} = H_0\left[\frac{\sqrt{2}\alpha_s(\sigma)\,n(\eta)}{\chi}e^{(\kappa-\varphi_s)I}+I\right] \tag{19}$$

in which χ is the single most important dimensionless parameter describing both storage and resistance effects of canal-aquifer interaction.

$$\chi = \frac{fB}{\sqrt{2}Tk_0} = B\sqrt{\frac{f}{Ts_c}} \tag{20}$$

The effects of the sediment layer and the coefficient of leakage of the aquifer also influence the solution. These effects can be incorporated into χ in (19) using the modification

$$\chi' = \chi\frac{\sqrt{2}}{\alpha_s(\sigma)\,n(\eta)} \tag{21}$$

in which $\alpha_s(\sigma)$ is defined using (16) and $n(\eta)$ is defined using (5). In unconfined or non-leaky confined aquifers, $\chi' = \chi/\alpha_s(\sigma)$. If there is no sediment resistance as well, $\chi' = \chi$.

The ratio of the change of head to the change of flow can be defined as a dimensionless parameter ξ. This parameter can be described using (19) as

$$\xi(\chi,\sigma,\eta) = \frac{H_0 fB}{q_0} = \frac{\chi'}{\sqrt{(4+(\chi')^2+4\chi'\sin(\kappa-\varphi_s))}} \tag{22}$$

The phase lag θ between the head and the discharge can also be obtained using (19) as

$$\theta(\chi,\sigma,\eta) = \cos^{-1}\left\{\frac{2\cos(\kappa-\varphi_s)}{\sqrt{(4+(\chi')^2+4\chi'\sin(\kappa-\varphi_s))}}\right\} \tag{23}$$

Equations (22) and (23) are similar to (16) and (17) in behavior. If there is no aquifer to interact, $\xi = 1$. If it is assumed that the interaction is negligible at $\xi > 0.95$, the corresponding condition is $\chi' > 27.6$. The canal amplitude is maximum under this condition. Similarly the interaction is maximum and there is significant damping of canal amplitude with $\xi < 0.05$ or $\chi' < 0.1$. Figure 5 shows the two cutoff values of 95% and 5% at both ends of the asymptotic curve. If the effect of the sediment layer is insignificant, $\sigma = 0$, and therefore $\varphi_s = 0$, $\alpha_s(\sigma) = 1$ and $\chi' = \chi$. Equation 22 then reduces to

$$\xi = \frac{H_0 fB}{q_0} = \frac{\chi}{\sqrt{2+(\sqrt{2}+\chi)^2}} \tag{24}$$

which relates the pulse response behavior to aquifer property χ.

The parameters χ and k_0 together are useful in obtaining primitive values of T and s_c. The parameter k_0 only gives the diffusivity T/s_c and χ gives Ts_c. They both have to be combined to obtain T and s_c

Numerical experiment to verify the analysis

Numerical experiments were carried out to determine the validity of (22) and (23) and understand relationships among relevant dimensionless variables. A 1-D fully implicit numerical model having a formulation similar to MODFLOW was used for this purpose with spatial and temporal discretizations of 100 m and 1hr respectively. In the model, a canal subjected to water level disturbances of period 16 hrs was simulated. Other model parameters were selected to give decent ranges for the dimensionless parameters investigated. The results shown in Figures 5 and 6 are independent of the actual physical dimensions of the problem. These results show how ξ and θ

vary with χ and σ. The solid line shows analytical values and the symbols show numerical model values. The results show that the numerical solution agrees with the analytical solutions.

Numerical experiment showing the applicability of the analytical solution to short canals

The analytical solutions derived in this paper are exact for infinitely long straight canals. Unfortunately some canals in South Florida are short. In this section, the applicability of the solution to short segments is tested by comparing the numerical solution in a 2-D model domain with the analytical solution. The complete analytical solution for a short segment is obtainable by superimposing point solutions of variable strength. This method that is not presented here, forms the basis of the transient analytic element method for Dupuit-Forchheimer flow (Bakker, 2004).

The numerical solution of the test problem used for the test is shown in Figure 7. It is obtained using the RSM model (Lal, et al. 2005) with a right triangular mesh of size 10 m and canal discretization of length 100 m. It shows dimensionless water levels around the closed end of a short canal. The distances used in the figure are in dimensionless units, created by dividing the actual length by a characteristic length $\lambda = \sqrt{T/(fs_c)}$. The contours of the amplitudes of ground water levels obtained numerically are plotted as a fraction of the amplitude of water level at the canal (H/H_0). The other parameters used in the experiment are: $P = 32$ Hrs, $T = 0.003\, m^2/s$ and $s_c = 0.2$. The sediment layer is assumed to be absent making $\alpha_s = 1.0$ and $\varphi_s = 0$. For the parameters selected, the characteristic length is $\lambda = 16.58\, m$. In order to obtain an analytical solution to compare with the numerical solution, the parameter χ is computed first as $\chi = 5.52$ using (20) and $B = 18.3\, m$. The dimensionless amplitude of the water level fluctuation is calculated next using (22) as $\xi = 0.78$. The corresponding dimensional value is $q_0 = 0.01$ as $H_0 = q_0\xi/(fB) = 7.81m$. For comparison, the numerical model result obtained using the RSM model shown in Figure 7 is 7.56 m. The difference between these values have to do more with the crude discretization. This experiment shows that (22) is a good approximation even for shorter canal segments.

The amplitudes of groundwater levels obtained analytically and numerically at an arbitrary distance of 20 m from the center of the canal are also compared next. The analytical solution computed using (2) and (8) is $H_y = H_0 \exp(-y/(\lambda\sqrt{2}))$. At a distance $y = 20m$, $H_y = 7.81 \times$

$\exp(-20/(16.58\times\sqrt{2})) = 3.32$ m. The value obtained using the RSM model, as shown in Figure 7 is 3.15 m. These results show that unless the canal is extremely short, the numerical solutions for groundwater and canal flow are reasonably close to the analytical solutions. Considering that the discretization is crude, the discrepancy has more to do with the numerical error.

Methods used to obtain the amplitude and the phase from time series data

The first step toward determining aquifer parameters involves analyzing the water level time series data to obtain the amplitudes and the phase lags. A number of techniques are available to carry out this task. Since the frequency of the disturbance is constant during the experiment, the problem involves the determination of amplitude a and the phase b when the data are fitted to $H = a\ \sin(ft + b)$. Before fitting to the curve, the data are de-trended to remove any regional influences. After that, three methods were used to obtain a and b values.

The first method used to calculate a and b is based on a least square best fit approach. This method can be used even with missing or short data records. With this approach, S is minimized for elapsed times t_i in which $i = 1, 2, \ldots n_t$; $n_t =$ number of time records.

$$S = \sum_{i=1}^{n} (Y_i - a\sin(ft_i + b))^2 \tag{25}$$

Conditions $\frac{\partial S}{\partial a} = 0$ and $\frac{\partial S}{\partial b} = 0$ give the following to be solved for a and b

$$\frac{\sum Y_i \sin(ft_i + b)}{\sum \sin^2(ft_i + b)} - \frac{\sum Y_i \cos(ft_i + b)}{\sum \sin(ft_i + b)\cos(ft_i + b)} = 0 \tag{26}$$

$$\frac{\sum Y_i \sin(ft_i + b)}{\sum \sin^2(ft_i + b)} = a \tag{27}$$

The second method is based on the cross correlation of the de-trended data. The phase lag and the ratio of the amplitudes that give the best correlations are selected as b and a respectively. A third approach was also used based on manually selected peak and trough points in the water level curve. The amplitude and the phase lag calculated manually are crude. However this last method can eliminate some known data problems.

APPLICATION TO THE L-31W TEST SITE

A pilot tetst was conducted in the L-31W canal in South Florida to see if the analytical expressions derived earlier can be put to practical use. This is accomplished by using them to understand the dynamics of the canal-aquifer system and calculate bulk aquifer parameters. The test can also teach lessons for future tests.

Description of the site and the test

The test site selected is the 11.5 km stretch of the L-31W canal in South Florida between structures S-174 and S-175. The L-31W canal built around 1971 is located in Dade County, FL, along the Eastern boundary of the Everglades National Park. The L-31W canal penetrates the extremely pervious surficial aquifer called the Biscayne aquifer. This aquifer is the most prolific aquifer in Dade County and contains highly permeable sands and limestones (Fish and Stewart, 1991). It is approximately 14 m thick near the canal, with the top 1/3 rd. made of marine limestone, and the bottom 2/3 rd. is referred to as the Ft Thompson formation. The ground elevation in the area is around 1.2 m - 1.8 m.

The test was started on 02/21/2003 at 0:00 Hrs with the rising phase of the cycle and lasted until 02/26/2003. During the test, sinusoidal water level disturbances of period $T_p = 48$ Hrs were created in the canal by using a structure S-174 in the North and S-175 in the south. The pumps and structures allowed a maximum flow rates of around 5 m^3/s in and out of the canal. The 48 Hr period allowed for a large enough amplitude, and avoided possible conflicts with the tidal cycles. Even if a large number of sine cycles would have been ideal, it had to be limited to a few in order to minimize the interference with the daily operation and management of the Everglades National Park and the south Florida conveyance system.

Summary of test results

A summary of test results at various stages of the calculation process is shown below. Figure 8 shows the raw water levels at the canal and a number of selected gages. It shows the influence of the test superimposed on the regional system behavior. The figure also shows the effect of a small rainfall measured at gage R127 on water levels. Figure 9 shows the detrended discharge and water level data, and the curves fitted to the data using the least square method described in (26)

and (27). The figure shows that water level in the aquifer varies smoothly when compared with pumping rate variation indicating that the aquifer is capable of smoothing many of the high frequency fluctuations. The noisy pumping rate is an indication of the effort made by the operators to maintain the sinusoidal water level targets. Some of the extremely noisy periods of the record were not used in the analysis. Table 2 shows the summary of the sinusoidal curve fits obtained using the three methods explained earlier. Statistical estimates associated with the fit are also shown. Some of these estimates may be used to determine the uncertainties of the parameters.

Transmissivity and vertical leakance near L-31W

Amplitude and phase characteristics of the sinusoidal water levels measured at different points in the aquifer are used to calculate transmissivities and vertical leakances of the aquifer. Table 2 shows the amplitudes and phases which are used to plot $-\log(H/H_c)$ versus x and φ_s versus x curves described in (3) and (4). Figures 10 and 11 show the plots. Table 3 shows the estimates of k_1 and k_2 obtained using the slopes. The results show $k_1 > k_2$ indicating the presence of a confining layer. The values of k_1 and k_2 are used to obtain η and k_0 as described earlier. They can be used to determine the aquifer diffusivity and the vertical leakance. If data are available for many gages, spatial distribution of the same properties can be plotted. Table 4 shows dimensionless parameter values obtained for L-31W.

Bottom sediment properties if L-31W

Effects of canal sediment resistance can be detected by the presence of intercepts in the $-\log(H/H_0)$ versus x curve and the φ_s versus x curve. Figures 10 and 11 both show the presence of this resistance. Since the functional relationship between σ and the intercept is known, the intercepts in (3) and (4) can be used to determine σ using (16) and (17). Table 4 shows the values of σ obtained for L-31W using the intercepts of (3) and (4).

Aquifer and canal storage properties of the L-31W surroundings

Storage parameters related to stream-aquifer interaction are determined using the amplitude and the phase lag of the discharge and the water level in (22) and (23). Using (22), the value of ξ can be calculated based on data in Table 2 as $\xi = H_0 fBL/Q_0 = 0.193 \times 3.636 \times 10^{-5} \times 18.3 \times 11500/5.805 = 0.254$. The value of χ' can now be solved using (22) as $\chi' = 0.54$. The value of χ'

can also be solved using (23) by first calculating phase $\theta =$ as 0.69 and then solving $\chi' = 1.44$. In order to calculate χ from the value of χ', equation $\chi = \chi' \alpha_s(\sigma)\ n(\eta)/\sqrt{2}$ is used. The parameter values used for this are $\alpha_s(\sigma) = 0.65$ and $n(\eta) = 2.0$. The final values of $\chi = 0.5$ and $\chi = 1.33$ are also shown in Table 4.

Table 4 shows the dimensionless parameters obtained for the overall L-31W system and the NTS1 zone. Table 5 shows the dimensional parameters. The uncertainty estimates of some of these parameters can be obtained using the standard error estimates in Table 2 if necessary.

Primitive variables of the L-31W surrounding

Dimensionless parameter groups obtained from the experiments can be used to calculate primitive variables. Primitive variables T ans s_c for example are calculated using T/s_c and Ts_c obtained from k_0 and χ. Using the least square method, it is possible to obtain $k_0 = 2.47 \times 10^{-4}$ as shown in Table 4. Aquifer diffusivity determined using k_0 is $T/s_c = \sqrt{f/(2k_0^2)} = 297\ m^2/s$ because $f = 3.636 \times 10^{-5}\ s^{-1}$. The value of $\chi = 0.50$ can be used with the definition (20) to calculate $Ts_c = B^2 f/\chi^2$ or $18.3^2 \times 3.636 \times 10^{-5}/0.50^2$ making $Ts_c = 0.0742\ m^2/s$. Combining with the value of diffusivity, it is possible to obtain $T = 4.49 m^s/s$ and $s_c = 0.0158$. Other primitive variables calculated in this manner are shown in Table 5.

DISCUSSION

Inaccuracies and problems with the field test and implications of the results are discussed in this section. The first type of inaccuracy discussed is due to ground surface features such as sloughs and agricultural ditches that influence the behavior of near-surface groundwater flow. Taylor slough shown in Figure 1 is a good example for a surface feature influencing the high water levels of E112. Figure 8 shows the artificially low amplitude of E112 resulting from water seepage out of the system during the high phase of the cycle. The same is true with gages in the Frogpond agricultural area because of the network of drainage canals that diffuse the high water levels in the cycles. Table 2 shows the amplitude data while Figures 10 and 11 show all the data in one plot. The figures show that some of the data anomalies. Experience with the test shows that identifying the affected gages closer to a wetland is not an easy task.

The second type of error discussed here is caused by unpredictable incidents of highly variable local rainfall affecting the water level as shown in Figure 8. In the current analysis, these effects are considered as data noise to make the analysis simple. A third error is due to the noise in the flow data when pumps and structures are used during operations aimed at maintaining target water levels. There are times when the structures and pumps had to be operated close to or beyond peak capacities almost clipping the peaks and troughs of the cycle.

Table 2 shows that the amplitude and phase characteristics of the collected data depend on the method of calculation. The table shows that data are clean for a number of gages that are not too far from the canal. For some of the gages, the standard errors are large compared to the amplitudes making them less useful. With and without error bars shown in Figures 10 and 11, knowledge about the scatter is useful in visually evaluating the quality of the data at various gages. Figures 10 and 11 also show that it is possible to obtain good straight line fits. Results in Table 3 indicate that the slopes, intercepts and aquifer properties vary from zone to zone.

Tables 4 and 5 also show the spatial variability of the properties around the canal. Results of a single test zone close to NTS1 and NTS10 are presented in this paper. The variability of the properties in the table can be attributed to the heterogeneity of the limestone aquifer in addition to errors in the data. The short duration of the test also has an effect on the accuracy of the results.

The second row of Table 5 shows the diffusivity computed assuming that the aquifer is not leaky. This is a simplifying assumption used by Carr and Van Der Camp (1969). They refer to the diffusivity computed using the amplitude as the effificncy based diffusivity. For the NTS1 zone, the value obtained is 132 m^2/s. For the same zone, the diffusivity computed using phase lag is 5233 m^2/s. The difference in diffusivities have also been observed by Smith and Hick (2001) and others as well. In the current analysis, this difference is explained using the leakiness in the confined aquifer. This result has a strong implication on groundwater model development. It show that if a leaky confined aquifer is modeled using a single layer confined aquifer or a single layer unconfined aquifer, the solution will be out of phase if the amplitudes match, or the solution will

have different amplitudes if the phases match.

The results of the test shown in Table 5 can be used to demonstrate the practical use of (8). For example, if it is necessary to determine the time scale of a transient problem near L31-W for which the confining layer becomes non-leaky for all practical purposes, a condition such as $\eta < 0.25$ can be used assuming a difference of less than 25% between k_1 and k_2 to be the deciding factor. This condition can be expressed as $(k_v/\delta_v)P/(2\pi s_c f) < 0.25$. With numbers from the table, $0.25 > 0.0315P/(2\pi \times 0.0158)$ gives $P < 0.8$ days. This means there is a need to have a second confined layer in a computer model when the water level fluctuations have a period shorter than 0.8 days. This also implies that the system can be considered as unconfined for all practical purposed when carrying out regional model applications with time steps larger than 1 day.

Looking at the results in Table 4 and Table 5, it is clear that water level and time data for field experiments have to be collected fairly accurately for the error to be reduced. It is also important to have as many gages are spatially spread in order to obtain the spatial distribution of diffusivity. Aquifer diffusivity is the most reliable property that can be calculated from the experiment because it is based only on the water level. However when other properties have to be calculated, there is only one discharge data set available for the purpose. This results in giving only one value of Ts_c for the entire canal segment. The individual values of T and s_c computed in this manner for a heterogeneous aquifer are less reliable because the computed values of T/s_c are local and computed values of Ts_c are regionally averaged.

Results of drawdown experiments carried out in the past in the L-31W area and the nearby L-31N area show a significant variability of the parameters. Fish and Stewart (1991) showed that the values of transmissivity can be as high as 1.8 m^2/s in the area and reaching 3.2 m^2/s near Krome Avenue close to Miami. Chin (1991) obtained values close to 1.3 m^2/s near L31-N. Genereaux and Guaridiaro (1998) observed a value close to 1.2 m^2/s for the Byscayne aquifer and $k_s/\delta_s = 35.2$ day^{-1} for the coefficient of leakage of the sediment. Results of multi-well aquifer tests reported by Reese and Cunningham (2000) suggest $T = 0.1m^2/s$, storativity= 0.0004 and $k_v/\delta_v = 0.007$

day^{-1} at Trail Center that is 50 km northwest of the site. Model calibration has also been used to obtain parameters. Nemeth, et al. (2000) obtained $s_c = 0.0002$, $k_v/\delta_v = 78\ day^{-1}$, $T = 1.5\ m^2/s$ using the MODBRANCH model.

SUMMARY AND CONCLUSIONS

The governing equations were analyzed to understand the dynamic behavior of a fully integrated canal-aquifer system. Results of the analysis include analytical expressions describing the response of the system to sinusoidal discharge stresses. Using the results, experimental methods were developed to help determine physical parameters of the system. When the analytical expressions were tested using numerical models applied to a number of test problems, the results show agreement. Dimensionless parameters that influence various processes were also identified using the equations. Table 1 shows a summary of the basic dimensional parameter groups responsible for various processes related to stream-aquifer interaction. Ranges of parameters controlling various processes are also shown in the table.

The dimensionless physical parameter groups that contribute to or explain various processes include η for leakage of the confined aquifer, σ for sediment resistance and χ for canal-aquifer storage relationship. Other parameters used to describe the system behavior include ξ for the response of the head in the canal to a given flow impulse. The analytical solutions needed to explain canal-aquifer interaction are explained in this paper for the case of sinusoidal stresses.

Results of the analysis show that aquifer leakance expressed in dimensionless form using η influences the propagation behavior. A curve showing the influence of η on the phase and the attenuation can be used to obtain a condition such as $\eta > 0.05$ for which an aquifer can be considered leaky confined for practical purposes, when detected at a 5% level. Results of the propagation behavior obtained using the MODFLOW model and the analytical expression are plotted against η showing that they agree. If η is very large, an aquifer system cannot be simulated numerically using just one layer alone. If only one layer is used, calibration cannot match both the phase and the amplitude of the solutions at the same time.

The analytical results show that for fully confined or unconfined aquifers, the canal can be completely cutoff from the aquifer due to sediment alone regardless of aquifer properties if $\sigma < 0.073$. Under such cutoff conditions, the canal and the aquifer can be considered moving independently. The same condition $\sigma < 0.33$ was obtained by Lal (2001) after studying the variation of longitudinal water levels along a canal. At the opposite end of cutoff, a canal is completely connected if $\sigma > 19.5$ assuming a detection level of 5%.

The analytical results also show that in addition to the sediment effects, canal can be completely cutoff because of aquifer properties and canal storage effects too, if $\chi' > 27.6$. In a previous study of longitudinal fllow profiles by Lal (2001), the same condition was obtained as $\chi' > 10$. At the opposite end of cutoff, the canal is completely connected to the aquifer and the canal and aquifer water levels are the same if $\chi' < 0.1$.

A separate test problem was used to investigate the applicability of the analytical method to relatively short segments. Using the test it was able to demonstrate that the analytical expressions derived for long canals can be used for fairly short canals as well. In carrying out the test, the flow around a short segment was solved numerically using both the RSM model and the analytical methods. The results show that the numerical results agree closely with the analytical solution even when the canal is relatively short.

Practical applications of the analytical methods developed in this paper include primarily the calibration of field parameters associated with canal-aquifer interaction. A second use of the equations is to assist in the calibation of numerical models by providing an exact solution for the numerical solution to be compared against. An application of this approach would involve carrying out a field test to determine the parameters first, and using the parameters in the numerical model to be compared against both the field data and the analytical solution.

ACKNOWLEDGEMENTS

The author wishes to acknowledge Joel Van Arman, Mark Wilsnack, Todd Tisdale, Steven Krupa, Cynthia Gefvert, for reviewing the manuscript, Ron Mierau, George Hwa, Cal Neidrauer and Paul Linton of the South Florida Water Management District for supporting and carrying out the test on a busy conveyance system, and Clay Brown for the GIS help. He also wishes to thank Kevin Kotun and others of the Everglades National Park, USACOE and the USFWS for their support of thee test, and the peers Randy Van Zee, Ken Konyha for healthy comments.

REFERENCES

Bakker, M. (2004). "Transient analytic elements for periodic Dupuit-Forchheimer flow", *Adv. Water Resources*, (27), 3-12.

Bear, J. (1979). *Hydraulics of groundwater*, Mc Graw-Hill, New York, NY.

Bruggeman, G. A. (1999). *Analytical solutions of geohydrological problems, developments in water science*, vol 46, Eq 228.01, Elsevier Publishers, Amsterdam.

Carr, P. A. and Van Der Kamp, G. S. (1969). "Determination of aquifer characteristics by the tidal method", *Water Resources Research*, 5(5), 1023-1031.

Chin, D. A. (1991). "Leakage of clogged channels that partially penetrate surficial aquifers", *J. Hydraul. Eng.,* 117(4), 487-488.

Cunningham, K. J., Carlson, J. L., Wingard, G. L., Robinson, E., and Wacker, M. A. (2004). "Characterization of Aquifer Heterogenity Using Cyclostratigraphy and Geophysical Method in the Upper Part of the Karstic Biscayne Aquifer, Southeastern Florida", *Water Resources Investigations Report 03-4208*, USGS.

Fish, J. E. and Stewart, M. (1991). *Hydrogeology of the surficial aquifer system*, USGS water resources investigation report 90-4108.

Genereaux, D. and Guadiario, J. (1998). "A canal drawdown experiment for determination of aquifer parameters", *J. Hydrologic Engrg.,* ASCE. 3(4), 294-302.

Klein, H., Armbruster, J. T., McPhearson, B. F., Freiberger, H. J., (1977). "Water and the south

Florida environment", *USGS Water resources investigation* 24-75, p-165.

Lal, A. M. W. (1998). "Calibration of riverbed roughness",

Lal, A. M. W. (2001). "Modification of canal flow due to stream-aquifer interaction", *J. Hydraul. Eng.,* 127(7), 567-576.

Lal, A. M. W., Van Zee, R. and Belnap, M. (1995) "Case Study: Model to Simulate Regional Flow in South Florida", *J Hydraul. Eng.*, 131(4), 1-12.

McDonald, M. G. and Harbaoug, A. W. (1988). "A Modular three dimensional finite difference groundwater flow model", US Geological Survey Techniques of Water Resources Investigations, Book 6, Reston, VA.

Miller, J. A. (1997). *Hydrogeology of Florida* in Randazzo, A. F., and Jones, D. S., The geology of Florida, Chapter 6, University of Florida press, Gainesville, FL., 69-88.

Motz, L. H. (2002). "Leaky one-dimensional flow with storage and skin effect in finite width sink", *J. Hydraul. Engr.,* 128(5), 298-304.

Drawdowns for leaky-aquifer flow with storage in finite width sink", *J. Hydraul. Eng.,* 120(4), 820-827.

Nemeth, M. S., Wilcox, W. M., Solo-Gabriele, H. M., Evaluation of the use of reach transmissivity to quantify leakage beneath levee L-31N, Miami Dade County, FL, USGS Water Resources Investigations Report 00-4066

Pinder, G. F., Bredehoeft, J. and Cooper, H. H. (1969). "Determination of aquifer diffusivity from aquifer response to fluctuations in river stage", *Water Resources Research*, 5(4), 850-855.

Reese, R. S. and Cunningham, K. J. (2000). "Hydrogeology of the gray limestone aquifer in Southern Florida", *USGS Water Resources Investigations Report 99-4213*, 51-59.

Singh, S. K. (2004). "Aquifer response to sinusoidal or arbitrary stage of semipervious stream", *J. Hydraul. Engrg.*, 130(11), 1108-1118.

Smith, A. J. and Hick, W. P. (2001). "Hydrogeology and Aquifer Tidal Propagation in Cockburn

Sound, Western Australia", *CSIRO Land and Water*, Technical Report 6/01, February 2001.

Swamee, P. K. and Singh, S. K. (2003). "Estimation of aquifer diffusivity from stream stage variation", *Journal of hydrologic engineering*, January/February, 20-24.

Zlotnik, V. A. and Huang, H. (1999). "Effect of shallow penetration and streambed sediments on aquifer response to stream stage fluctuations", *Groundwater*, 37(4), 599-604.

NOTATION

The following symbols were used in the paper.

B	width of the canal, (m).
f	angular frequency, (s^{-1}).
$h(t)$	water level in the overlying phreatic aquifer, (m).
H	water head in the aquifer, (m).
H_0	water level in the canal, (m).
H_1	water level just outside the canal and the sediment layer, (m).
H_2	water head in the aquifer, (m).
k_0	value of k_1 and k_2 for fully confined aquifers, (m^{-1}).
k_1	amplitude decay constant, (m^{-1})
k_2	wave number (m^{-1})
k_s/δ_s	coefficient of leakage of the sediment layer, (s^{-1})
k_v/δ_v	coefficient of leakage or leakance of the semipervious confining layer, (s^{-1})
p	wetted perimeter, (m)
P	period of the disturbance
q	discharge into the canal per unit length, (m^2/s)
R	1-D aquifer recharge per unit length, (m/s)
α_s	reduction of amplitude at the sediment layer
s_c	storage coefficient of the aquifer
T	transmissivity of the aquifer, (m^2/s)
η	dimensionless parameter describing the leakiness of the aquifer
λ	characteristic length of the aquifer, (m)
σ	dimensionless sediment conductance parameter
χ	dimensionless parameter describing resistance and storage effects of canal-aquifer interaction
χ'	parameter χ modified by the sediment layer and the leakiness
φ	phase lag at a distance x from canal
φ_s	sudden phase lag due to canal sediment
ξ	dimensionless parameter describing change in head per change in discharge

TABLES

Table 1: Summary of important parameters and their ranges

Description of the parameter and the range	expression
Parameter describing vertical leakiness of the confined aquifer η: aquifer is confined if $\eta < 0.05$ and extremely leaky confined if $\eta > 100$	$\eta = \frac{1}{s_c f}\frac{k_v}{\delta_v}$
Wave number and log decay rate in a fully confined or an unconfined aquifer	$k_0 = \sqrt{\frac{s_c f}{2T}}$
Wave number in a leaky confined aquifer $k_2 < k_0$	$k_2 = k_0\sqrt{(\sqrt{1+\eta^2}-\eta)}$
Decay constant in a leaky confined aquifer $k_1 > k_0$	$k_1 = k_2(\sqrt{1+\eta^2}-\eta)$
Dimensionless sediment conductance parameter σ: if $\sigma < 0.073$ there is full cutoff; if $\sigma > 19.5$ the sediment is fully pervious. Values described here are at a 5% detection level	$\sigma = p\frac{k_s}{\delta_s}\sqrt{\frac{2}{fs_cT}}$
Dimensionless stream-aquifer interaction parameter χ: with no sediments, if $\chi > 27.5$, there is cutoff and therefore no interaction. If $\chi < 0.1$, there is full interaction and the canal and the aquifer move in unison. Values described here are at a 5% detection level.	$\chi = B\sqrt{\frac{f}{Ts_c}}$
Stream-aquifer interaction parameter modified by sediment resistance; if $\chi > 27.5$ there is cutoff or no interaction; if $\chi' < 0.1$, there is full interaction.	$\chi' = \frac{\chi}{\alpha_s(\sigma)n(\eta)}$
Water level response per for a given discharge impulse $\xi(\chi',\sigma)$ with $0 < \xi < 1.0$. If $\xi > 0.95$, there is no interaction; if $\xi < 0.05$ there is full cutoff at a 5% detection level.	$\xi = \frac{H_0 fB}{q_0}$
Phase lag between discharge impulse and head response, $\theta(\chi',\sigma)$ with $0 < \theta < \pi/4$. With no interaction, $\theta = 0$.	θ

Table 2: Amplitudes and phases of observed data fitted to $Y = a\ \sin(ft + b)$

Gage		Least square method			Cross correlation method			Manual method	
Name	Dist.	a	b	s_e	H/H_c	b	$corr$	a	b
	m	m	rad	m		rad		m	
L-31W	0	0.193	0.000	0.027	1.000	-	-	0.183	0.000
NTS6	14	0.126	0.065	0.029				0.123	0.065
NTS5	17	0.124	0.065	0.031				0.120	0.065
NTS4	21	0.115	0.098	0.031				0.108	0.098
NTS1	280	0.112	0.317	0.017	0.533	0.267	0.98	0.109	0.263
NTS10	1510	0.072	0.396	0.022	0.317	0.377	0.90	0.076	0.458
NTS18	235	0.117	0.327	0.018	0.568	0.052	0.99	0.111	-
NTS1.16	238	0.102	0.258	0.028				0.111	0.208
E112	1490	0.042	1.520	0.014	0.153	-	0.87	0.037	-
FROGP+	1698	0.032	1.741	0.015	-	-	-	0.031	0.625
FROGPD2	2612	0.031	1.770	0.016	-	-	-	0.030	0.624
Q	0	5.805 m^3/s	-0.690	1.796	-	-	-	-	-

$a =$ amplitude of the sine representation $y = a\ \sin(ft + b)$

$b =$ phase of the sine representation

$corr =$ correlation coefficient between gage and canal water levels

$s_e =$ standard error estimate

Table 3: Table of the slopes and the intercepts the fits of log amplitude and phase

Method	Linear plot of log ampl		Linear plot of phase lag	
	intercept $(-\ln(\alpha_s))$	slope (k_1)	intercept (φ_s)	slope (k_2)
Least square, (overall)	4.638×10^{-1}	3.467×10^{-4}	1.550×10^{-1}	1.905×10^{-4}
Cross Corr. (overall)	4.826×10^{-1}	4.438×10^{-4}	1.116×10^{-1}	1.787×10^{-4}
Manual (overall)	4.304×10^{-1}	2.985×10^{-4}	1.058×10^{-1}	2.491×10^{-4}
Least square, (NTS1,NTS10)	4.259×10^{-1}	3.699×10^{-4}	3.078×10^{-1}	5.894×10^{-5}

Table 4: Table of dimensionless parameters

Domain	Overall	Overall	Overall	Zone NTS1,NTS10
Method	LSQ	Cross corr	Manual	LSQ
η	0.635	1.040	0.182	3.058
k_0	2.473×10^{-4}	2.831×10^{-4}	2.636×10^{-4}	1.866×10^{-4}
σ (ampl)	2.503	2.604	2.339	3.749
σ (phase)	3.527	4.065	7.764	-
α_s (ampl)	0.629	0.617	0.650	0.653
ξ (ampl)	0.254	0.254	0.254	0.254
χ (ampl)	0.405	0.412	0.397	0.501
χ (phase)	0.688	0.844	0.452	1.332
θ	0.690	0.690	0.690	0.690

Explanations

(ampl) = Values computed using ξ or amplitude ratio of head and discharge

(phase) = Values computed using θ or the phase lag between head and discharge

Table 5: Table of primitive variable computed using various methods

Domain	Overall	Overall	Overall	Zone NTS1, NTS10
Method	LSQ	Cross corr	Manual	LSQ
1. Aquifer diffusivity T/s_c, (m^2/s)	297	227	261	522
2. Ampl based diffusivity T/s_c, (m^2/s) (assuming non-leaky)	151	92	204	132
3. Aquifer T s_c (ampl), (m^2/s)	0.0742	0.0716	0.0768	0.0484
4. Aquifer T s_c (phas), (m^2/s)	0.0257	0.0170	0.0595	0.0068
5. Transmissivity T,(ampl) m^2/s	4.69	4.03	4.48	5.03
6. Transmissivity T,(phas) m^2/s	2.76	1.96	3.94	1.89
7. Storage coeff s_c	0.0158	0.0177	0.0171	0.0096
8. Coeff of leakage (sediment) k_s/δ_s (day^{-1})	13.72	14.03	13.06	16.62
9. Coeff of leakage (aquifer) k_v/δ_v (day^{-1})	0.0315	0.0581	0.0098	0.0925

Explanation of the rows in the table

2. Referred to as effi ciency based diffusivity by Carr and Van Der Camp (1969)

3. Computed using ξ or amplitude ratio of head and discharge

4. Computed using θ or the phase lag between head and discharge

5. Computed using ξ or amplitude ratio of head and discharge

6. Computed using θ or the phase lag between head and discharge

FIGURES

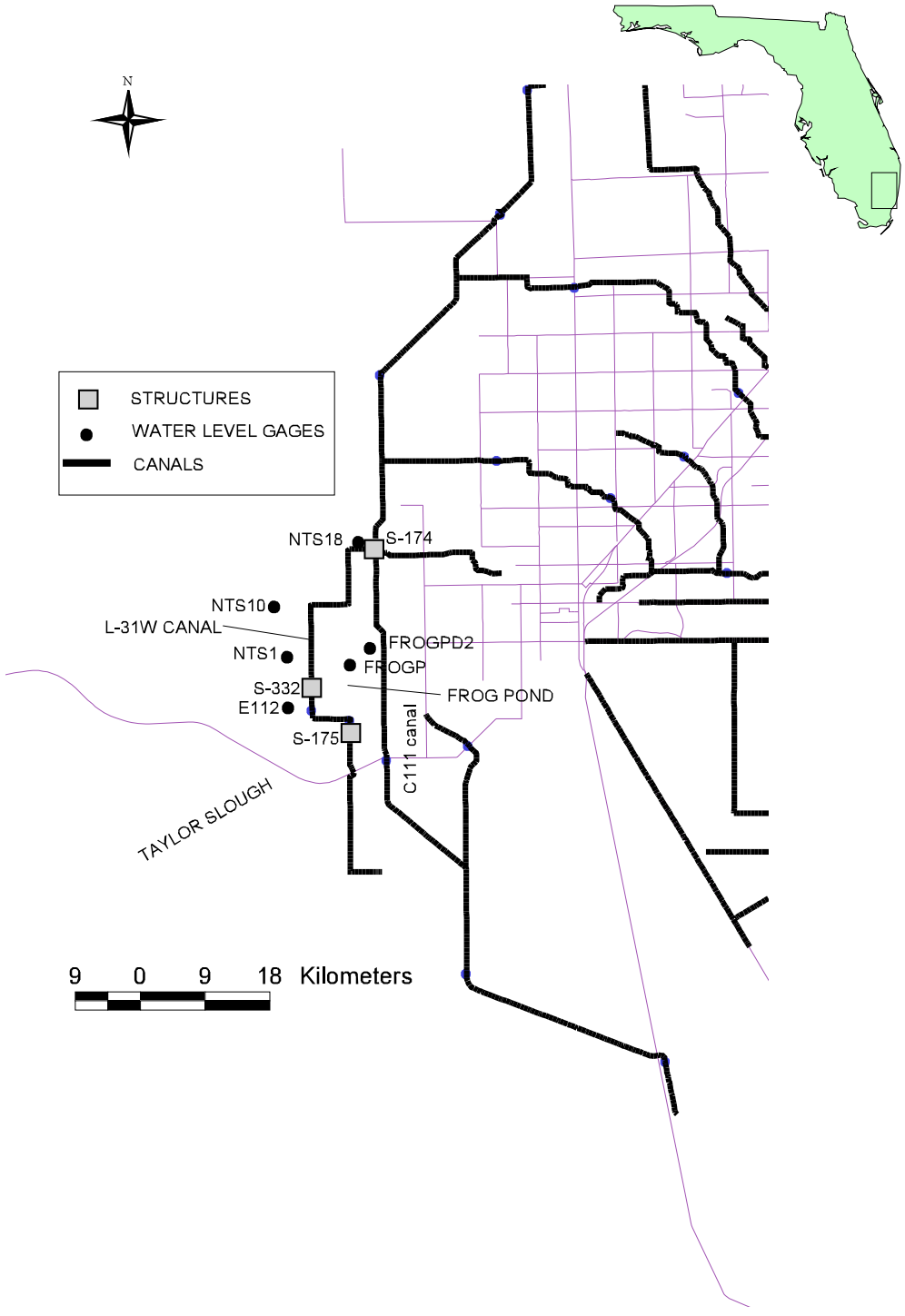

Figure 1: Study site in Dade County, Florid showing the canals and the structures

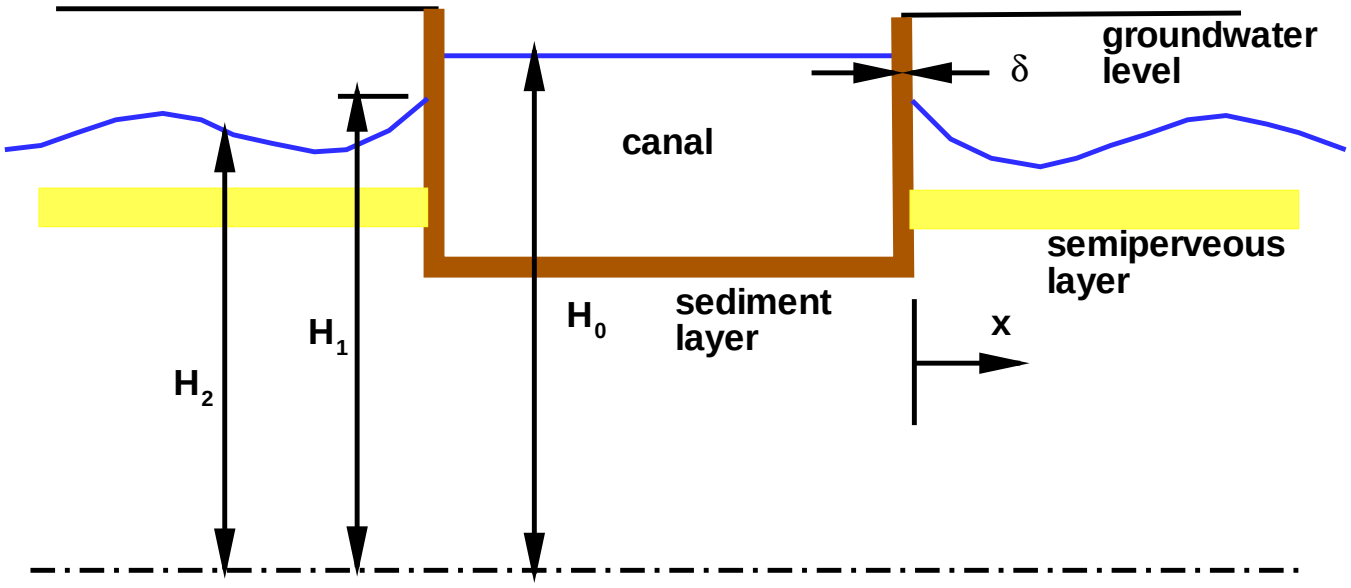

Figure 2: Definition sketch of a canal cross section

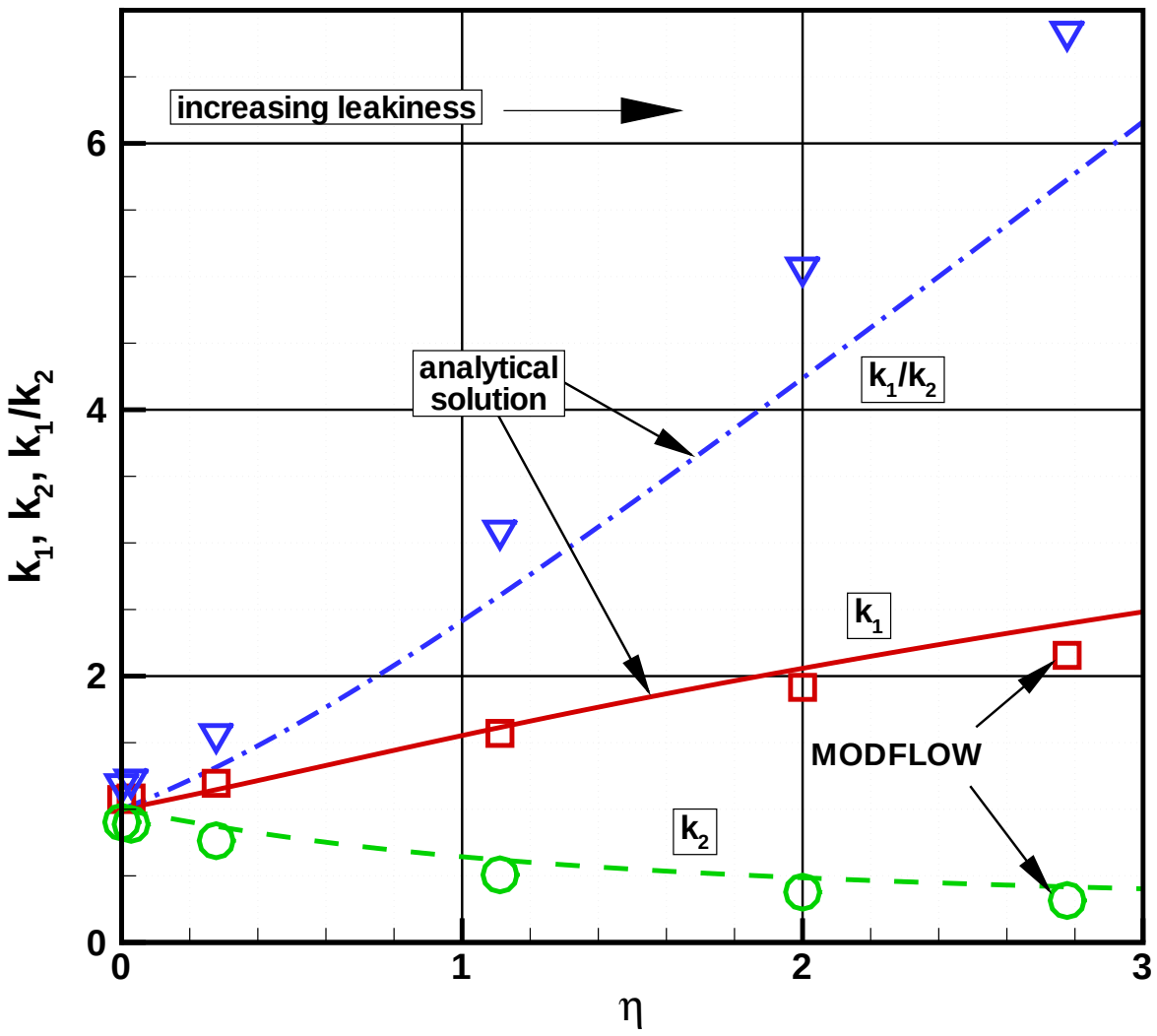

Figure 3: Plot of decay constant k_1, delay constants k_2, and k_1/k_2 with vertical leakiness parameter η

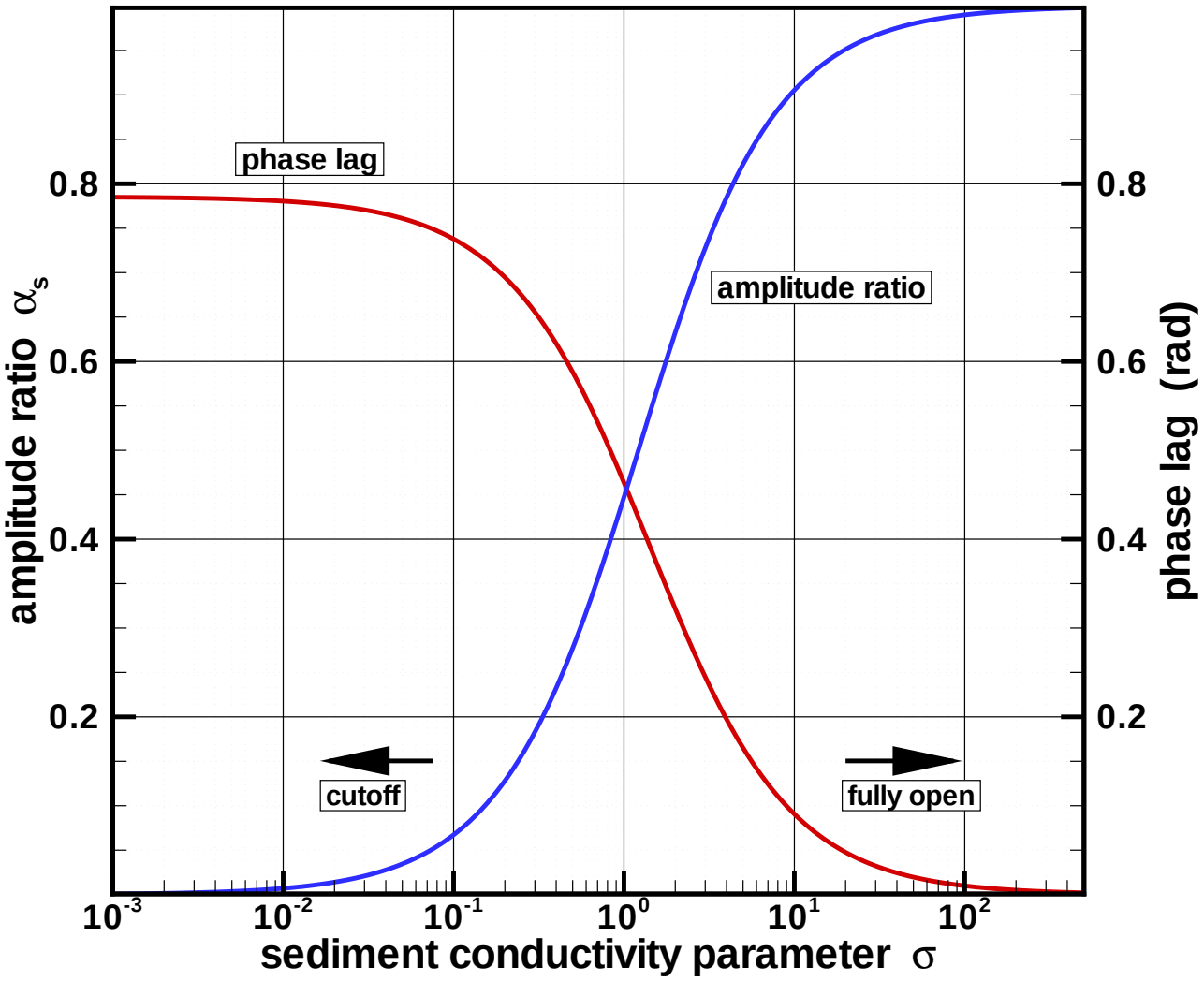

Figure 4: Plot of amplitude attenuation α_s and phase lag φ_s across the sediment layer versus σ. This plot is similar to a plot of ξ and θ versus $\chi'/\sqrt{2}$

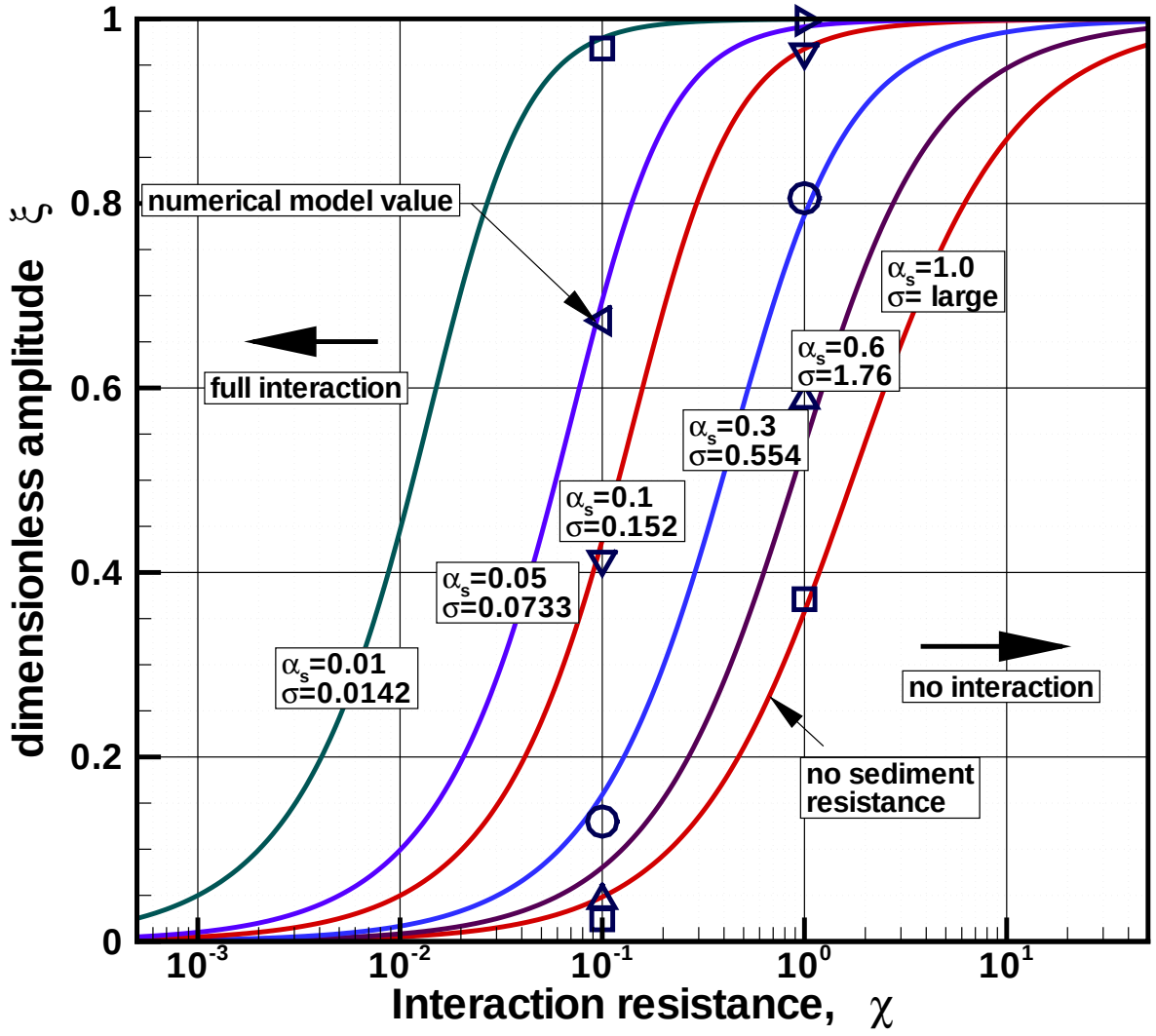

Figure 5: Plot of ξ versus χ and σ

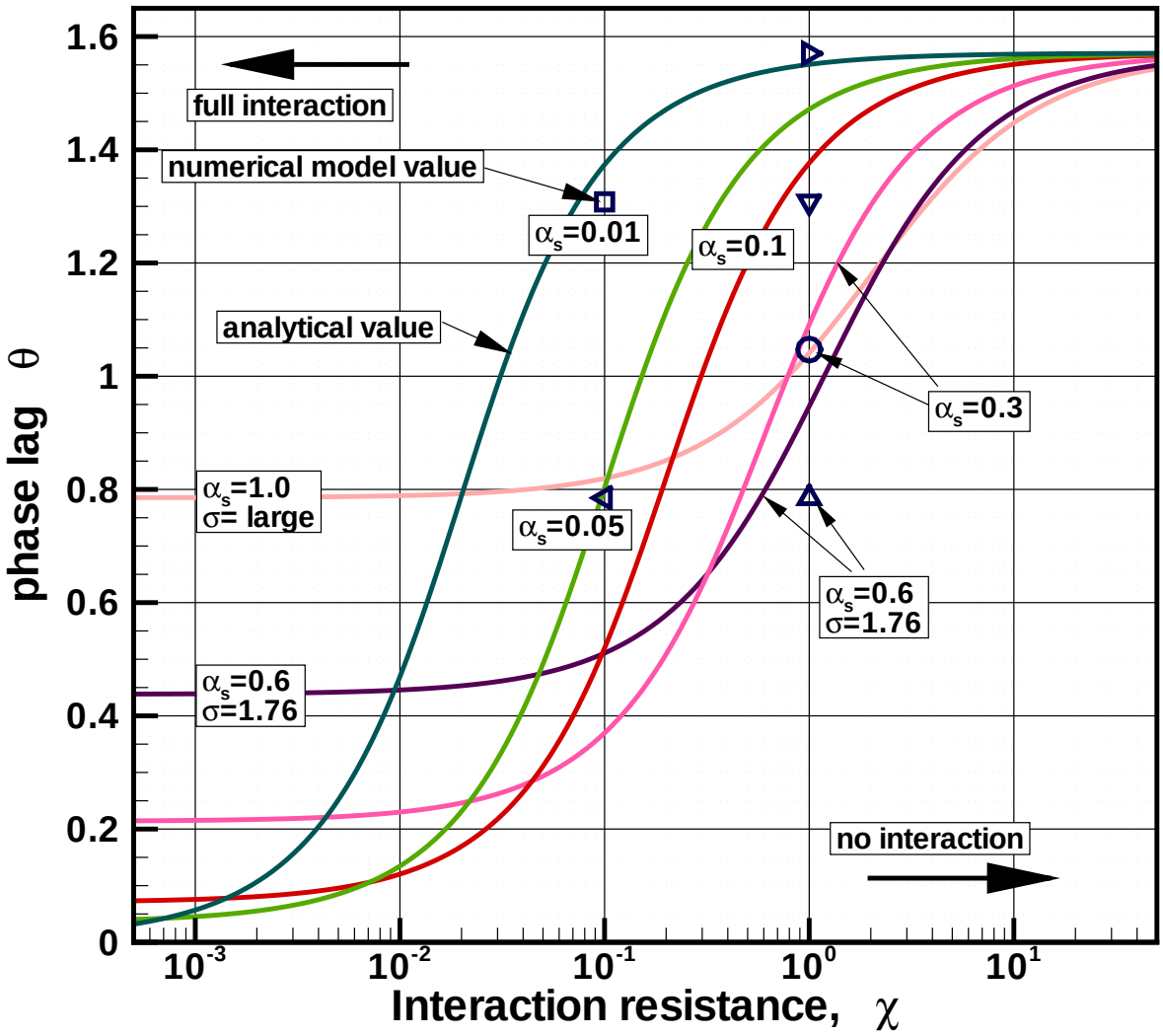

Figure 6: Plot of θ versus χ and σ

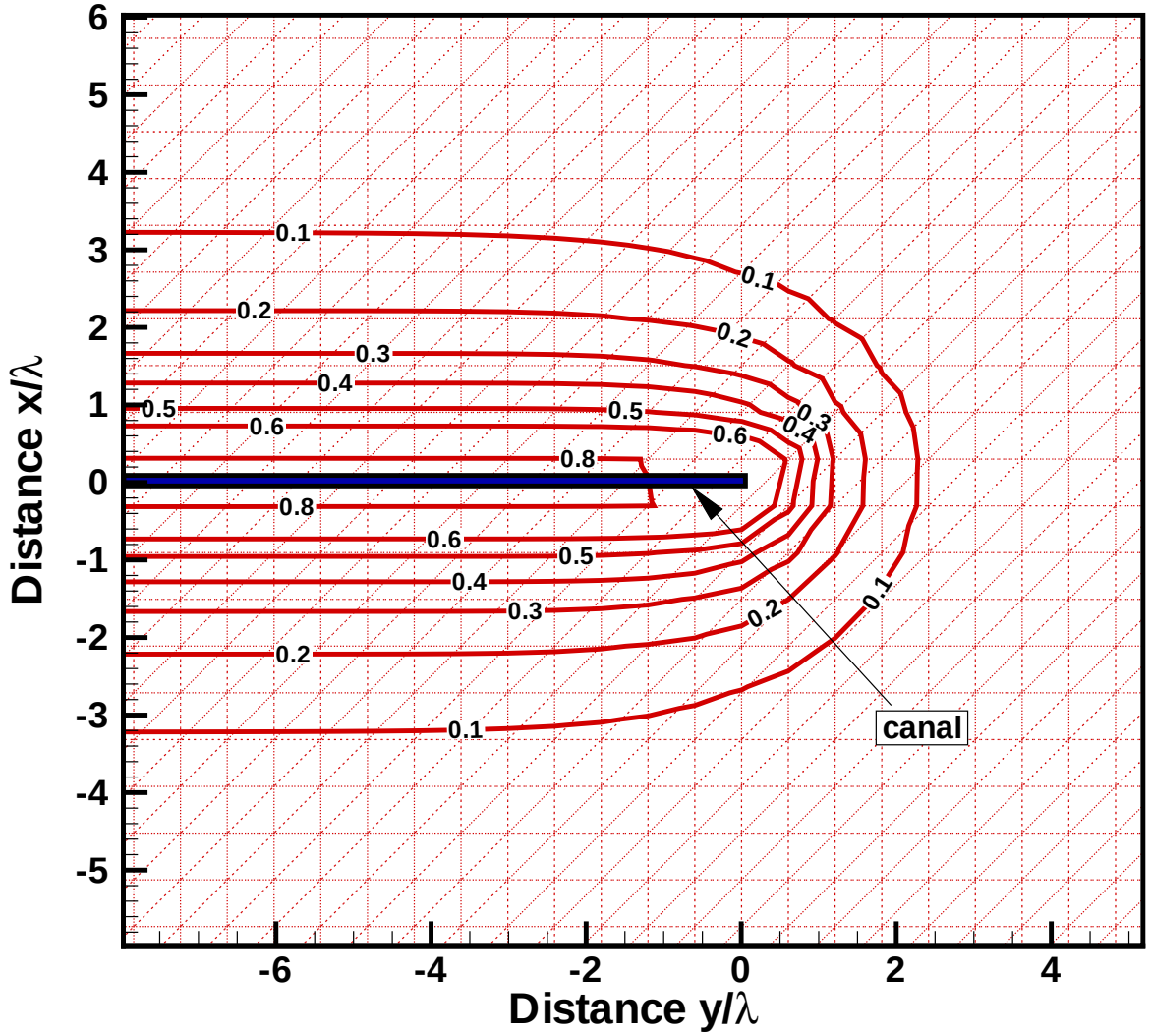

Figure 7: Contours of dimensionless amplitudes H/H_0 at a canal end obtained using RSM. H_0 is the maximum analytical water level at the canal

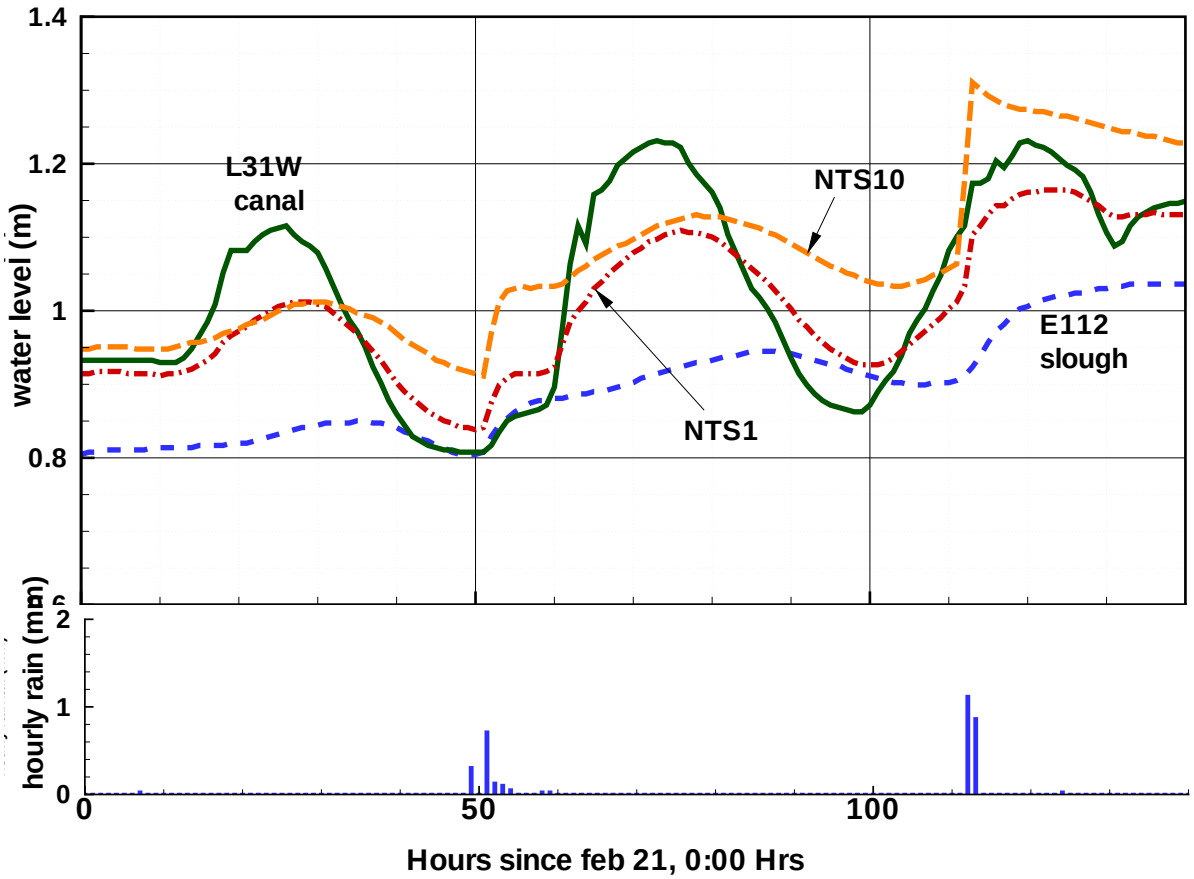

Figure 8: Raw time series data and rainfall for selected stations.

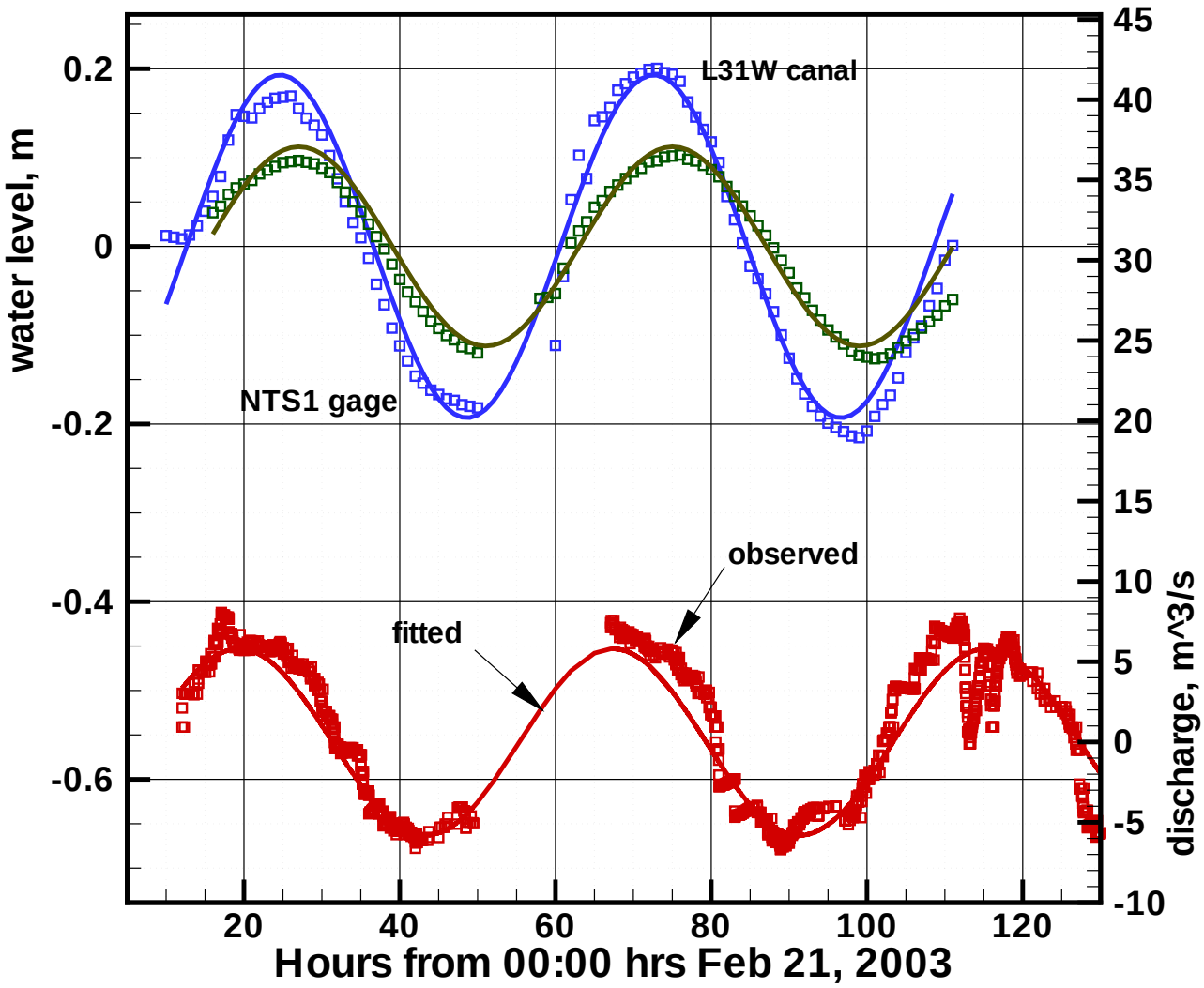

Figure 9: Water level and net inflow rate data and their sinusoidal fits

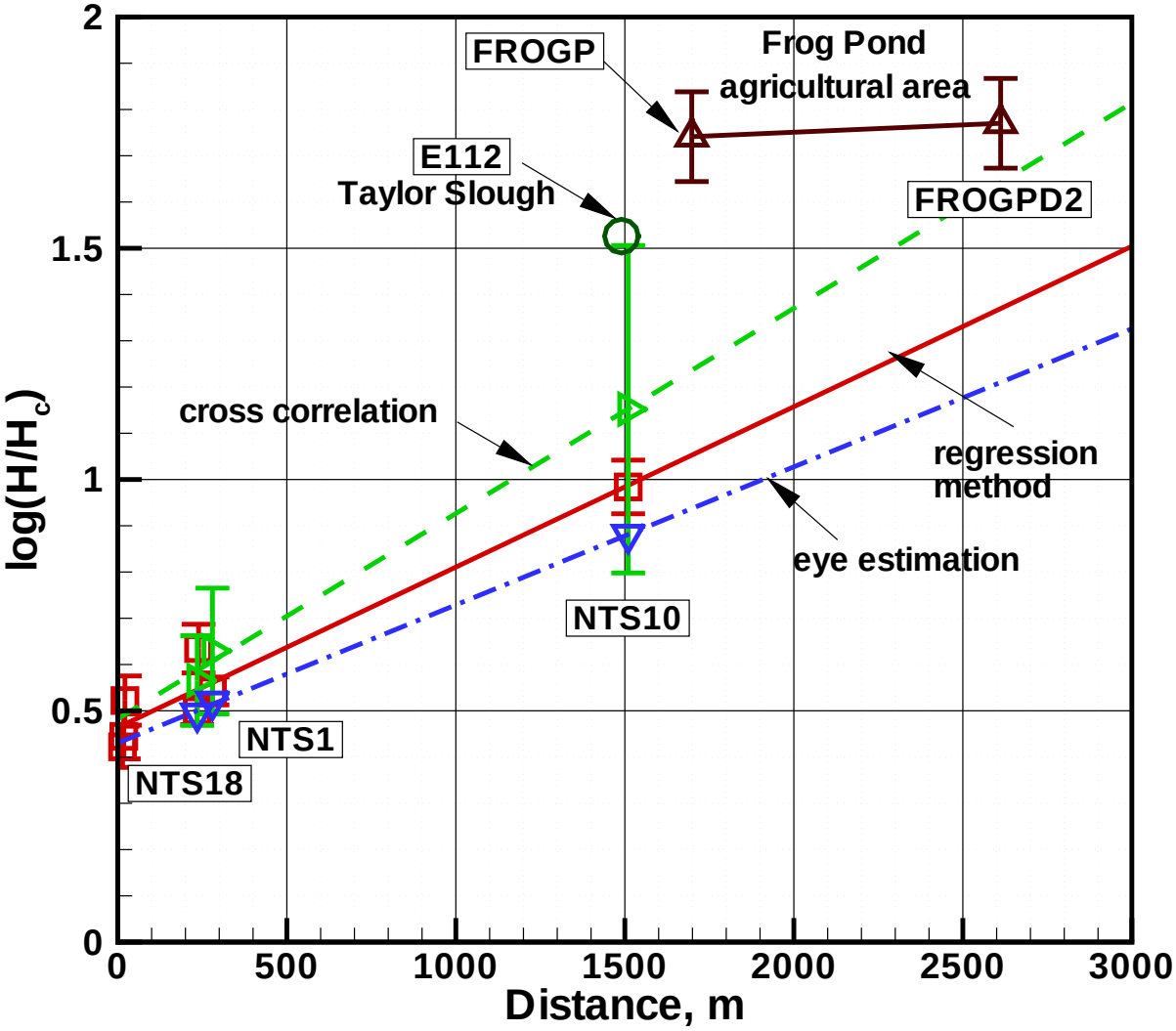

Figure 10: Plot of $\log(H/H_0)$ against distance from gage to canal

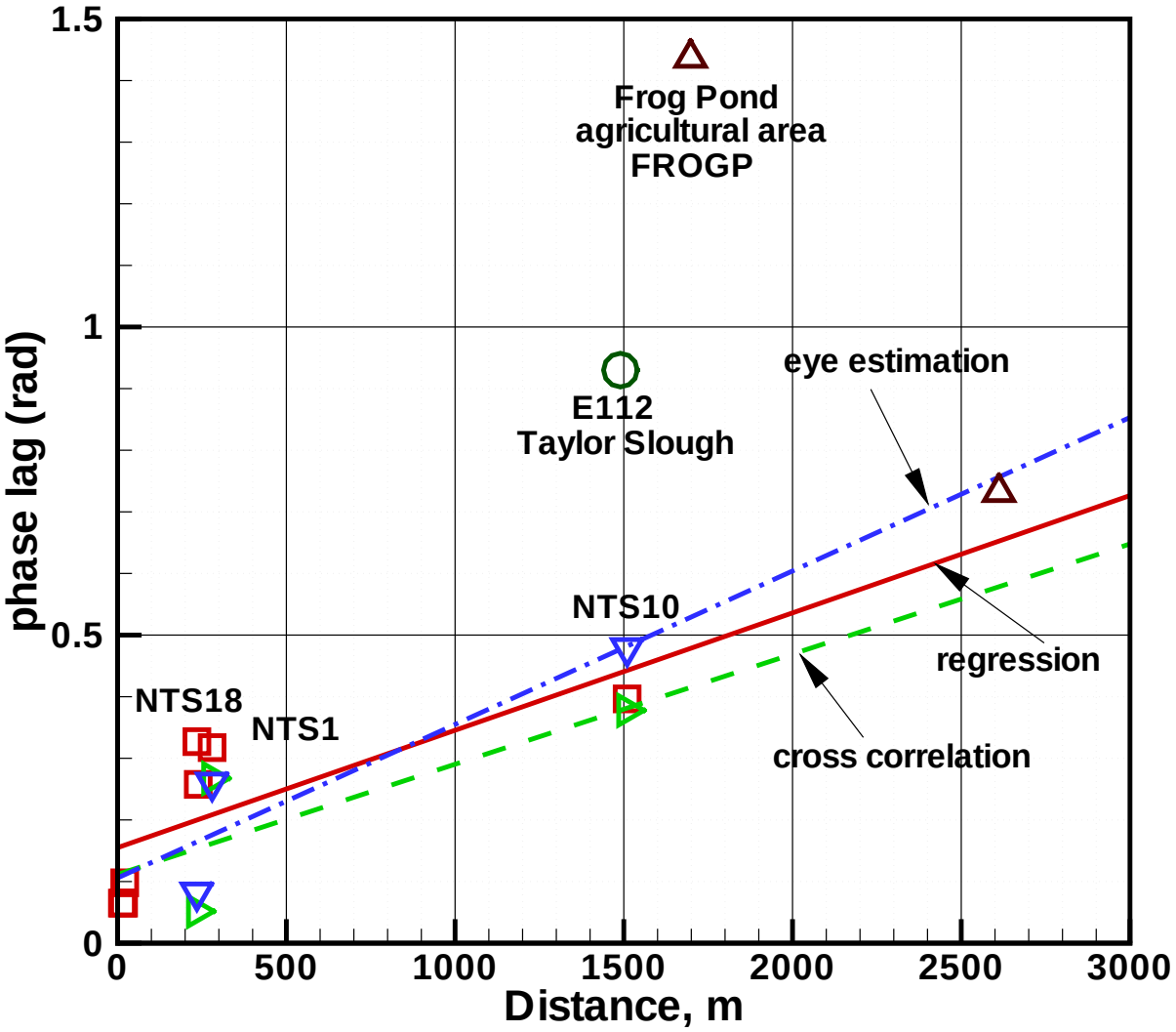

Figure 11: Plot of phase lag versus the distance from gage to canal

C.5 Hydrologic process modules of the Regional Simulation Model: An overview

HPM White Paper is not yet available

C.6 Management simulation engine of the Regional Simulation Model: An overview

Management Simulation Engine of the Regional Simulation Model: An Overview

Joseph Park
Office of Modeling
South Florida Water Management District
West Palm Beach, Florida, USA

January 25 2005

Abstract

The Regional Simulation Model (RSM) is a conjunctive aquifer-stream-surface hydrological model under development at the South Florida Water Management District (SFWMD). The model is designed to allow a flexible, extensible expression of a wide variety of natural hydrologies, as well as anthropogenic water resource control schemes in order to facilitate alternative management scenario evaluations. The management module of the RSM is the Management Simulation Engine (MSE). The MSE is based on a multi-level hierarchical control architecture, which naturally encompasses the local control of hydraulic structures, as well as the coordinated subregional and regional control of multiple structures. MSE emphasizes the decoupling of hydrological state information from the managerial decision algorithms, facilitating the interoperation and compatibility of diverse management algorithms. The overall hierarchy and operational capabilities of the MSE are described, and compared to management capabilities of some of the leading hydrological models.

1 Introduction

The advent of numerical estimation and simulation software packages has produced a profound impact on the ability of scientists and engineers to model a wide variety of physical phenomena across a broad spectrum of disciplines. Certainly the fields of electrical and mechanical engineering have benefited enormously from the evolution and application of finite- element techniques applied to constrained field equations of the electromagnetic and mechanical stress fields. Likewise, the disciplines of hydrodynamics and aerodynamics have enjoyed significant progress owing to the development of numerical models enabling the evaluation of spatially extended flow regimes over a wide range of Reynolds numbers. Similarly, the discipline of hydrology has profitably leveraged these developments to the point where there currently exists a nearly overwhelming proliferation of hydraulic and hydrological computational numerical models aimed at addressing the major engineering issues facing the hydrological community.

While the performance and applicability of these hydrological solutions has matured considerably, there still exists room for improvement in the modeling of human intervention in the control of hydraulic structures. Indeed, it has been recognized that the need exists for comprehensive integration of management features in conjunctive hydrological models [1]. This is not to say that the synthesis of control system and decision making software has failed to be successful in many of these models, rather, that careful design and decomposition of the hydraulic structure management algorithms (or state information-processing filters) can result in model implementations which provide a natural, flexible and extensible architecture for the expression and implementation of complex hydraulic management scenarios. Such management scenarios include the local control of individual water control structures, the coordinated control of multiple local structures to meet local demands and constraints, as well as regional (global) management operations required to satisfy water supply, flood control, and environmental concerns.

To address these needs, the South Florida Water Management District is developing the Regional Simulation Model (RSM), a conjunctive hydrological model composed of two primary, coupled components: the Hydrological Simulation Engine (HSE), and the Management Simulation Engine (MSE). The MSE consists of a multi-level hierarchical control scheme, incorporating a wide selection of control algorithms and decision making tools, each of which is integrated seamlessly with the hydrological computations of the HSE. From a hydroinformatics perspective, the RSM architecture empha-

sizes the decoupling of hydrological state information from the management information processing applied to the states. Given a well defined interface between the two, this approach enables multiple information processing algorithms to execute in parallel, with higher levels of the hierarchical management able to synthesize the individual results which are best suited to the managerial objectives.

The RSM is therefore designed to provide numerical hydrological solutions incorporating complex anthropogenic control schemes in a flexible, extensible, clear and consistent manner. The focus of this paper is to communicate the overall design structure of the MSE and illustrate the enhancements it provides in relation to the current state-of-the-art towards addressing the emerging needs of complex management scenarios applied to regional scale conjunctive hydrological models.

1.1 Hydrological Model Management Schemes

Even a cursory examination of the hydrological literature reveals a wealth of advanced management techniques applied to water resource models [2, 3]. For example, linear programming [4], artificial neural networks [5, 6] fuzzy control [7, 8], dynamic programming [9], simulated annealing [10], genetic algorithms [11], hybrids of all of these, as well as others. However, these hydrological models tend to be specialized, requiring non-standard input formats, and limited in scope to either reservoir routing or local hydrological control. Instead, we will focus on models which incorporate the following attributes:

- Widely available and accepted by the hydrological community
- Implement stream flow & hydraulic structures
- Allow control of hydraulic structures
- Extensive body of model implementations

While there are many models which meet the above criteria to varying degrees, we have focused on the widely used and accepted models listed in Table 1. A list of the acronyms is provided in appendix 7.

Model	Source	Language
MODBRANCH	USGS	FORTRAN
MIKE SHE/11	DHI	Pascal
FEQ	USGS	FORTRAN
RSM	SFWMD	C++
HMS-RAS	HEC	C++/FORTRAN
SWMM	EPA	C
FLDWAV	NWS	FORTRAN
FLO-2D	Tetra Tech	FORTRAN

Table 1. Hydrologic models used in comparison

The primary features of each of these models, with emphasis on the hydraulic structure control and management capabilities is summarized in Appendix 6. The RSM model is described separately in section 2. Table 2 presents a synopsis of some of these primary features for each of these models. The first column lists the primary feature, each row refers to the specific model. An X entry indicates that the feature is fully implemented in the model, x denotes that the features is partially available, and * is used to represent features that do not apply, for example the coupling of ground water and stream flow in one-dimensional stream conveyance models. The reader is cautioned that the purpose of this comparison is not to argue for superiority of any one model over another. Indeed, the applicability of this diverse set of tools targets a wide spectrum of hydrological conditions for which there are disjoint functional overlaps between several of the models. Rather, the comparison focuses on the managerial capabilities of these leading applications which are well accepted in the hydrological community.

Function	MB	MS	FEQ	RSM	HEC	SM	FW	FLO
Metadata Input				X				
Non Rectangular			*	X			*	
Coupled G W/SF	X	X	*	X	X		*	*
Coupled GW/SW/SF		X	*	X	X		*	*
Rating Curves	X	X	X	X	X	X	X	X
Dynamic Control		x		X				
Arbitrary Control		x	x	X	x	x		
Multi Supervision		x		X				
Optimization		X		X				

Table 2. Comparison of Modern Hydrological Models.
MB - MODBRANCH, MS - MIKE SHE/11, FEQ - FEQ, RSM - RSM,
HEC - HEC HMS, SM - SWMM, FW - FLDWAV, FLO - FLO-2D

The primary features have the following meanings:

Metadata Input This indicates that the model inputs are specified in a self-describing format in which the inputs are contextually specified. A prime example would be the use of the Extensible Markup Language (XML) employed by the RSM [12]. An XML input specification enables implicit syntax and input value validation, coherently organizes the data into a structured hierarchy, provides a common cross-platform and application generic input dataset, among other advantages. The use of standardized metadata input represents a significant step forward in data representations when compared to the typical implementations relying on application-specific input formats based on proprietary or non-standard formatting specifications.

Non Rectangular This refers to the shape of the spatial computational elements in the hydrological numerical representation. While this is not directly implicated in the functionality of the hydraulic structure modeling, it does represent a significant difference between the RSM and other models. The RSM operates on arbitrary triangular elements, which may provide more efficient geo-spatial matching and representation than is easily obtainable with rectangular elements. The HSE is a finite volume formulation, consequently, the computational elements are not limited to rectangular grid cells as imposed by pragmatics of applying finite difference formulations.

Coupled GW/SF The groundwater and streamflow are integrated in the hydrologic solution.

Coupled GW/SW/SF The groundwater, surfacewater and streamflow are integrated in the hydrologic solution.

Rating Curves Hydraulic structures can have transfer functions specified by rating curves defined as lookup tables.

Arbitrary Control The modeler can implement an arbitrary control or management algorithm. This feature is considered fully implemented if one can write the control algorithm using standard computer code. The code is compiled into a shared library which is loaded at run-time, with I/O data passed between the control library and the model through a well defined interface. The control code is able to access arbitrary hydrological state information from the model, and is able to dictate hydraulic structure control to the model. The feature is partially implemented if the model restricts the expression of control algorithms to a set of rules, or limits the inputs to a restricted set hydraulic and temporal variables.

Dynamic Control This feature refers to the ability to dynamically alter or adjust the control behavior of hydraulic structures. For example, a closed loop feedback controller such as a PID may have it's target value, or, any adjustable parameter of the controller changed in response to a dynamic variable. Another feature is to provide for dynamic switching of management algorithms. For instance, a rule-based fuzzy algorithm optimized for flood-control operations can dynamically replace a rule-curve or setpoint controller of a hydraulic structure in response to any observable state variable.

Multi Supervision The management algorithms are capable of multi-input, multi-output operations. For example, a management object is capable of setting the structure flow characteristics for multiple structures simultaneously. This is strictly possible with MIKE 11, but requires careful design and PASCAL code programming to implement. In the MSE, the management hierarchy defines objects which explicitly control the behavior of multiple hydraulic structures. This can be done with user defined computer code, fuzzy rules, LP, graph flow algorithms or heuristics.

Optimization The model incorporates an optimization package able to solve constrained optimization problems directed at allocating hydraulic structure flows, water storage control, or other resource management decisions.

2 Regional Simulation Model (RSM)

The Regional Simulation Model (RSM) is designed to simulate the complex natural and anthropogenic flow of an integrated aquifer-stream flow model. It consists of two interoperative computational modules, the Hydrologic Simulation Engine (HSE) [13, 14, 15, 16, 17, 18] and the Management Simulation Engine (MSE) [19, 20, 21]. The HSE is described briefly in the following section, one may refer to the citations for more detail. The MSE is detailed in the subsequent sections with an emphasis on the information processing characteristics inherent in it's design.

2.1 Hydrologic Simulation Engine (HSE)

HSE can simulate two-dimensional overland flow, two-dimensional or three-dimensional groundwater flow, one-dimensional canal flow, and flow in and out of reservoirs. The overland and groundwater flow domains are discretized in the horizontal 2-D domain using unstructured triangular cells. The groundwater aquifer layers may consist of any number of variable depth layers, each of which can span an arbitrary extent of horizontal 2-D cells. The stream flow network is discretized using piecewise linear canal segments, with variable geometry rectangular or trapezoidal cross-sections. The triangular 2-D meshes and 1-D stream networks are independent, and may overlap partially, fully, or not at all. A wide variety of local and micro-hydrologic functions associated with urban and natural land use, agricultural management practices, irrigation practices, and local routing are handled with a feature known as pseudocells. The pseudocells also provide various ET and rain function interactions, as well as unsaturated flow distributions.

The numerical solution is based on a semi-implicit finite volume approximation of the diffusion flow transport equations. The computational method is unconditionally stable, and is achieved through use of the PETSC sparse linear system solver [22]. The model is fully integrated. All coupled aquifer, overland and stream flow regional components are solved simultaneously.

The RSM is an object-oriented code, which relies heavily on the features of abstraction and inheritance. Within the HSE, the abstraction 'waterbody' is used to represent objects which contain conservative variables while the 'watermover' class represents fluxes between waterbodies. A watermover class for each type of hydraulic structure is implemented when dictated by the model input descriptions. These hydraulic structure watermovers are the primary interface for hydraulic control signals from the MSE. In the absence of a control signal, the watermover transports the flow imposed

by the hydraulic structure transfer function in response to the hydrological state variables. When a control signal is applied, some fraction of the total possible flow is allowed as specified by the control value.

2.2 Management Simulation Engine (MSE)

The MSE design is based on the hydroinformatic principle that operational and managerial decisions applied to water control structures can be viewed as information processing algorithms decoupled from the hydrological state information on which they operate. Essentially, the HSE provides hydrological and hydraulic state information (Σ), while external policies dictate managerial constraints and objectives (Λ).

In the MSE this state and process information can be functionally transformed by an independent set of filters, which can be viewed as information pre-processors. These processors are denoted as Assessors (A) and Filters. For example, an Assessor may perform statistical filtering such as spatio-temporal expectations, amplitude or time-delay modulation, or any other suitable data filtering operation. The MSE is then tasked with appropriately processessing the assessed state information in order to produce water management control signals (χ, μ) which are applied to the hydraulic control structures in order to satisfy the desired constraints and objectives. Figure 1 illustrates this overall cyclic flow of state and management information in the RSM.

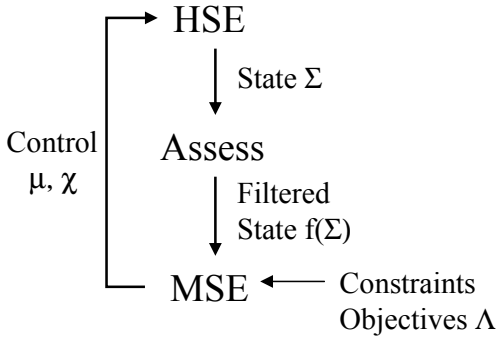

Figure 1: RSM state and management information flow

More specifically, the MSE architecture is based on a multilayered hierarchy, with individual water control structures regulated by 'controllers' while the regional coordination and interoperation of controllers is imposed

by 'supervisors'. Supervisors can change the functional behavior of controllers, completely switch control algorithms for a structure, or override the controller output based on integrated state information and/or rules. A schematic depiction of the HSE-MSE layered hierarchy is shown in figure 2.

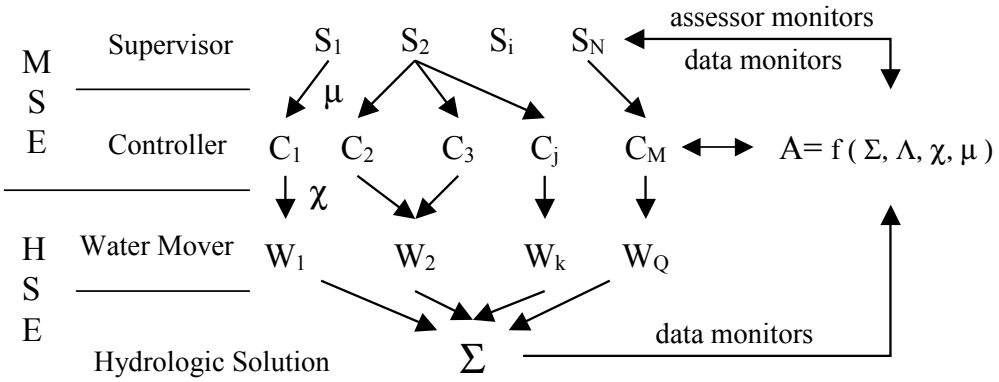

Figure 2: HSE MSE schematic

At the lowest layer is the hydrological state information (Σ) computed by the HSE. This information includes water stages, flow values, rainfall, ET, hydrologic boundary conditions, or any other state variable used as input or computed as output by the HSE. All such variables are made available to the MSE and Assessors through the implementation of a uniform data monitor interface. The data monitor interface extends naturally to the MSE input/output variables. Therefore, the input state information available to a controller or supervisor is not limited to water levels or flow values, but can include control information, decision variables, constraints or any other management variable from any other controller or supervisor in the model. This transparency of state and process information throughout the model is central to the efficient synthesis and processing of heterogeneous information required to simplify and naturally express complex water management policies.

The top level of the MSE is the supervisory layer. There is no limit on the number of supervisory algorithms, or constraint on the number of controllers that a supervisor may influence. Based on state and process information, which optionally may have been filtered or assessed, the function of a supervisor is to produce the supervisory control signal (μ) for a single, or collection of hydraulic structure controllers. The supervisors are therefore able to comprehensively coordinate the global behavior of multiple

independent, or coupled hydraulic structures. A description of the available supervisors is given in section 2.5.

The intermediate layer consists of the hydraulic structure watermover controllers. A controller is responsible for local regulation of structure flow. It is possible to attach multiple controllers to a structure watermover, although only one controller at a time is activated. This activation is controlled by a supervisor. For example, a fuzzy controller optimized for wet condition operations may be selected by a supervisor during significant rain events, while a standard rulecurve could be enforced during normal operations. In this manner the MSE provides for dynamic switching of hydraulic structure control functions in response to state or process information.

Once the controllers have computed their respective control values (χ), these signals are applied as flow constraints to the structure watermovers in the HSE. Each watermover will compute a maximum flow capacity based on the hydrological state conditions and hydraulic transfer function of the structure. The resultant controlled flow will be some fraction of the currently available maximum flow capacity.

2.3 Assessors & Filters

The role of assessors in the MSE is to perform data preprocessing required for operational control decisions. By decoupling the conditioning and filtering of state and process information from the decision making algorithms, the decision processors can be simplified and modularized. Therefore, an assessor is a information processor intended to provide specialized aggregation or differentiation of state variables particular to a managerial decision process. For example, the water supply needs (WSN) assessor estimates the volumetric flow in a canal water control unit which is required to meet a downstream water supply demand. This assessor considers both upstream and downstream supply & demand from connected water control units. Once this assessment is completed, a supervisory algorithm can synthesize information from other assessors or operational constraints to arrive at a control decision. Since the supervisor is not concerned with the particulars of how the assessments are made, only with their results, the management algorithms are isolated to information processing relevant to the decision process, and do not include code or rules to perform data filtering and assessment.

Related to the assessors, are MSE filters. Filters are generic information processors implemented to perform simple, often redundant data filtering operations. For example, a filter may apply a scalar or timeseries amplitude modulation consisting of the usual arithmetic operations (multiplication,

division, addition, subtraction) or may compute simple timeseries or spatial variable statistics such as arithmetic, geometric, or other expectations, or may act as an accumulator.

The RSM implements a unified design approach for monitors, filters, and assessors based on object oriented design principles. As a result, the interfacing of these constructs from the user's perspective is particularly simple, and powerful. Assessor and filters operate in a piped FIFO fashion, as exemplified by the XML fragments below and in figure 3.

```
<WcuAssessor asmtID="101" name="Reach1" mode="wsneeds">
   <target> <dss file="Reach1Target.dss"/> </target>
</WcuAssessor>

<filter type="offset">
   <offset><dss file="Reach1Offset.dss"/></offset>
   <filter type="MovingAvg" numAvg="15">
      <assessormonitor id="101" attr="flow"></assessormonitor>
   </filter>
</filter>
```

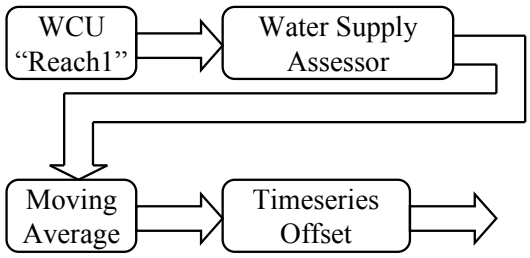

Figure 3: Unified interfacing of data preprocessors allows piped operations.

The first XML section defines a water control unit assessor (WcuAssessor) attached to the canal unit Reach1. The assessor is in water supply needs mode, which computes the flow required in the control unit to satisfy the target levels specified in the timeseries file Reach1Target.dss. The second section defines a dual-stage filter applied to the assessed flow values. An assessormonitor is used to reference the assessed flow, and serves as input to a moving average filter. The output of the moving average filter is input to an offset filter, with offset values specified by the timeseries Reach1Offset.dss. To change the data source, order, or type of operations, one simply recon-

figures the XML specification. This procedure can be automated with the use of a graphical user interface software application.

A crucial aspect of effectively storing and accessing assessed state information for water resource management purposes is the maintenance of an efficient storage mechanism which associates hydrological state information with the proper managerial abstractions. In the RSM this is done by storing assessed information relevant to a particular water control unit (WCU) in a data storage object defined in the MSE network. The MSE network is an abstraction of the reservoirs, stream flow network, and water control structures dedicated to representing the managerial architecture of the model, it is discussed in section 2.6

A result of these data handling abstractions and interfaces is the desired decoupling of state variable processing from managerial decision processing based on a flexible, data driven specification which is easily modified providing a level of plug-and-play functionality not commonly found in conjunctive hydrological models.

2.4 MSE Controller Layer

The MSE controller layer is the intermediary between the hydraulic structure watermovers and the regional-scale supervisory coordinators. The controllers can operate independently of the supervisors, in fact they are not required at all for uncontrolled operation of a hydraulic structure. The essential purpose of a controller is to regulate the maximum available flow through a structure to satisfy a local constraint. A controller may take as an input variable any state or process information which can be monitored within the RSM. Since the interface between a structure watermover and any controller is uniform, it is possible to change controllers dynamically with a supervisory command, or manually with a simple XML input change. The unitary interface also allows for the modeler to mix and match controllers in a particular model application so that the local control schemes are a hybridization of any of the available control algorithms.

The currently available controller modules in the RSM include:

- One & two dimensional rulecurves
- Piecewise linear transfer function
- Proportional Integral Derivative (PID) feedback control
- Sigmoid PI feedback control
- Fuzzy control
- User defined finite state machine

Each of these is briefly described in the following sections. Detailed information regarding the usage, applicability, and examples of model implementations are described in [20].

2.4.1 One & two dimensional rulecurves

All of the models examined in section 1.1 implement rulecurves in some fashion as a method of controlling the flow transfer function of hydraulic structures. The MSE provides for one or two variable interpolated lookup tables as a means of structure control. Notable in the MSE implementation is that the selected variables can be taken from any HSE or MSE variable which can be monitored, not just water level or flow variables.

2.4.2 Piecewise linear transfer function

With the piecewise linear transfer function controller, the user specifies a control function as a combination of two or three linear segments as shown in figure 4. The upper and lower control values are C_H and C_L, with the control output determined by the value of the input state variable ϕ in relation to the upper and lower threshold values τ_H and τ_L. This controller can act as either a binary switch between the output control values of C_H and C_L, or can provide linear interpolation between the control points (τ_L, C_L) and (τ_H, C_H) along with lower and upper saturation values at C_L and C_H.

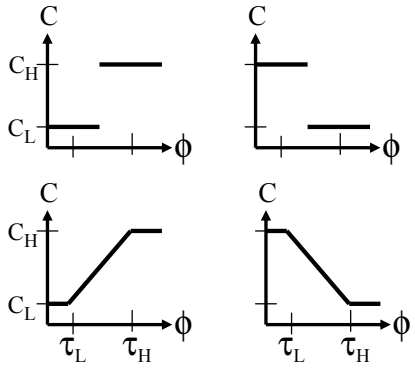

Figure 4: Piecewise linear transfer functions.

2.4.3 Proportional Integral Derivative (PID) feedback control

MSE implements a standard closed-loop feedback PID controller based on the time difference approximation

$$C(i) = \gamma_P \, \epsilon_i + \gamma_D \frac{\triangle \epsilon_i}{\triangle t} + \gamma_I \sum_{i=1}^{n} \epsilon_i \triangle t \tag{1}$$

where γ_P γ_D and γ_I represent gain factors for the proportional, derivative and integral terms, the system state variable to be controlled is $\phi(t)$ and the desired system target state is $T(t)$ at timestep t. The system error is computed as $\epsilon(t) = \phi(t) - T(t)$.

2.4.4 Sigmoid PI feedback control

The sigmoid controller is essentially a PI controller with a single nonlinear activation function (the sigmoid) filtering the controller output. The PI portion of the controller is implemented as specified in equation 1 without the derivative term. Once a preliminary PI control output is available C_{PI}, the output is processed by a nonlinear sigmoidal activation function commonly known as the logistic or sigmoid function which is specified by

$$S(cx) = \frac{1}{1 + e^{-cx}}. \tag{2}$$

with $c > 0$. The value of c determines the slope of the activation function at the origin, and can change the functional behavior from that of a slowly rising transition (c→0) to one of a unit step function ($c \to \infty$). This function serves to limit the possibly unbounded control outputs to the interval [0,1], while also providing an adjustable derivative for the linear portion of the activation function. Finally, the processed control signal is scaled by a constant scale factor α. The resultant sigmoid control signal is therefore given by

$$C(i) = \alpha \, S\left(C_{PI}(i)\right) \tag{3}$$

The sigmoid controller has been shown to increase stability and tolerance of closed loop feedback PI control to large variations of input state variables [19].

2.4.5 Fuzzy control

The MSE incorporates a generic fuzzy controller as defined by the International Electrotechnical Commission (IEC) standard for Fuzzy Control Programming [23]. The fuzzy controller constitutes a rule-based expert system utilizing an inferencing engine coupled with multiple constraint aggregation. Fuzzy control can be useful in cases where there exists an experiential reference base that can be expressed in terms of rules. In contradiction to many canonical control processors, fuzzy control doesn't require knowledge of the system transfer function, that the transfer function be expressible in closed form, or that the system has to be linear. An additional advantage is that the rule base is expressed in a linguistically natural format and can be easily understood by non-specialists.

The definition of a fuzzy controller is expressed in the Fuzzy Control Language (FCL) [23]. The FCL specifies the input/output variables, fuzzy membership functions, and rule-base. The fuzzy controller supports five types of input/output terms for fuzzification and defuzzification illustrated in figure 5.

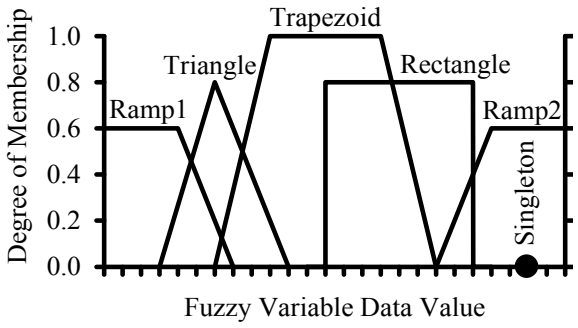

Figure 5: MSE fuzzy I/O terms

An example FCL excerpt for a simple pump station controller is shown below.

```
// Fuzzy Controller for Pump Station
VAR_INPUT
        CanalStage : REAL;
END_VAR
VAR_OUTPUT
        PumpOut : REAL;
END_VAR
FUZZIFY CanalStage
        TERM low    := (9, 1) (10, 0);
        TERM medium := (9, 0) (10, 1) (12, 1) (13, 0);
        TERM high   := (12, 0) (13, 1);
END_FUZZIFY
DEFUZZIFY PumpOut
          TERM off        := 0.;
          TERM mediumLow  := (0.3, 1) (0.6, 0);
          TERM mediumHigh := (0.4, 0) (0.7, 1);
          TERM on         := 1.;
END_DEFUZZIFY
RULEBLOCK No1
          RULE 1: IF CanalStage IS high THEN PumpOut IS on;
          RULE 2: IF CanalStage IS medium AND CanalStage IS high
                  THEN PumpOut IS mediumHigh;
          RULE 3: IF CanalStage IS medium AND CanalStage IS low
                  THEN PumpOut IS mediumLow;
          RULE 4: IF CanalStage IS low THEN PumpOut IS off;
END_RULEBLOCK
```

The corresponding fuzzy input/output terms for this example are shown in figure 6.

To completely implement this fuzzy controller, the XML specification read by the RSM must specify the structure watermover to which the controller is applied, the source of the input state variable(s), and the name of the output variable exemplified below. As with the other controllers, the input state variables can be obtained from any monitored data source in the RSM. Although only one input variable is demonstrated in this example, multiple inputs are supported.

```
<fuzctrl cid="101" wmID="1" fcl="pump.fcl">
   <varIn name="CanalStage">
     <segmentmonitor id="34" attr="head"></segmentmonitor>
   </varIn>
   <varOut name="PumpOut"> </varOut>
</fuzctrl>
```

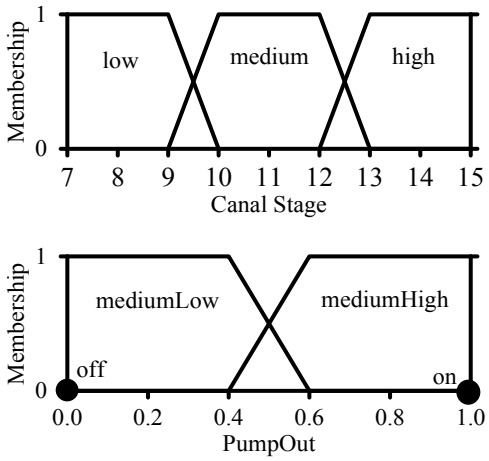

Figure 6: Fuzzy input output terms for pump example

2.4.6 User defined finite state machine

In certain cases, a canonical fixed transfer function or rule-based expert system controller may not best suit the needs of a hydraulic structure watermover controller. To accommodate this, the MSE allows the user to develop arbitrary finite state machine algorithms through the development of C or C++ shared libraries. MSE implements a dynamic shared library loader and function pointer interface which calls the user defined control function(s) at each timestep. Each controller maintains it's own shared object and function pointer information, allowing the user to define multiple control functions inside a single shared object. The control functions can receive multiple input state variables from any data source that can be monitored within the RSM. The input-output interface to the user functions are detailed in [20].

An example of the RSM XML specification for a user defined controller is shown below. To manually replace this controller with the previously mentioned fuzzy controller, or any other controller, a simple edit of the XML input file is all that is required.

```
<userctrl cid="102" wmID="2" module="./UserCtrl.so" func="myControl">
   <varIn name="Canal1">
      <segmentmonitor id="25" attr="head"></segmentmonitor>
   </varIn>
   <varOut name="GateOpen"> </varOut>
</userctrl>
```

2.5 MSE Supervisor Layer

An MSE supervisor is effectively a meta-controller, a controller of controllers. The addition of this supervisory layer considerably simplifies the control expression of multiple, coordinated hydraulic structures. In addition to the organizational simplification of control algorithms, it is likely that the additional layer enables representation of management functions which are not realizable with a single control layer. This assertion is based on analogy with the universal approximation theorem for artificial neural networks (ANN).

The universal approximation theorem states that any real valued (linear or nonlinear) continuous function can be approximated arbitrarily closely by an artificial neural network having only two adjustable weight layers which are processed by sigmoidal activation functions. The proof of this theorem [24, 25] builds on seminal work of Kolmorogorov concerning the decomposition of continuous functions [26].

In relation to the multi-level control hierarchy of the MSE as depicted in figure 2, the computational architecture can be viewed as an analog of the universal approximation artificial neural network as follows. Consider that the MSE control signal outputs μ and χ are analogous with the adjustable weight matrix of an artificial neural network. In an ANN the weights are adjusted in a learning or evolution process based on the optimization of an error metric in relation to a desired goal. In the MSE control scenario, the control signals converge on values dictated by optimization of the system response in relation to the desired control objectives. Concerning the MSE control and supervisory processors S_i and C_j, it is clear that the control signal output for physically based control structures is stable and finite. Therefore, the processor transfer function of these stable and bounded control processors must also be stable and bounded. Such process functions are functionally analogous to the sigmoidal functions which are inherently stable and bounded process functions (equ. 2). Based on this analogy, it is expected that the multi-layered control hierarchy of the MSE provides a computational architecture capable of modeling the majority of water re-

source management policies.

In relation to the controllers, which are multi-input, single-output (MISO) processors, the supervisors are multi-input, multi-output (MIMO) processors. Supervisors have the ability to change individual response characteristics of controllers, or, in the case of multiple controllers attached to a watermover, to dynamically select and activate a specific controller for a watermover. Specifically, the supervisory functions include

- Synoptic assessment of state and process information
- Controlling multiple parameters of multiple controllers
- Dynamic switching of multiple controllers
- Flow regulation override for controller(s)

This is done through a uniform interface to the controllers ensuring interoperability between different supervisory processors and any controller.

There is no practical limit on the number of supervisors allowed in a model, or on the number of controllers that a supervisor may affect. It is common to have a hybrid selection of different supervisors, each one regulating a specific sub-regional collection of hydraulic structures. The ability to selectively tailor management control algorithms, as well as the flexibility to easily reconfigure them in a plug-and-play fashion lends considerable power to the implementation of diverse and complex operational management scenarios.

The currently available supervisor modules in the MSE include:

- Fuzzy supervision
- User defined finite state machine
- Linear Programming
- Graph flow
- Heuristic Object Routing Model

The fuzzy supervisor is derived from the same fuzzy library modules as the fuzzy controller described in section 2.4.5. It's operational characteristics and fuzzy control language usage are the same. The user defined supervisor is an extension of the user defined controller described in section 2.4.6 from a multi-input, single-output controller, to a multi-input, multi-output supervisor. The multi-outputs allow for the coordinated operation, or behavioral changes to multiple watermover controllers. The user supervisor allows one to define arbitrary supervisory algorithms in dynamically loaded shared libraries.

The remaining supervisory modules are briefly described in the following sections. Detailed information regarding the usage, applicability, and examples of model implementations for all supervisors are described in [21].

2.5.1 Linear Programming supervision

MSE provides an interface to the GNU Linear Programming Kit (GLPK) [27]. The GLPK package is intended for solving large-scale linear programming (LP), mixed integer programming (MIP), and other related optimization problems. GLPK supports the GNU MathProg language, which is a subset of the AMPL language. AMPL is a comprehensive and powerful algebraic modeling language for linear and nonlinear optimization problems, in discrete or continuous variables. AMPL lets you use common notation and familiar concepts to formulate optimization models and examine solutions.

The MSE GLPK supervisor is defined by a MathProg model definition file which specifies the parameters, variables, and optimization function of the supervisor. The model definition file may also contain a data section which defines parametric values, and initial values for variables. If the data section is not included in the model definition file, then a separate data definition file must exist. The MSE GLPK supervisor reads these files, creates the GLPK problem objects, and calls the appropriate GLPK API routines to solve the supervisory constrained optimization problem.

2.5.2 Graph flow supervision

From the perspective of mathematical graph theory, there is a well developed body of work regarding the assessment of flows in interconnected networks [28, 29]. Graph representations of flow networks for water distribution and stream flow networks are common, and useful [30, 31]. The MSE maintains a graph theory based representation of the managed canal network as described in section 2.6. The MSE Graph supervisor implements the maxflow, feasible flow, and mincost feasible flow algorithms. These algorithms are essentially minimal numerical procedures which solve constrained optimization problems on the network flow by taking advantage of the network properties, rather than solving a set of simultaneous equations explicitly. The constraints consist of the canal arc capacity, the hydraulic structure capacity, demand and supply flows at the structures, and flow cost weights assigned to the canal arcs.

Each graph supervisor solves the network flow based on it's own network representation, however, this can be degenerate with other supervisor net-

work representations. As a result, a graph supervisor can solve the flow for the entire network, or for any subset of the network for which a graph has been defined.

2.5.3 Heuristic Object Routing Model supervision

In addition to the generic supervisory information processors described above, there is also a heuristic operational management module specific to the South Florida region. This module is termed the Object Routing Model (ORM) and was derived from the longstanding legacy application [32] which incorporates many years of water resource management and numerical hydrological experience.

The ORM is a basin routing model that follows a binary decision tree in the determination of hydraulic structure flow settings. Assessors quantify the water supply and flood control needs of a basin which are to be resolved by basin flow transfers. Management objectives are expressed as policies which dictate the structure of the decision tree.

2.5.4 Supervisor XML

Several of MSE supervisors require external information dictating the information processing model of the particular supervisor. For example, the fuzzy supervisor requires an FCL file, the user supervisor a C or C++ algorithm and the LP supervisor a MathProg file. However, all supervisors share a common input/output interface with the RSM state variables, and are described in the RSM model input with an XML entry. An example XML excerpt is shown below. In this example, two watermover controllers have their lower trigger threshold value adjusted according to the control algorithm coded in the user defined C++ function `SetTrigLow`. This supervisor accepts two input variables, and sets two output variables.

```
<user_supervise id="804" module="./UserSprv.so" func="SetTrigLow">
   <ctrlID> 103 104 </ctrlID>
   <varIn name="segment1Head">
      <segmentmonitor id="1" attr="head"></segmentmonitor>
   </varIn>
   <varIn name="segment4Head">
      <segmentmonitor id="4" attr="head"></segmentmonitor>
   </varIn>
   <varIn name="season">
      <tkprmonitor attr="month"></tkprmonitor>
   </varIn>
   <varOut ctrlID="103" func="triglow" name="103_TrigLow"> </varOut>
   <varOut ctrlID="104" func="triglow" name="104_TrigLow"> </varOut>
</user_supervise>
```

2.6 MSE Network

A central feature of the MSE which enables decoupling of the hydrological state information maintained by the HSE and the operational process information of the MSE is the MSE network. The MSE network is an abstraction of the stream flow network and control structures suited to the needs of water resource routing and decisions. It is based on a standard graph theory representation of a flow network comprised of arcs and nodes [29]. The MSE network data objects serve as state and process information repositories for management processes. They maintain assessed and filtered state information, parameter storage relevant to WCU or hydraulic structure managerial constraints and variables, and serve as an integrated data source for any MSE algorithm seeking current state information. It also provides a mathematical representation of a constrained, interconnected flow network which facilitates the efficient graph theory solution of network connectivity and flow algorithms.

From the hydrological perspective, the HSE stream network is composed of an interconnected network of flow segments, with each segment maintaining parameters relevant to aquifer-stream interaction, flow resistance, spatial coordinates and other physical properties. The spatial representation of HSE segments are typically dictated by topographic and physical parameters. From the water resource management viewpoint of the MSE, the important features of the flow network are it's connectivity, flow capacities, flow regulation structures, and assessed state information relevant to managed sections of the network. The MSE network maintains a mapping

between these two representations.

The primary stream object in the MSE network is the Water control unit (WCU). A WCU maps a collection of HSE stream segments that are operationally managed as a discrete entity to a single arc in the MSE network. WCU's are typically bounded by hydraulic control structures, which are represented as nodes in the MSE network. Each WCU includes associative references to all inlet and outlet hydraulic flow nodes. Some of the variables stored in a structure (node) object include:

1. current flow capacity
2. maximum design flow capacity
3. reference to hydraulic watermover
4. reference to structure controller
5. operational policy water levels
6. supply
7. demand

while the WCU (arc) objects incorporate:

1. flow capacity
2. seasonal maintenance levels
3. inlet flow
4. outlet flow
5. water depth
6. water volume

Each WCU in the MSE network is referenced by a unique label, and has an associative data storage object which dynamically allocates storage for assessment results. This allows multiple, independent assessments of the WCU state. For example, one assessment of WCU inlet structure flows might come from a graph algorithm, while another could be stored from a LP model.

This abstraction from hydrological objects to managerial objects condenses the network representation facilitating the organization and storage of relevant assessed state and process information. As an example, figure 7 depicts an HSE stream network consisting of 63 nodes and 62 segments. Some of the nodes correspond to locations of hydraulic control structures, though the association is not apparent from examination of the HSE network. Each stream segment has a unique identifier which allows the modeler or MSE processor to monitor state information of the segment. However,

as pointed out earlier, it may be appropriate to make water management decisions based on some assessed or filtered version of aggregated stream segment states.

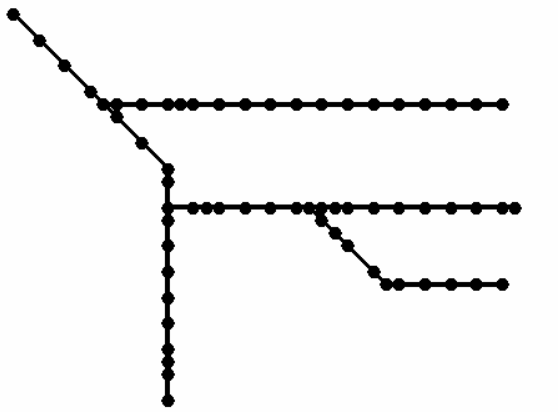

Figure 7: Example HSE stream network segments and nodes.

Consider now an abstraction of the HSE network into 10 WCU's, regulated by 11 hydraulic structures. An example of such a MSE network is presented in figure 8. In the MSE network each line segment represents a WCU, while each node represents a hydraulic structure which regulates a WCU. The modeler or MSE processor is able to directly monitor information stored in any of these object data containers, information which has already been assessed and automatically stored in the appropriate WCU data object at each timestep.

As with other RSM model inputs, the WCU mapping from the HSE stream network is performed with an input XML entry. The excerpt below shows basic elements in the construction of an MSE network. The `mse_arc` establishes a collection of HSE stream segments as a single entity, and defines the nodes which connect to this arc. The `mse_node` supplies optional parameter and data values for nodes, while the `mse_unit` aggregates the `mse_arc` into WCU's.

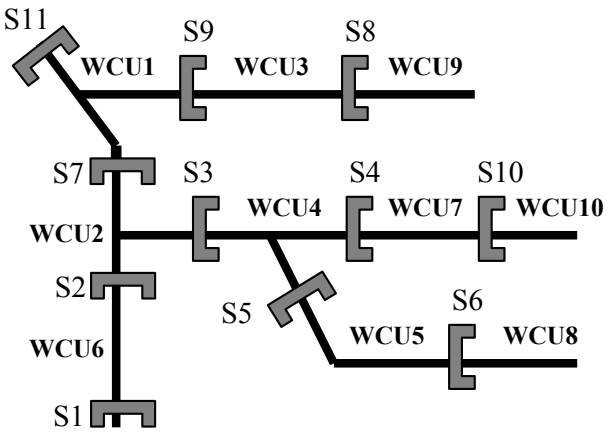

Figure 8: Example MSE network abstraction of HSE network into WCU's and structures.

```
<mse_network name="Test Network">
  <mse_arcs>
    <mse_arc name="Reach_1" capacity="1400">
      <hse_arcs> 100 101 102 103 </hse_arcs>
      <node_source> "S11"    </node_source>
      <node_sink>   "S11_A"  </node_sink>
    </mse_arc>
    <!-- more mse_arc entries.... -->
  </mse_arcs>
  <mse_nodes>
    <mse_node name="S11" purpose="WaterSupply" designCap="3000.">
      <supply name="S11 Supply"> <const value="100"> </const> </supply>
      <open   name="S11 Open">   <rc id="2"></rc> </open>
      <close  name="S11 Close">  <const value="5.5"> </const> </close>
    </mse_node>
    <!-- more mse_node entries.... -->
  </mse_nodes>
  <mse_units>
    <mse_unit name="WCU1">
      <unit_arcs> "Reach_1" "Reach_1S" "Reach_1E" </unit_arcs>
      <maintLevel name="maint"> <const value="5.5"> </const> </maintLevel>
      <inlet  name="S11 inlet">  "S11" </inlet>
      <outlet name="S7 outlet" > "S7"  </outlet>
      <outlet name="S9 outlet" > "S9"  </outlet>
    </mse_unit>
    <!-- more mse_unit entries.... -->
  </mse_units>
</mse_network>
```

3 RSM Integrated Example

In this section we demonstrate some basic MSE operational controls applied to a RSM model application which represents the Florida lower east coast. This model covers roughly the area from Lake Okeechobee in the northwest to southern Miami-Dade county in the southeast. The HSE model consists of 1124 mesh cells representing a single layer aquifer and ground surface, coupled with a stream network consisting of 455 canal segments. The model period of record is from January 1 1998 to March 31 1999, this period encompasses the May-September rainy season, as well as an exceptional rain event from a tropical storm which passed over the area on October 5, 1988. Figure 9 illustrates the HSE mesh and canal network.

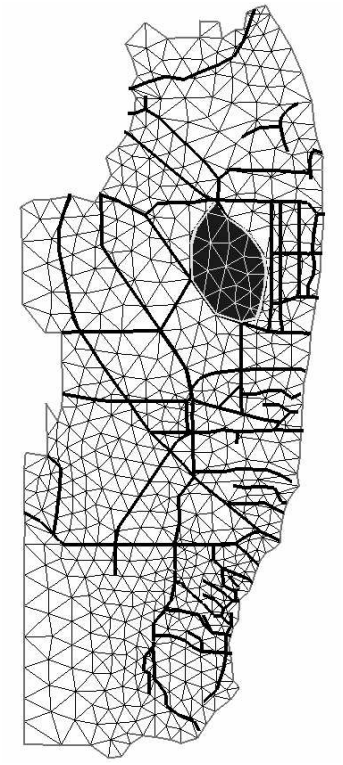

Figure 9: Example RSM application mesh and canal network, WCA1 is highlighted.

Regarding the MSE implementation of this model, there are 192 hydraulic structure watermovers, with a controller assigned to each water-

mover. The MSE implements 12 supervisors to control coordination of multiple controllers. The HSE canal network has been aggregated into 56 water control units (WCU's) forming the MSE network. Figure 10 shows a graphic comparison of the HSE and MSE networks.

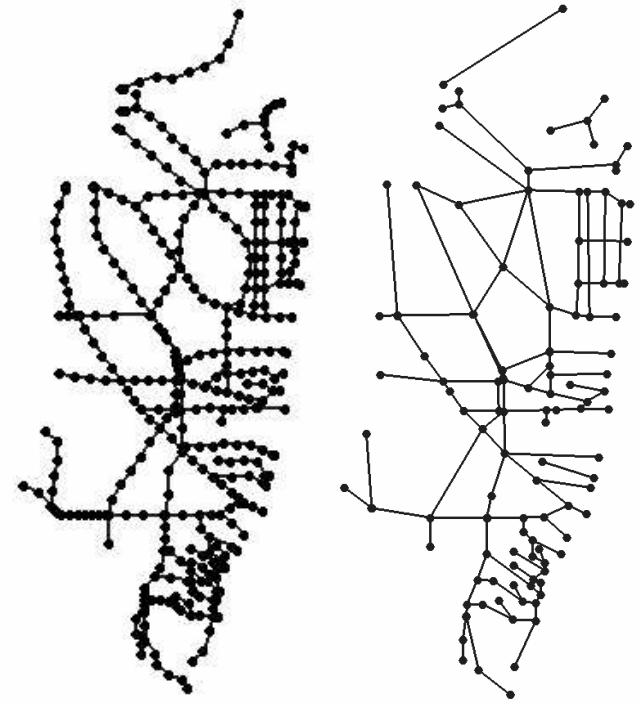

Figure 10: Comparison of HSE (left) and MSE networks (right).

The highlighted area in figure 9 corresponds to the northernmost extent of the Everglades. It is a federally protected wetland, the Arthur R. Marshall Loxahatchee National Wildlife Refuge. The refuge is commonly referred to as Water Conservation Area 1 (WCA1). The refuge is surrounded by a canal and levee system which effectively isolates it from the adjacent lands. Water levels inside WCA1 are controlled through a series of inlet and outlet hydraulic structures located on the perimeter canals of the basin. Figure 11 depicts a schematic representation of the WCA1 model representation with the major flow control structures indicated as arrows.

The primary outlet flow structures from WCA1 are the series of S10 structures along the lower left canal rim. These structures discharge into the

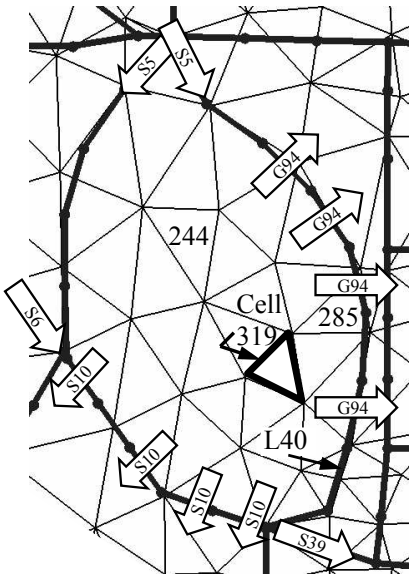

Figure 11: WCA1 model conceptualization.

adjacent Everglades referred to as Water Conservation Area 2 (WCA2). The hydraulic structure S39 controls the flow from the southern rim canal into a coastal outlet canal. Additionally, the series of G94 structures are capable of discharging from WCA1 into the adjacent drainage district (though these structures are usually controlled by the drainage district into which they discharge.) In the model, the controllers for the S10 and G94 structures are piecewise linear transfer functions while the S39 controller is a user defined (C++) finite state machine module. When the supervisor is not in effect, these controllers regulate the flow through the structures.

In this demonstration, a supervisor has been created from a user defined C++ module to coordinate the operation of the S10, S39 and G54 structures in an attempt to lower the canal and aquifer levels in WCA1 in response to stage and rainfall state information. The input stage information is an assessed spatial average of watertable levels in the three mesh cells 244, 285 and 319 (figure 11). The input rainfall is a spatio-temporal moving average assessed over the same three cells and a 24 hour period. The assessor XML for these inputs is shown below, the resultant assessed stage and rainfall is depicted in figure 12.

```
<statassessor asmtID="2" attr="ave" name="WCA-1 3-gage avg">
  <cellmonitor id="244" attr="head"/>
  <cellmonitor id="285" attr="head"/>
  <cellmonitor id="319" attr="head"/>
</statassessor>

<statassessor asmtID="3" attr="ave" name="WCA-1 rain avg">
  <filter type="movingavg" numAvg="4">
     <cellmonitor id="244" attr="rain"/>
  </filter>
  <filter type="movingavg" numAvg="4">
     <cellmonitor id="285" attr="rain"/>
  </filter>
  <filter type="movingavg" numAvg="4">
     <cellmonitor id="319" attr="rain"/>
  </filter>
</statassessor>
```

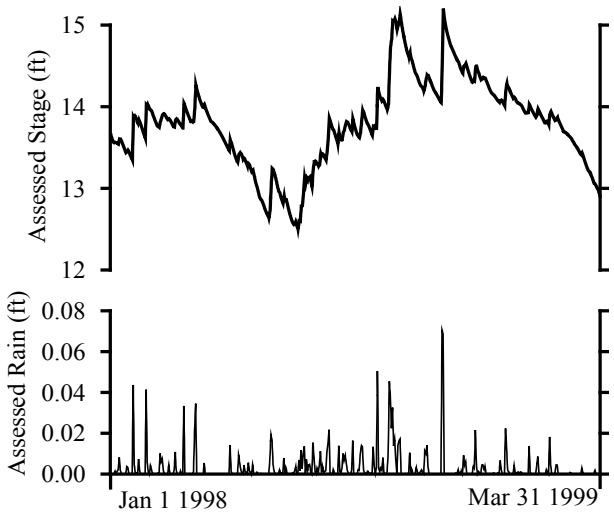

Figure 12: Assessed stage and rainfall in WCA1.

The user defined supervisor receives the assessed stage and rainfall information as input state variables, and then assigns structure control outputs to the S10, G94 and S39 structures based on two modes of operation. In the default mode the control outputs are set for each structure based only

on the assessed stage values decomposed into four ranges of average stage s: $(s < 12)$, $(12 <= s < 13)$, $(13 <= s < 14)$, $(s >= 14)$ ft. The supervisor also computes a threshold comparison on accumulated values of the assessed rainfall. A sliding accumulator stores assessed rainfall over a three day moving window. If the sum of the accumulated rainfall exceeds a threshold (0.01 ft) and the assessed stage is greater than 12 ft, then an alternate set of control values are applied to the structures intended to increase the outflow from WCA1. This algorithm is not patterned after an actual water management policy for WCA1, but serves to illustrate some of the possibilities afforded with the combination of assessors and supervisors.

The model was run in two modes. In the first run the supervisor which controls the WCA1 outlet structures was switched off. In this mode the local controllers for each WCA1 outlet structure are regulating the flow according to their operational criteria. In the second mode, the supervisor is activated, and overrides the control function of the individual structure controllers as described above. The control signals and resultant structure flows for one of the S10 and G94 structures, and for the S39 are shown in figures 13 and 14 respectively.

The second model run was conducted with the WCA1 outflow supervisor activated. Control signals and selected structure flows for this case are shown in figures 15 and 16 respectively. Comparison of the unsupervised and supervised control and flow graphs shows a significant behavioral difference, where as expected, the supervisory control provides significantly increased outflow.

A comparison of the modeled canal stage in the L40 canal segment with and without supervision is depicted in figure 17. The lower portion of figure 17 plots the model input observed rainfall applied to cell 319, which was used as one of the inputs to the assessed rainfall. The supervisory control has lowered the L40 canal stage by approximately 18 inches. The model output of water levels in the mesh cell 319 are presented in figure 18. The effect of the supervisory control is clearly evident in the lower water levels achieved with the coordinated outlet flows.

This simplistic demonstration is by no means comprehensive in terms of utilizing the wide spectrum of tools and capabilities available in the RSM. Rather, it serves to illustrate a simple coordinated structure control scenario which makes use of assessors, filters, controllers and supervisors.

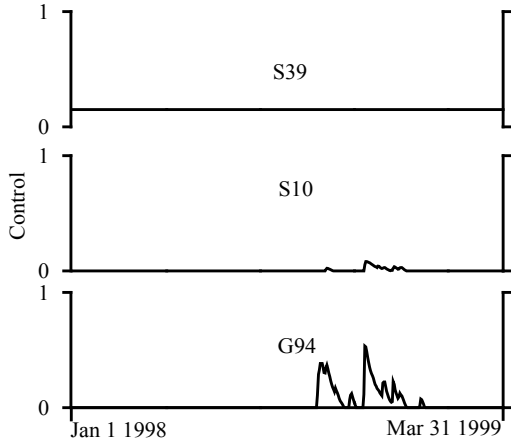

Figure 13: WCA1 outlet structure control signals without supervision.

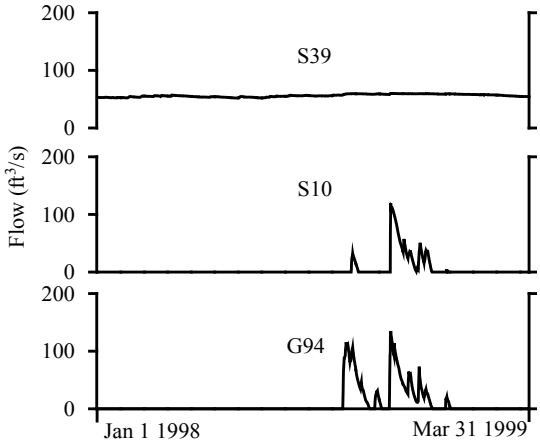

Figure 14: WCA1 outlet structure flows without supervision.

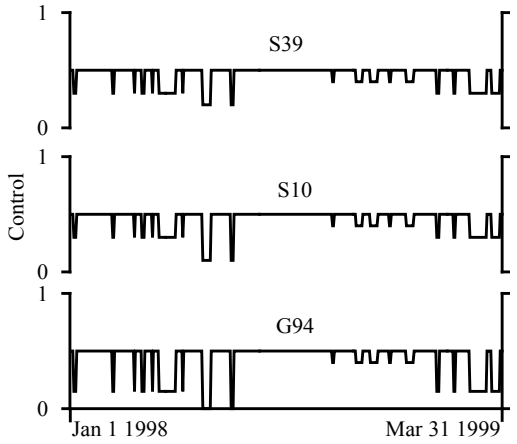

Figure 15: WCA1 outlet structure control signals with supervision.

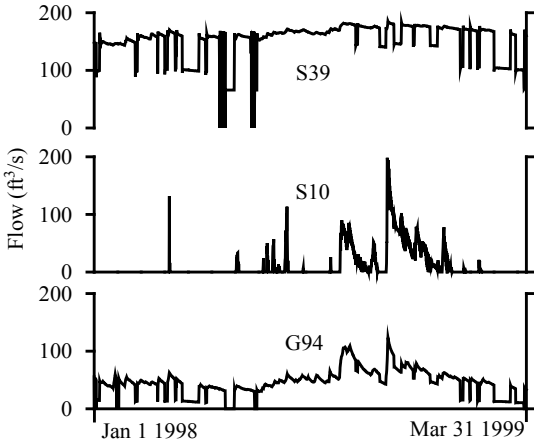

Figure 16: WCA1 outlet structure flows with supervision.

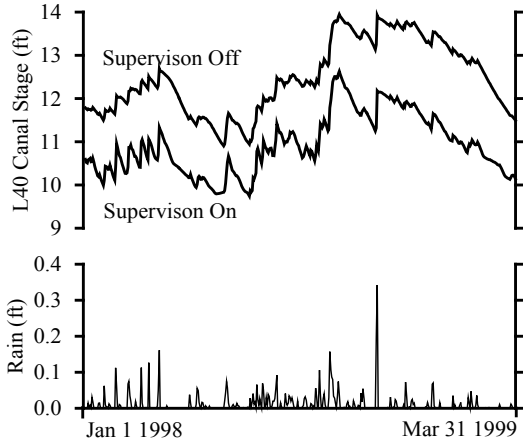

Figure 17: L40 canal stage comparison with and without supervision.

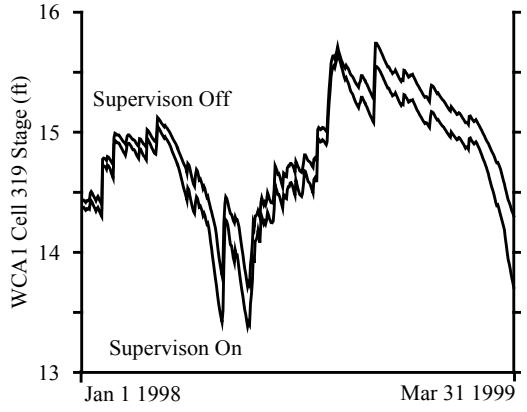

Figure 18: Cell 319 aquifer stage comparison with and without supervision.

4 Future work

To continue progress towards the comprehensive integration of management features in conjunctive hydrological models, there are several areas of continuation relevant to the RSM that deserve attention. At the controller level, there are plans to extend the controller library to include canonical state estimation filters. In the linear domain with Gaussian statistics this includes the addition of a Kalman filter, while for nonlinear transfer functions and non-Gaussian statistics the extended Kalman filter and artificial neural networks.

In the supervisory realm it would be useful to enact a form of arbitration between supervisors. For example, a basin might have one supervisor defined to optimize public water supply deliveries based on synoptic rainfall and aquifer levels, while a competing supervisor for the same basin might be computing optimal solutions for a conservation area or estuarine water quality. One way to address potential conflict resolutions is to extend the control layer hierarchy to include another layer above the supervisors, a managerial layer. This top level would have access to all raw and assessed state information, as well any external constraints required to resolve the conflict by selecting a 'winner' supervisory algorithm at a particular time. The available information processors (LP, fuzzy, finite state machine) could all be extended for this function.

An alternative would be to implement an arbitration processor below the supervisory layer. This processor would take the multiple supervisory inputs, and based on external constraint information will compute which supervisory functions will be applied. An advantage of this approach is that it would be possible to synthesize a supervisory control signal from disparate supervisors to produce an effective supervisory signal. This could be done by an LP optimization, through the aggregation and inferencing of a fuzzy processor, or with the use of a knowledge base and case-based or model-based reasoning inference processor, or artificial intelligence processor.

Another useful extension would be the development of scenario management tools. These would provide the ability to comprehensively specify alternative predefined supervisory or control schemes based on user defined, or state variable information.

5 Conclusion

This paper has explored the general features and capabilities of the Management Simulation Engine component of the Regional Simulation Model. The MSE has been designed based on principles of interoperability of control algorithms, decoupling of hydrologic state and managerial process information, and a multi-level control hierarchy. The combination of these features results in a powerful, extensible methodology to express a wide variety of anthropogenic water resource control policies.

This level of functionality is not typical of some of the leading hydraulic routing, hydrological, and conjunctive aquifer-stream models in use today. Most of these models provide a limited set of water resource management expressions, such as the use of rulecurves based only on hydraulic or hydrological state variables. One notable exception to this is the MIKE SHE suite of modeling tools. MIKE SHE implements a mature and expansive set of management features, arguably the most comprehensive set available in commercial conjunctive models. The RSM and MSE extend this functionality and provide a new set of tools and features not previously available. A list of the essential features of the RSM and MSE which highlight this level of functionality is presented below.

XML input:
Data driven, industry standard XML input specifications

Multilayer control hierarchy:
Local control algorithms for individual hydraulic structures, supervisory control of multiple controllers for synoptic and coordinated structure operations

Integrated structure control algorithms:

1. Closed loop feedback PID control
2. Sigmoid activated closed loop feedback PID control
3. Piecewise linear transfer function
4. Fuzzy logic
5. User defined finite state machine

Integrated supervisory structure coordination algorithms/models:

1. Fuzzy logic
2. User defined finite state machine

3. LP
4. Graph flow
5. Heuristic

Stream flow network abstraction:
Management objects are defined in terms of hydrological entities aggregated into Water Control Units and their associated hydraulic structures, which are internally represented using graph theory. Necessary aggregation and assessment of hydrological state variables is implicit.

Network dynamic data store:
Assessed hydrologic state variables, operational control parameters, and other water resource management variables are dynamically stored and updated in the stream flow network abstraction providing a central data store for managerial algorithms.

Decoupled hydrologic state and management information:
Enables isolation of hydraulic control algorithms from hydraulic and hydrological state algorithms.

Control process interoperability:
Decoupled state and process information with a uniformly designed interface allows compatibility between various control algorithms.

Dynamic switching of control processors:
Multilayered control hierarchy with management process interoperability allows dynamic switching of control algorithms based on hydrological state or management process variables.

Integrated state and information variable monitoring:
Input and output variables for both hydrologic state, and managerial process variables are accessed with a uniform interface known as monitors, allowing MSE objects to access any needed state information.

Suite of assessors:
Provides specialized quantification of hydrological state variables, freeing managerial algorithms from data preprocessing.

Generalized data filtering:
Common statistical and mathematical functions are implemented as a series of piped filters, enabling simple, yet powerful and flexible modulation of state variables.

References

[1] Belaineh, G., Peralta, R. C., Hughes, T. C., Simulation/ Optimization Modeling for Water Resources Management, ASCE Journal Water Resources Planning Management, 125(3), p 154-61, 1999

[2] M. A. Brdys, B. Ulanicki, Operational Control of Water Systems: Structures, Algorithms, and Applications, Prentice Hall, 1994, ISBN 0136389740

[3] Mays, L. W., Tung, Y, Hydrosystems Engineering and Management, McGraw-Hill, 1991, ISBN 0070411468

[4] Eschenbach, E. A., et. al., Goal Programming Decision Support System for Multiobjective Operation of reservior Systems, ASCE Journal Water Resources Planning Management, 127(2), p 108-20, 2001

[5] Sivakumar, B., Jayawardena, A.W., Fernando, T.M.K.G., "River flow forecasting: use of phase-space reconstruction and artificial neural networks approaches", 2002, J. Hydrol., 265, p225-45

[6] Lambrakis, N., et. al., "Nonlinear analysis and forecasting of a brackish karstic spring", 2000, Water Resour. Res., 36 (4), p875-84

[7] Dubrovin, T., Jolma, A., Turunen, E., Fuzzy Model for Real-Time Reservior Operation, ASCE Journal Water Resources Planning Management, 128(1), p 66-73, 2002

[8] Shrestha, B.P., Duckstein, L., Stakhiv, E.Z., Fuzzy Rule-Based Modeling of Reservior Operations, ASCE Journal Water Resources Planning Management, 122(4), p 262-69, 1996

[9] Foufoula-Georgiou, E., Kitandis, P.K., Gradient Dynamic Programming for stochastic optimal control of multidimensional water resources systems, Water Resour. Res., 24(8), p 1345-59, 1988

[10] da Conceicao Cunha, M., Sousa, Joaquim, Water Distribution Network Design Optimization: Simulated Annealing Approach, ASCE Journal Water Resources Planning Management, 125(4), p 215-21, 1999

[11] Wardlaw, R., Sharif, M., Evaluation of Genetic Algorithms for Optimal Reservior System Operation, ASCE Journal Water Resources Planning Management, 125(1), p 25-33, 1999

[12] Extensible Markup Language (XML) 1.0 (Third Edition), W3C Recommendation 04 February 2004, http://www.w3.org/TR/2004/REC-xml-20040204/

[13] Lal, Wasantha A. M., Weighted implicit finite-volume model for overland flow, ASCE Journal of Hydraulic Eng., 124(9), Sep 1998, pp 941-950

[14] Lal, Wasantha, A. M., Van Zee, Randy and Belnap, Mark, Case Study: Model to Simulate Regional Flow in South Florida, ASCE Journal of Hydraulic Engineering, in publication, manuscript HY/2003/023398, April 2005

[15] Lal, Wasantha, A. M. and Van Zee, Randy, Error analysis of the finite volume based regional simulation model RSM, Proceedings, World Water and Environmental Resources Congress, June 23-26, 2003, Philadelphia

[16] Lal, Wasantha, A. M., Jayantha Obeysekera, Randy Van Zee, Sensitivity and uncertainty analysis of a regional simulation model for the natural system in South Florida, Proceedings of the 27 th Congress of the IAHR/ASCE Conference, San Francisco, CA, August 10-17, 1997, pp. 560-565

[17] Lal, Wasantha, A. M., Modification of canal flow due to stream-aquifer interaction, ASCE Journal of Hydraulic Engrg., 127(7), July, 2001

[18] Regional Simulation Model (RSM) User's Manual, Hydrologic Simulation Engine (HSE) Components, South Florida Water Management District, Model Development Division (4540), 3301 Gun Club Road, West Palm Beach, FL November 2004

[19] Park, J.C., et. al., Sigmoidal Activation of PI Control Applied to Water Management, Journal of Water Resources Planning and Management, in publication, manuscript WR/2003/022696

[20] Regional Simulation Model (RSM) User's Manual, Management Simulation Engine (MSE) Controllers, South Florida Water Man-

agement District, Model Development Division (4540), 3301 Gun Club Road, West Palm Beach, FL March 2004

[21] Regional Simulation Model (RSM) User's Manual, Management Simulation Engine (MSE) Supervisors, South Florida Water Management District, Model Development Division (4540), 3301 Gun Club Road, West Palm Beach, FL March 2004

[22] PETSc Users Manual, Argonne National Laboratory, ANL-95/11 - Revision 2.1.5 http://www.mcs.anl.gov/petsc, 2004

[23] International Electrotechnical Commission (IEC), Technical Committee No. 65, Industrial Process Measurement and Control Subcommittee 65B: Devices, IEC 1131 - Programmable Controllers, Part 7 - Fuzzy Control Programming

[24] Cybenko, G., Approximations by superpositions of sigmoidal functions. Mathematics of Control, Signals, and Systems, 2, p 303-14, 1989

[25] Hornik, K, Multilayer feedforward networks are universal approximators, Neural Networks, 2, p 359-66, 1989

[26] Kolmogorov, A. N., On the representation of continuous functions of many variables by superpositions of continuous functions of one variable and addition. Dokl. Akad. SSSR, 114, p 953-6, 1957

[27] GNU Linear Programming Kit (GLPK), Version 4.2, November 2003, http://www.gnu.org/software/glpk/glpk.html

[28] Ford, L. R., Fulkerson, D. R., Flows in Networks, Princeton University Press, 1962

[29] Ahuja, R. K., Magnanti, T. I., Orlin, J. B., Network Flows: Theory, Algorithms, and Applications, Prentice Hall, 1993

[30] Diba, A., Louie, P. W. F., Mahjoub, M. Yeh, W., Planned Operation of Large-Scale Water-Distribution System, J. Water Resour. Plng. and Mgmt, 121(3), p 260-9, 1995

[31] Ostfeld, A., Water Distribution Systems Connectivity Analysis, J. Water Resour. Plng. and Mgmt, 131(1), p. 58-66, 2005

[32] A Primer to the South Florida Water Management Model, South Florida Water Management District, Model Development Division (4540), 3301 Gun Club Road, West Palm Beach, FL

[33] Harbaugh, A.W., and McDonald, M.G., 1996, User's documentation for MODFLOW-96, an update to the U.S. Geological Survey modular finite-difference ground-water flow model: U.S. Geological Survey Open-File Report 96485, 56 p.

[34] McDonald, M.C., and Harbaugh, A.W., 1988, A modular three-dimensional finite-difference ground-water flow model: U.S. Geological Survey Techniques of Water-Resources Investigations, book 6, chap. A1, 586 p.

[35] United States Geological Survey, MODFLOW Fact Sheet, http://water.usgs.gov/pubs/fs/FS-121-97/

[36] Prudic, D.E., 1989, Documentation of a computer program to simulate stream-aquifer relations using a modular, finite-difference, ground-water flow model: U.S. Geological Survey Open-File Report 88-729, 113 p.

[37] Swain, E.D., and Wexler, E.J., 1996, A coupled surface-water and ground-water flow model (MODBRNCH) for simulation of stream-aquifer interaction: U.S. Geological Survey Techniques of Water-Resources Investigations, book 6, chap. A6, 125 p.

[38] Schaffranek, R.W., Baltzer, R.A., and Goldberg, D.E., 1981, A model for simulation of flow in singular and interconnected channels: U.S. Geological Survey Techniques of Water-Resources Investigations, book 7, chap. C3, 110 p.

[39] Schaffranek, R.W., 1987, Flow model for open-channel reach or network: U.S. Geological Survey Professional Paper 1384, 12 p.

[40] DHI Water & Environment, Agern All 5, DK-2970 Hrsholm, Denmark, http://www.dhisoftware.com/mikeshe/

[41] DHI Water & Environment, Agern All 5, DK-2970 Hrsholm, Denmark, MIKE SHE Components,
http://www.dhisoftware.com/mikeshe/Components/

[42] United States Environmental Protection Agency Ariel Rios Building 1200 Pennsylvania Avenue, N.W. Washington, DC 20460 http://www.epa.gov/ednnrmrl/swmm/index.htm

[43] Institute for Water Resources U.S. Army Corps of Engineers 7701 Telegraph Road Alexandria, Virginia 22315 Hydrologic Engineering Center 609 Second Street Davis, CA 95616-4687 http://www.hec.usace.army.mil/

[44] Barkau, R., 1997, UNET One-Dimensional Unsteady Flow Through a Full Network of Open Channels, User's Manual, U.S. Army Corps of Engineers, Hydrologic Engineering Center, 609 Second Street Davis, CA 95616-4687

[45] National Weather Service 1325 East West Highway, Silver Spring, MD 20910
http://www.nws.noaa.gov/oh/hrl/rvrmech/fld_release.htm

[46] FLO-2D Software, Inc., Tetra Tech, P.O. Box 66, Nutrioso, AZ, 85932 http://www.flo-2d.com/

[47] Franz, D.D., and Melching, C.S., 1997, Full Equations (FEQ) model for the solution of the full, dynamic equations of motion for one-dimensional unsteady flow in open channels and through control structures: U.S. Geological Survey Water-Resources Investigations Report 96-4240, 258 p.

[48] email communication 12/7/04 from Soren Tjerry, Hydraulic Engineer DHI Inc, 319 SW Washington, Suite 614 Portland, OR 97204, e-mail: snt@dhi.us. Dr. Tjerry indicates that MIKE refers to the seminal contributions of Professor Michael B. (Mike) Abbott in the establishment and development of the MIKE family of numerical models. See also: http://www.hydroinformatics.org/hi/abbott/default.htm

6 Appendix A: Review of commonly used models

6.1 MODFLOW MODBRNCH

The modular finite-difference ground-water flow model (MODFLOW) [33, 34] is a three dimensional finite-difference groundwater model capable of simulating steady and nonsteady flow in an irregularly shaped boundary in which aquifer layers can be confined, unconfined, or a combination of both. The ground-water flow equation is solved using the finite-difference approximation wherein the flow region is subdivided into blocks in of uniform medium properties. The MODFLOW spatial domain is discretized into variably spaced rectangular blocks which must constitute a grid of mutually perpendicular lines. Currently, MODFLOW is the most widely used program in the world for simulating ground-water flow [35].

Surface and groundwater interactions can be simulated by the coupled BRANCH and USGS modular, three dimensional, finite- difference groundwater flow (MODFLOW) models, referred to as MODBRNCH [37].

The Branch-Network Dynamic Flow Model BRANCH [38, 39] is used to simulate steady or unsteady flow in a single open-channel reach (branch) or throughout a system of branches (network) connected in a dendritic or looped pattern. BRANCH uses a weighted four-point, implicit, finite- difference approximation of the unsteady-flow equations. The effects of hydraulic control structures within the model domain are treated by a multi-parameter rating method.

6.2 MIKE SHE

MIKE SHE is a modeling tool that can simulate the entire land phase of the hydrologic cycle encapsulated in an integrated modeling environment that allows components to be used independently and customized to local needs [40].

MIKE SHE includes a traditional 2D or 3D finite-difference groundwater model, which is very similar to MODFLOW. MIKE SHE's overland-flow component includes a 2D finite difference diffusive wave approach using the same 2D mesh as the groundwater component. Overland flow interacts with the river, the unsaturated zone, and saturated groundwater zone.

MIKE SHE's river modeling component is the MIKE 11 modeling system for river hydraulics. MIKE 11 is a dynamic, 1-D modeling tool for the design, management and operation of river and channel systems. MIKE 11 supports any level of complexity and offers simulation engines that covers

the entire range from simple Muskingum routing to the Higher Order Dynamic Wave formulation of the Saint-Venant equations. MIKE 11 is the most widely used hydraulic modeling system in the world [41].

MIKE 11 provides for hydraulic analysis/design of structures including bridges, as well as optimization of river and reservoir operations. A wide range of structures can be represented with native computational methods and user defined functions. The structures are included in the MIKE 11 hydrodynamic module (HD), which provides computational formulations applicable to flow over a variety of structures that include:

- Broad-crested weirs
- Culverts
- Bridges
- Pumps
- Regulating structures
- Control structures
- Dam-break structures
- User-defined structures
- Tabulated structures

Further, operational control strategies for a number of different standard structures are included in the structure operation (SO) module for the following structures:

- Sluice gates
- Overflow gates
- Radial gates
- Pumps
- Reservoir releases

Control strategies for gate operations can be defined in the following ways:

1. A direct determination of the gate operation by description of the gate level as a function of time or as a function of hydraulic or species concentration variables at specified locations inside the model area.
2. The gate is determined by PID operation. The set-point for this can be chosen on the basis of hydraulic variables and concentrations within the model area.

3. An iterative determination of the gate level. With this approach iteration is performed on the gate level until a requested set-point value is obtained. This facility is ideal for flood control purposes.

The functional representation of the control strategy can be specified by rating curves, a binary decision tree which selects alternative strategies, or by user- defined functions developed in the Pascal programming language and compiled into a dynamic load library (DLL).

6.3 EPA SWMM

The EPA Storm Water Management Model (SWMM) [42] is a dynamic rainfall-runoff simulation model used for single event or long-term (continuous) simulation of runoff quantity and quality from primarily urban areas. The runoff component of SWMM operates on a collection of subcatchment areas that receive precipitation and generate runoff and pollutant loads. The routing portion of SWMM transports this runoff through a system of pipes, channels, storage/treatment devices, pumps, and regulators. SWMM also contains a flexible set of hydraulic modeling capabilities used to route runoff and external inflows through the drainage system network of pipes, channels, storage/treatment units and diversion structures. These include the ability to apply user-defined dynamic control rules to simulate the operation of pumps, flow dividers, orifice openings, and weir crest levels. The SWMM model allows the user to specify control functions based on a user specified set of rules, where the rules are decomposed into condition-action components. The conditions evaluate to boolean expressions composed from an if-and-or syntax. The correspondingly selected actions are specified in terms of then-else constructs, with optional priority fields assigned to each potential action.

6.4 HEC HMS-RAS-RESSIM

The Hydrologic Engineering Center (HEC) [43] Hydrologic Modeling System (HMS) is designed to simulate the precipitation-runoff processes of dendritic watershed systems. Several hydraulic structures can be modeled including bridges, culverts, weirs or other hydraulic control structures. Hydraulic structures are simulated by user specified discharge rating curves or rating tables assigned to either channel or floodplain elements. Culvert flow can occur between grid elements that are not contiguous. Reference elevations for headwater depth and tailwater effects can be considered.

A variety of hydrologic routing methods are included for simulating flow in open channels. Routing with no attenuation can be modeled with the lag method. The traditional Muskingum method is also included. The modified Puls method can be used to model a reach as a series of cascading, level pools with a user-specified storage-outflow relationship. Channels with trapezoidal, rectangular, triangular, or circular cross sections can be modeled with the kinematic wave or Muskingum-Cunge method. Channels with overbank areas can be modeled with the Muskingum-Cunge method and an 8-point cross section.

The HEC River Analysis System (HEC-RAS) is designed to perform one-dimensional hydraulic calculations for a full network of natural and constructed channels. The system can handle a full network of channels, a dendritic system, or a single river reach. The steady flow component is capable of modeling subcritical, supercritical, and mixed flow regimes water surface profiles. The effects of various structures such as bridges, culverts, weirs, pump stations, navigation dams, and culvert flap gates may be considered in the computations.

Special features of the steady flow component include:

- multiple plan analyses
- multiple profile computations
- multiple bridge and/or culvert opening analyses
- split flow optimization

The HEC-RAS modeling system is also capable of simulating one-dimensional unsteady flow through a full network of open channels. The unsteady flow equation solver was adapted from Dr., Robert L. Barkau's UNET model [44].

The HEC Reservoir System Simulation program, HEC-ResSim is dedigned for reservoir operation modeling at one or more reservoirs for a variety of operational goals and constraints. A network of rivers and streams, called a stream alignment, is created in the watershed setup module, This stream alignment is used as a back bone on which the reservoir network schematic is developed. The network schematic elements include reservoirs, routing reaches, diversions, and junctions. The reservoirs are complex elements that are made up of the pool, the dam, and one or more outlets.

The criteria for reservoir release decisions is called an operation set which is made up of a set of discrete zones and rules. The zones divide the pool by elevation and contain a set of rules that describe the goals and constraints that should be followed when the reservoir's pool elevation is within the zone.

6.5 NWS FLDWAV

The U.S. National Weather Service Flood Wave (FLDWAV) program [45] is a generalized flood routing program capable of modeling single stream or a an interconnected system of flow channels. A four-point finite-difference approximation of the one-dimensional St. Venant equations is the basis of the formulation. Boundary conditions include dams, bridges, weirs and other common flow controls. FLDWAV can model time-dependent gate controls, and has the ability to read generic rating curves applied to control structures. The model incorporates equations for spillway flows, bridge and embankment effects, tidal flap gates, dams, tributary inflows, river sinuosity, and tidal effects. The user may specify multiple routing techniques (dynamic-implicit/ explicit, diffusion, level-pool) throughout the stream system.

6.6 FLO-2D

FLO-2D [46] is a dynamic flood routing model that simulates channel flow, overland unconfined flow and street flow. It predicts the progression of a flood hydrograph over a system of square grid elements while conserving volume. The model uses the full dynamic wave momentum equation and a central finite difference routing scheme to distribute the flow. The potential flow surface topography is represented in a FLO-2D simulation by a square grid format.

The model has number of components that enhance flood routing detail including channel-floodplain discharge exchange, loss of storage due to buildings, flow obstructions, rill and gully flow, street flow, hydraulic structure controls, levee and levee failure, mud and debris flow, sediment transport, rainfall and infiltration. Hydraulic structures can represent bridges, culverts, weirs or other control structures. Structures are simulated by user specified discharge rating curves or rating tables assigned to either channel or floodplain elements. Culvert flow can occur between grid elements that are not contiguous. Reference elevations for headwater depth and tailwater effects can be considered.

6.7 FEQ

The Full Equations model (FEQ) [47] simulates flow in a stream system by solving the full, dynamic equations of motion for one-dimensional unsteady flow in open channels and through control structures. FEQ stream systems are subdivided into three broad classes of flow paths:

1. stream reaches (branches)
2. stream segments for which complete information on flow and depth are not required (dummy branches)
3. level-pool reservoirs

These components are connected by special features or hydraulic control structures, such as junctions, bridges, culverts, dams, waterfalls, spillways, weirs, side weirs, pumps, and others. The hydraulic characteristics of channel cross sections and special features are stored in function tables calculated by the companion program FEQUTL. The FEQ model uses keyword and format-specific input files.

7 Appendix B: List of Acronyms

AMPL	-	A Modeling Language for Mathematical Programming
ANN	-	Artificial Neural Network
API	-	Application Programming Interface
DHI	-	Danish Hydraulic Institute Water & Environment
EPA	-	United States Environmental Protection Agency
FCL	-	Fuzzy Control Language
FLDWAV	-	Flood Wave
FLO-2D	-	FLO-2D Software
FEQ	-	Full Equations model
GLPK	-	GNU Linear Programming Kit
GNU	-	GNU's not Unix
GW	-	Ground Water
HEC	-	Hydrologic Engineering Center
HSE	-	Hydrologic Simulation Engine
HMS	-	Hydrologic Modeling System
LP	-	Linear Programming
MODFLOW	-	Modular finite-difference ground-water flow model
MODBRANCH	-	Coupled MODFLOW & BRANCH model
MIKE	-	Anecdotally attributed to Michael B. Abbott [48]
MIP	-	Mixed Integer Programming
MSE	-	Management Simulation Engine
NWS	-	United States National Weather Service
ORM	-	Object Routing Model
RSM	-	Regional Simulation Model
RAS	-	River Analysis System
RESSIM	-	Reservoir System Simulation
SF	-	Stream Flow
SFWMD	-	South Florida Water Management District
SFWMM	-	South Florida Water Management Model
SHE	-	Systeme Hydrologique Europeen
SW	-	Surface Water
SWMM	-	Storm Water Management Model
USGS	-	United States Geological Survey
WCA	-	Water Conservation Area
WCU	-	Water Control Unit
XML	-	Extensible Markup Language